MycoKeys 68: 1–21 (2020)
doi: 10.3897/mycokeys.68.51667
http://mycokeys.pensoft.net

RESEARCH ARTICLE

A peer-reviewed open-access journal
MycoKeys
Launched to accelerate biodiversity research

Three new *Curvularia* species from clinical and environmental sources

Isabel Iturrieta-González[1], Josepa Gené[1], Nathan Wiederhold[2], Dania García[1]

1 *Unitat de Micologia, Facultat de Medicina i Ciències de la Salut and IISPV, Universitat Rovira i Virgili, Reus, Spain* **2** *Fungus Testing Laboratory, Department of Pathology and Laboratory Medicine, University of Texas Health Science Center, San Antonio, TX, USA*

Corresponding author: Josepa Gené (josepa.gene@urv.cat)

Academic editor: N. Wijayawardene | Received 3 March 2020 | Accepted 18 April 2020 | Published 17 June 2020

Citation: Iturrieta-González I, Gené J, Wiederhold N, García D (2020) Three new *Curvularia* species from clinical and environmental sources. MycoKeys 68: 1–21. https://doi.org/10.3897/mycokeys.68.51667

Abstract

Curvularia is a Pleosporalean monophyletic genus with a great diversity of species, including relevant phytopathogenic, animal and human pathogenic fungi. However, their microscopic identification is difficult due to overlapping morphological features amongst species. In recent years, multi-locus sequence analysis using the ITS region of the rDNA and fragments of the genes *gapdh* and *tef*1 revealed numerous cryptic species, especially in isolates that commonly produced 3-septate conidia. Therefore, based on sequence analysis of the above-mentioned DNA barcodes recommended for species delineation in *Curvularia*, we propose three novel species, *C. paraverruculosa*, *C. suttoniae* and *C. vietnamensis*, isolated from soil, human clinical specimens and plant material, respectively, collected in different countries. These new species are morphologically characterised and illustrated in the present study. *Curvularia paraverruculosa* differs from its counterparts, *C. americana* and *C. verruculosa*, mainly by its narrower conidia. *Curvularia suttoniae* and *C. vietnamensis* are closely related to *C. petersonii*, but the former two have larger conidia.

Keywords

Ascomycetes, Dematiaceous hyphomycetes, phylogeny, Pleosporaceae, taxonomy

Introduction

The genus *Curvularia* Boedijn (1933), typified by *C. lunata* (Wakker) Boedijn, belongs in Pleosporaceae, Pleosporales (Wijayawardene et al. 2018). Members of *Curvularia* show different life modes, i.e. saprophytic, endophytic and also pathogenic on plants and animals (Marin-Felix et al. 2017a). Phytopathogenic species can affect wild grasses

and staple crops, such as rice, maize, wheat or sorghum and give rise to serious losses in agricultural production (Gautam et al. 2013, Manamgoda et al. 2015, Marin-Felix et al. 2017a, Tan et al. 2018). The endophytic species have garnered interest in recent years for their use in the production of bio-based products that are beneficial to living organisms and the environment (Bengyella et al. 2019). Since the first report of *Curvularia* as a human pathogen in a patient with mycetoma (Baylet et al. 1959), other clinical presentations have been reported, such as superficial and deep infections that mainly affect the respiratory tract but can even cause cerebral phaeohyphomycosis with an extremely poor prognosis (de Hoog et al. 2000).

The genus is morphologically distinguished mainly by its asexual morph, which shows sympodial conidiophores with mono- to polytretic conidiogenous cells and transversally septate conidia. Typically, the conidia in *Curvularia* are curved due to the hypertrophy of one of the intermediate cells and they are euseptate (Ellis 1971), although other authors opine that the conidia in *Curvularia* are distoseptate (Sivanesan 1987, Seifert et al. 2011, Madrid et al. 2014). The species of *Bipolaris* and *Exserohilum* have typically straight and distoseptate conidia; however, some of them have been transferred to *Curvularia*, based on their DNA sequence analyses (Manamgoda et al. 2012, Hernández-Restrepo et al. 2018, Tan et al. 2018). Furthermore, due to the overlapping of morphological characters amongst certain species of *Curvularia*, such as conidial size, shape and septation, an accurate identification at the species level is difficult without a DNA sequence analysis (da Cunha et al. 2013, Madrid et al. 2014, Manamgoda et al. 2015). Several cryptic species have been described recently using only multi-locus sequence analyses of the recommended DNA barcodes for species delimitation, i.e. the internal transcribed spacer (ITS) region of the rDNA and the protein-coding loci glyceraldehyde-3-phosphate dehydrogenase (*gapdh*) and translation elongation factor 1-a (*tef*1) (Marin-Felix et al. 2017a, Tan et al. 2018). Nearly 130 species have so far been accepted in *Curvularia*, including the species classified previously in the teleomorphic genera *Cochliobolus* and *Pseudocochliobolus* after applying the current criteria for fungal nomenclature (Manamgoda et al. 2012, 2015, Madrid et al. 2014, Hyde et al. 2017, Marin-Felix et al. 2017a, 2017b, Dehdari et al. 2018, Heidari et al. 2018, Hernández-Restrepo et al. 2018, Liang et al. 2018, Mehrabi-Koushki et al. 2018, Tan et al. 2018, Tibpromma et al. 2018, Kiss et al. 2019, Raza et al. 2019, Zhang et al. 2020).

Based on a polyphasic approach, combining morphological and phylogenetic analyses, three novel *Curvularia* species are proposed here, isolated from human clinical specimens in the USA, soil in Mexico and seed and plant debris in Vietnam and Indonesia, respectively.

Material and methods

Origin of isolates

Five unidentified *Curvularia* isolates, maintained in the fungal collection of the Medical School of the Rovira i Virgili University (FMR; Reus, Spain), were included in the

study. Two of these (FMR 10992, FMR 11690) were isolated from human specimens in the USA by Deana A. Sutton of the Fungus Testing Laboratory at the University of Texas Health Sciences Center (UTHSC; San Antonio, USA) and the other three (FMR 11956, FMR 17656, FMR 17659) were isolated from environmental samples; the first from sorghum seeds collected in Indonesia, the second from soil collected in the Mexican region of Michoacán and the third from unidentified plant material collected in the north-east of Vietnam.

DNA extraction, PCR, sequencing and phylogenetic analysis

The fungal DNA was extracted from colonies growing on potato dextrose agar (PDA; Pronadisa, Madrid, Spain) for 7 to 10 days at 25 °C in darkness and following the protocol of Müller et al. (1998). The ITS barcode, including the 5.8S gene and the genes *gapdh* and *tef*1 were analysed following Marin-Felix et al. (2017a). Amplification was carried out using the primer pairs ITS5/ITS4 for the ITS region (White et al. 1990), gpd1/gpd2 for *gapdh* (Berbee et al. 1999) and EF983/2218R for *tef*1 (Schoch et al. 2009). The PCR products were purified and stored at -20 °C until sequencing. The same pairs of primers used for the amplification were also used to obtain the DNA sequences, which were processed at Macrogen Europe (Macrogen Inc., Madrid, Spain). The sequences of each isolate were edited using SeqMan v. 7.0.0 (DNAStar Lasergene, Madison, WI, USA) to obtain the consensus sequences.

We made a preliminary comparison of *gapdh* sequences generated from our isolates with those of the National Center for Biotechnology Information (NCBI) using the Basic Local Alignment Search Tool (BLASTn) for their molecular identification. To establish the phylogenetic position of unidentified isolates with respect to the most accepted species in *Curvularia*, we carried out individual (data not shown) and combined alignments of the three loci complemented by all available sequences of the ex-type and reference strains of *Curvularia* species retrieved from NCBI (Table 1). Based on this first phylogeny of the genus, a more restricted multi-locus analysis was carried out, including only those *Curvularia* species most related to the isolates under study. The alignments were made in the MEGA (Molecular Evolutionary Genetics Analysis) software v.6.0. (Tamura et al. 2013), using ClustalW algorithm (Thompson et al. 1994), refined with MUSCLE (Edgar 2004) in the same platform and manually adjusted as necessary. Phylogenetic reconstructions were made using Maximum Likelihood (ML) and Bayesian Inference (BI) approaches under RAxML-HPC2 on XSEDE v.8.2.12 (Stamatakis et al. 2014) in CIPRES Science gateway portal (Miller et al. 2010) and MrBayes v. 3.2.6 (Ronquist et al. 2012), respectively.

For the ML analysis, the best nucleotide substitution model for the combined analysis of ITS, *gapdh* and *tef*1, determined using the MEGA programme, was Kimura 2-parameters with Gamma distribution (K2+G); the combined analysis of these three phylogenetic markers was tested through Incongruence Length Difference (ILD) implemented in the Winclada programme (Farris et al. 1994). ML bootstrap values (bs) ≥ 70% were considered significant.

Table 1. Species included in this study, their substrate, origin and GenBank accession numbers.

Species	Strain no[1]	Substrate	Country	Genbank accession no.[2]		
				ITS	*gapdh*	*tef1*
Bipolaris maydis	CBS 136.29 T	*Zea mays*	USA	AF071325	KM034846	KM093794
B. saccharicola	CBS 155.26 T	Unknown	Unknown	KY905674	KY905686	KY905694
Curvularia aeria	CBS 294.61 T	Air	Brazil	HF934910	HG779148	–
C. affinis	CBS 154.34 T	Unknown	Indonesia	KJ909780	KM230401	KM196566
C. ahvazensis	CBS 144673 T	*Zinnia elegans*	Iran	KX139029	MG428693	MG428686
C. akaii	CBS 317.86	*Themada triandra* subsp. *japonica*	Japan	KJ909782	KM230402	KM196569
C. akaiiensis	BRIP 16080 T	Unknown	India	KJ415539	KJ415407	KJ415453
C. alcornii	MFLUCC 10-0703 T	*Z. mays*	Thailand	JX256420	JX276433	JX266589
C. americana	UTHSC 08-3414 T	Human ankle	USA	HE861833	HF565488	–
	UTHSC 07-2649	Human toe tissue	USA	HE861834	HF565486	–
	UTHSC 08-84	Human nasal sinus	USA	HG779015	HG779115	–
	UTHSC 08-278	Human peritoneal dialysis fluid	USA	HE861832	HF565487	–
	UTHSC 08-2697	Human leg	USA	HG779016	HG779117	–
C. annelliconidiophori	CGMCC3.19352 T	Roots of *Saccharum officinarum*	China	MN215641	MN264077	MN263935
C. asiatica	MFLUCC 10-0711 T	*Panicum* sp.	Thailand	JX256424	JX276436	JX266593
C. australiensis	BRIP 12044 T	*Oryza sativa*	Australia	KJ415540	KJ415406	KJ415452
	CBS 172.57	*O. sativa* seeds	Vietnam	JN601026	JN601036	JN601003
C. australis	BRIP 12521 T	*Sporobolus caroli*	Australia	KJ415541	KJ415405	KJ415451
C. bannonii	BRIP 16732 T	*Jacquemontia tamnifolia*	USA	KJ415542	KJ415404	KJ415450
C. beasleyi	BRIP 10972 T	*Chloris gayana*	Australia	MH414892	MH433638	MH433654
	BRIP 15854	*Leersia hexandra*	Australia	MH414893	MH433639	MH433655
C. beerburrumensis	BRIP 12942 T	*Eragrostis bahiensis*	Australia	MH414895	MH433634	MH433657
C. boeremae	IMI 164633 T	*Portulaca oleracea*	India	MH414911	MH433641	–
C. borreriae	CBS 859.73	Volcanic ash soil	Chile	HE861848	HF565455	–
C. bothriochloae	BRIP 12522 T	*Bothriochloa bladhii*	Australia	KJ415543	KJ415403	KJ415449
C. brachyspora	CBS 186.50	Soil	Indonesia	KJ922372	KM061784	KM230405
C. buchloes	CBS 246.49 T	*Buchloë dactyloides*	USA	KJ909765	KM061789	KM196588
C. carica-papayae	CBS 135941 T	*Carica papaya*	India	HG778984	HG779146	–
C. chiangmaiensis	CPC 28829 T	*Z. mays*	Thailand	MF490814	MF490836	MF490857
C. chlamydospora	UTHSC 07-2764 T	Human toe nail	USA	HG779021	HG779151	–
C. chonburiensis	MFLUCC 16-0375 T	Dead leaf of *Pandanus* sp.	Thailand	MH275055	MH412747	–
C. clavata	BRIP 61680	*Oryza* sp.	Australia	KU552205	KU552167	KU552159
C. cymbopogonis	CBS 419.78	*Yucca* leaf spot	Netherlands	HG778985	HG779129	–
C. coatesiae	BRIP 24261 T	*Litchi chinensis*	Australia	MH414897	MH433636	MH433659
C. coicis	CBS 192.29 T	*Coix lacryma-jobi*	Japan	AF081447	AF081410	JN601006
C. coimbatorensis	SZMC 22225 T	Human corneal scraping	India	MN628310	MN628306	MN628302
C. colbranii	BRIP 13066 T	*Crinum zeylanicum*	Australia	MH414898	MH433642	MH433660
C. comoriensis	CBS 110673	Unknown	Unknown	LT631357	LT715841	–

Species	Strain no[1]	Substrate	Country	Genbank accession no.[2]		
				ITS	*gapdh*	*tef1*
C. crassiseptum	CBS 503.90 T	Plant material	Nigeria	LT631310	LT715882	–
C. crustacea	BRIP 13524 T	*Sporobolus* sp.	Indonesia	KJ415544	KJ415402	KJ415448
C. dactyloctenicola	CPC 28810 T	*Dactyloctenium aegyptium*	Thailand	MF490815	MF490837	MF490858
C. dactyloctenii	BRIP 12846 T	*Dactyloctenium radulans*	Australia	KJ415545	KJ415401	KJ415447
C. deightonii	CBS 537.70	*Sorghum vulgare*	Denmark	LT631356	LT715839	–
C. determinata	CGMCC3.19340 T	Leaves of *S. officinarum*	China	MN215653	MN264088	MN263947
C. elliptiformis	CGMCC3.19351 T	Roots of *S. officinarum*	China	MN215656	MN264091	MN263950
C. ellisii	CBS 193.62 T	Air	Pakistan	JN192375	JN600963	JN601007
C. eragrosticola	BRIP 12538 T	*Eragrostis pilosa*	Australia	MH414899	MH433643	MH433661
C. eragrostidis	CBS 189.48	*Sorghum* seed	Indonesia	HG778986	HG779154	–
C. falsilunata	CGMCC3.19329 T	Roots of *S. officinarum*	China	MN215660	MN264093	MN263954
C. flexuosa	CGMCC3.19447 T	Roots of *S. officinarum*	China	MN215663	MN264096	MN263957
C. gladioli	CBS 210.79	Gladiolus leaf	Romania	HG778987	HG779123	–
C. geniculata	CBS 187.50	*Andropogon sorghum* seed	Indonesia	KJ909781	KM083609	KM230410
C. graminicola	BRIP 23186 T	*Aristida ingrata*	Australia	JN192376	JN600964	JN601008
C. guangxiensis	CGMCC3.19330 T	Roots of *S. officinarum*	China	MN215667	MN264100	MN263961
C. gudauskasii	DAOM 165085	Unknown	Unknown	AF071338	AF081393	–
C. harveyi	BRIP 57412 T	*Triticum aestivum*	Australia	KJ415546	KJ415400	KJ415446
C. hawaiiensis	BRIP 11987 T	*O. sativa*	USA	KJ415547	KJ415399	KJ415445
C. heteropogonicola	BRIP 14579 T	*Heteropogon contortus*	India	KJ415548	KJ415398	KJ415444
C. heteropogonis	CBS 284.91 T	*H. contortus*	Australia	KJ415549	JN600969	JN601013
C. hominis	CBS 136985 T	Human cornea	USA	HG779011	HG779106	–
C. homomorpha	CBS 156.60 T	Air	USA	JN192380	JN600970	JN601014
C. inaequalis	CBS 102.42 T	Soil	France	KJ922375	KM061787	KM196574
C. intermedia	CBS 334.64	*Avena versicolor*	USA	HG778991	HG779155	–
C. ischaemi	CBS 630.82 T	*Ischaemum indicum*	Solomon Islands	MH861533	JX276440	–
C. kenpeggii	BRIP 14530 T	*Triticum aestivum*	Australia	MH414900	MH433644	MH433662
C. kusanoi	CBS 137.29	*Eragrostis major*	Japan	JN192381	LT715862	JN601016
C. lamingtonensis	BRIP 12259 T	*Microlaena stipoides*	Australia	MH414901	MH433645	MH433663
C. lunata	CBS 730.96 T	Human lung biopsy	USA	JX256429	JX276441	JX266596
C. malina	CBS 131274 T	*Zoysia matrella*	USA	JF812154	KP153179	KR493095
C. manamgodae	CGMCC3.19446 T	Roots of *S. officinarum*	China	MN215677	MN264110	MN263971
	LC13495	Roots of *S. officinarum*	China	MN215678	MN264111	MN263972
C. mebaldsii	BRIP 12900 T	*Cynodon transvaalensis*	Australia	MH414902	MH433646	MH433664
	BRIP 13983	*Cynodon dactylon* x *C. transvaalensis*	Australia	MH414903	MH433647	MH433665
C. micropus	CBS 127235 ET	*Paspalum notatum*	Georgia	HE792934	LT715859	–

Species	Strain no[1]	Substrate	Country	Genbank accession no.[2]		
				ITS	*gapdh*	*tef1*
C. microspora	GUCC 6272 T	*Hippeastrum striatum*	China	MF139088	MF139106	MF139115
C. miyakei	CBS 197.29 T	*Eragrostis pilosa*	Japan	KJ909770	KM083611	KM196568
C. mosaddeghii	IRAN 3131C T	*Syzygium cumini*	Iran	MG846737	MH392155	MH392152
C. muehlenbeckiae	CBS 144.63 T	*Sorghum* sp.	USA	MH858242	HG779108	KM196578
C. neergaardii	BRIP 12919 T	*O. sativa*	Ghana	KJ415550	KJ415397	KJ415443
	CBS 276.91	Unknown	Australia	LT631362	LT715848	–
C. neoindica	IMI 129790 T	*Brassica nigra*	India	MH414910	MH433649	MH433667
C. nicotiae	BRIP 11983 T	Soil	Algeria	KJ415551	KJ415396	KJ415442
C. nodosa	CPC 28800 T	*Digitaria ciliaris*	Thailand	MF490816	MF490838	MF490859
	CPC 28801	*Brachiaria reptans*	Thailand	MF490817	MF490839	MF490860
C. nodulosa	CBS 160.58	*Eleusine indica*	Unknown	JN601033	JN600975	JN601019
C. oryzae	CBS 169.53 T	*O. sativa*	Vietnam	KP400650	KP645344	KM196590
C. ovariicola	CBS 470.90 T	*Eragrostis interrupta*	Australia	JN192384	JN600976	JN601020
C. pallescens	CBS 156.35 T	Air	Indonesia	KJ922380	KM083606	KM196570
C. palmicola	MFLUCC 14-0404 T	Dead branches of *Acoelorrhaphe wrightii*	Thailand	MF621582	–	–
C. pandanicola	MFLUCC 15-0746 T	Dead leaf of *Pandanus* sp.	Thailand	MH275056	MH412748	MH412763
C. papendorfii	CBS 308.67 T	*Acacia karroo*	South Africa	KJ909774	KM083617	KM196594
C. paraverruculosa	**FMR 17656 T**	**Soil**	**Mexico**	**LR736641**	**LR736646**	**LR736649**
C. petersonii	BRIP 14642 T	*D. aegyptium*	Australia	MH414905	MH433650	MH433668
C. perotidis	CBS 350.90 T	*Perotis rara*	Australia	JN192385	KJ415394	KM230407
C. phaeospara	CGMCC3.19448 T	Roots of *S. officinarum*	China	MN215686	MN264118	MN263980
C. pisi	CBS 190.48 T	*Pisum sativum*	Canada	KY905678	KY905690	KY905697
C. plantarum	CGMCC3.19342 T	Roots of *S. officinarum*	China	MN215688	MN264120	MN263982
C. platzii	BRIP 27703b T	*Cenchrus clandestinum*	Australia	MH414906	MH433651	MH433669
C. polytrata	CGMCC3.19338 T	Roots of *S. officinarum*	China	MN215691	MN264123	MN263984
C. portulacae	BRIP 14541 T	*Portulaca oleracea*	USA	KJ415553	KJ415393	KJ415440
C. prasadii	CBS 143.64 T	*Jasminum sambac*	India	KJ922373	KM061785	KM230408
C. protuberans	CGMCC3.19360 T	Leaves of *S. officinarum*	China	MN215693	MN264125	MN263986
C. protuberata	CBS 376.65 T	*Deschampsia flexuosa*	UK	KJ922376	KM083605	KM196576
C. pseudobrachyspora	CPC 28808 T	*Eleusine indica*	Thailand	MF490819	MF490841	MF490862
C. pseudolunata	UTHSC 09-2092 T	Human nasal sinus	USA	HE861842	HF565459	–
C. pseudorobusta	UTHSC 08-3458	Human nasal sinus	USA	HE861838	HF565476	–
C. radici-foliigena	CGMCC3.19328 T	Roots of *S. officinarum*	China	MN215695	MN264127	MN263988
	LC11956	Roots of *S. officinarum*	China	MN215698	MN264130	MN263991
C. radicicola	CGMCC3.19327 T	Roots of *S. officinarum*	China	MN215699	MN264131	MN263992
	LC11953	Roots of *S. officinarum*	China	MN215700	MN264132	MN263993
C. ravenelii	BRIP 13165 T	*Sporobolus fertilis*	Australia	JN192386	JN600978	JN601024
C. reesii	BRIP 4358 T	Air	Australia	MH414907	MH433637	MH433670

Species	Strain no[1]	Substrate	Country	Genbank accession no.[2]		
				ITS	*gapdh*	*tef1*
C. richardiae	BRIP 4371 T	*Richardia brasiliensis*	Australia	KJ415555	KJ415391	KJ415438
C. robusta	CBS 624.68 T	*Dichanthium annulatum*	USA	KJ909783	KM083613	KM196577
C. rouhanii	CBS 144674 T	*Syngonium vellozianum*	Iran	KX139030	MG428694	MG428687
C. ryleyi	BRIP 12554 T	*Sporobolus creber*	Australia	KJ415556	KJ415390	KJ415437
C. saccharicola	CGMCC3.19344 T	Roots of *S. officinarum*	China	MN215701	MN264133	MN263994
C. sacchari-officinarum	CGMCC3.19331 T	Leaves of *S. officinarum*	China	MN215705	MN264137	MN263998
C. senegalensis	CBS 149.71	Unknown	Nigeria	HG779001	HG779128	–
C. shahidchamranensis	IRAN 3133C T	Crude oil contaminated soil	Iran	MH550084	MH550083	–
C. soli	CBS 222.96 T	Soil	Papua New Guinea	KY905679	KY905691	KY905698
C. sorghina	BRIP 15900 T	*Sorghum bicolor*	Australia	KJ415558	KJ415388	KJ415435
C. spicifera	CBS 198.31	*Capsicum anuum*	Cyprus	HF934916	HG779136	–
	CBS 274.52	Soil	Spain	JN192387	JN600979.	JN601023
C. sporobolicola	BRIP 23040b T	*Sporobolus australasicus*	Australia	MH414908	MH433652	MH433671
C. subpapendorfii	CBS 656.74 T	Soil	Egypt	KJ909777	KM061791	KM196585
C. suttoniae	**FMR 10992 T**	**Human leg wound**	**USA**	HE861828	HF565479	**LR736651**
	FMR 11690	**Human sphenoid sinus**	**USA**	HE861826	HF565477	**LR736650**
C. tamilnaduensis	SZMC 22226 T	Human corneal scraping	India	MN628311	MN628307	MN628303
	SZMC 26758	Human corneal scraping	India	MN628308	MN628304	MN628300
	SZMC 26759	Human corneal scraping	India	MN628309	MN628305	MN628301
C. thailandicum	MFLUCC 15-0747 T	Decaying leaves of *Pandanus* sp.	Thailand	MH275057	MH412749	MH412764
C. trifolii	CBS 173.55	*Trifolium repens*	USA	HG779023	HG779124	–
C. tripogonis	BRIP 12375 T	*Tripogon loliiformis*	Australia	JN192388	JN600980	JN601025
C. tropicalis	BRIP 14834 T	*Coffea arabica*	India	KJ415559	KJ415387	KJ415434
C. tsudae	ATCC 44764 T	*Chloris gayana*	Japan	KC424596	KC747745	KC503940
	BRIP 10967	Leaf tip blight of *C. gayana*	Australia	KC424604	KC747754	KC503949
C. tuberculata	CBS 146.63 T	*Z. mays*	India	JX256433	JX276445	JX266599
C. umbiliciformis	CGMCC3.19346 T	Roots of *S. officinarum*	China	MN215711	MN264142	MN264004
C. uncinata	CBS 221.52 T	*O. sativa*	Vietnam	HG779024	HG779134	–
C. variabilis	CPC 28815 T	*Chloris barbata*	Thailand	MF490822	MF490844	MF490865
	CPC 28816	*Imperata cylindrica*	Thailand	MF490823	MF490845	MF490866
C. verruciformis	CBS 537.75	*Lobibyx* sp. feather	New Zealand	HG779026	HG779133	–
C. verruculosa	CBS 149.63	*Elaeis guineensis*	Nigeria	HF934909	HG779110	–
	CBS 150.63	*Punica granatum* leaf	India	KP400652	KP645346	KP735695
	CPC 28792	*C. dactylon*	Thailand	MF490825	MF490847	MF490868
	CPC 28809	*E. indica*	Thailand	MF490824	MF490846	MF490867

Species	Strain no[1]	Substrate	Country	Genbank accession no.[2]		
				ITS	*gapdh*	*tef*1
C. vietnamensis	**FMR 17659 T**	**Unidentified dead leaves**	**Vietnam**	**LR736642**	**LR736644**	**LR736647**
	FMR 11956	***Sorghum* seed**	**Indonesia**	**LR736652**	**LR736643**	**LR736648**
C. warraberensis	BRIP 14817 T	*D. aegyptium*	Australia	MH414909	MH433653	MH433672
C. xishuangbannaensis	KUMCC 17-0185 T	Decaying leaves of *Pandanus amaryllifollus*	China	MH275058	MH412750	MH412765

[1] ATCC: American Type Culture Collection, Virginia, USA; BRIP: Queensland Plant Pathology Herbarium, Brisbane, Australia; CBS: Culture collection of the Westerdijk Fungal Biodiversity Institute, Utrecht, the Netherlands; CGMCC: China General Microbiological Culture Collection Center, China; CPC: Culture collection of Pedro Crous, housed at Westerdijk Fungal Biodiversity Institute; DAOM: Plant Research Institute, Department of Agriculture (Mycology), Ottawa, Canada; FMR: Facultat de Medicina, Universitat Rovira i Virgili, Reus, Spain; GUCC: Department of Plant Pathology, Agriculture College, Guizhou University, P.R. China; IMI: International Mycological Institute, Kew, UK; IRAN: Iranian Fungal Culture Collection, Iranian Research Institute of Plant Protection, Iran; KUMCC: Culture Collection of Kunming Institute of Botany, Kunming, China; LC: Personal culture collection held in the laboratory of Prof. Lei Cai, China; MFLUCC: Mae Fah Luang University Culture Collection, Chiang Ria, Thailand; MUCL: Mycothe`que de l'Universite´ Catholique de Louvain, Louvain-la-Neuve, Belgium; SZMC: Szeged Microbiological Collection at the Department of Microbiology, Faculty if Science and Informatics, University of Szeged, Hungary; UTHSC: Fungus Testing Laboratory, Department of Pathology at the University of Texas Health Science Center, San Antonio, Texas, USA. T and ET indicate ex-type and ex-epitype strain.
[2]Sequences newly generated in this study and novel species proposed are indicated in bold.

For the BI phylogenetic analysis, the best nucleotide substitution model was determined using jModelTest (Posada 2008). For the ITS region, we used Kimura 2-parameter with Invariant sites (K80+I), for *gapdh* General Time Reversible with gamma distribution (GTR+G) and for *tef*1 General Time Reversible with invariant sites (GTR+I). The parameter settings used were two simultaneous runs of 5M generations, four Markov chains, sampled every 1000 generations. The 50% majority-rule consensus tree and posterior probability values were calculated after discarding the first 25% of the samples. A posterior probability (pp) value of ≥ 0.95 was considered significant.

Sequence data generated in the present study were deposited in GenBank (Table 1) and the alignments in TreeBASE (http://treebase.org).

Phenotypic study

Macroscopic characterisation of the colonies was made on PDA, oatmeal agar (OA; oatmeal 30 g, agar 13 g, distilled water 1 litre) and potato carrot agar (PCA; potato 20 g, carrot 20 g, agar 13 g, distilled water 1 litre), after 7 days at 25 °C in darkness. Colours of the colonies in descriptions were based on Kornerup & Wanscher (1978). Cardinal temperatures for growth were obtained on PDA after 7 days in darkness.

Microscopic features were studied from the specimens mounted in Shear's solution growing on the same media (Madrid et al. 2014). At least 30 measurements were taken for the calculation of conidial and conidiophores length and width ranges, which are also reported as the mean plus or minus standard deviation in the descriptions.

Photomicrographs were taken using a Zeiss Axio-Imager M1 light microscope (Zeiss, Oberkochen, Germany) with a DeltaPix Infinity X digital camera.

Nomenclatural novelties and descriptions were deposited in MycoBank (Crous et al. 2004). Ex-type cultures and holotypes, which were dried cultures, were deposited at the Westerdijk Fungal Biodiversity Institute from Utrecht (CBS, The Netherlands).

Results

BLASTn results with *gapdh* sequences showed that the isolate FMR 17656 was ≤ 97.6%, similar to *C. verruculosa* CPC 28792; FMR 11956 and FMR 17659 showed a similarity of 93.31% and 93.6%, respectively, with *C. spicifera* CBS 198.31; and isolates FMR 10992 and FMR 11690 both exhibited a similarity of 94.7% with the ex-type strain of *C. petersonii* (BRIP 14642). Sequence similarity with this marker between FMR 11956/17659 and FMR 10992/11690 was 97%. These values suggested that the unidentified isolates represented putative new species for the genus, which were then confirmed by multi-locus sequence analysis of ITS, *gapdh* and *tef*1 barcodes. The combined analysis included 128 sequences representing 126 taxa in the genus *Curvularia* and these were rooted with *Bipolaris maydis* (CBS 136.29) and *B. saccharicola* (CBS 155.26) (Suppl. material 1: Fig. S1). The alignment comprised a total of 1928 bp (ITS 432, *gapdh* 573 bp and *tef*1 923 bp), including 546 variable sites (ITS 119 bp, *gapdh* 253 bp and *tef*1 174 bp) and 445 phylogenetically informative (ITS 83 bp, *gapdh* 233 bp and *tef*1 129 bp). The unidentified isolates were allocated to three single lineages in the same clade (74/0.99) together with sequences of the ex-type strains of *C. americana* (UTHSC 08-3414), *C. petersonii* (BRIP 14642) and *C. verruculosa* (CBS 150.63), but with enough distance to be considered distinct species. The two clinical isolates (FMR 10992 and FMR 11690) formed a fully-supported clade closely related to isolates FMR 11956 and FMR 17659, which were collected in Indonesia and Vietnam, respectively and to *C. petersonii*. The fifth isolate (FMR 17656) was related to *C. verruculosa* and *C. americana*, but formed an independent and distant branch from the previously-mentioned species.

In order to evaluate possible intra- and inter-specific variability within the species and to confirm the novelty of these fungi, we performed a multi-locus analysis, including only those sequences of the species that were more related to the unidentified *Curvularia* isolates (Fig. 1). The alignment comprised a total of 1894 bp (ITS 409, *gapdh* 562 bp and *tef*1 923 bp), with 298 variable sites (ITS 66 bp, *gapdh* 135 bp and *tef*1 97 bp) and 240 being phylogenetically informative (ITS 51 bp, *gapdh* 117 bp and *tef*1 72 bp). The phylogenetic analyses show that these isolates indeed represent three new species, which are described and illustrated in the Taxonomy section. The species can be morphologically differentiated mainly by features of their conidia (Table 2).

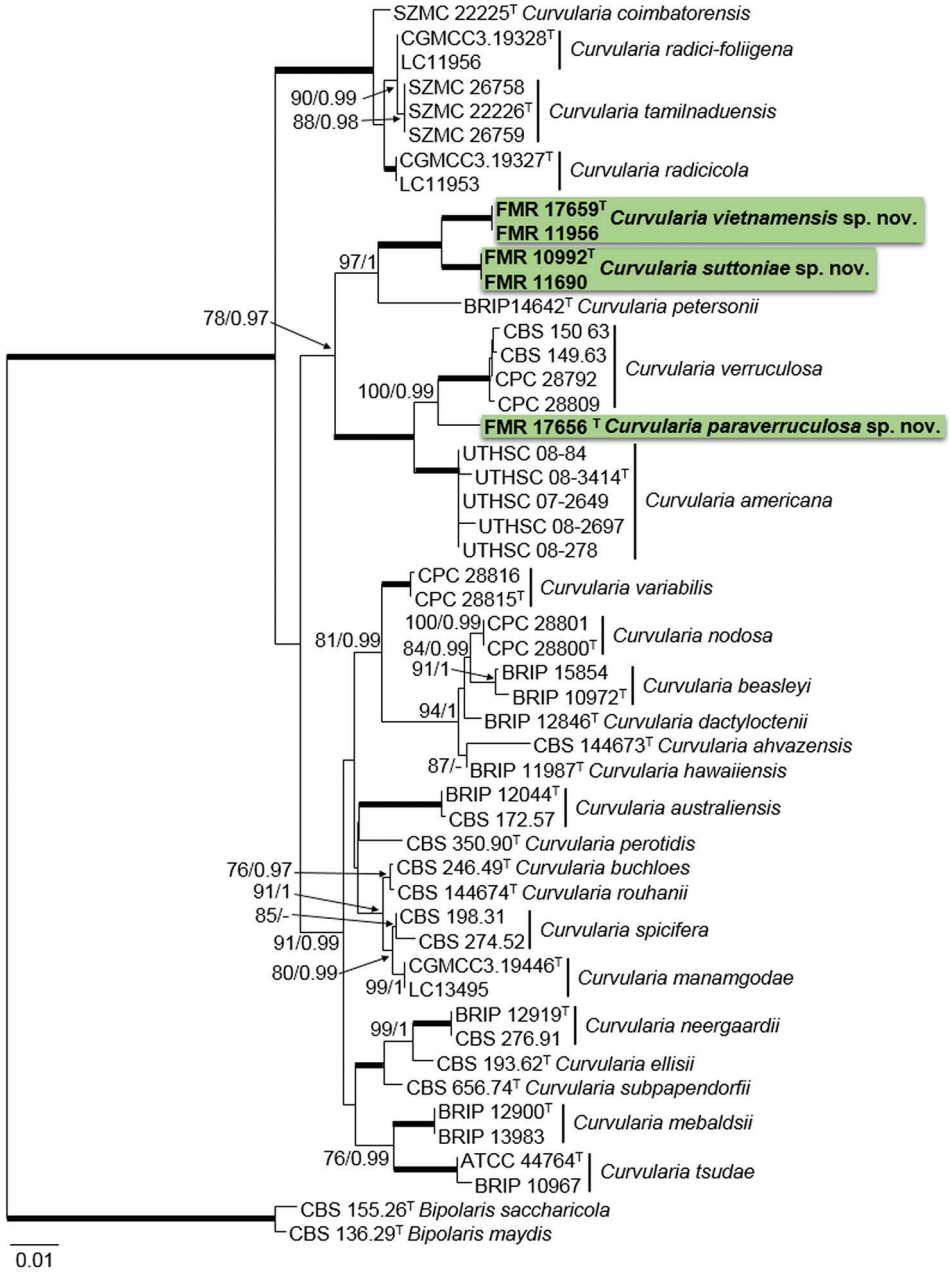

Figure 1. Phylogenetic tree of the *Curvularia* species most related to the new taxa based on Maximum Likelihood analysis obtained by RAxML, using the combined analysis of ITS, *gapdh* and *tef*1 and rooted with *Bipolaris maydis* CBS 136.29 and *Bipolaris saccharicola* CBS 155.26. Bootstrap values (bs) greater than 70% and Bayesian posterior probabilities (pp) greater than 0.95 are given at the nodes (bs/pp). Bold branches indicate bs/pp of 100/1. The novel species are highlighted in bold. Ex-type isolates are marked with a superscript T.

Table 2. Conidial features of the novel *Curvularia* species proposed here and of their closest relatives.

Species	Size (µm)	Septum no.	Ornamentation	References
C. americana	13–28 × 7–15	3–4	Smooth upper cells, verruculose basal cell	Madrid et al. (2014)
C. palmicola	23.9–34.7 × 9.3–15.7	3	Smooth	Hyde et al. (2017)
C. paraverruculosa	11–37 × 8–12	3(–4)	Verruculose to verrucose	Present study
C. petersonii	(15–)17–19(–21) × (5–)5.5–6(–7)	3	Smooth	Tan et al. (2018)
C. suttoniae	8–22 × 5–9	(2–)3	Smooth upper cells, verruculose basal cell	Present study
C. verruculosa	20–40 × 12–17	3	Rough to verruculose	Sivanesan (1987)
C. vietnamensis	15–28 × 5–12	(1–)3(–4)	Smooth	Present study

Taxonomy

Curvularia paraverruculosa **Iturrieta-González, Gené & Dania García, sp. nov.**
MycoBank No: 833024
Fig. 2

Etymology. Name refers to the phylogenetic closeness to *Curvularia verruculosa*.

Type. Mexico, Michoacán, Villa Jiménez, from soil, Sept 2016, *E. Rosas de Paz.* (holotype CBS H-24293, culture ex-type FMR 17656, CBS 146220).

Description (PDA at 25 °C). *Mycelium* composed of branched, septate, subhyaline to pale brown, thin- and smooth-walled hyphae, 2–4 µm wide. *Conidiophores* semi- to macronematous, mononematous, septate, straight or flexuous, geniculate at upper part, unbranched or slightly branched, smooth-walled, yellowish-brown to brown, 19–85(–145) × 3–6 µm (av. (±SD) 49.6 (±43.8) × 4.6 (±0.69)). *Conidiogenous cells* terminal or intercalary, polytretic, proliferating sympodially, yellowish-brown, with darkened scars, subcylindrical, 4–6 µm wide. *Conidia* 3(–4)-septate, mostly curved at the third cell from base which is usually larger than the others, sometimes apically bifurcate, verruculose to verrucose, apical and basal cells subhyaline to pale brown, middle cells brown, 11–37 × 8–12 µm (av. (±SD) 24 (±18.38) × 9.58 (±1.66)); hila slightly protuberant, thickened and darkened. Sexual morph not observed.

Culture characteristics (7 d at 25 °C). *Colonies* on PDA reaching 45 mm diam., dark green (30F8), final edge whitish, velvety, flat, margin regular and fimbriate; reverse dark green (30F8). On PCA and OA, reaching 58–60 mm diam., dark green (30F8), final edge whitish, slightly floccose, flat, margin regular and fimbriate; reverse dark green (30F8). Sporulation was abundant on the three media.

Cardinal temperature for growth. Optimum 30 °C, maximum 37 °C, minimum 15 °C.

Distribution. Mexico.

Notes. *Curvularia paraverruculosa* is allocated phylogenetically to a strongly-supported clade (100/1) with *C. verruculosa* and *C. americana* (Fig. 1). All three species commonly have 3-septate conidia, but these can be distinguished by their size and

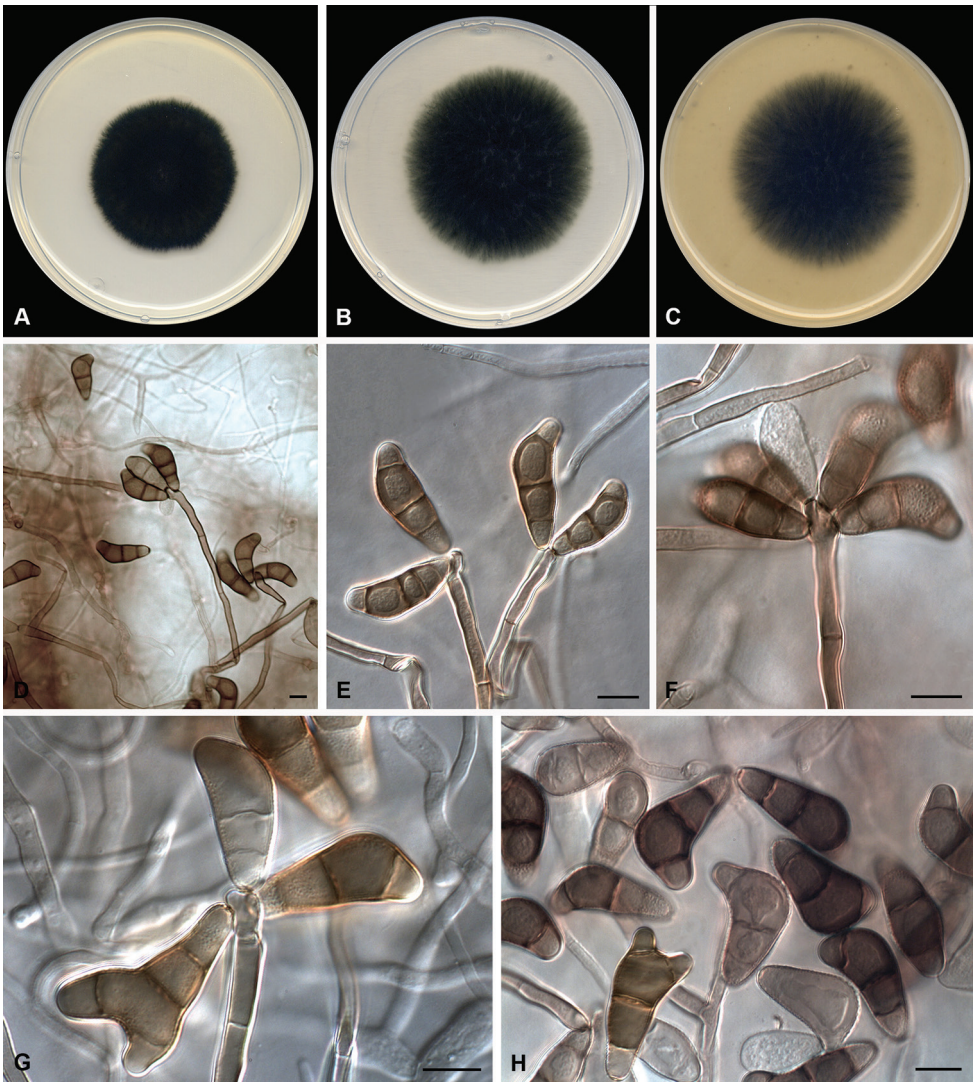

Figure 2. *Curvularia paraverruculosa* sp. nov. (ex-type FMR 17656). **A–C** Colonies on PDA, PCA and OA, respectively, at 25 °C after 7 d **D–H** conidiophores and conidia. Scale bars: 10 µm.

ornamentation. Although conidia in *C. verruculosa*, the closest phylogenetic species and *C. paraverruculosa* are entirely verruculose, they are larger in the former (20–40 × 12–17 µm) (Sivanesan 1987). Furthermore, *C. paraverruculosa* also produces apically bifurcate conidia (Fig. 2), which have not been described in *C. verruculosa*. The conidia of *C. americana* are smaller (13–28 × 7–15 µm) and smooth-walled with a slightly verruculose basal cell (Madrid et al. 2014). In addition, microconidiation, described in *C. americana*, has not been observed in *C. paraverruculosa*.

Curvularia suttoniae **Iturrieta-González, Wiederhold, Gené & Dania García, sp. nov.**
MycoBank No: 833025
Fig. 3

Etymology. Named in honour of the American mycologist Deanna A. Sutton for her contribution to the body knowledge of microfungi.

Type. USA, Texas, from a human leg wound, 2009, *D.A. Sutton* (holotype CBS H-24294, culture ex-type UTHSC 09-3575, CBS 146221, FMR 10992).

Description (PDA at 25 °C). *Mycelium* consisting of branched, septate, pale brown, smooth-walled to verruculose hyphae, 1–4 µm wide. *Conidiophores* mononematous, semi- to macronematous, erect to slightly flexuous, geniculate at the apex, unbranched or branched, smooth-walled to verruculose, pale brown, 43–103 × 3–5 µm (av. (±SD) 80 (±32.35) × 3.7 (±0.67)). *Conidiogenous cells* terminal, subterminal or intercalary, polytretic, proliferating sympodially, pale brown, darkened scars, subcylindrical to slightly swollen, 3–5 µm wide. *Conidia* (2–)3-septate, straight or curved, with the third cell often larger than the rest, apical and middle cells smooth-walled, basal cell verruculose, pale brown to brown, apical and basal cells paler than the middle cells, 8–22 × 5–9 µm (av. (±SD) 15 (±9.89) × 6.88 (±1.18)); hila protuberant, thickened and darkened. Sexual morph not observed.

Culture characteristics (7 d at 25 °C). Colonies on PDA reaching 66–68 mm diam., yellowish-grey (4B2), velvety, flat, margin slightly irregular and fimbriate; reverse black to brownish-orange (5C4); soluble pigment brown (6E6) present in cultures between 30–37 °C. On PCA, reaching 67 mm diam., olive grey (3D2), slightly floccose at the centre, flat, margin regular and whitish; reverse olive grey (3D2), whitish towards periphery. On OA, reaching 64 mm diam., olive grey (3F2), slightly floccose at the centre, flat, margin regular and whitish; reverse olive grey (3F2). Scarce sporulation on the three media.

Cardinal temperature for growth. Optimum 25–30 °C, maximum 37 °C, minimum 5 °C.

Distribution. USA.

Additional specimen examined. USA, South Carolina, from human sphenoid sinus, 2008, *D.A. Sutton* (UTHSC 08-809, FMR 11690).

Notes. *Curvularia suttoniae* is included in a well-supported clade with *C. petersonii* and *C. vietnamensis*, the latter also described here. Although the three species are clearly differentiated phylogenetically (Fig. 1), they can be distinguished only by subtle morphological features. While the conidia of *C. petersonii* and *C. vietnamensis* are entirely smooth, those of *C. suttoniae* show verruculose basal cells. Furthermore, the conidia in *C. petersonii* are narrower (5–7 µm wide) (Tan et al. 2018) and, in *C. vietnamensis*, they are larger (15–28 × 5–12 µm) than those of *C. suttoniae* (8–22 × 5–9 µm). In addition to these morphological features, *gapdh* sequences easily distinguish the two latter species.

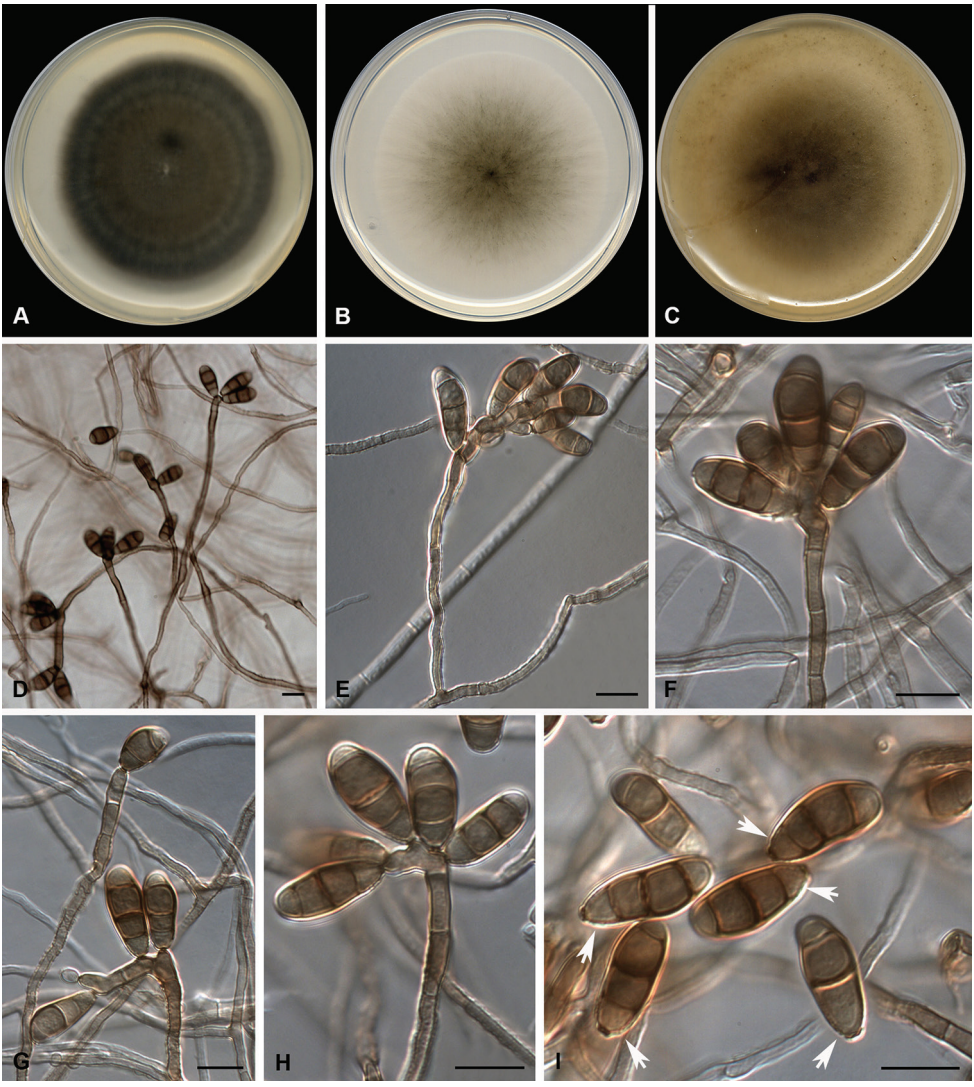

Figure 3. *Curvularia suttoniae* sp. nov. (ex-type FMR 10992). **A–C** Colonies on PDA, PCA and OA, respectively, at 25 °C after 7 d **D–I** conidiophores and conidia with verruculose basal cells (arrows). Scale bars: 10 µm.

Curvularia vietnamensis **Iturrieta-González, Gené & Dania García, sp. nov.**
MycoBank No: 833027
Fig. 4

Etymology. Name refers to the country where the species was collected.

Type. Vietnam, north-east region, on an unidentified dead leaf, Aug 2011, *J. Guarro* (holotype CBS H-24295, culture ex-type CBS 146222, FMR 17659).

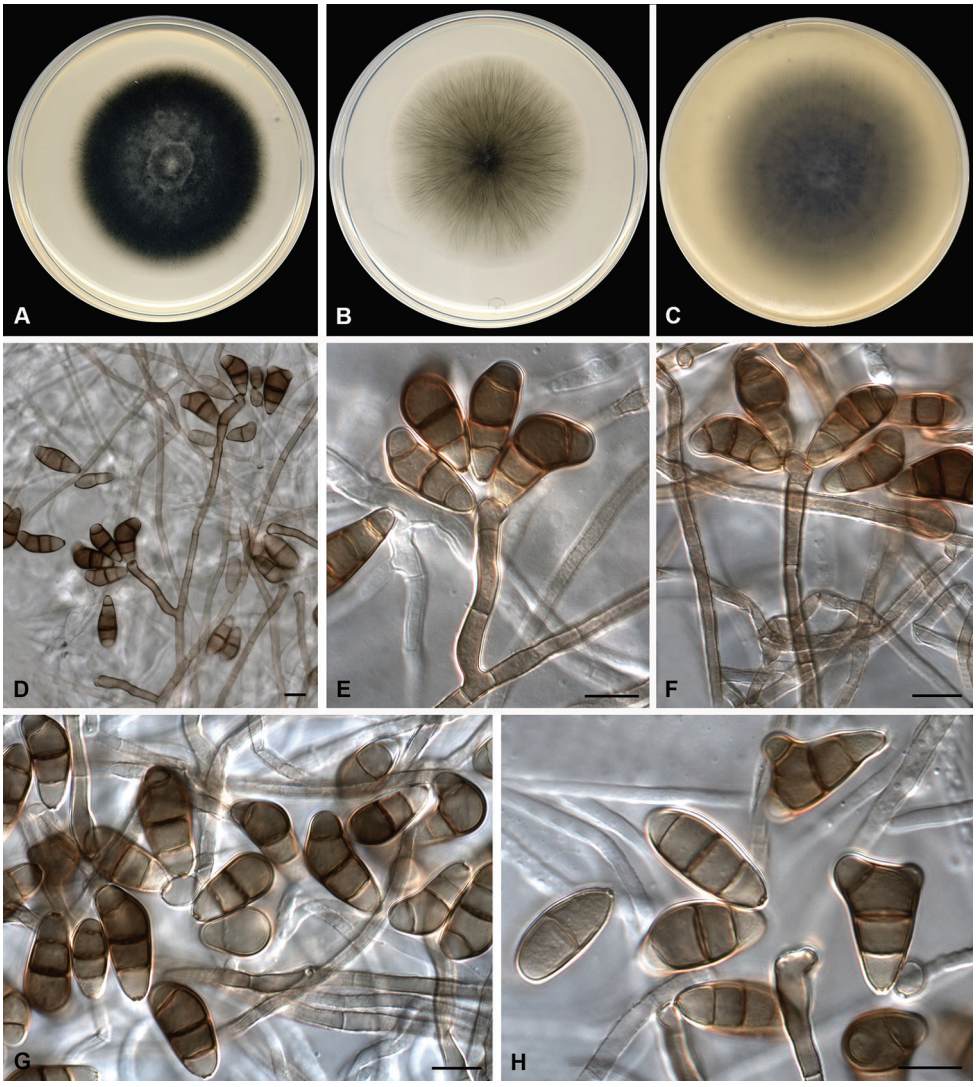

Figure 4. *Curvularia vietnamensis* sp. nov. (ex-type FMR 17659). **A–C** Colonies on PDA, PCA and OA, respectively, at 25 °C after 7 d **D–H** conidiophores and conidia. Scale bars: 10 µm.

Description (PDA at 25 °C). *Mycelium* composed of branched, septate, subhyaline to pale brown, thin and smooth-walled to verruculose hyphae, 2–4 µm wide. *Conidiophores* macronematous, mononematous, septate, straight or flexuous, sometimes slightly geniculate at upper part, unbranched to slightly branched, smooth to verruculose, pale brown to brown, 11–136(–194) × 3–6 µm (av. (±SD) 92.2 (±72.86) × 4.21 (±0.85)). *Conidiogenous cells* terminal or intercalary, mono- or polytretic, proliferating sympodially, pale brown, with darkened scars, subcylindrical to swollen, 3–7 µm wide.

Conidia (1–)3(–4)-septate, curved, with the third cell from base unequally enlarged, some apically bifurcate, smooth-walled, apical and basal cells pale brown, middle cells brown, 15–28 × 5–12 µm (av. (±SD) 21.38 (± 3.44) × 9.34 (±1.83)); hila slightly protuberant, thickened and darkened. Sexual morph not observed.

Culture characteristics (7 d at 25 °C). *Colonies* on PDA reaching 62 mm diam., greenish-grey to dark green (28C2/29F8), final edge white, umbonate, densely floccose, margin regular; reverse grey (29F1), final edge pale grey (1B2). On PCA, reaching 58 mm diam., olive grey to grey (3F2/3B1), slightly floccose at the centre, margin regular, final edge whitish; reverse olive grey to grey (3F2/3B1). On OA, reaching 74 mm diam., olive (2F3) slightly floccose at the centre, margin regular, flat; reverse olive to greenish-grey (2F3/1C2). Sporulation abundant mainly on PCA and OA.

Cardinal temperature for growth. Optimum 30 °C, maximum 37 °C, minimum 15 °C.

Distribution. Indonesia and Vietnam.

Additional specimen examined. Indonesia, from Sorghum seed, 1948, *J. van der Vecht* (CBS 188.48 = FMR 11956).

Notes. See *C. suttoniae* described above.

Discussion

As in other Pleosporalean genera, *Curvularia* is currently a well-delineated genus on the basis of molecular data (Manamgoda et al. 2015, Marin-Felix et al. 2017a). However, morphological features and analyses of the ITS barcode are insufficient to accurately identify *Curvularia* species. Thus, the multi-locus sequence analysis of different gene markers (i.e. LSU, ITS, *gapdh*, *rpb*2 and *tef*1) has been used to study the species diversity in *Curvularia* and phylogentic relationships with other similar genera (Hernández-Restrepo et al. 2018, Manamgoda et al. 2012, 2015, Madrid et al. 2014, Marin-Felix et al. 2017a, 2017b, Tan et al. 2018). Marin-Felix et al. (2017a) regarded ITS, *gapdh* and *tef*1 as the DNA barcodes for species delineation in the genus. During the last three years, numerous new *Curvularia* species have been introduced (Hyde et al. 2017, Marin-Felix et al. 2017a, 2017b, Dehdari et al. 2018, Heidari et al. 2018, Liang et al. 2018, Mehrabi-Koushki et al. 2018, Tan et al. 2018, Tibpromma et al. 2018, Kiss et al. 2019, Raza et al. 2019, Zhang et al. 2020). Novel species are found, not only on fresh material collected in various geographical regions, but also in re-evaluation of *Curvularia* isolates deposited in fungal collections and earlier identified by morphological features or ITS sequence analysis.

The five isolates, studied here, showed morphological similarity with *C. americana* or *C. lunata* (Sivanesan 1987, Madrid et al. 2014), but they also showed subtle variations that did not match with these species. Multi-locus analysis of the recommended barcodes facilitated the delineation of the novel species *C. paraverruculosa*, *C. suttoniae* and *C. vietnamensis*, which were closely related to the known species *C. americana*, *C. petersonii* and *C. verruculosa* (Fig 1).

As in the case of *C. suttoniae*, other related species, such as *C. americana* and *C. verruculosa*, have also been associated with clinical specimens previously (da Cunha et al. 2013, Madrid et al. 2014). However, the role of all these fungi in human diseases has never been proven. Contrary to that, the recently described species *C. coimbatorensis* and *C. tamilnaduensis* were shown to be causal agents of fungal keratitis in India (Kiss et al. 2019). These two latter species, as with *C. suttoniae* and *C. vietnamensis* in our case, could only be molecularly differentiated by *gapdh* and *tef*1 loci; ITS sequence similarity between *C. coimbatorensis* and *C. tamilnaduensis* was 99% (Kiss et al. 2019) and between *C. suttoniae* and *C. vietnamensis*, it was 100%. Therefore, considering clinical laboratories commonly use ITS barcode for fungal diagnosis, not only will the diversity of *Curvularia* species remain obscure in the clinical setting, but also, subsequently, the epidemiology of its species associated with human or animal diseases. Our results suggest that *gapdh* and *tef*1 loci could be good alternatives as barcodes for *Curvularia* identification, since both have a high discriminatory power amongst species. However, *gapdh* would be the recommended locus because there are more sequences available for different species in the genus.

The ITS analysis revealed that *C. palmicola*, only known for its type specimen found on dead branches of *Acoelorrhaphe wrightii* in Thailand (Hyde et al. 2017), is also closely related to the novel species described here. However, this fungus was not included in our concatenate analysis since sequences of *gapdh* and *tef*1 were not available for comparison. Nevertheless, *C. palmicola* can be distinguished morphologically from our species mainly by having conidia with constricted wall at the septum level. Furthermore, *C. palmicola* has longer conidia (23.9–34.7 µm) than *C. suttoniae* (8–22 µm) and C. *vietnamensis* (15–28 µm) and it differs from *C. paraverruculosa* by its smooth-walled conidia.

Despite the fact that DNA sequence analysis is currently mandatory for *Curvularia* identification, two species were recently characterised exclusively, based on morphological data and host association, i.e. *C. tremae* on living leaves of *Trema orientalis* (Haldar 2017) and *C martyniicola* on *Martynia annua* (Kumar and Singh 2018), both from India. *Curvularia tremae* produces up to 4-septate and larger conidia (average length 152.21 µm and 67.75 µm wide at the broadest part) than those described here. Despite the conidia being mostly 3-sepetate, as in our species, *C. martyniicola* differs by having longer conidiophores (95–200 µm) than those of *C. paraverruculosa* (19–85(–145) µm) and *C. suttoniae* (43–103 µm) and by larger conidia (25–45 × 10–15 µm) than those observed in *C. vietnamensis* (15–28 × 5–12 µm).

Acknowledgements

The authors are grateful to Sándor Kocsubé of the University of Szeged (Hungary) for sending the sequences of *C. tamilnaduensis* and *C. coimbatorensis* used in this study. The study was supported by the Spanish Ministerio de Economía y Competitividad, grant CGL2017-88094-P.

References

Baylet J, Camain R, Segretain G (1959) Identification of the agents of maduromycoses of Senegal and Mauritania. Description of a new species. Bulletin de la Societe de Pathologie Exotique et de ses Filiales 52: 448–477.

Bengyella L, Iftikhar S, Nawaz K, Fonmboh DJ, Yekwa EL, Jones RC, Njanu YM, Roy P (2019) Biotechnological application of endophytic filamentous *Bipolaris* and *Curvularia*: a review on bioeconomy impact. World Journal of Microbiology and Biotechnology 35: 69. https://doi.org/10.1007/s11274-019-2644-7

Berbee ML, Pirseyedi M, Hubbard S (1999) *Cochliobolus* phylogenetics and the origin of known, highly virulent pathogens, inferred from ITS and glyceraldehyde-3-phosphate dehydrogenase gene sequences. Mycologia 91: 964–977. https://doi.org/10.1080/00275514.1999.12061106

Boedijn KB (1933) Über einige phragmosporen Dematiazen. Bulletin du Jardin Botanique de Buitenzorg 13: 120–134.

Crous PW, Gams W, Stalpers JA, Robert V, Stegehuis G (2004) MycoBank: an online initiative to launch mycology into the 21st century. Studies in Mycology 50: 19–22.

da Cunha KC, Sutton DA, Fothergill AW, Gené J, Cano J, Madrid H, de Hoog S, Crous PW, Guarro J (2013) In vitro antifungal susceptibility and molecular identity of 99 clinical isolates of the opportunistic fungal genus *Curvularia*. Diagnostic Microbiology and Infectious Disease 76: 168–174. https://doi.org/10.1016/j.diagmicrobio.2013.02.034

Dehdari F, Mehrabi-Koushki M, Hayati J (2018) *Curvularia shahidchamranensis* sp. nov., a crude oil-tolerant fungus. Current Research in Environmental & Applied Mycology 8: 572–584. https://doi.org/10.5943/cream/8/6/2

de Hoog GS, Guarro J, Gené J, Figueras MJ (2000) Atlas of Clinical Fungi (2nd edn). Baarn, The Netherlands: Centraalbureau voor Schimmelcultures, 1126 pp.

Edgar RC (2004) MUSCLE: multiple sequence alignment with high accuracy and high throughput. Nucleic Acids Research 32: 1792–1797. https://doi.org/10.1093/nar/gkh340

Ellis MB (1971) Dematiaceous Hyphomycetes. Commonwealth Mycological Institute, United Kingdom, 608 pp.

Farris JS, Källersjö M, Kluge AG, Bult C (1994) Testing significance of incongruence. Cladistics 10: 315–319. https://doi.org/10.1111/j.1096-0031.1994.tb00181.x

Gautam AK, Kant M, Thakur Y (2013) Isolation of endophytic fungi from Cannabis sativa and study their antifungal potential. Archives of Phytopathology and Plant Protection 46: 627–635. https://doi.org/10.1080/03235408.2012.749696

Haldar D (2017) Two new cercosporoid fungi from India. International Journal of Current Research 9: 46566–46569.

Heidari K, Mehrabi-Koushki M, Farokhinejad R (2018) *Curvularia mosaddeghii* sp. nov., a novel species from the family *Pleosporaceae*. Mycosphere 9: 635–646. https://doi.org/10.5943/mycosphere/9/4/2

Hernandez-Restrepo M, Madrid H, Tan YP, Da Cunha KC, Gene J, Guarro J, Crous PW (2018) Multi-locus phylogeny and taxonomy of *Exserohilum*. Persoonia 41: 71–108. https://doi.org/10.3767/persoonia.2018.41.05

Hyde KD, Norphanphoun C, Abreu VP, Bazzicalupo A, Chethana KT, Clericuzio M, Dayarathne MC, Dissanayake AJ, Ekanayaka AH, He MQ, Hongsanan S (2017) Fungal diversity notes 603–708: taxonomic and phylogenetic notes on genera and species. Fungal Diversity 87: 1–235. https://doi.org/10.1007/s13225-017-0391-3

Kiss N, Homa M, Manikandan P, Mythili A, Krizsán K, Revathi R, Varga M, Papp T, Vágvölgyi C, Kredics L, Kocsubé S (2019) New species of the genus *Curvularia*: *C. tamilnaduensis* and *C. coimbatorensis* from fungal keratitis cases in South India. Pathogens. 9(1). pii: E9. https://doi.org/10.3390/pathogens9010009

Kornerup A, Wanscher JH (1978) Methuen handbook of colour, 3rd edition. London, Methuen, 256 pp.

Kumar S, Singh R (2018) *Curvularia martyniicola*, a new species of foliicolous hyphomycetes on *Martynia annua* from India. Studies in Fungi 3: 27–33. https://doi.org/10.5943/sif/3/1/4

Liang Y, Ran SF, Bhat J, Hyde KD, Wang Y, Zhao DG (2018) *Curvularia microspora* sp. nov. associated with leaf diseases of *Hippeastrum striatum* in China. Mycokeys 29: 49–61. https://doi.org/10.3897/mycokeys.29.21122

Madrid H, Da Cunha KC, Gené J, Dijksterhuis J, Cano J, Sutton DA, Guarro J, Crous P (2014) Novel *Curvularia* species from clinical specimens. Persoonia 33: 48–60. https://doi.org/10.3767/003158514X683538

Manamgoda DS, Cai L, McKenzie EH, Crous PW, Madrid H, Chukeatirote E, Shivas RG, Tan YP, Hyde KD (2012) A phylogenetic and taxonomic re-evaluation of the *Bipolaris* – *Cochliobolus* – *Curvularia* Complex. Fungal Diversity 56: 131–144. https://doi.org/10.1007/s13225-012-0189-2

Manamgoda DS, Rossman AY, Castlebury LA, Chukeatirote E, Hyde KD (2015) A taxonomic and phylogenetic re-appraisal of the genus *Curvularia* (*Pleosporaceae*): human and plant pathogens. Phytotaxa 212: 175–198. https://doi.org/10.11646/phytotaxa.212.3.1

Marin-Felix Y, Groenewald JZ, Cai L, Chen Q, Marincowitz S, Barnes I, Bensch K, Braun U, Camporesi E, Damm U, De Beer ZW (2017a) Genera of phytopathogenic fungi: GOPHY 1. Studies in Mycology 86: 99–216. https://doi.org/10.1016/j.simyco.2017.04.002

Marin-Felix Y, Senwanna C, Cheewangkoon R, Crous PW (2017b) New species and records of *Bipolaris* and *Curvularia* from Thailand. Mycosphere 8(9): 1556–1574. https://doi.org/10.5943/mycosphere/8/9/11

Mehrabi-Koushki M, Pooladi P, Eisvand P, Babaahmadi G (2018) *Curvularia ahvazensis* and *C. rouhanii* spp. nov. from Iran. Mycosphere 9: 1173–1186. https://doi.org/10.5943/mycosphere/9/6/7

Miller MA, Pfeiffer W, Schwartz T (2010) Creating the CIPRES Science Gateway for inference of large phylogenetic tree. Proceedings of the Gateway Computing Environments workshop (GCE), November 14, 2010. New Orleans, Louisiana, 1–8. https://doi.org/10.1109/GCE.2010.5676129

Müller FM, Werner KE, Kasai M, Francesconi A, Chanock SJ, Walsh TJ (1998) Rapid extraction of genomic DNA from medically important yeasts and filamentous fungi by high-speed cell disruption. Journal of Clinical Microbiology 36: 1625–1629. https://doi.org/10.1128/JCM.36.6.1625-1629.1998

Posada D (2008) jModelTest: Phylogenetic Model Averaging. Molecular Biology and Evolution 25: 1253–1256. https://doi.org/10.1093/molbev/msn083

Raza M, Zhang ZF, Hyde KD, Diao YZ, Cai L (2019) Culturable plant pathogenic fungi associated with sugarcane in southern China. Fungal Diversity 99: 1–104. https://doi.org/10.1007/s13225-019-00434-5

Ronquist F, Teslenko M, Van Der Mark P, Ayres DL, Darling A, Höhna S, Larget B, Liu L, Suchard MA, Huelsenbeck JP (2012) MrBayes 3.2: efficient Bayesian phylogenetic inference and model choice across a large model space. Systematic Biology 61: 539–542. https://doi.org/10.1093/sysbio/sys029

Schoch CL, Crous PW, Groenewald JZ, Boehm EW, Burgess TI, De Gruyter J, De Hoog GS, Dixon LJ, Grube M, Gueidan C, Harada Y (2009) A class-wide phylogenetic assessment of Dothideomycetes. Studies in Mycology 64: 1–15. https://doi.org/10.3114/sim.2009.64.01

Seifert K, Morgan-Jones G, Gams W, Kendrick B (2011) The genera of hyphomycetes. CBS Biodiversity Series 9. CBS-KNAW Fungal Biodiversity Centre, Utrecht, The Netherlands, 997 pp.

Sivanesan A (1987) Graminicolous species of *Bipolaris*, *Curvularia*, *Drechslera*, *Exserohilum* and their teleomorphs. Mycological Papers 158: 1–261.

Stamatakis A (2014) RAxML Version 8: A tool for phylogenetic analysis and post-analysis of large phylogenies. Bioinformatics 30(9): 1312–1313. https://doi.org/10.1093/bioinformatics/btu033

Tamura K, Stecher G, Peterson D, Filipski A, Kumar S (2013) MEGA6: Molecular evolutionary genetics analysis version 6.0. Molecular Biology and Evolution 30: 2725–2729. https://doi.org/10.1093/molbev/mst197

Tan YP, Crous PW, Shivas RG (2018) Cryptic species of *Curvularia* in the culture collection of the Queensland Plant Pathology Herbarium. MycoKeys 35: 1–25. https://doi.org/10.3897/mycokeys.35.25665

Thompson JD, Higgins DG, Gibson TJ (1994) CLUSTAL W: improving the sensitivity of progressive multiple sequence alignment through sequence weighting, position-specific gap penalties and weight matrix choice. Nucleic Acids Research 22: 4673–4680. https://doi.org/10.1093/nar/22.22.4673

Tibpromma S, Hyde KD, McKenzie EH, Bhat DJ, Phillips AJ, Wanasinghe DN, Samarakoon MC, Jayawardena RS, Dissanayake AJ, Tennakoon DS, Doilom M (2018) Fungal diversity notes 840–928: microfungi associated with *Pandanaceae*. Fungal Diversity 93: 1–160. https://doi.org/10.1007/s13225-018-0408-6

White TJ, Bruns T, Lee S, Taylor J (1990) Amplification and direct sequencing of fungal ribosomal RNA genes for phylogenetics. In: Innis MA, Gelfand DH, Sninsky JJ, et al. (Ed.) PCR protocols: a guide to methods and applications. Academic Press, New York, NY, 315–322. https://doi.org/10.1016/B978-0-12-372180-8.50042-1

Wijayawardene NN, Hyde KD, Lumbsch HT, Liu JK, Maharachchikumbura SS, Ekanayaka AH(2018) Outline of Ascomycota: 2017. Fungal Diversity 88: 167–263. https://doi.org/10.1007/s13225-018-0394-8

Zhang Q, Yang Z-F, Cheng W, Wijayawardene NN, Hyde KD, Chen Z, Wang Y (2020) Diseases of *Cymbopogon citratus* (Poaceae) in China: *Curvularia nanningensis* sp. nov. MycoKeys 63: 49–67. https://doi.org/10.3897/mycokeys.63.49264

Supplementary material 1

Figure S1. Phylogenetic tree of the genus *Curvularia* based on Maximum Likelihood analysis obtained by RAxML, using the combined analysis of ITS, *gapdh* and *tef*1 and rooted with *Bipolaris maydis* CBS 136.29 and *Bipolaris saccharicola* CBS 155.26

Authors: Isabel Iturrieta-González, Josepa Gené, Nathan Wiederhold, Dania García

Data type: phylogenetic tree

Explanation note: Bootstrap values (bs) greater than 70% and Bayesian posterior probabilities (pp) greater than 0.95 are given at the nodes (bs/pp). Bold branches indicate bs/pp of 100/1. The novel species are highlighted in bold. Ex-type and ex-epitype strain are marked with a superscript T and ET, respectively.

Link: https://doi.org/10.3897/mycokeys.68.51667.suppl1

MycoKeys 68: 23–48 (2020)
doi: 10.3897/mycokeys.68.50035
http://mycokeys.pensoft.net

RESEARCH ARTICLE

A peer-reviewed open-access journal
MycoKeys
Launched to accelerate biodiversity research

Two new species of Ophiostomatales (Sordariomycetes) associated with the bark beetle *Dryocoetes alni* from Poland

Beata Strzałka[1], Robert Jankowiak[1], Piotr Bilański[1], Nikita Patel[2], Georg Hausner[2], Riikka Linnakoski[3], Halvor Solheim[4]

1 *Department of Forest Ecosystems Protection; University of Agriculture in Krakow, Al. 29 Listopada 46, 31-425, Krakow, Poland* **2** *Department of Microbiology, Buller Building 213, University of Manitoba, Winnipeg, R3T 2N2, Canada* **3** *Natural Resources Institute Finland (Luke), Latokartanonkaari 9, 00790, Helsinki, Finland* **4** *Norwegian Institute of Bioeconomy Research, P.O. Box 115, 1431, Ås, Norway*

Corresponding author: Robert Jankowiak (rljankow@cyf-kr.edu.pl)

Academic editor: K. D. Hyde | Received 10 January 2020 | Accepted 26 April 2020 | Published 17 June 2020

Citation: Strzałka B, Jankowiak R, Bilański P, Patel N, Hausner G, Linnakoski R, Solheim H (2020) Two new species of Ophiostomatales (Sordariomycetes) associated with the bark beetle *Dryocoetes alni* from Poland. MycoKeys 68: 23–48. https://doi.org/10.3897/mycokeys.68.50035

Abstract

Bark beetles belonging to the genus *Dryocoetes* (Coleoptera, Curculionidae, Scolytinae) are known vectors of fungi, such as the pathogenic species *Grosmannia dryocoetidis* involved in alpine fir (*Abies lasiocarpa*) mortality. Associations between hardwood-infesting *Dryocoetes* species and fungi in Europe have received very little research attention. Ectosymbiotic fungi residing in *Ceratocystiopsis* and *Leptographium* (Ophiostomatales, Sordariomycetes, Ascomycota) were commonly detected in previous surveys of the *Dryocoetes alni*-associated mycobiome in Poland. The aim of this study was to accurately identify these isolates and to provide descriptions of the new species. The identification was conducted based on morphology and DNA sequence data for six loci (ITS1-5.8S, ITS2-28S, ACT, CAL, TUB2, and TEF1-α). This revealed two new species, described here as *Ceratocystiopsis synnemata* **sp. nov.** and *Leptographium alneum* **sp. nov**. The host trees for the new species included *Alnus incana* and *Populus tremula*. *Ceratocystiopsis synnemata* can be distinguished from its closely related species, *C. pallidobrunnea*, based on conidia morphology and conidiophores that aggregate in loosely arranged synnemata. *Leptographium alneum* is closely related to *Grosmannia crassivaginata* and differs from this species in having a larger ascomatal neck, and the presence of larger club-shaped cells.

Keywords

Bark beetle, *Ceratocystiopsis*, hardwoods, *Leptographium*, ophiostomatoid fungi, taxonomy, two new species

Introduction

Bark beetles in the genus *Dryocoetes* (Coleoptera: Curculionidae: Scolytinae) are mainly secondary pests infesting dead, injured, and felled or windthrown conifer- and hardwood hosts. For this reason, most members of *Dryocoetes* have no or only minor economic importance, although *Dryocoetes confusus*, the most destructive species in the genus, may cause extensive mortality of subalpine fir (*Abies lasiocarpa*) in North America (Bright 1963; Negrón and Popp 2009). The biology of hardwood-infesting *Dryocoetes* species is poorly understood in Poland. One of them is *Dryocoetes alni* (Georg), which has a wide geographical distribution, extending from France in the west to Siberia in the east, and from Fennoscandia in the north to Italy and Asia Minor in the south (Dodelin 2010). In Poland it occurs rarely, but probably it is widespread. This beetle species attacks weakened or dead trees of *Alnus* spp., *Populus* spp. and *Corylus avellana* (Gutowski and Jaroszewicz 2001; Borowski et al. 2012).

Dryocoetes beetles live in close association with fungi; most notably with members of the Ophiostomatales (Ascomycota, Sordariomycetes) that are well-recognized associates of bark- and wood-dwelling beetles (Kirisits 2004; Wingfield et al. 2017). According to Six (2012), associations among bark beetles and fungi range from mutualistic to commensal, and from facultative to obligate. Some fungi are highly specific and associated only with a single beetle species, while others can be associated with many beetle species. The majority of fungi vectored by *Dryocoetes* cause sapstain but some are responsible for serious tree diseases, such as the pathogenic species of *Leptographium*, *Grosmannia dryocoetidis* which is involved in *A. lasiocarpa* mortality (Molnar 1965). Ophiostomatales is comprised of two families, Kathistaceae and Ophiostomataceae, the latter comprising several several phylogenetic lineages that include, among others, *Ceratocystiopsis*, *Graphilbum*, *Leptographium*, *Ophiostoma*, *Raffaelea* and *Sporothrix* (Hyde et al. 2020). Members of these lineages have similar morphological and ecological characteristics. These fungi are also referred to as so-called ophiostomatoid fungi, a polyphyletic grouping characterized by the production of sticky spore masses at the apices of the flask-shaped sexual fruiting structures and their association with different arthropods (De Beer and Wingfield 2013; De Beer et al. 2013a, b, 2016; Hyde et al. 2020).

Leptographium sensu lato is a broadly defined polyphyletic group of morphologically similar species (De Beer and Wingfield 2013). To date, *Leptographium sensu lato* includes ten species complexes and some smaller lineages with uncertain taxonomic positions (De Beer and Wingfield 2013; Jankowiak et al. 2017). The genus *Leptographium* contains more than 150 described taxa, most of which are associated with phloem- and wood breeding beetles that affect a wide range of plants worldwide (Jacobs and Wingfield 2001). *Leptographium* species colonizing the roots of conifers may cause tree health problems, such as members of the *Leptographium wageneri* species complex that are responsible for black stain root disease (BSRD) on conifers in western North America (Goheen and Cobb 1978). Morphologically, species of *Leptographium sensu lato* are characterized by mononematous, darkly pigmented conidiophores terminating in penicillate branches. In addition, species belonging to the *Grosmannia olivacea* species complex also form synnematous conidiophores. Some members of *Leptographium sensu lato* produce sporothrix-like or

hyalorhinocladiella-like synanamorphs. Many *Leptographium sensu lato* also form sexual morphs characterized by globose ascomata with elongated necks (Jacobs and Wingfield 2001) and these were often included in the genus *Grosmannia* Goid. (Goidànich 1936).

Leptographium species have historically been classified into various genera including *Grosmannia*, *Ceratocystis* Ellis and Halst. (Upadhyay 1981), and *Ophiostoma* Syd. and P. Syd. (Seifert et al. 1993). Phylogenetic analyses based on the ribosomal large subunit (LSU) and beta-tubulin sequence data carried out by Zipfel et al. (2006) documented distinct differences between *Ophiostoma* and *Grosmannia*, and redefined the latter genus to include all *Leptographium* with sexual morphs. De Beer and Wingfield (2013) re-evaluated the taxonomy of *Leptographium* and *Grosmannia*, considering all available DNA sequence data for all species. The authors concluded that sequence data for additional gene regions would be necessary to fully resolve the delineation of *Leptographium* and *Grosmannia*. De Beer and Wingfield (2013) suggested that all known *Leptographium* and *Grosmannia* placed in *Leptographium sensu lato* based on phylogenetic inference, should be treated in their current genera (*Leptographium* or *Grosmannia*). However, new species, excluding those residing in the *G. penicillata* species complex, should provisionally be treated in *Leptographium*, irrespective of their sexual or asexual morphs.

In contrast to species of *Leptographium sensu lato*, members of *Ceratocystiopsis* are less widespread globally. The genus *Ceratocystiopsis* currently includes nearly 20 taxa, most of which are collected from plants infested by phloem and wood-breeding beetles. *Ceratocystiopsis* species have short-necked perithecia, elongated ascospores, and hyalorhinocladiella-like asexual morphs (Upadhyay 1981; De Beer and Wingfield 2013).

Surveys of hardwood-infesting bark beetles in Poland have recently led to the recovery of an unknown *Leptographium* species from *Dryocoetes alni* (Jankowiak et al. 2019a). In addition, several isolates resembling *Ceratocystiopsis* have also been isolated from *D. alni* in association with *Populus tremula* L. In this study, all known *Leptographium* and *Ceratocystiopsis* species as well as the newly collected isolates were compared based on morphology and DNA sequence data for six nuclear loci, with the overall aim of providing accurate identifications for these fungi.

Materials and methods

Isolates and herbarium specimens

Isolations were made from the bark beetle *D. alni* and its galleries established in *P. tremula* logs. Strains were collected in beech-alder stand in southern Poland (Paprocice: 50°48'56.10"N, 21°2'51.23"E) during March–September 2018. The isolation procedures were the same as described by Jankowiak et al. (2019a). Isolates were also collected from *Alnus incana* (L.) Moench and *P. tremula* infested by *D. alni* and from *Malus sylvestris* (L.) Mill. infested by *Scolytus mali* (Bechstein) during studies conducted by Jankowiak et al. (2019a).

All fungal isolates used in this study are listed in Table 1. The isolates are maintained in the culture collection of the Department of Forest Pathology, Mycology

Table 1. Fungal isolates used in the present study.

Species[1]	Isolate no[2]			Herbarium no[3]	Host	Insect vector	Origin	GenBank accession no[4]					
	CMW	CBS	KFL and NRIF	TUR				ITS1-5.8S-ITS2-28S	ITS2-28S	TUB2	TEF1-α	ACT	CAL
Taxon 1													
***Ceratocystiopsis synnemata* sp. nov.**			16216DA	http://mus.utu.fi/TFU.207991	*Alnus incana*	*Dryocoetes alni*	Resko	**MN900984**		**MN901005**	**MN901014**	not obtained	not obtained
			13418DA	http://mus.utu.fi/TFU.207992	*Populus tremula*	*Dryocoetes alni*	Paprocice	**MN900985**		**MN901006**	**MN901015**	not obtained	not obtained
			149a18DA	http://mus.utu.fi/TFU.207993	*Populus tremula*	*Dryocoetes alni*	Paprocice	**MN900986**		**MN901007**	**MN901016**	not obtained	not obtained
			149b18DA	http://mus.utu.fi/TFU.207994	*Populus tremula*	*Dryocoetes alni*	Paprocice	**MN900987**		**MN901008**	**MN901017**	not obtained	not obtained
			16918DA[H]	http://mus.utu.fi/TFU.207995	*Populus tremula*	*Dryocoetes alni*	Paprocice	**MN900988**		**MN901009**	**MN901018**	not obtained	not obtained
			17718DA	http://mus.utu.fi/TFU.207996	*Populus tremula*	*Dryocoetes alni*	Paprocice	**MN900989**		**MN901010**	**MN901019**	not obtained	not obtained
Taxon 2													
***Leptographium alneum* sp. nov.**	52067	144905	13116RJDA	http://mus.utu.fi/TFU.207559	*Alnus incana*	*Dryocoetes alni*	Resko	**MN900990**	MH283185	MH283218	MH283406	**MN901029**	**MN901041**
	52072	144904	16016bRJDA	http://mus.utu.fi/TFU.207997	*Alnus incana*	*Dryocoetes alni*	Resko	**MN900991**		MH283219	MH283407	**MN901030**	**MN901042**
		144903	16216bRJDA	http://mus.utu.fi/TFU.207998	*Alnus incana*	*Dryocoetes alni*	Resko	**MN900992**	MH283186	MH283220	MH283408	**MN901031**	**MN901043**
	52070		7617RJDA		*Populus tremula*	*Dryocoetes alni*	Paprocice	**MN900993**		MH283221	**MN901020**	**MN901032**	**MN901044**
	52075	144902	7717RJDA	http://mus.utu.fi/TFU.207558	*Populus tremula*	*Dryocoetes alni*	Paprocice	**MN900994**		MH283222	**MN901021**	**MN901033**	**MN901045**
	52069		8417RJDA		*Populus tremula*	*Dryocoetes alnil*	Paprocice	**MN900995**		MH283223	**MN901022**	**MN901034**	**MN901046**
			8617RJDA		*Populus tremula*	*Dryocoetes alni*	Paprocice	**MN900996**		MH283224	**MN901023**	**MN901035**	**MN901047**
	52076[H]	144901[H]	8917RJDA[H]	http://mus.utu.fi/TFU.207557	*Populus tremula*	*Dryocoetes alni*	Paprocice	**MN900997**		MH283225	**MN901024**	**MN901036**	**MN901048**
			9117RJDA		*Populus tremula*	*Dryocoetes alni*	Paprocice	**MN900998**		MH283226	**MN901025**	**MN901037**	**MN901049**
			88616RJSM		*Malus sylvestris.*	*Scolytus mali*	Rozpucie	**MN900999**	MH283187	MH283227	MH283409	**MN901038**	**MN901050**
	52071	144900	88716aRJSM	http://mus.utu.fi/TFU.207556	*Malus sylvestris*	*Scolytus mali*	Rozpucie	**MN901000**	MH283188	MH283228	MH283410	**MN901039**	**MN901051**

Species[1]	Isolate no[2]			Herbarium no[3]	Host	Insect vector	Origin	GenBank accession no[4]					
	CMW	CBS	KFL and NRIF	TUR				ITS1-5.8S-ITS2-28S	ITS2-28S	TUB2	TEF1-α	ACT	CAL
Leptographium piriforme	52066		297NBRZ16AO		*Betula pendula*	Wound	Żohatyn	**MN901001**	MH740931	MH740984	MH741134	not obtained	not obtained
			10618DA		*Alnus incana*	*Dryocoetes alni*	Paprocice	**MN901002**		**MN901011**	**MN901026**	not obtained	not obtained
Grosmannia crassivaginata	134	119144			unknown	unknown	unknown	**MN901003**		**MN901012**	**MN901027**	**MN901040**	not obtained
Ceratocystiopsis pallidobrunnea			WIN(M) 51		*Populus tremuloides*	unknown	Duck Mountain[5]	**MN901004**		**MN901013**	**MN901028**	not obtained	not obtained

[1]Boldtype = new species in the present study.

[2]CMW Culture Collection of the Forestry and Agricultural Biotechnology Institute (FABI), University of Pretoria, Pretoria, South Africa; CBS Westerdijk Fungal Biodiversity Institute, Utrecht, The Netherlands; KFL Culture collection of the Department of Forest Pathology, Mycology and Tree Physiology; University of Agriculture in Krakow, Poland; NRIF The Natural Resources Institute Finland (Luke), Helsinki, Finland; WIN the University of Manitoba (Winnipeg); Canada. H = ex-holotype

[3]TFU the TUR Herbarium of the University of Turku, Finland

[4]ITS1-5.8S-ITS2-ITS2-28S = the internal transcribed spacer 1 and 2 regions of the nuclear ribosomal DNA gene, 5.8S rRNA gene; and the 28S large subunit of the nrDNA gene; ACT= Actin; TUB2 = Beta-tubulin; CAL= Calmodulin; TEF1-α = Translation elongation factor 1-alpha; **Bold** type = GenBank accession numbers of sequences obtained in the present study.

[5]Duck Mountain Provincial Forest, Manitoba, Canada.

and Tree Physiology; University of Agriculture in Krakow, Poland, and in the culture collection of the Natural Resources Institute Finland (Luke), Finland. The ex-type isolates of the new species described in this study were deposited in the Westerdijk Fungal Biodiversity Institute (**CBS**), Utrecht, the Netherlands, and in the culture collection (**CMW**) of the Forestry and Agricultural Biotechnology Institute (**FABI**), University of Pretoria, South Africa. Herbarium specimens have been deposited in the Herbarium of the University of Turku (**TUR**), Finland. Three reference strains were obtained from collections. These included a living culture of *Ceratocystiopsis pallidobrunnea* (WIN(M)51) from the culture collection of University of Manitoba (Canada), and cultures of *Grosmannia crassivaginata* (CBS 119444) and *Leptographium piriforme* (CMW 52066) (Table 1). Taxonomic descriptions and nomenclatural data have been registered in MycoBank (www.MycoBank.org) (Robert et al. 2013).

DNA extraction, PCR and sequencing

DNA extractions were done as described by Jankowiak et al. (2018). For sequencing and phylogenetic analyses, six loci were amplified: internal transcribed spacer 1 and 2 (ITS1-5.8S-ITS2), internal transcribed spacer 2 and large subunit (ITS2-28S), actin (ACT), beta-tubulin (TUB2), calmodulin (CAL) and the translation elongation factor 1-alpha (TEF1-α) using the primers listed in Table 2.

DNA fragments were amplified in a 25 µL reaction mixture containing 0.25 µL of Phusion High-Fidelity DNA polymerase (Finnzymes, Espoo, Finland), 5 µL Phusion HF buffer (5x), 0.5 µL of dNTPs (10 mM), 0.75 µL DMSO (100%) and 0.5 µL of each primer (25 µM). Amplification reactions were performed in the LabCycler Gradient thermocycler (Sensoquest Biomedical Electronics GmbH, Germany). Amplification of the various loci was performed under the following conditions: a denaturation step at 98 °C for 30 s was followed by 35 cycles of 5 s at 98 °C, 10 s at 52–64 °C (depending on the primer melting temperature and fungal species) and 30 s at 72 °C, and a final elongation step at 72 °C for 8 min. The PCR products were visualized under UV light on a 2% agarose gel stained with Midori Green DNA Stain (Nippon Genetic Europe).

Amplified products were sequenced with the BigDye Terminator v 3.1 Cycle Sequencing Kit (Applied Biosystems, Foster City, CA, USA) and the products were re-

Table 2. Information on PCR primers used in this study.

Locus	Primers	Fungi
ITS1-5.8S	ITS1-F (Gardes and Bruns 1993), ITS4 (White et al. 1990)	*Ceratocystiopsis*, *Leptographium*
28S	LR0R, LR5 (Vilgalys and Hester 1990)	*Ceratocystiopsis*
ITS2-28S	ITS3 (White et al. 1990), LR3 (Vilgalys and Hester 1990)	*Leptographium*
TUB2	Bt2a, Bt2b (Glass and Donaldson 1995)	*Ceratocystiopsis*
	T10 (O'Donnell and Cigelnik 1997), Bt2b (Glass and Donaldson 1995)	*Leptographium*
ACT	Lepact-F, Lepact-R (Lim et al. 2004)	*Leptographium*
CAL	CL3F, CL3R (De Beer et al. 2016)	*Leptographium*
TEF1-α	F-728F (Carbone and Kohn 1999), EF2 (O'Donnell et al. 1998)	*Ceratocystiopsis*
	EF1F, EF2R (Jacobs et al. 2004)	*Leptographium*

Table 3. Morphological comparisons of closely related species to *Ceratocystiopsis synnemata* sp. nov.

Species	*Ceratocystiopsis pallidobrunnea* (Olchowecki and Reid 1974)	*Ceratocystiopsis pallidobrunnea* (Upadhyay 1981)	*Ceratocystiopsis synnemata* sp. nov.
Sexual state	Present	Present	unknown
Ascomata base	40–60	40–75	
Ascomatal neck length (µm)	15–60	21.2–66	
Ascospore shape	allantoid or falcate with truncate ends in side view, cylindrical or fusiform with truncate ends in face view	falcate with truncate or obtuse ends in side view, fusiform or ellipsoid-fusiform in face view	
Ascospore size (in face view, µm)	(-3.5)4.5–7.5 × 0.7–1 excluding sheath	14–17.5(-22.5) × 1–1.5(-1.8) including sheath	
Conidial shape	allantoid or oblong with obtuse ends	cylindrical, allantoid	oblong-elliptical
Conidial size (µm)	2.5–5 × 0.7–1.2	2–7 × 0.7–2.5	2.4–4 × 1–1.4
Branched conidiophores	present, to 50 µm long	present	present, 76.9 µm long
Conidiophores aggregate into synnemata	absent	absent	present
Optimal growth temp on MEA	–	–	
Growth rate at optimum	–	–	
Host	*Populus tremuloides*	*Populus tremuloides*	*Alnus incana*, *Populus tremula*
Arthropods	unknown	unknown	*Dryocoetes alni*,
Distribution	Manitoba, Canada	Manitoba, Canada	Poland

solved with an ABI PRISM 3100 Genetic Analyzer (Applied Biosystems), at the DNA Research Centre (Poznań, Poland) using the same primers that were used for the PCR. The sequences (Table 1) were compared with sequences retrieved from GenBank using the BLASTn algorithm (Altschul et al. 1990). Newly obtained sequences were deposited in NCBI GenBank and added to previous alignments for the ITS1-5.8S-ITS2-28S and ITS2-28S regions (Jankowiak et al. 2019a). Alignments were adjusted to accommodate the new sequences and the data sets were used to obtain consensus sequences and the two data sets were concatenated.

Phylogenetic analyses

BLAST searches (Altschul et al. 1990) using the BLASTn algorithm were performed to retrieve similar sequences from GenBank (http://www.ncbi.nlm.nih.gov) and accession numbers for these sequences are presented in the corresponding phylogenetic trees (Figs 1–4). Datasets were curated with the Molecular Evolutionary Genetic Analysis (MEGA) v6.06 program (Tamura et al. 2013).

The phylogenetic position of Taxon 1 was determined from their concatenated ITS1-5.8S-ITS2-28S sequences within a dataset that covered all ITS1-5.8S and ITS2-28S sequences of *Ceratocystiopsis* available in GenBank, as well as sequences of *C. pallidobrunnea* obtained in this study (Fig. 1). The outgroup taxa for the ITS1-5.8S-ITS2-28S dataset analysis were *Ophiostoma karelicum* and *O. quercus*. The TUB2 dataset included all available sequences for reference species in *Ceratocystiopsis* that could be retrieved from GenBank and six of our isolates (Fig. 2) in order to identify isolates to the species level.

In the case of Taxon 2, the ITS2–28S dataset included most of the available sequences for reference species in *Leptographium sensu lato* that could be retrieved from GenBank (Fig. 3) to show the placement of our isolates within this group. The outgroup taxa for the ITS2–28S dataset analysis was *O. karelicum* and *O. novo-ulmi*. The concatenated constructs of sequences for multiple loci (ITS1-5.8S-ITS2–28S + TUB2 + TEF1-α + ACT) were also used for 11 of our isolates, *Grosmannia crassivaginata*, and *L. piriforme* (Fig. 4). Before individual data sets for the ITS2-28S, ACT, TUB2, and the TEF1-α gene regions were used for 11 of our isolates, *Grosmannia crassivaginata*, and *L. piriforme*. The outgroup taxa for the ITS1-5.8S-ITS2–28S + TUB2 + TEF1-α + ACT datasets analysis were *Leptographium flavum* and *L. vulnerum.* Datasets concerning the protein coding sequences were concatenated. Sequence alignments were performed using the online version of MAFFT v7 (Katoh and Standley 2013). The ITS1-5.8S, ITS2-28S, ACT, TUB2, and TEF1-α datasets were aligned using the E-INS-i strategy with a 200PAM/k=2 scoring matrix, a gap opening penalty of 1.53 and an offset value of 0.00. The alignments were checked manually with BioEdit v.2.7.5 (Hall 1999). The resulting alignments and trees were deposited into TreeBASE (http://purl.org/phylo/treebase/phylows/study/TB2:S25615). Aligned data sets of the protein-coding genes were compared to gene maps constructed by Yin et al. (2015) to determine the presence or absence of introns and to confirm that introns and exons were appropriately aligned (Suppl. material 1: Tables S1–S3). Single nucleotide polymorphisms (SNPs) for different gene regions between the new taxa and the phylogenetically closest related species were also identified by comparative sequence analysis.

Phylogenetic trees were inferred for each of the datasets using three different methods: Maximum likelihood (ML), Maximum Parsimony (MP) and Bayesian inference (BI). For ML and BI analyses, the best-fit substitution models for each aligned dataset were established using the corrected Akaike Information Criterion (AICc) in jModelTest 2.1.10 (Guindon and Gascuel 2003; Darriba et al. 2012). ML analyses were carried out with PhyML 3.0 (Guindon et al. 2010), utilizing the Montpelier online server (http://www.atgc-montpellier.fr/phyml/). The ML analysis included bootstrap analysis (1000 bootstrap pseudoreplicates) in order to assess node support values and the overall reliability of the tree topology.

The best evolutionary substitution model for ITS2-28S (*Leptographium*) and the ITS1-5.8S-ITS2–28S (*Ceratocystiopsis*) was GTR+I+G. The best evolutionary substitution model for TUB2 (*Ceratocystiopsis*) and for the combined ITS1-5.8S-ITS2–28S, ACT, TUB2, and TEF1-α, datasets for *Leptographium* was GTR+G.

MP analyses were performed with PAUP* 4.0b10 (Swofford 2003). Gaps were treated as fifth state. Bootstrap analysis (1000 bootstrap replicates) was conducted to determine the levels of confidence for the nodes within the inferred tree topologies. Tree bisection and reconnection (TBR) was selected as the branch swapping option. The tree length (TL), Consistency Index (CI), Retention Index (RI), Homoplasy Index (HI) and Rescaled Consistency Index (RC) were recorded for each analysed dataset after the trees were generated.

BI analyses using Markov Chain Monte Carlo (MCMC) methods were carried out with MrBayes v3.1.2 (Ronquist and Huelsenbeck 2003). The four MCMC chains were run for 10 million generations applying the best-fit model for each data set. Trees were sampled every 100 generations, resulting in 100,000 trees. The Tracer v1.4.1 program (Rambaut and Drummond 2007) was utilized to determine the burn-in value for each dataset. The remaining trees were utilized to generate a 50% majority rule consensus tree, which allowed for calculating posterior probability values for the nodes.

Morphology, growth studies and mating tests

Morphological characters were examined for selected isolates and for the herbarium specimens chosen to represent the type specimens for the newly proposed species. Cultures were grown on 2% MEA agar [MEA: 20 g Bacto malt extract (Becton Dickinson and Company, Franklin Lakes, USA), 20 g agar (Bacto agar powder from Becton Dickinson and Company, Franklin Lakes, USA), 1 l deionized water] with or without host tree twigs to induce potential ascocarp formation. Autoclaved twigs with bark were positioned in the centre of the MEA agar plates. Fungal cultures were derived from single spores, and crossings were made following the technique described by Grobbelaar et al. (2010). To encourage the production of ascomata for species descriptions, single conidial isolates were crossed in all possible combinations. Cultures were incubated at 25 °C and monitored regularly for the appearance of fruiting structures.

Morphological features were examined by mounting materials in 80% lactic acid on glass slides, and observing various fruiting structures using a Nikon Eclipse 50*i* microscope (Nikon Corporation, Tokyo, Japan) with an Invenio 5S digital camera (DeltaPix, Maalov, Denmark) to capture photographic images. Microscopy was done as previously described by Kamgan Nkuekam et al. (2011). Color designations were based on the charts of Kornerup and Wanscher (1978).

For each taxonomically relevant structure fifty measurements were made, whenever possible, with the Coolview 1.6.0 software (Precoptic, Warsaw, Poland). Averages, ranges and standard deviations were calculated for the measurements, and these are presented in the format '(min–)(mean-SD)–(mean+SD)(–max)'.

Growth characteristics for the two newly proposed species and *Grosmannia crassivaginata* (isolate CBS 119144) were determined by analyzing the radial growth for five isolates in pure culture that represent each of the studied species (Table 1). Agar disks (5 mm diam.) were cut from actively growing margins of fungal colonies for each of the tested isolates and these disks were placed in the center of plates containing 2% MEA. Four replicate plates for each of the proposed new species and *G. crassivaginata* were incubated at 5, 10, 15, 20, 25, 30 and 35 °C. The radial growth (two measurements per plate) were determined 7 d (Taxon 1) and 4 d (Taxon 2, and *G. crassivaginata*) after inoculation, and growth rates were calculated as mm/d.

Results

Morphological characteristics

The two new taxa showed differences with regards to growth rates in culture and color differences ranging from white (Taxon 1) to brownish gray (Taxon 2). Taxon 1 produced a hyalorhinocladiella-like asexual morph with simple and highly branched conidiophores, which often aggregate in loosely synnemata that were arranged either singly or in groups topped with white mucilaginous spore drops. Taxon 2 produced short mononematous conidiophores with allantoid conidia, and stalked club-shaped cells. A sexual morph could be induced in all isolates of Taxon 2; the most distinct features observed in both the herbarium specimens and the studied isolates were the short ascomatal necks and falcate ascospores with gelatinous sheaths. Sexual morph was not observed for Taxon 1 in any of the crosses done between different isolates. Morphological differences among these new taxa and the most closely related species are listed in Tables 3, 4, and discussed in the Notes under the new species descriptions in the Taxonomy section.

The optimal growth temperatures were 25 °C for Taxon 1 and 30 °C for Taxon 2. No growth was observed at 5 °C for Taxon 2.

Phylogenetic analyses

Alignments for the *Ceratocystiopsis* data set of ITS1-5.8S-ITS2-28S contained 1278 characters and for the TUB2 512 characters (including gaps). Alignments for the ITS2-28S and the concatenated combined *Leptographium* data set of ITS1-5.8S-ITS2-28S+ACT+TUB2, TEF1-α, contained 637, and 13276 characters (including gaps), respectively. The exon/intron arrangement of the TUB2 *Ceratocystiopsis* species complex data included exons 3, 4, 5 and 6, interrupted with introns 3, 4, and 5. The exon/intron arrangement of the TUB2 *Leptographium* data included exons 3, 4, and 5/6, interrupted with introns 3 and 4, but lacking intron 5. The aligned TEF1-α gene region consisted of introns 3, 5 and exons 4/5, 6, while lacking intron 4. The alignment of the ACT dataset contained exons 5 and 6, interrupted with intron 5.

The ITS1-5.8S-ITS2-28S (Fig. 1) and ITS2-28S (Fig. 3) trees show the placement of the Polish isolates (referred to as Taxon 1 and Taxon 2) within the Ophiostomatales. Taxon 1 resided among sequences representing species that are members of *Ceratocystiopsis* (Fig. 1), while Taxon 2 grouped with other species in the *Leptographium sensu lato* (Fig. 3). Taxon 1 was closely related with *C. pallidobrunnea* (Fig. 1), while Taxon 2 formed a separate lineage within *Leptographium sensu lato* that included *Leptographium piriforme* and *Grosmannia crassivaginata* (Fig. 3). Taxon 1 had unique ITS1-5.8S-ITS2-28S sequences compared with other *Ceratocystiopsis* species (Fig. 1), while isolates of Taxon 2 had ITS2-28S sequences that were almost identical with sequences noted in *G. crassivaginata* (Fig. 3).

Table 4. Morphological comparisons of closely related species to *Leptographium alneum* sp. nov.

Species*	*G. crassivaginata* (Griffin 1968), holotype DAOM 110144)	*G. crassivaginata* (Jacobs and Wingfield 2001), holotype DAOM 110144)	*G. crassivaginata* (Upadhyay 1981), RWD 858, WIN(M) 69-12	*G. crassivaginata* (this study, CBS119144)	*L. piriforme* (Greif et al. 2006)	*L. alneum* sp. nov.
Sexual state	Present	Present	Present	Absent	Unknown	Present
Ascomata base	40–90	40–90	35–110			59–108
Ascomatal neck length (µm)	40–60	40–60	37–70 including ostiolar hyphae		–	58–114 excluding ostiolar hyphae
Ostiolar hyphae length (µm)	10–25, septate	–	septate			14.6–22.7, non-septate
Ascospore shape	Falcate in side view, fusiform in face view	Fusiform,	Falcate in side view, fusiform in face view		–	Falcate in side view, fusiform in face view
Ascospore size (in face view, µm)	5–7 × 1.excluding sheath, 10–11.5×5–6.5 including sheath	10–11 × 5–6 including sheath	9–12 × 5–7 including sheath		–	6.9–10.3 × 1.8–3.3 excluding sheath, 8.9–12.2 × 4.5–7 including sheath
Conidiophores length (µm)	to 50	25–105 (-120)	to 85	(28.6–)33.2–63.2(–109.1)		(48.1–)59.3–84.2(–102.9)
Stipe length (µm)		8–60(-85)		(5.6–)3.7–26(–58.6)	7–45.6	(7.6–)14.3–39.2(–48.5)
Conidiogenous apparatus length (µm)		15–55 (-60)		(22.3–)27–41.3(–54.7)		(20–)26.5–38.6(–48.7)
Conidial shape	Cylindrical to allantoid	Oblong to obovoid	Clavate, curved	Oblong to allantoids, often clavate	Curved	Cylindrical to allantoid
Conidial size (µm)	3–6 × 1–1.5	4–10×1–2	2.5–12 × 1–2	(2.4–)3.2–5(–8.1) × (0.7–)0.9–1.3(–1.7)	2.4–4.6 × 1.0–1.4	(3.2–)3.7–5.9(–9.7) × (0.8–)1–1.8(–2.8)
Club-shaped cells size (µm)	12–20 × 8–12 on short hyphal branches	–	9–23 × 7–14 on immersed hyphal branches	(6.5–)8.5–14.1(–18.5) × (5–)6.5–10.8(–13.5), born terminally or laterally on a non-septate or 2–3 septate stalk, 4.8–41.5 long, 2.5–7.3 wide below primary septa	14.4–31.2 × 7.2–16., borne on a one- to four celled stalk, 7.2–45.6 × 4.8–7.2	(11.5–)14.8–25.6(–33.3) × (7.7–)11.3–15.1(–18.2), born terminally on a multicelled stalk, 7.2–124.2 long , 4.4–9.7 wide below primary septa
Colony color and optimal growth temp on MEA	Brown, -	Olivaceous, 30,	Pale to dark brown or chaetura brown, -	Olive brown, 30	Light brown, 35	Brownish grey, 30
Radial growth rate (mm/d) at optimum	–	–		6.9 mm	–	8.8 mm
Host	*Picea mariana*, *Populus grandidentata*, *P. tremuloides*	*Picea mariana*, *P. glauca*, *Pinus resinosa*, *P. sylvestris*, *P. strobus*, *Fraxinus nigra*, *Populus grandidentata*, *P. tremuloides*	*Populus tremuloides*	unknown	Unknown (Greif et al. 2006); *Pinus sylvestris* (Jankowiak and Kolařík 2010); *Betula verrucosa* (Jankowiak et al. 2019c); *Populus tremula* (this study)	*Populus tremula*, *Malus sylvestris* (Jankowiak et al. 2019a, this study)
Arthropods	Unknown		–	Unknown	Coleoptera, Diptera,Araneae, Acari,Hemiptera, Lepidoptera, Collembola, Psocoptera,Trichoptera, and Hymenoptera: Formicidae, *D. alni* (this study)	*Dryocoetes alni*, *Scolytus mali*
Distribution	Ontario, Canada	Ontario, Canada,USA	Fort Collins, Colarado (USA), Monitoba (Canada)	Unknown	Alberta, Canada, Poland	Poland

*format 'min-max' or (min–)(mean-SD)–(mean+SD)(–max) for some morphological structures of *G. crassivaginata* (CBS119144) and *L. alneum* sp. nov.

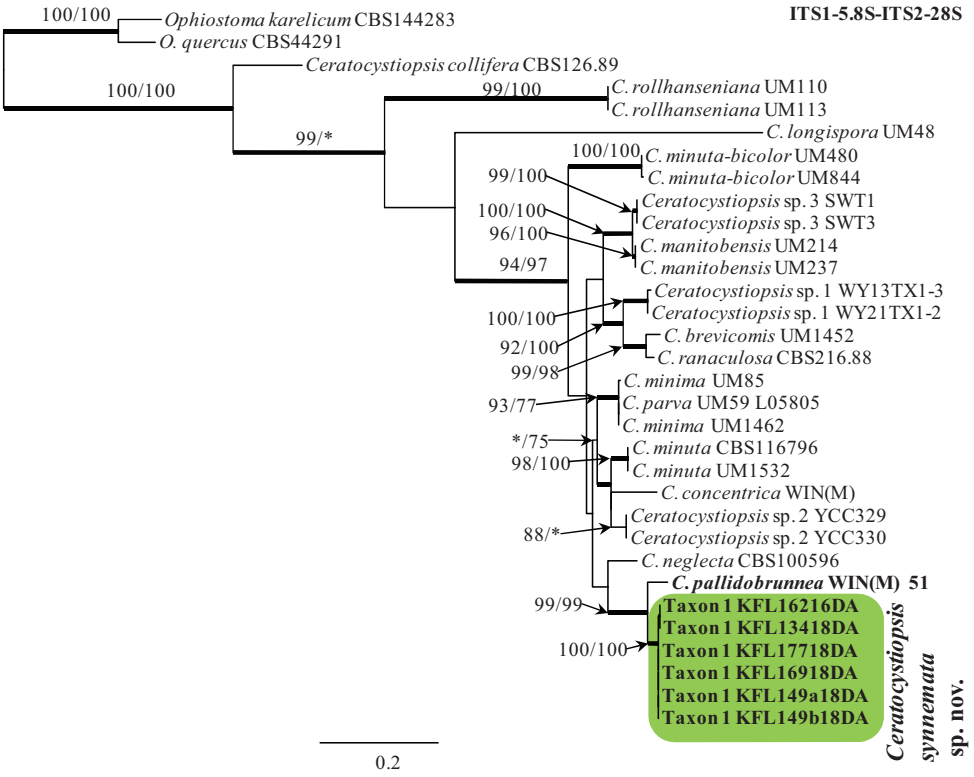

Figure 1. Phylogram obtained from Maximum Likelihood (ML) analyses of the ITS1-5.8S-ITS2-28S data for the *Ceratocystiopsis* spp. Sequences obtained during this study are presented in bold type. The Bootstrap values ≥ 75% for ML and Maximum Parsimony (MP) analyses are presented at nodes as follows: ML/MP. Bold branches indicate posterior probabilities values ≥ 0.95 obtained from Bayesian Inference (BI) analyses. * Bootstrap values <75%. The tree is drawn to scale (see bar) with branch length measured in the number of substitutions per site. *Ophiostoma karelicum* and *Ophiostoma quercus* represent the outgroup.

The MP, ML and BI analyses of the individual dataset (ITS2-28S, ACT, TUB2, TEF1-α) provided trees with similar topologies (data not shown). In the TUB2 tree (Fig. 2), Taxon 1 formed a well-supported lineage that clearly separated this newly proposed species from all the other known species in *Ceratocystiopsis* and the most closely related species *C. pallidobrunnea* (Fig. 2). The combined analyses of the ITS1-5.8S-ITS2-28S+TUB2+ACT+TEF1-α data grouped isolates of Taxon 2 in a lineage together with *L. piriforme* and *G. crassivaginata*, in agreement with the ITS2-28S tree. However, this taxon formed a well-supported lineage next to a clade containing *G. crassivaginata* (Fig. 4).

The six isolates of Taxon 1 obtained in this study were distinguished from *C. pallidobrunnea* using SNP analyses for each of the ITS1-5.8S-ITS2-28S, TUB2, TEF1-α gene region sequences. The total number of SNP differences between the six isolates and *C. pallidobrunnea* for all three genes was 166 (26 for ITS1-5.8S-ITS2-28S, 60 for

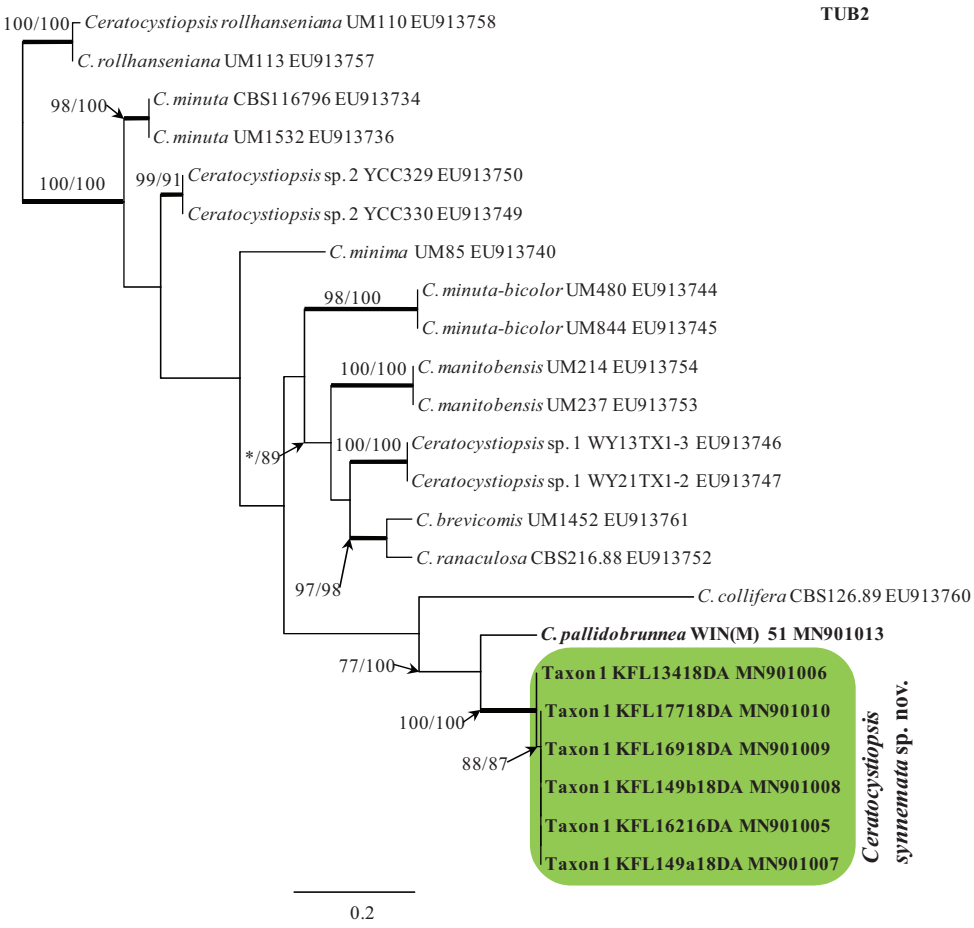

Figure 2. Phylogram obtained from Maximum Likelihood (ML) analyses of TUB2 data for the *Ceratocystiopsis* spp. Sequences obtained during this study are presented in bold type. The Bootstrap values ≥ 75% for ML and Maximum Parsimony (MP) analyses are presented at nodes as follows: ML/MP. Bold branches indicate posterior probabilities values ≥ 0.95 obtained from Bayesian Inference (BI) analyses. * Bootstrap values <75%. The tree is drawn to scale (see bar) with branch length measured in the number of substitutions per site.

TUB2, and 80 for TEF1-α). Little intraspecific sequence variation was found within 6 isolates of Taxon 1. Intraspecific variability of the ITS1-5.8S-ITS2-28S, TUB2 and TEF1-α genes was detected for Taxon 1 in one position, i.e. 387, two positions, i.e. 212, 217, and one position i.e. 482, respectively (Suppl. material 1: Tables S1, S2).

The 11 isolates of Taxon 2 obtained in this study were distinguished from *G. crassivaginata* using SNP analyses for each of the ITS1-5.8S-ITS2-28S, TUB2, TEF1-α, ACT gene region sequences. The total number of SNP differences between the 11 isolates and *G. crassivaginata* for all four genes was 59 (8 for ITS1-5.8S-ITS2-28S, 16 for TUB2, 25 for TEF1-α, and 10 for ACT). The intraspecific sequence variation was greater for 11 isolates of Taxon 2 than for Taxon 1. Intraspecific variability of the

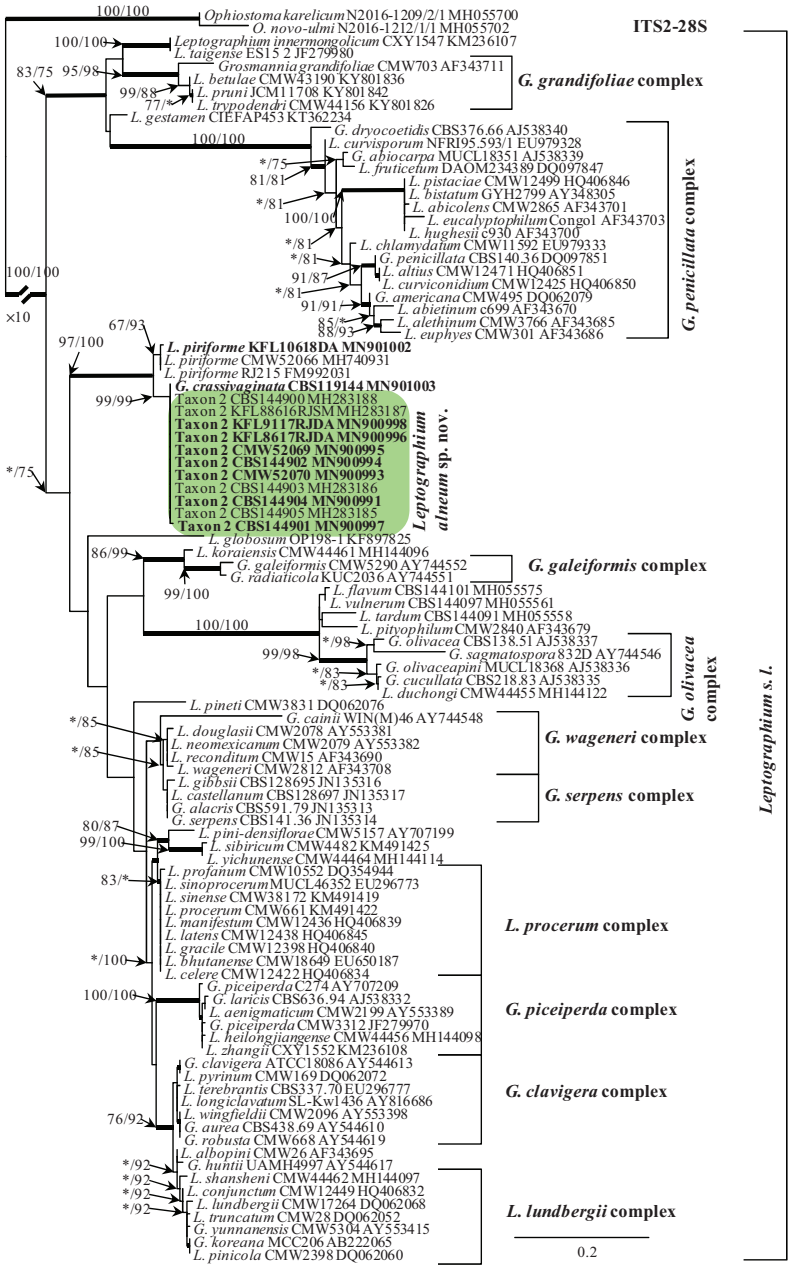

Figure 3. Phylogram obtained from Maximum Likelihood (ML) analyses of the ITS2-28S for selected species of *Leptographium sensu lato*. Sequences obtained during this study are presented in bold type. The Bootstrap values ≥ 75% for ML and Maximum Parsimony (MP) analyses are presented at nodes as follows: ML/MP. Bold branches indicate posterior probabilities values ≥ 0.95 obtained from Bayesian Inference (BI) analyses. * Bootstrap values <75%. The tree is drawn to scale (see bar) with branch length measured in the number of substitutions per site. *Ophiostoma karelicum* and *O. quercus* represents the outgroup in analyses of ITS2-28S.

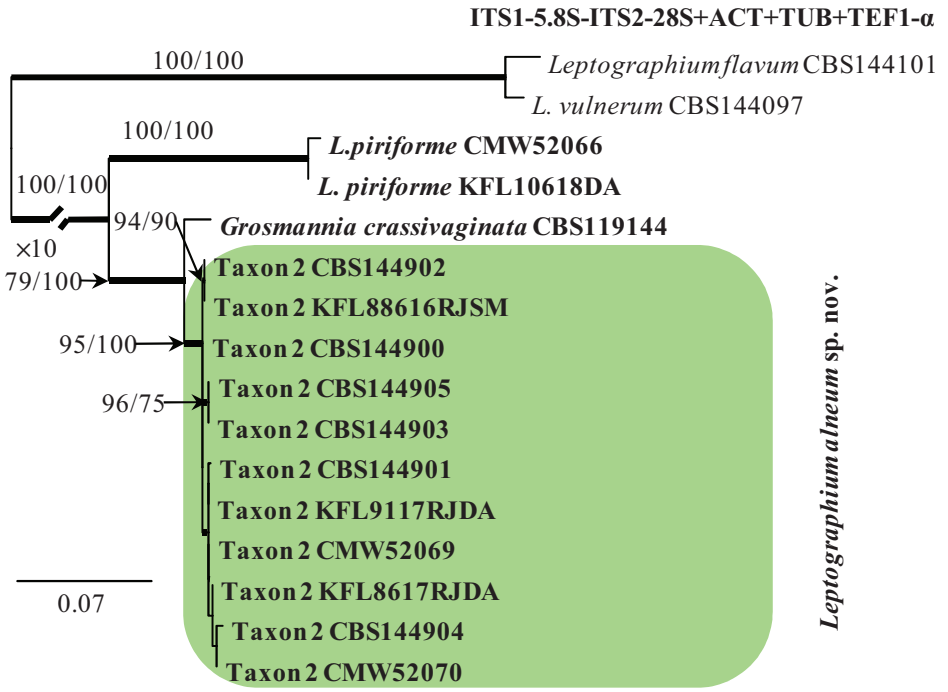

Figure 4. Phylogram obtained from Maximum Likelihood (ML) analyses of the combined datasets of ITS1-5.8S-ITS2-28S+ACT+TUB2+TEF1-α for selected species of *Leptographium sensu lato*. Sequences obtained during this study are presented in bold type. The Bootstrap values ≥ 75% for ML and Maximum Parsimony (MP) analyses are presented at nodes as follows: ML/MP. Bold branches indicate posterior probabilities values ≥ 0.95 obtained from Bayesian Inference (BI) analyses. * Bootstrap values <75%. The tree is drawn to scale (see bar) with branch length measured in the number of substitutions per site. *Leptographium flavum* and *L. vulnerum* represents the outgroup in analyses of the combined datasets of ITS1-5.8S-ITS2-28S+ACT+TUB2+TEF1-α.

TUB2, TEF1-α, and ACT genes was detected for Taxon 2 in eight positions, i.e. 36, 82, 83, 87, 215, 230–232; nine positions, i.e. 14, 21, 31, 46, 101, 196, 272, 352, 549; and five positions, i.e. 402, 749, 754, 755, 766, respectively (Suppl. material 1: Table S3).

These results indicate that the six isolates of Taxon 1 within *Ceratocystiopsis* and the 11 isolates of Taxon 2 within *Leptographium* represent novel species.

Taxonomy

The morphological characterization and phylogenetic comparisons based on six genetic loci, showed that two taxa associated with *D. alni* from Poland are distinct from each other and from other known taxa in the *Ophiostomatales*. Therefore, they are described here as new species:

Taxon 1

Ceratocystiopsis synnemata **B. Strzałka, R. Jankowiak & G. Hausner, sp. nov.**
MycoBank No: 835151
Fig. 5

Etymology. The epithet (synnemata) refers to the synnematous conidiomata formed by this fungus.

Type. Poland, Paprocice, from *Dryocoetes alni* beetle infesting *Populus tremula*, 5 Oct 2018, *K. Miśkiewicz* (TUR 207995 http://mus.utu.fi/TFU.207995 ***holotype***, ex-holotype cultures: NRIF 16918DA = KFL 16918DA).

Description. ***Sexual morph*****:** not observed. ***Asexual morph*****:** hyalorhinocladiella-like. ***Conidiophores*** micronematous or macronematous. The micronematous con-

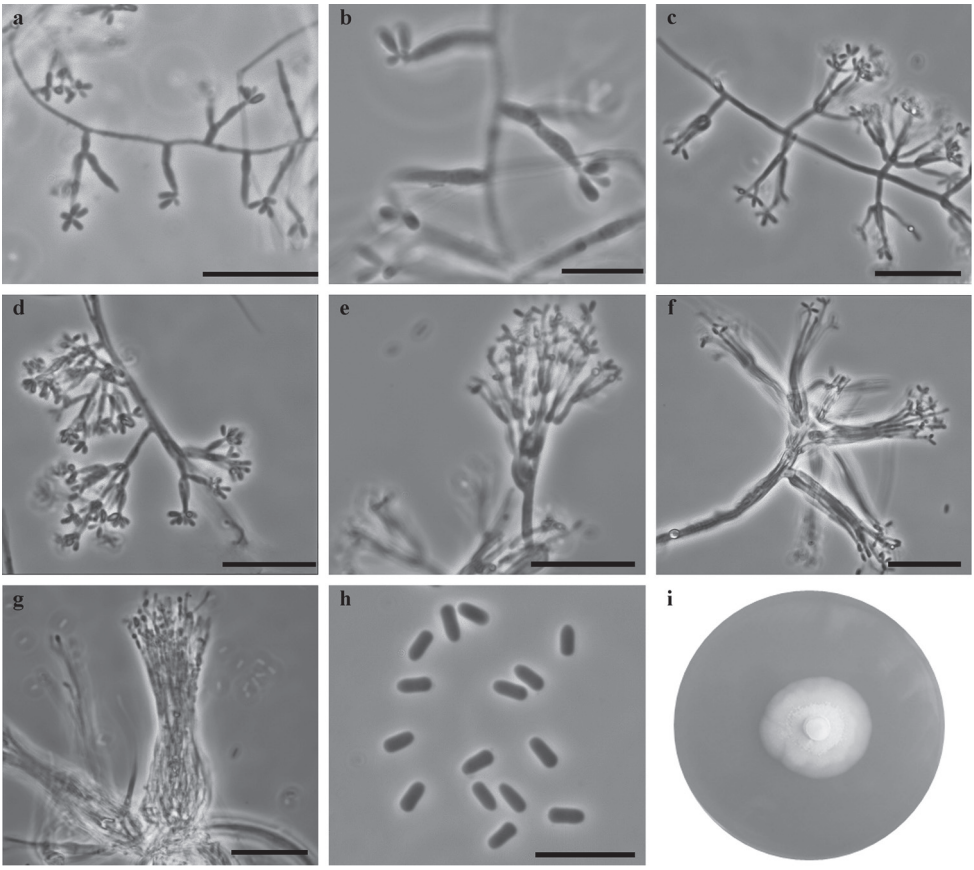

Figure 5. *Ceratocystiopsis synnemata* sp. nov. (NRIF 16918DA=KFL 16918DA) **a, b** micronematous conidiophores **c–e** macronematous conidiophores **f, g** conidiophores aggregate in synnemata **h** conidia **i** fourteen-day-old culture on MEA. Scale bars: 25 µm (**a**), 10 µm (**b**), 25 µm (**c–g**), 10 µm (**h**).

idiophores, hyaline, consist of conidiogenous cells arising singly from the vegetative hyphae (6–)8.6–16.4(–23.2) × (0.6–)0.9–1.3(–1.6) µm. The macronematous conidiophores are much larger, (14.5–)17.3–39.8(–76.9) µm long than the preceding forms and from a basal cell, (3.1–)5.3–11.2(–17) × (0.9–)1.1–1.9(–2.6) µm. The basal cells branch lateral or penicillate and form 1–5 branches (mostly 1–2) producing conidiogenous cells at their apices. ***Conidiophores*** often aggregate in loosely synnemata, (43.2–)52.3–86.4(–114.7) µm long, (2.4–)3.6–8.2(–12.9) µm wide at the tip. ***Conidia*** hyaline, smooth, unicellular, oblong-elliptical, (2.4–)2.8–3.5(–4) × (1–)1.1–1.3(–1.4) µm. ***Cultural characteristics*:** Colonies with optimal growth at 25 °C on 2% MEA with radial growth rate 1.4 (± 0.1) mm/d, growth very well at 30 °C (1.3 mm/d) and 35 °C (1.0 mm/d). Colonies yellowish gray, margin smooth. Hyphae pale gray in color, smooth, submerged in the medium and aerial mycelium rare, not constricted at the septa, 0.4–2.6 (mean 1.1±0.6) µm diam., asexual morph moderately abundant, very abundant after adding twigs.

Host trees. *Alnus incana*, *Populus tremula*

Insect vector. *Dryocoetes alni*

Distribution. Poland

Note. *Ceratocystiopsis synnemata* can be distinguished from *C. pallidobrunnea* by the shape and size of the conidia. *Ceratocystiopsis synnemata* has shorter and oblong-elliptical conidia in contrast to the allantoid conidia of *C. pallidobrunnea* (*C. synnemata*: 2.4–4 ×1–1.4 µm; *C. pallidobrunnea*: 2.5–5 × 0.7–1.2 µm (Olchowecki and Reid 1974), 2–7 × 0.7–2.5 µm (Upadhyay 1981) (Table 3). In addition, *C. synnemata* produces conidiophores that aggregate into loosely arranged synnemata.

Taxon 2

Leptographium alneum **B. Strzałka, R. Jankowiak & P. Bilański, sp. nov.**
MycoBank No: 835146
Fig. 6

Etymology. The epithet (alneum) refers to the species name of the bark beetle vector of this fungus, *Dryocoetes alni*.

Type. Poland, Paprocice, from *Dryocoetes alni* beetle infesting *Populus tremula*, 2 Nov 2017, *K. Miśkiewicz*, (TUR 207557 http://mus.utu.fi/TFU.207557 ***holotype***, ex-holotype cultures: CBS 144091 = CMW 51789).

Description. ***Sexual morph*:** Ascomata developing after 30 d on sterilized *Populus* twigs when two mating types were paired: superficially or partly embedded in the agar or wood, single. Bases light brown to dark brown, globose, unornamented, (59–)66–90(–108) µm in diameter, necks dark brown, cylindrical, straight or curved, (58–)68–88(–114) µm long (excluding ostiolar hyphae), (18.7–)20.7–27.9(–31) µm wide at base, (10.2–)11.8–15.3(–17.8) µm wide at the tip. ***Ostiolar hyphae*** present, pale brown, straight, non-septate or sporadically one-septate, numerous, divergent, pointed at the

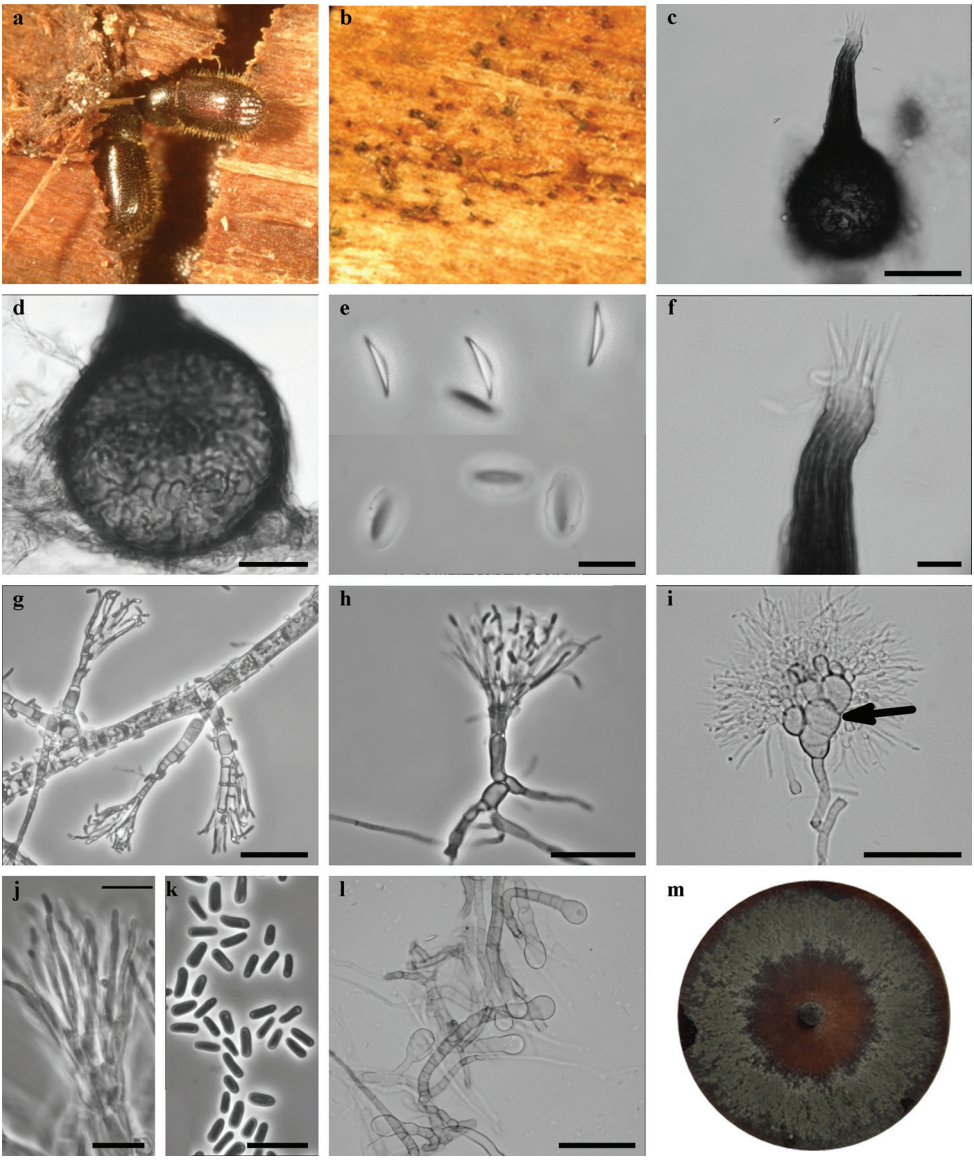

Figure 6. *Leptographium alneum* sp. nov. (CBS 144901) **a** *Dryocoetes alni*-infested *Populus tremula* tree **b** galleries of *D. alni* with ascomata **c** ascoma **d** ascomatal base **e** ascospores **f** ostiolar hyphae **g–i** conidiophores, black arrow indicates barrel-shaped cells **j** conidiogenous **k** conidia **l** club-shape cells **m** fourteen-day-old culture on MEA. Scale bars: 50 µm (**c**), 25 µm (**d**), 10 µm (**e**), 10 µm (**f**), 25 µm (**g**), 25 µm (**h**), 50 µm (**i**), 10 µm (**j**), 10 µm (**k**), 50 µm (**l**).

tip, (14.6–)15.9–19(–22.7) µm long, 5 to 12 in number. ***Asci*** not seen. ***Ascospores*** one-celled, hyaline, falcate in side view, (7.4–)8.1–11.1(–14.3) × (1.2–)1.5–2.1(–2.4) µm; fusiform in face view, (6.9–)7.4–8.8(–10.3) × (1.8–)2–2.8(–3.3) µm; end view not seen,

excluding hyaline gelatinous sheath, (8.9–)10–11.5(–12.2) × (4.5–)5.5–6.7(–7) µm in face view including sheath, accumulated in orange yellow-colored mass at the tip of the neck. Gelatinous sheath 0.5–3 µm thick, oval in face view.

Asexual morph*: *conidiophores macronematous, arising directly from hyphae, single solitary, without rhizoidal hyphae at the bases, often with barrel-shaped or globose cells, (48.1–)59.3–84.2(–102.9) µm in length. ***Stipes*** erect, light olivaceous, 1–4 septate (mostly 2), (7.6–)14.3–39.2(–48.5) µm long (from first basal septum to below primary branches), (2–)2.4–5.4(–15.6) µm wide below primary branches, apical cell often strongly swollen, (3.2–)3.8–5.2(–6.1) µm wide at base, basal cell rarely swollen. Conidiophores often composed of barrel or globose cells. ***Conidiogenous apparatus*** (20–)26.5–38.6(–48.7) µm long (excluding conidial mass) consisting of 2–3 series of branches-type B (more than two branches) (Jacobs and Wingfield 2001). Primary branches light olivaceous, cylindrical or swollen, smooth, (5.1–)5.8–12.7(–23.1) × (1.2–)1.6–4.2(–6.8) µm. ***Conidiogenous cells*** hyaline, tapering from base to apex, (11.6–)13.2–19(–23.7) × (0.8–)0.9–2(–3.5) µm. ***Conidia*** hyaline, mostly allantoid, sometimes oblong to obovoid (3.2–)3.7–5.9(–9.7) × (0.8–)1–1.8(–2.8) µm, accumulating around the conidiogenous apparatus as a creamy mucilaginous mass.

***Cultural characteristics*:** Colonies with optimal growth at 30 °C on 2% MEA with radial growth rate 8.8 (± 0.9) mm/d, good growth observed at 35 °C (8.3 mm/d) and better than at 25 °C (7.9 mm/d). Colonies brownish gray with distinct silvery gloss, margin smooth. Hyphae olive yellow in color, smooth, submerged in the medium and aerial mycelium abundant, not constricted at the septa, 1.1–5.5 (mean 2.5±1) µm diam., asexual morph very abundant, which gives a shade of gray. Club-shaped cells terminal on septate hyphal branches present, (11.5–)14.8–25.6(–33.3) × (7.7–)11.3–15.1(–18.2) µm, born on a multicelled stalk, (7.2–)14.7–82.4(–124.2) µm long, (4.4–)5.1–7.7(–9.7) µm wide below primary septa, (2.9–)4–6(–7.4) µm wide at base. Perithecia and asexual morph co-occur in culture.

Host trees. *Alnus incana*, *Malus sylvestris*, *Populus tremula*

Insect vector. *Dryocoetes alni*, *Scolytus mali*

Distribution. Poland

Note. Morphologically, *Leptographium alneum* differs from *Grosmannia crassivaginata* in having longer ascomatal necks (*L. alneum*: 58–114 µm: *G. crassivaginata*: 40–60 µm), and the presence of larger club-shaped cells (*L. alneum*: 11.5–33.3 × 7.7–18.2 µm; *G. crassivaginata*: 12–20 × 8–12 µm (Griffin 1968), 6.5–18.5 × 5–13.5 µm (CBS 119144), (Table 4). In addition, *L. alneum* has aseptate or sporadically 1-septate ostiolar hypahe, which are septate in *G. crassivaginata*. *Leptographium alneum* frequently produces conidiophores with barrel-shaped or globose cells, while in *G. crassivaginata* the cells of the conidiophore are slightly swollen at most. In contrast to *G. crassivaginata* (CBS 119144), *L. alneum* has larger conidia, especially in regard to width (*L. alneum*: (3.2–)3.7–5.9(–9.7) × (0.8–)1–1.8(–2.8) µm: *G. crassivaginata*: (2.4–)3.2–5(–8.1) × (0.7–)0.9–1.3(–1.7) µm) (Table 4). *Leptographium alneum* has brownish gray colony with silvery gloss cultures in contrast to the olive brown colored colonies of *G. crassivaginata* (isolate CBS 119144). The optimal growth on MEA for

L. alneum and *G. crassivaginata* (isolate CBS 119144) is 30 °C. However, *L. alneum* grows much faster than *G. crassivaginata* (*L. alneum* 8.8 mm/d, *G. crassivaginata* 6.9 mm/d) and grows faster at 35 °C (8.3 mm/d) than at 25 °C (7.9 mm/d). In contrast, *G. crassivaginata* grows much faster at 25 °C (5.6 mm/d) than 35 °C (4.4 mm/d).

Discussion

This study identified two new species of ophiostomatoid fungi associated with *Dryocoetes alni* on *Alnus incana* and *Populus tremula* in hardwood ecosystems in Poland. DNA sequence comparisons and morphological features supported these as novel. The species were named *Ceratocystiopsis synnemata* and *Leptographium alneum*. The results confirm earlier findings that many species of the Ophiostomatales are associated with hardwood-infesting bark beetles in Poland (Jankowiak et al. 2017, 2018, 2019a; Aas et al. 2018).

The results of this study revealed one new species of *Ceratocystiopsis* bringing the total number of species in the genus to 17. The newly described species is morphologically similar to other species of *Ceratocystiopsis*, with hyalorhinocladiella-like asexual morph (De Beer et al. 2013a). In contrast to other *Ceratocystiopsis* species, *C. synnemata* produces simple as well as highly branched conidiophores reminiscent of *C. pallidobrunnea* (Olchowecki and Reid 1974; Upadhyay 1981) or *C. rollhanseniana* (Hausner et al. 2003). In addition, *C. synnemata* forms synnemata with loosely packed conidiophores that appear to be a unique feature of *Ceratocystiopsis*.

Ascomata in *Ceratocystiopsis* tended to be globose with short necks, and falcate ascospores surrounded by a gelatinous sheath (De Beer and Wingfield 2013). Generally, *Ceratocystiopsis* species produce perithecia in varying degrees of abundance and maturity (Upadhyay 1981; Plattner et al. 2009). *Ceratocystiopsis synnemata* did not form a sexual state in crosses between different isolates. That would suggest that this species is heterothallic or produces perithecia very sparsely.

Most of the formally described species of *Ceratocystiopsis* are known only from Pinaceae including those in the genera *Picea*, *Pinus* and *Pseudotsuga*. For example, in Poland, two species of *Ceratocystiopsis* have previously been reported: *C. minuta* and species of uncertain status, *C. alba*, which both have been isolated from spruce-infesting bark beetles (Jankowiak et al. 2009). Only *C. pallidobrunnea* was collected from hardwood tree species, *Populus tremuloides* in Canada (Olchowecki and Reid 1974; Plattner et al. 2009). The discovery of *C. synnemata* on *Populus tremula* in this study clearly show that *Ceratocystiopsis* species are also distributed in hardwood forest ecosystems in Europe.

A new species of *Leptographium* was discovered from *Dryocoetes alni* in this study. This new taxon is closely related to *Leptographium piriforme* and *Grosmannia crassivaginata* forming a well-supported lineage distinct from other species of *Leptographium sensu lato*. All these three species have the curved conidia formed on short conidiophores, club-shaped cells, short-necked perithecia, and falcate, sheathed ascospores. These features clearly distinguish them from the other species recognized in the various species complexes currently recognized within *Leptographium sensu lato*.

Based on DNA sequence comparisons, *L. alneum* described in this study is closely related to *G. crassivaginata*, a species described from *Picea mariana*, *Populus grandidentata* and *P. tremuloides* in Canada (Griffin 1968). Morphologically, *L. alneum* most closely resembles *G. crassivaginata*. The asexual morph of *L. alneum* produced short conidiophores, and stalked club-shaped cells, similar to those of *G. crassivaginata*. Other similarities are the presence of short-necked perithecia, and fusiform-falcate, sheathed ascospores. *Leptographium alneum*, however, differs from *G. crassivaginata*, in having longer ascomatal neck and larger club-shaped cells. Moreover, *L. alneum* has larger conidia than *G. crassivaginata* (CBS 119144), especially with regard to the width of the conidia. Other differences are the presence of barrel-shaped or globose cells that make up the conidiophores, which in *G. crassivaginata* are occasionally only slightly swollen. There are also differences in characteristics of cultures. *Leptographium alneum* has brownish gray cultures in contrast to olive brown culture of *G. crassivaginata* (isolate CBS 119144). Both species belong to fast-growing species on MEA, however *L. alneum* grows much faster than *G. crassivaginata*, especially at 35 °C.

Leptographium species are generally considered as saprotrophs or pathogens of conifer trees (Jacobs and Wingfield 2001). However, the results of the present study confirm previous Polish investigations that some of the *Leptographium* species have a close affinity to hardwoods in Europe. Recently, *L. betulae*, *L. tardum*, and *L. trypodendri* were collected from hardwood-infesting bark beetles in Poland (Jankowiak et al. 2017, 2018), while three other *Leptographium* species have been isolated and formally described from hardwood wounds (Jankowiak et al. 2018, 2019c).

There was no information on *D. alni*-associated fungi before 2019. Recent Polish research reported that only *L. alneum* (named as *Leptographium* sp. 7) is an associate of *D. alni* (Jankowiak et al. 2019a). However, the additional isolations conducted in 2018 demonstrated that this beetle species apart from *L. alneum*, was also associated with other ophiostomatoid species including *C. synnemata* and *L. piriforme*. Among them, only *C. synnemata* and *L. alneum* were commonly found in association with *D. alni*. The common occurrence of these species suggests their important role as fungal associates of *D. alni* in Poland. The results of the present study and other Polish findings (Jankowiak et al. 2019a) indicated that *C. synnemata* and *L. alneum* have been found only occasionally from other beetle species and therefore can be considered as regular and possible specific associates of *D. alni*. *Leptographium piriforme* is less specific and can be found with other beetle species (Jankowiak and Kolařík 2010) or hardwood wounds (Jankowiak et al. 2019c) in low numbers.

This work represents the most detailed survey of Ophiostomatales associated with *D. alni* in Europe. Two new species were described. Ophiostomatoid fungi on hardwoods have been relatively well investigated in Poland (Jankowiak et al. 2017, 2018, 2019a, b, c; Aas et al. 2018), but in other parts of Europe they are still poorly studied. In addition, many ophiostomatoid species have not been formally described and our study has contributed to filling this knowledge gap. The findings of this study clearly showed that the diversity and taxonomic placement of many members of the Ophiostomatales associated with hardwoods-infesting bark beetles in Europe are still poorly understood.

Acknowledgements

This work was supported by the National Science Centre, Poland (contract No. UMO-2014/15/NZ9/00560) and the Ministry of Science and Higher Education of the Republic of Poland.

References

Aas T, Solheim H, Jankowiak R, Bilański P, Hausner G (2018) Four new *Ophiostoma* species associated with hardwood-infesting bark beetles in Norway and Poland. Fungal Biology 122: 1142–1158. https://doi.org/10.1016/j.funbio.2018.08.001

Altschul SF, Gish W, Miller W, Myers EW, Lipman DJ (1990). Basic local alignment search tool. Journal of Molecular Biology 215: 403–410. https://doi.org/10.1016/S0022-2836(05)80360-2

Borowski J, Piętka J, Szczepkowski A (2012) Insects found on black alder *Alnus glutinosa* (L.) Gaertn. when stands are dying back. Forest Research Papers 73: 355–362. https://doi.org/10.2478/v10111-012-0034-0

Bright DE (1963) Bark beetles of the genus *Dryocoetes* (Coleoptera: Scolytidae) in North America. Annals of the Entomological Society of America 56: 103–115. https://doi.org/10.1093/aesa/56.1.103

Carbone I, Kohn LM (1999) A method for designing primer sets for speciation studies filamentous ascomycetes. Mycologia 91: 553–556. https://doi.org/10.2307/3761358

Darriba D, Taboada GL, Doallo R, Posada D (2012) jModelTest 2: more models, new heuristics and parallel computing. Nature Methods 9: 1–772. https://doi.org/10.1038/nmeth.2109

De Beer ZW, Wingfield MJ (2013) Emerging lineages in the Ophiostomatales. In: Seifert KA, De Beer ZW, Wingfield MJ (Eds) Ophiostomatoid fungi: Expanding frontiers, CBS Biodiversity Series. CBS-KNAW Fungal Biodiversity Centre, Utrecht 12: 21–46.

De Beer ZW, Seifert KA, Wingfield MJ (2013a) A nomenclator for ophiostomatoid genera and species in the Ophiostomatales and Microascales. In: Seifert KA, De Beer ZW, Wingfield MJ (Eds) Ophiostomatoid fungi: Expanding frontiers, CBS Biodiversity Series. CBS-KNAW Fungal Biodiversity Centre, Utrecht 12: 261–268.

De Beer ZW, Seifert KA,Wingfield MJ (2013b) The ophiostomatoid fungi: their dual position in the Sordariomycetes. In: Seifert KA, De Beer ZW, Wingfield MJ (Eds) Ophiostomatoid fungi: Expanding frontiers, CBS Biodiversity Series. CBS-KNAW Fungal Biodiversity Centre, Utrecht 12: 1–19.

De Beer ZW, Duong TA, Wingfield MJ (2016) The divorce of *Sporothrix* and *Ophiostoma*: solution to a problematic relationship. Studies of Mycology 83: 165–191. https://doi.org/10.1016/j.simyco.2016.07.001

Dodelin B (2010) *Dryocoetes alni* (Georg), un scolyte méconnu (Coleoptera, Curculionidae, Scolytinae). Bulletin mensuel de la Société linnéenne de Lyon 79: 271–273. https://doi.org/10.3406/linly.2010.13795

Gardes M, Bruns TD (1993) ITS primers with enhanced specificity for Basidiomycetes – application to the identification of mycorrhiza and rusts. Molecular Ecology 2: 113–118. https://doi.org/10.1111/j.1365-294X.1993.tb00005.x

Glass NL, Donaldson GC (1995) Development of primer sets designed for use with the PCR to amplify conserved genes from filamentous ascomycetes. Applied and Environmental Microbiology 61: 1323–1330. https://doi.org/10.1128/AEM.61.4.1323-1330.1995

Goidànich G (1936) II genre di Ascorniceti 'Grosmanni' G. Goid. Bolletino della Stazione di Patologia vegetale di Roma 16: 26–40.

Goheen DJ, Cobb FW (1978) Occurrence of *Verticicladiella wageneri* and its perfect state, *Ceratocystis wageneri* sp. nov., in insect galleries. Phytopathology 68: 1192–1195. https://doi.org/10.1094/Phyto-68-1192

Greif MD, Gibas CF, Currah RS (2006) *Leptographium piriforme* sp. nov., from a taxonomically diverse collection of arthropods collected in an aspen-dominated forest in western Canada. Mycologia 98: 771–780. https://doi.org/10.1080/15572536.2006.11832648

Griffin HD (1968) The genus *Ceratocystis* in Ontario. Canadian Journal of Botany 46: 689–718. https://doi.org/10.1139/b68-094

Grobbelaar J, De Beer ZW, Bloomer P, Wingfield MJ, Wingfield BD (2010) *Ophiostoma tsotsi* sp. nov., a wound- infesting fungus of hardwood trees in Africa. Mycopathologia 169: 413–423. https://doi.org/10.1007/s11046-009-9267-8

Guindon S, Gascuel O (2003) A simple, fast and accurate method to estimate large phylogenies by maximum-likelihood. Systematic Biology 52: 696–704. https://doi.org/10.1080/10635150390235520

Guindon S, Dufayard JF, Lefort V, Anisimova M, Hordijk W, Gascuel O (2010) New algorithms and methods to estimate maximum-likelihood phylogenies: assessing the performance of PhyML 3.0. Systematic Biology 59: 307–321. https://doi.org/10.1093/sysbio/syq010

Gutowski JM, Jaroszewicz B (2001) Catalogue of the fauna of Bialowieza Primeval Forest. Instytut Badawczy Leśnictwa, Warszawa.

Hall TA (1999) BioEdit: a user-friendly biological sequence alignment editor and analysis program for Windows 95/98/NT. Nucleic Acids Symposium, Ser 41: 95–98.

Hausner G, Eyjólfsdóttir GG, Reid J (2003) Three new species of *Ophiostoma* and notes on *Cornuvesica falcata*. Canadian Journal of Botany 81: 40–48. https://doi.org/10.1139/b03-009

Hyde KD, Norphanphoun C, Maharachchikumbura SSN, Bhat DJ, Jones EBG, Bundhun D, Chen YJ, Bao DF, Boonmee S, Calabon MS, Chaiwan N, Chethana KWT, Dai DQ, Dayarathne MC, Devadatha B, Dissanayake AJ, Dissanayake LS, Doilom M, Dong W, Fan XL, Goonasekara ID, Hongsanan S, Huang SK, Jayawardena RS, Jeewon R, Karunarathna A, Konta S, Kumar V, Lin CG, Liu JK, Liu NG, Luangsa-ard J, Lumyong S, Luo ZL, Marasinghe DS, McKenzie EHC, Niego AGT, Niranjan M, Perera RH, Phukhamsakda C, Rathnayaka AR, Samarakoon MC, Samarakoon SMBC, Sarma VV, Senanayake IC, Shang QJ, Stadler M, Tibpromma S, Wanasinghe DN, Wei DP, Wijayawardene NN, Xiao YP, Yang J, Zeng XY, Zhang SN, Xiang MM (2020) Refined families of Sordariomycetes. Mycosphere 11(1): 305–1059.

Jacobs K, Wingfield MJ (2001) *Leptographium* species: tree pathogens, insect associates, and agents of blue-stain. American Phytopathological Society, Minnesota.

Jacobs K, Bergdahl DR, Wingfield MJ, Halik S, Seifert KA, Bright DE, Wingfield BD (2004) *Leptographium wingfieldii* introduced into North America and found associated with exotic *Tomicus piniperda* and native bark beetles. Mycological Research 108: 411–418. https://doi.org/10.1017/S0953756204009748

Jankowiak R, Kolařík M (2010) *Leptographium piriforme* – first record for Europe and of potential pathogenicity. Biologia 65: 754–757. https://doi.org/10.2478/s11756-010-0065-z

Jankowiak R, Kacprzyk M, Młynarczyk M (2009) Diversity of ophiostomatoid fungi associated with bark beetles colonizing branches of *Picea abies* in southern Poland. Biologia 64: 1170–1177. https://doi.org/10.2478/s11756-009-0188-2

Jankowiak R, Strzałka B, Bilański P, Linnakoski R, Aas T, Solheim H, Groszek M, de Beer ZW (2017) Two new *Leptographium* spp. reveal an emerging complex of hardwood-infecting species in the Ophiostomatales. Antonie van Leeuwenhoek 110: 1537–1553. https://doi.org/10.1007/s10482-017-0905-8

Jankowiak R, Ostafińska A, Aas T, Solheim H, Bilański P, Linnakoski R, Hausner G (2018) Three new *Leptographium* spp. (Ophiostomatales) infecting hardwood trees in Norway and Poland. Antonie van Leeuwenhoek 111: 2323–2347. https://doi.org/10.1007/s10482-018-1123-8

Jankowiak R, Strzałka B, Bilański P, Kacprzyk M, Wieczorek P, Linnakoski R (2019a) Ophiostomatoid fungi associated with hardwood-infesting bark and ambrosia beetles in Poland: taxonomic diversity and vector specificity. Fungal Ecology 39: 152–167. https://doi.org/10.1016/j.funeco.2019.02.001

Jankowiak R, Bilański P, Strzałka B, Linnakoski R, Bosak A, Hausner G (2019b) Four new *Ophiostoma* species associated with conifer- and hardwood-infesting bark and ambrosia beetles from Czech Republic and Poland. Antonie van Leeuwenhoek 112: 1501–15021. https://doi.org/10.1007/s10482-019-01277-5

Jankowiak R, Bilański P, Ostafińska A, Linnakoski R (2019c) Ophiostomatales associated with wounds on hardwood trees in Poland. Plant Pathology 68: 1407–1424. https://doi.org/10.1111/ppa.13061

Kamgan Nkuekam G, De Beer ZW, Wingfield MJ, Roux J (2011) A diverse assemblage of *Ophiostoma* species, including two new taxa on eucalypt trees in South Africa. Mycological Progress 11: 515–533. https://doi.org/10.1007/s11557-011-0767-9

Katoh K, Standley DM (2013) MAFFT multiple sequence alignment software version 7, improvements in performance and usability. Molecular Biology and Evolution 30: 772–780. https://doi.org/10.1093/molbev/mst010

Kirisits T (2004) Fungal associates of European bark beetles with special emphasis on the ophiostomatoid fungi. In: Lieutier F, Day KR, Battisti A, Grégoire JC, Evans H (Eds) Bark and Wood Boring Insects in Living Trees in Europe, A Synthesis, Dordrecht, Kluwer, 185–223. https://doi.org/10.1007/978-1-4020-2241-8_10

Kornerup A, Wanscher JH (1978) Methuen Handbook of Colour. Third Edition. Eyre Methuen, London, 252 pp.

Lagerberg T, Lundberg G, Melin E (1927) Biological and practical researches into blueing in pine and spruce. SkogsvĺrdsföreningensTidskrift 25: 145–272.

Lim YW, Massoumi Alamouti S, Kim JJ, Lee S, Breuil C (2004) Multigene phylogenies of *Ophiostoma clavigerum* and closely related species from bark beetle-attacked *Pinus* in North America. FEMS Microbiology Letters 237: 89–96. https://doi.org/10.1111/j.1574-6968.2004.tb09682.x

Molnar AC (1965) Pathogenic fungi associated with a bark beetle on alpine fir. Canadian Journal of Botany 43: 563–570. https://doi.org/10.1139/b65-062

Negrón JF, Popp JB (2009) The flight peridiocity, attack patterns, and life history of *Dryocoetes confusus* Swaine (Coleoptera: Curculionida: Scolytinae), the western balsam bark beetle, in north central Colorado. Western North American Naturalist 69: 447–458. https://doi.org/10.3398/064.069.0404

O'Donnell K, Cigelnik E (1997) Two divergent intragenomic rDNA ITS2 types within a monophyletic lineage of the fungus *Fusarium* are nonorthologous. Molecular Biology and Evolution 7: 103–116. https://doi.org/10.1006/mpev.1996.0376

O'Donnell K, Kistler HC, Cigelnik E, Ploetz RC (1998) Multiple evolutionary origins of the fungus causing Panama disease of banana: concordant evidence from nuclear and mitochondrial gene genealogies. Proceedings of the National Academy of Sciences of the United States of America 95: 2044–2049. https://doi.org/10.1073/pnas.95.5.2044

Olchowecki A, Reid J (1974) Taxonomy of the genus *Ceratocystis* in Manitoba. Canadian Journal of Botany 52: 1675–1711. https://doi.org/10.1139/b74-222

Plattner A, Kim J-J, Reid J, Hausner G, Lim YW, Yamaoka Y, Breuil C (2009) Resolving taxonomic and phylogenetic incongruence within species *Ceratocystiopsis minuta*. Mycologia 101: 878–887. https://doi.org/10.3852/08-132

Rambaut A, Drummond AJ (2007) Tracer v1.4. http://beast.bio.ed.ac.uk/Tracer

Robert V, Vu D, Amor ABH, Van de Wiele N, Brouwer C, Jabas B, Szoke S, Dridi A, Triki M, ben Daoud S, Chouchen O, Vaas L, de Cock A, Stalpers JA, Stalpers D, Verkley GJM, Groenewald M, dos Santos FB, Stegehuis G, Li W, Wu L, Zhang R, Ma J, Zhou M, Gorjón SP, Eurwilaichitr L, Ingsriswang S, Hansen K, Schoch C, Robbertse B, Irinyi L, Meyer W, Cardinali G, Hawksworth DL, Taylor JW, Crous PW (2013) MycoBank gearing up for new horizons. IMA Fungus 4: 371–379. https://doi.org/10.5598/imafungus.2013.04.02.16

Ronquist F, Huelsenbeck JP (2003) MrBayes 3: Bayesian phylogenetic inference under mixed models. Bioinformatics 19: 1572–1574. https://doi.org/10.1093/sysbio/sys029

Seifert KA, Wingfield MJ, Kendrick WB (1993) A nomenclator for described species of *Ceratocystis*, *Ophiostoma*, *Ceratocystiopsis*, *Ceratostomella* and *Sphaeronaemella*. In: Wingfield MJ, Seifert KA, Webber J (Eds) *Ceratocystis* and *Ophiostoma*: Taxonomy, Ecology and Pathogenicity. APS Press, St. Paul, 269–287.

Six DL (2012) Ecological and Evolutionary Determinants of Bark Beetle – Fungus Symbioses. Insects 3: 339–366. https://doi.org/10.3390/insects3010339

Swofford DL (2003) PAUP* 4.0: phylogenetic analysis using parsimony (*and other methods). Sinauer Associates, Sunderland.

Tamura K, Stecher G, Peterson D, Filipski A, Kumar S (2013) MEGA6: molecular evolutionary genetics analysis version 6.0. Molecular Biology and Evolution 30: 2725–2729. https://doi.org/10.1093/molbev/mst197

Vilgalys R, Hester M (1990) Rapid genetic identification and mapping of enzymatically amplified ribosomal DNA from several *Cryptococcus* species. Journal of Bacteriology 172: 4238–4246. https://doi.org/10.1128/JB.172.8.4238-4246.1990

Upadhyay HP (1981) A Monograph of *Ceratocystis* and *Ceratocystiopsis*. Athens, University of Georgia Press.

White T, Bruns T, Lee S, Taylor J (1990) Amplification and direct sequencing of fungal ribosomal RNA genes for phylogenetics. In: Innis MA, Gelfand DH, Snisky JJ, White TJ (Eds) PCR Protocols: a Guide to Methods and Applications. Academic Press, New York, 315–322. https://doi.org/10.1016/B978-0-12-372180-8.50042-1

Wingfield MJ, Barnes I, De Beer ZW, Roux J, Wingfield BD, Taerum SJ (2017) Novel associations between ophiostomatoid fungi, insects and tree hosts: current status–future prospects. Biological Invasions 19: 3215–3228. https://doi.org/10.1007/s10530-017-1468-3

Yin M, Duong TA, Wingfield MJ, Zhou XD, De Beer ZW (2015) Taxonomy and phylogeny of the *Leptographium procerum* complex, including *L. sinense* sp. nov. and *L. longiconidiophorum* sp. nov. Antonie Van Leeuwenhoek 107: 547–563. https://doi.org/10.1007/s10482-014-0351-9

Zipfel RD, De Beer ZW, Jacobs K, Wingfield BD, Wingfield MJ (2006) Multi-gene phylogenies define *Ceratocystiopsis* and *Grosmannia* distinct from *Ophiostoma*. Studies in Mycology 55: 75–97. https://doi.org/10.3114/sim.55.1.75

Supplementary material 1

Tables S1–S3

Authors: Beata Strzałka, Robert Jankowiak, Piotr Bilański, Nikita Patel, Georg Hausner, Riikka Linnakoski, Halvor Solheim

Data type: molecular data

Explanation note: **Table S1.** Comparison of polymorphic sites of 18S–ITS1–5.8S–ITS2–28S and TUB2 genes of *Ceratocystiopsis pallidobrunnea* and Taxon 1. **Table S2.** Comparison of polymorphic sites of TEF1-α gene of *Ceratocystiopsis pallidobrunnea* and Taxon 1. **Table S3.** Comparison of polymorphic sites of 18S–ITS1–5.8S–ITS2–28S and protein-coding genes of *Grosmannia crassivaginata* and Taxon 2.

Link: https://doi.org/10.3897/mycokeys.68.50035.suppl1

MycoKeys 68: 49–73 (2020)
doi: 10.3897/mycokeys.68.53264
http://mycokeys.pensoft.net

RESEARCH ARTICLE

A peer-reviewed open-access journal
MycoKeys
Launched to accelerate biodiversity research

Hygrophorus subsection *Hygrophorus* (Hygrophoraceae, Agaricales) in China

Chao-Qun Wang[1], Tai-Hui Li[1], Ming Zhang[1], Xiao-Lan He[2], Wei-Qiang Qin[3], Tie-Zhi Liu[4], Nian-Kai Zeng[5], Xiang-Hua Wang[6], Jian-Wei Liu[6], Tie-Zheng Wei[7], Jiang Xu[1], Yue-Qiu Li[1], Ya-Heng Shen[1]

1 *Guangdong Provincial Key Laboratory of Microbial Culture Collection and Application, State Key Laboratory of Applied Microbiology Southern China, Guangdong Institute of Microbiology, Guangdong Academy of Sciences, Guangzhou 510070, Guangdong, China* **2** *Soil and Fertilizer Institute, Sichuan Academy of Agricultural Sciences, Chengdu 610066, Sichuan, China* **3** *Jishou University, Zhangjiajie 427000, Hunan, China* **4** *College of Life Sciences, Chifeng University, Chifeng 024000, Inner Mongolia, China* **5** *College of Pharmacy-Transgenic Laboratory, Hainan Medical University, Haikou 571199, Hainan, China* **6** *Key Laboratory for Plant Diversity and Biogeography of East Asia, Kunming Institute of Botany, Chinese Academy of Sciences, Kunming 650201, Yunnan, China* **7** *State Key Laboratory of Mycology, Institute of Microbiology, Chinese Academy of Sciences, Beijing 100101, China*

Corresponding author: Tai-Hui Li (mycolab@263.net)

Academic editor: María P. Martín | Received 15 April 2020 | Accepted 16 May 2020 | Published 26 June 2020

Citation: Wang C-Q, Li T-H, Zhang M, He X-L, Qin W-Q, Liu T-Z, Zeng N-K, Wang X-H, Liu J-W, Wei T-Z, Xu J, Li Y-Q, Shen Y-H (2020) *Hygrophorus* subsection *Hygrophorus* (Hygrophoraceae, Agaricales) in China. MycoKeys 68: 49–73. https://doi.org/10.3897/mycokeys.68.53264

Abstract

Hygrophorus subsect. *Hygrophorus* has been relatively well-studied in Europe and North America, but studies on the taxa in Asia, particularly in China, are still limited. In this study, phylogenetic overviews of genus *Hygrophorus*, based on the nuclear large subunit (LSU) ribosomal RNA gene and of subsect. *Hygrophorus*, based on the nuclear ribosomal internal transcribed spacer (ITS) regions were generated. Four new species, i.e. *H. brunneodiscus*, *H. fuscopapillatus*, *H. glutiniceps* and *H. griseodiscus* are described from southern China; and a rarely reported edible species *H. hedrychii* is described in detail, based upon the materials from north-eastern China. The main characteristics of the species under subsect. *Hygrophorus* worldwide are summarised in a table.

Keywords

East Asia, molecular systematics, taxonomy, waxycap, woodwax

Introduction

Hygrophorus Fr. (Hygrophoraceae, Agaricales, Basidiomycota) is a cosmopolitan fungal genus, mainly distributed in the northern hemisphere. The characteristics that distinguish the genus are: the ectomycorrhizal habit, robust basidiomata, usually viscid pileus surface, waxy, thick and distant lamellae, divergent lamellar trama and white or hyaline thin-walled basidiospores (Candusso 1997, Young 2005). The divergent lamellar trama morphologically distinguishes *Hygrophorus* from the other genera in the family Hygrophoraceae (Singer 1986, Lodge et al. 2014). According to the recent phylogenetic study, *Hygrophorus* can be divided into three subgenera [subg. *Camarophylli* Fr., subg. *Colorati* (Bataille) E. Larss. and subg. *Hygrophorus*], while subg. *Hygrophorus* is divided into three sections [sect. *Discoidei* (Bataille) Konrad & Maubl., sect. *Hygrophorus* and sect. *Picearum* E. Larss.] and sect. *Hygrophorus* consists of subsect. *Fulventes* E. Larss. and subsect. *Hygrophorus*, which includes the generic type species *H. eburneus* (Bull.: Fr.) Fr. (Lodge et al. 2014).

Morphologically, members in subsect. *Hygrophorus* share the characteristics of glutinous and white or pallid pileus, almost white and sometimes darkening lamellae, glutinous stipe and *Cossus*-odour, resembling the smell of *Cossus cossus* (Lepidoptera) (Larsson and Jacobsson 2004, Lodge et al. 2014). Five known species are currently included in subsect. *Hygrophorus*, i.e. *H. cossus* (Sow.) Fr., *H. discoxanthus* (Fr.) Rea, *H. eburneus*, *H. hedrychii* (Velen.) K. Kult. and *H. scabrellus* A. Naseer & A.N. Khalid, according to Larsson and Jacobsson (2004), Lodge et al. (2014) and Naseer et al. (2019).

Phylogenetically, the relationships of subsect. *Hygrophorus* are still controversial. The ITS-LSU-SSU-RPB2 combined analysis in Lodge et al. (2014) showed that subsect. *Hygrophorus* was a polyphyletic group; ITS analysis in Endo et al. (2018) showed subsect. *Hygrophorus* as a polyphyletic group since *H. discoxanthus* was located at the base of sect. *Hygrophorus*. ITS analysis in Lodge et al. (2014) showed that subsection was mostly monophyletic with an unstable support, but *H. discoideus* should belong to subsect. *Discoidei.* The ITS-LSU combined analysis in Lodge et al. (2014) and ITS analysis in Naseer et al. (2019) indicated subsect. *Hygrophorus* as a monophyletic group.

During the authors' study on the diversity of subsect. *Hygrophorus* in China, five species were discovered. In order to assess their phylogenetic positions, a phylogenetic overview of genus *Hygrophorus* was conducted, based on all available sequences of the nuclear large subunit (LSU) ribosomal RNA gene from GenBank (Benson et al. 2017) and the newly-obtained Chinese sequences in this study; and a phylogenetic overview of subsect. *Hygrophorus* was also made with the available sequence data of nuclear ribosomal internal transcribed spacer (ITS) regions from GenBank and UNITE (Nilsson et al. 2019) and the newly-obtained sequences from the Chinese materials. Through morphological comparisons along with the phylogenetic analyses, four new species, i.e. *H. brunneodiscus* from Central South China, *H. fuscopapillatus* and *H. griseodiscus* from south-western China and *H. glutiniceps* from southern China, are firstly introduced in this paper; and the presence of *H. hedrychii* in China is confirmed using molecular data, based on fungal collections from north-eastern China and also described and elucidated, based on macro- and micromorphological observations.

Materials and methods

Morphological observation and descriptions

Specimens are deposited in the Mycological Herbarium of Chifeng University (CFSZ), Fungal Herbarium of Hainan Medical University (FHMU), Fungarium of Guangdong Institute of Microbiology (GDGM), Herbarium of Mycology, Academia Sinica (HMAS) and Mycological Herbarium of Soil and Fertilizer Institute, Sichuan Academy of Agricultural Sciences (SAAS). Macro-morphological characteristics are described on the basis of field notes and photos and colour codes followed Kornerup and Wanscher (1978). Micro-morphological characteristics are measured when tissues are mounted in 5% aqueous potassium hydroxide (KOH) and 1% Congo Red solution under an Olympus BX51 microscope (Olympus Co., Tokyo, Japan). Twenty basidiospores and ten basidia from mature lamellae are measured for each specimen, Q refers to the ratio of length to width and Q_m refers to the mean value of Q values of all spores; pileipellis and stipitipellis are observed using the hand-sliced tissues approximately at the surface of the mid-radius of the pileus and the middle of the stipe length, respectively. Description terms for morphological characteristics mainly follow Vellinga (1988).

DNA extraction, PCR amplification and sequencing

The total genomic DNA extracted from dry samples using a HiPure Fungus DNA Mini kit (Megen Biotech Co. Ltd., Guangzhou, China) according to the manufacturer's instructions. Gene regions of the large subunit (LSU) and the internal transcribed spacer (ITS) nuclear ribosomal RNA gene are amplified by Polymerase Chain Reactions with the primers LR5 and LR0R (https://sites.duke.edu/vilgalyslab/rdna_primers_for_fungi/) and ITS1/ITS5 and ITS4 (White et al. 1990, Gardes and Bruns 1993), respectively. Sequencing of both directions was performed on an ABI 3730 sequencer analyser (Applied Biosystems, Foster City, CA, USA) using the same PCR primers at Beijing Liuhe Co. Ltd. Raw sequences are assembled by using SEQMAN version 7.1.0 of LASERGENE software (DNAStar, Madison, WI, USA). Newly-obtained consensus sequences are deposited in GenBank (Table 1).

Sequence alignments and phylogenetic analyses

For the LSU dataset, the newly-obtained sequences and all available *Hygrophorus* sequences longer than 300 bps from GenBank are treated as ingroups and the sequences of *Cantharocybe gruberi* (A.H. Sm.) H.E. Bigelow & A.H. Sm. are selected as outgroup, based on Razaq et al. (2014) and Naseer et al. (2019); for the ITS dataset, the newly-obtained sequences and the downloaded sequences from GenBank and UNITE longer than 300 bps and of subsect. *Hygrophorus* are combined as ingroups and the sequences

Table 1. Taxa, vouchers, geographic origin and GenBank accession numbers of the newly-generated sequences in this study.

Taxon	Voucher	Geographic origin	ITS	LSU
H. brunneodiscus	GDGM73213	China: Hunan	MN378318	MT093623
	GDGM75489	China: Hunan	MN378317	MT093622
	GDGM76934	China: Hunan	MT093605	MT093621
H. eburneus	GDGM70059 (BHS2011-11)	USA	MT093608	
H. fuscopapillatus	GDGM44412	China: Sichuan	MN378337	MT093625
	LJW1858	China: Yunnan	MT093606	MT093626
	XHW6609	China: Yunnan	MT093607	MT093627
H. griseodiscus	FHMU1578 (Zeng2452)	China: Hainan	MN378311	
	FHMU2013 (Zeng3052)	China: Hainan	MN378312	MT093614
	GDGM42140	China: Guangdong	MN378310	MT093619
	GDGM42188	China: Guangdong	MN378313	MT093618
	GDGM42217	China: Guangdong	MN378309	MT093617
	GDGM45220	China: Hainan	MN378315	MT093620
	GDGM53153	China: Jiangxi	MT093603	MT093615
	GDGM53496	China: Hunan	MN378314	
	HMAS273294	China: Guangdong	MT093604	
	SAAS462	China: Sichuan	MN378338	MT093624
H. hedrychii	CFSZ2559	China: Inner Mongolia	MT093610	
	CFSZ2851	China: Inner Mongolia	MN378306	MT093628
	CFSZ4268	China: Inner Mongolia	MT093609	
	CFSZ10761	China: Inner Mongolia	MT093611	
	CFSZ18159	China: Inner Mongolia	MN378308	MT093629
	CFSZ18269	China: Inner Mongolia	MN378307	MT093630

of *H. arbustivus* Fr. are selected as outgroups, since *H. arbustivus* is the type species of the sister group subsect. *Fulventes*, according to Lodge et al. (2014). Both datasets are combined, using GENEIOUS software (Biomatters Ltd.) and aligned by MAFFT (Multiple Alignment using Fast Fourier Transform) online service version 7 (Katoh et al. 2017). Maximum Likelihood analyses are performed by IQ-TREE web server with 1000 rapid bootstrap (BS) replicates (Trifinopoulos et al. 2016). The trees are viewed and edited in ITOL (Interactive Tree of Life) web server (Letunic and Bork 2016).

Results

Molecular phylogenetic results

For the aligned LSU dataset, 121 sequences with 980 sites were included, amongst them 119 *Hygrophorus* sequences are placed in the ingroups and two sequences of

Cantharocybe gruberi are in the outgroups. In the LSU phylogenetic tree (Fig. 1), both sect. *Hygrophorus* and subsect. *Hygrophorus* are presented as monophyletic groups with low support values, 61% BS and 54% BS, respectively; in addition, the sequences named as "*H. lindtneri*" (MK278193), "*H. marzuolus*" (MK278194) and "*H.* cf. *arbustivus*" (MK278183) are present within these clades. Three sequences from three samples (GDGM44412, LJW1858 and XHW6609) of *H. fuscopapillatus* are present as a monophyletic clade with high support value (100% BS), *H. griseodiscus* is present as a sister clade to *H. fuscopapillatus* with 100% BS, and, together, they form a sister clade to *H. cossus* with 75% BS; three sequences of *H. brunneodiscus* samples (GDGM73213, GDGM75489 and GDGM76934) and seven sequences of *H. glutiniceps* samples (GDGM42140, GDGM42154, GDGM42188, GDGM42217, GDGM45220, GDGM53153 and Zeng3052) form two independent monophyletic clades with high support values (100% BS) respectively; in addition, three sequences of *H. hedrychii* specimens (CFSZ2851, CFSZ18159 and CFSZ18269) form a monophyletic clade with high support value (99% BS).

For the aligned ITS dataset, 88 sequences with 689 sites were included, two sequences of *H. arbustivus* are treated as the outgroups and 86 sequences of subsect. *Hygrophorus* are within the ingroups. At least thirteen respectively-supported clades that correspond to different species were recovered in the ITS phylogenetic tree (Fig. 2), five of them coming from China. Two newly-generated sequences of *H. griseodiscus* from two different fruit-bodies of SAAS462 fall together in a supported clade with two GenBank downloaded sequences (KU836529–30) from Sichuan province in China and an uncultured *Hygrophorus* sequence (LC175568) from Hokkaido in Japan and the support value of the *H. griseodiscus*-clade is 91% BS. Three sequences from samples (GDGM44412, LJW1858 and XHW6609) of *H. fuscopapillatus* form a clade with 85% BS. Three sequences of *H. brunneodiscus* samples (GDGM73213, GDGM75489 and GDGM76934) form a clade with strong support value (100% BS). Nine sequences of *H. glutiniceps* specimens (GDGM42140, GDGM42188, GDGM42217, GDGM45220, GDGM53153, GDGM53496, HMAS273294, Zeng2452 and Zeng3052) are also clustered with strong support value (100% BS). Six newly-generated sequences of *H. hedrychii* samples (CFSZ2559, CFSZ2851, CFSZ4268, CFSZ10761, CFSZ18159 and CFSZ18269) from Inner Mongolia Autonomous Region of China are clustered with other *H. hedrychii* sequences from China (KX497168) and Sweden (AY242854 and AY463490) with 92% BS; in addition, MK575431 named as "*H. eburneus*" from Wisconsin in USA and DQ367904, labelled as "*H. eburneus* var. *eburneus*" from Canada, form a clade with 98% BS, this North American clade being the sister clade with the Eurasian *H. hedrychii*-clade with 100% BS.

Species of subsect. *Hygrophorus* known from China

According to the molecular phylogenetic analyses (Figs 1, 2) and morphological examinations on the Chinese specimens in this study, at least five species of *Hygrophorus* subsect. *Hygrophorus* are present in China, including *H. brunneodiscus*,

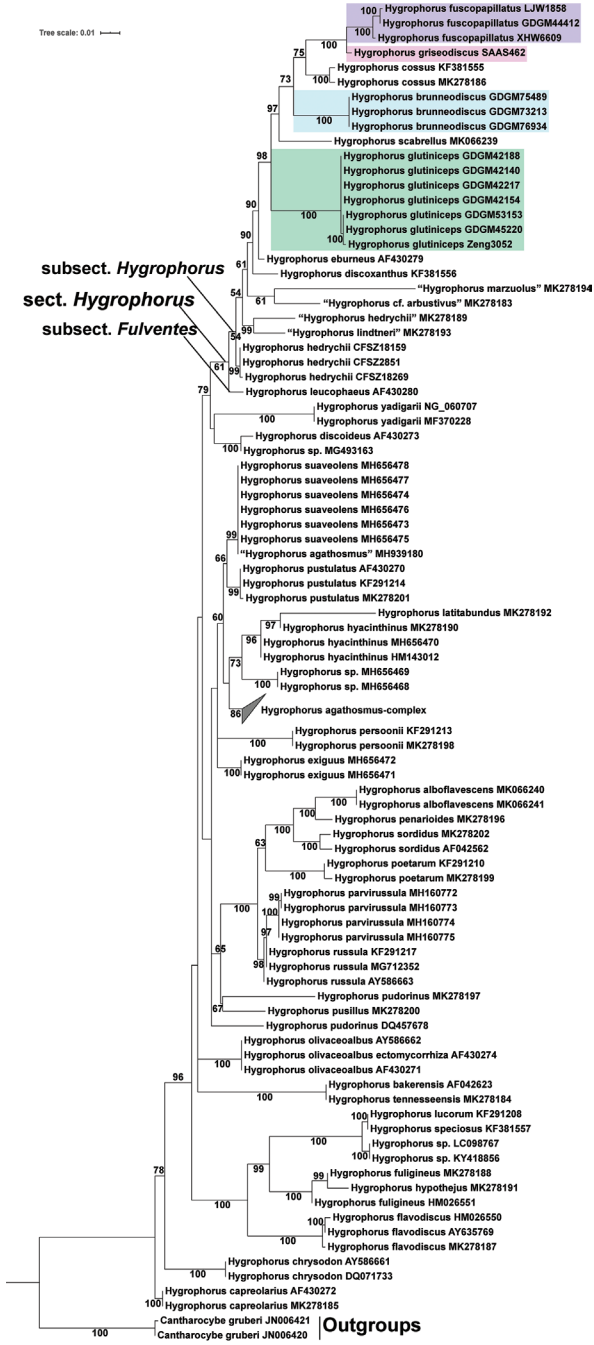

Figure 1. Phylogram showing the interspecific relationships under the genus *Hygrophorus* inferred from a LSU dataset using IQ-tree. Sequences of *Cantharocybe gruberi* were selected as outgroups. Bootstrap values greater than 50% are indicated around the branches. For downloaded sequences, specimen names and GenBank accession numbers are presented; for newly-generated sequences, species names and specimen vouchers are listed. Four newly-described species' sequences are highlighted in colour; sequences with quotation marks are incorrect names.

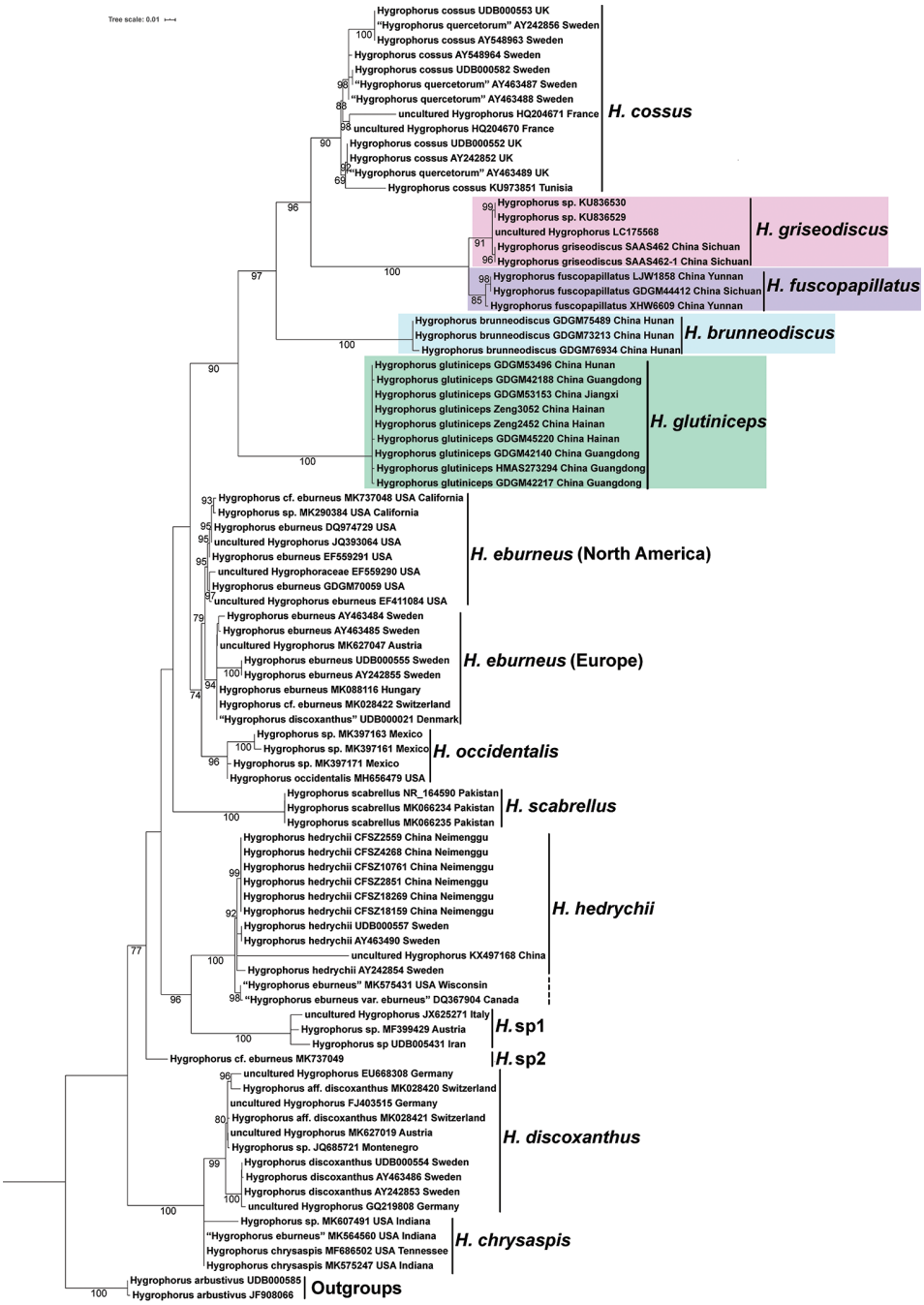

Figure 2. Phylogram of species under subsect. *Hygrophorus* inferred from an ITS dataset using IQ-tree. Sequences of *Hygrophorus arbustivus* were selected as outgroups. Bootstrap values greater than 50% are indicated around the branches. For downloaded sequences, specimen names, GenBank accession numbers and locations are presented; for newly-generated sequences, species names, specimen vouchers and locations are listed. Four newly-described species' sequences are highlighted in colour; sequences with incorrect names are marked with quotation marks.

H. fuscopapillatus, *H. glutiniceps*, *H. griseodiscus* and *H. hedrychii*. Although *H. cossus* and *H. eburneus* of subsect. *Hygrophorus* have been reported in China (Chen and Li 2013), but they are not described in the present study, because no DNA sequences or fresh specimens of these two species have been obtained from China in this study.

Taxonomy

Hygrophorus brunneodiscus **C.Q. Wang & T.H. Li, sp. nov.**
Fungal Names: FN 570664
Figure 3

Typification. China, Hunan Province, Zhangjiajie City, Zhangjiajie Campus of Jishou University, on the ground of a forest dominated by *Quercus fabri* and *Q. serrata*, elev. ca. 220 m, 29°8'24"N, 110°27'42"E, 26 May 2019, W.Q. Qin (GDGM73213, Holotype!), ITS MN378318.

Etymology. "*brunneo-*": brown, "*-discus*": pileus disc. The species epithet "*brunneodiscus*" (Lat.) refers to the brown pileus disc of this new taxon.

Diagnosis. *Hygrophorus brunneodiscus* differs from *H. cossus* by the smaller pileus (20–50 mm broad), brownish pileus disc, thinner stipe (4–7 mm wide) and the shorter basidia (32–48 μm long); differs from *H. fuscopapillatus* and *H. griseodiscus* by the low elevation distribution and brown pileus disc.

Description. *Pileus* 20–50 mm broad, hemispherical or conical with a slightly involute or slightly revolute margin when young, becoming convex with an expanded margin when mature, whitish to brownish as a whole, brownish-orange, light brown, yellowish-brown (5C4–5, 5D4–5, 5E5–8) at the disc (about one fourth part of the radius from the centre to the margin), becoming paler to greyish-yellow (4B3–4), greyish-white (4B1) or whitish outwards and white at the margin or with a white marginal zone of 1–2 mm wide, viscid, covered with a glutinous layer of transparent materials when wet. *Lamellae* short decurrent to decurrent, white, waxy, with 36–40 complete lamellae and 1–3 lamellulae between two complete lamellae; lamella edge concolorous, entire. *Stipe* 40–90 × 4–7 mm, cylindrical, hollow, nearly equal to slightly thinner at apex and tapering towards the base; pale yellow to greyish-yellow (4A3, 4B3), white to yellowish-white (4A2) at apex, sometimes white at base; sticky, covered with a layer of transparent materials when wet, easily-sticking debris on the slime layer, usually fibrillose or with scattered white fibrillose dots at apex. *Context* thin, white to light brown, with slight fishy odour.

Basidiospores (6.5)7–9(9.5) × 4–5.5(6) μm [mean length = 7.6 μm, mean width = 4.6 μm], Q = (1.3)1.4–2(2.1), Qm = 1.68, ellipsoid to oblong, smooth. *Basidia* 32–48 × 6–8.5 μm, Q = 4.1–6.6, Qm = 5.3, clavate, thin-walled, 4-spored, with sterigmata 5.5–7(9) μm long. *Pileipellis* an ixotrichoderm, composed of septate cylindrical hyphae, covered with a gelatinous layer; hyphae thin-walled, 2.5–5 μm wide, slightly yellowish and glutinous in KOH. *Hymenophoral trama* divergent, composed of septate, thin-walled and cylindrical hyphae; hyphal cells 45–70 × 6–10 μm, hyaline. *Clamp connections* present.

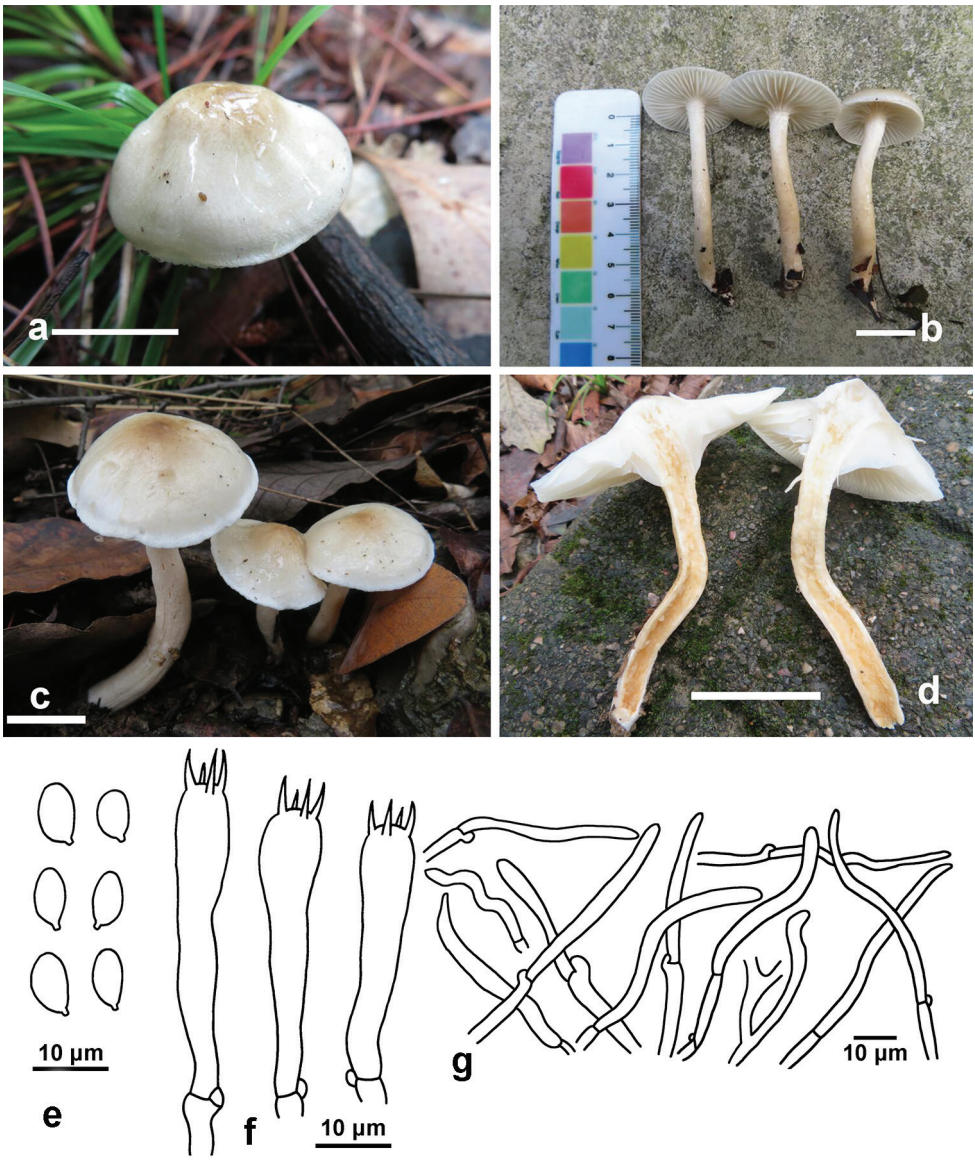

Figure 3. *Hygrophorus brunneodiscus*. **a, b** Basidiomata (GDGM73213, Holotype) **c, d** Basidiomata (GDGM75489) **e** Basidiospores (GDGM73213) **f** Basidia (GDGM73213) **g** Elements of pileipellis (GDGM73213). Scale bars: 2 cm (**a–d**).

Habit, habitat and distribution. Solitary to scattered, on the ground of subtropical broad-leaf forest dominated by *Quercus*, so far only known from Hunan Province in South Central China.

Additional specimens examined. China, Hunan Province, Zhangjiajie City, Zhangjiajie Campus of Jishou University, 26 October 2018, W.Q. Qin (GDGM75489); ibidem, 30 June 2019, W.Q. Qin (GDGM76934).

Remarks. *Hygrophorus brunneodiscus* is characterised by its brown tint on pileus disc, sticky pileus and stipe surface, basidiospores (6.5)7–9(9.5) × 4–5.5(6) µm, basidia 32–48 × 6–8.5 µm and subtropical and low elevation distribution.

Hygrophorus brunneodiscus can be easily recognised within subsect. *Hygrophorus* for its brownish colour on the pileus disc. Apart from that, *H. cossus* differs from *H. brunneodiscus* by having pale ochraceous grey colour at the pileus centre and more slender basidia (48–60 × 7–8.5 µm) (Larsson and Jacobsson 2004). *Hygrophorus discoxanthus* differs in the pure white mature basidiomata as young, rusty-brown pileus margin and discolouration of rusty brown at the lamellar edge and different host-association (with *Fagus*) (Candusso 1997, Larsson and Jacobsson 2004). *Hygrophorus eburneus* differs from it by having more carnose pileus and thicker stipe (4–10 mm wide), forming an ectomycorrhizal relationship with *Fagus* (Larsson and Jacobsson 2004). *Hygrophorus hedrychii* differs from it by having larger and more robust fruit-bodies (pileus 30–80 mm in diam. and stipe 5–10 mm in width), forming an ectomycorrhizal relationship with *Betula* (Larsson and Jacobsson 2004, Campo 2015). *Hygrophorus scabrellus* differs from it by owning smaller (24–28 mm in diam.) and off-white with dark green colour pileus, smaller basidiospores (mean length = 6.5 µm, mean width = 3.84 µm) and distribution in temperate forests under *Quercus* trees (Naseer et al. 2019).

Hygrophorus fuscopapillatus C.Q. Wang & T.H. Li, sp. nov.

Fungal Names: FN 570701
Figure 4

Typification. China, Sichuan Province, Panzhihua City, Yanbian County, Gesala Ecotourism Area, elev. ca. 2900 m, 27°08'10"N, 101°11'33"E, 25 August 2013, M. Zhang & C.Q. Wang (GDGM44412, Holotype!), ITS MN378337.

Etymology. "*fusco-*": dark brown, "*-papillatus*": papillate. The species epithet "*fuscopalillatus*" (Lat.) refers to the dark brown or grey brown papilla on the pileus of the new species.

Diagnosis. Differs from *H. griseodiscus* by the host association with Fagaceae, solitary habit, adnate to subdecurrent lamellae and slightly smaller basidispores measuring (6)7–9.5(10) × (4)4.5–5.5(6) µm. The ITS sequence is 95% similar to *H. griseodiscus*.

Description. *Pileus* 20–30 mm broad, convex to hemispherical when young, applanate to plano-concave when mature, with a papilla or small umbo in the centre, white to pale grey (1B1), grey or brownish-grey to olive brown (4E2–3,4F1–3) at papilla, gradually becoming lighter from centre to margin, white to pale grey (1B1) at margin, glutinous when wet; margin even, occasionally split. *Lamellae* adnate to subdecurrent, white, thick, with 30–36 complete lamellae per pileus and 1–3 lamellulae between two entire lamellae. *Stipe* 40–60 × 4–5 mm, cylindrical, white to yellowish-grey (4B2), covered by a glutinous layer. *Context* thin, whitish.

Basidiospores (6)7–9.5(10) × (4)4.5–5.5(6) µm [mean length = 8.2 µm, mean width = 5 µm], Q =1.3–1.9, Qm =1.65, broadly ellipsoid, ellipsoid to oblong, smooth, hyaline. *Basidia* (32)35–46(48) × (6)6.5–8.5(9) µm, Q = 4.4–6.8, Qm = 5.5, clavate,

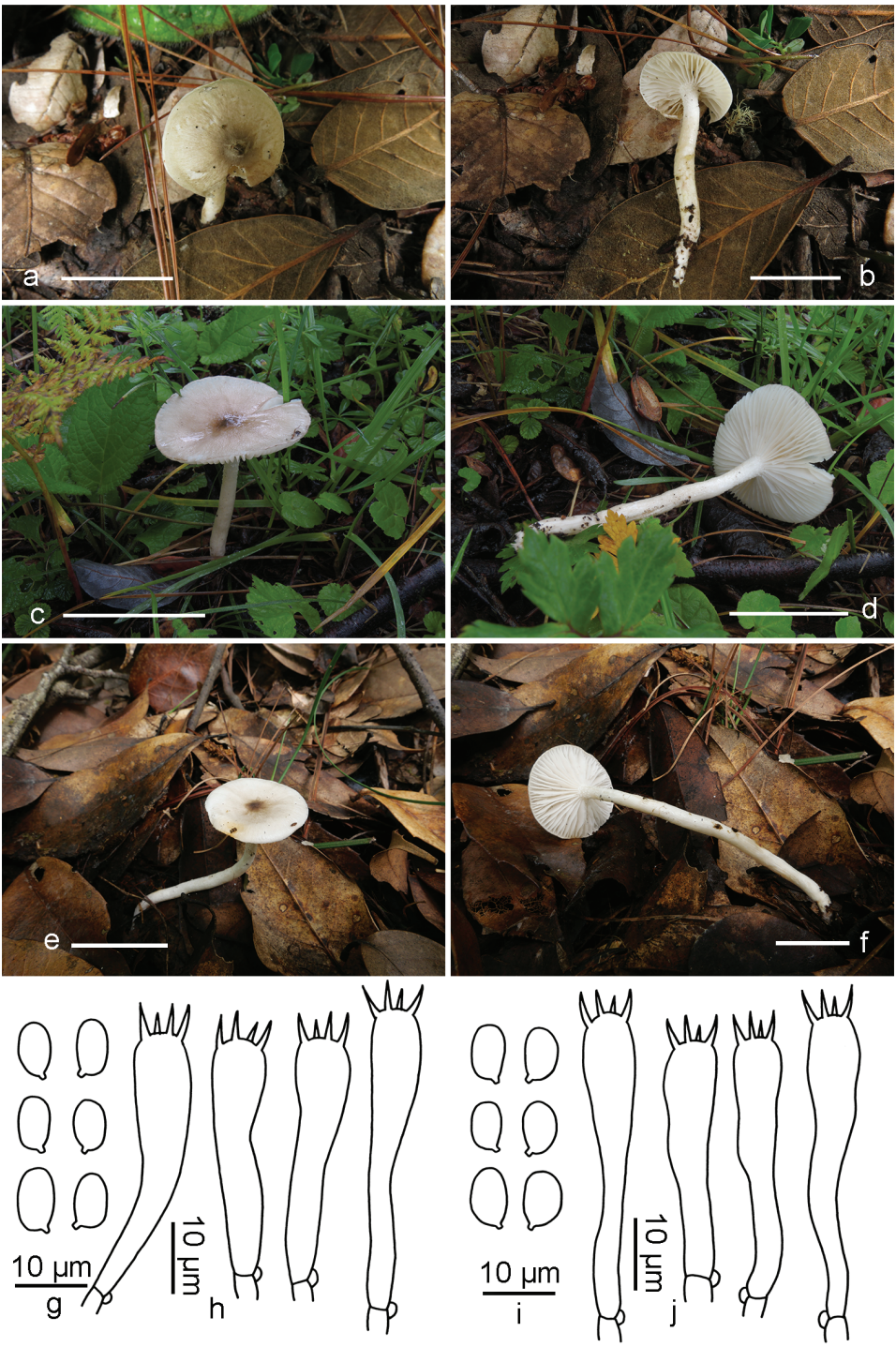

Figure 4. *Hygrophorus fuscopapillatus*. **a, b** Basidiomata (GDGM44412, Holotype) **c, d** Basidiospores Basidiomata (LJW1858) **e, f** Basidiospores and Basidia (XHW6609) **g, h** Basidiospores and Basidia (GDGM44412) **i, j** Basidiospores and Basidia (LJW1858). Scale bars: 2 cm (**a–f**).

thin-walled, 4-spored, with sterigmata 5–7.5 µm long. *Pileipellis* an ixotrichoderm, composed of septate and thin-walled cylindrical hyphae, covered with a gelatinous layer; hyphal cells 3–5 µm broad. *Hymenophoral trama* divergent, composed of septate, thin-walled and cylindrical hyphae; hyphal elements 13–31.5 µm broad. *Clamp connections* present.

Habit, habitat and distribution. Solitary, on the ground of Fagaceae-dominated forests, so far only known from Sichuan and Yunnan provinces in Southwest China.

Additional specimens examined. China, Yunnan Province, Yulong County, Jade Dragon Snow Mountain, Lijiang Alpine Botanic Garden, on the ground of *Quercus pannosa* dominated forest, elev. ca. 3267 m, 27°00'02"N, 100°10'52"E, 31 August 2019, J.W. Liu (LJW1858); Binchuan County, Jizushan, on the ground of *Castanopsis* and *Lithocarpus* dominated forest, elev. ca. 2853 m, 25°58'06"N, 100°21'39"E, 18 September 2019, X.H. Wang (XHW6609).

Remarks. *Hygrophorus fuscopapillatus* is distinguished by the solitary basidiomes, the brownish-grey to olive brown papilla in the pileus centre, the broadly ellipsoid, ellipsoid to oblong basidiospores measuring (6)7–9.5(10) × (4)4.5–5.5(6) µm.

Amongst the members of subsect. *Hygrophours*, *H. griseodiscus* closely resembles *H. fuscopapillatus*; however, *H. griseodiscus* differs from *H. fuscopapillatus* by the host association with Pinaceae, the larger pileus (2–4.5 cm broad), the emarginate lamellae with decurrent tooth, the larger basidispores measuring (7)8–10(10.5) × (4)4.5–6(6.5) µm and the broader basidia (7–11 mm broad). In addition, *H. brunneodiscus* is distinguished from *H. fuscopapillatus* by the broader pileus (2–5 cm in diam.) and the brownish pileus disc. *Hygrophorus cossus* is separated by the larger pileus (3–9 cm in diam.), greyish-white lamellae with a cream yellow tint and a thicker stipe (0.6–2 cm broad) (Larsson and Jacobsson 2004). *Hygrophorus discoxanthus* differs by the rusty brown lamellae when mature and the wider stipe (up to 1.2 cm broad); *H. eburneus* is distinguished by the gregarious habit, the more robust basidiomes and the white pileus (Candusso 1997, Larsson and Jacobsson 2004). *Hygrophorus glutiniceps* differs by the subtropical to tropical distribution and smaller basidiospores measuring (5)6–8.5(10) × (3.5)4–6 µm. *Hygrophorus hedrychii* is separated by the larger basidiomes (pileus up to 8 cm in diam.) and the reddish-yellow pileus centre (Larsson and Jacobsson 2004). *Hygrophorus scabrellus* is distinguished by the off-white with dark green pileus, the off-white to beige lamellae and the much smaller basidiospores measuring 6.5 × 3.84 µm (Naseer et al. 2019).

Hygrophorus glutiniceps C.Q. Wang & T.H. Li, sp. nov.

Fungal Names: FN 570663
Figures 5, 6

Typification. China, Guangdong Province, Guangzhou City, Tianluhu Forest Park, on the ground of a forest dominated by *Castanopsis fissa*, elev. ca. 250 m, 23°13'39"N, 113°25'53"E, 6 September 2012, M. Zhang (GDGM42188, Holotype!), ITS MN378313.

Figure 5. Basidiomata of *Hygrophorus glutiniceps*. **a, b** GDGM42140 **c** GDGM42154 **d** GDGM42188 (Holotype) **e** GDGM42217 **f** GDGM45220. Scale bars: 2 cm.

Etymology. "*glutini-*": glutinous, "*-ceps*": pileus. The species epithet "*glutiniceps*" (Lat.) refers to the glutinous surface of pileus.

Diagnosis. *Hygrophorus glutiniceps* differs from *H. discoxanthus* by the subtropical to tropical distribution, the darker lamellae and the thinner stipe (3–6 mm broad).

Description. *Pileus* 8–40 mm broad, hemispherical to convex, often with an inconspicuous umbo and a usually involute margin when young, broad-convex to depressed with a slightly incurved to rarely uplifting margin when mature, covered with a layer of gelatine-like or transparent gluey materials when wet, white with cream or light yellow to orange tint (4A2–4) at disc, becoming light to yellowish-brown (5E8) with age (especially at margin and in wounded area), usually brownish-orange

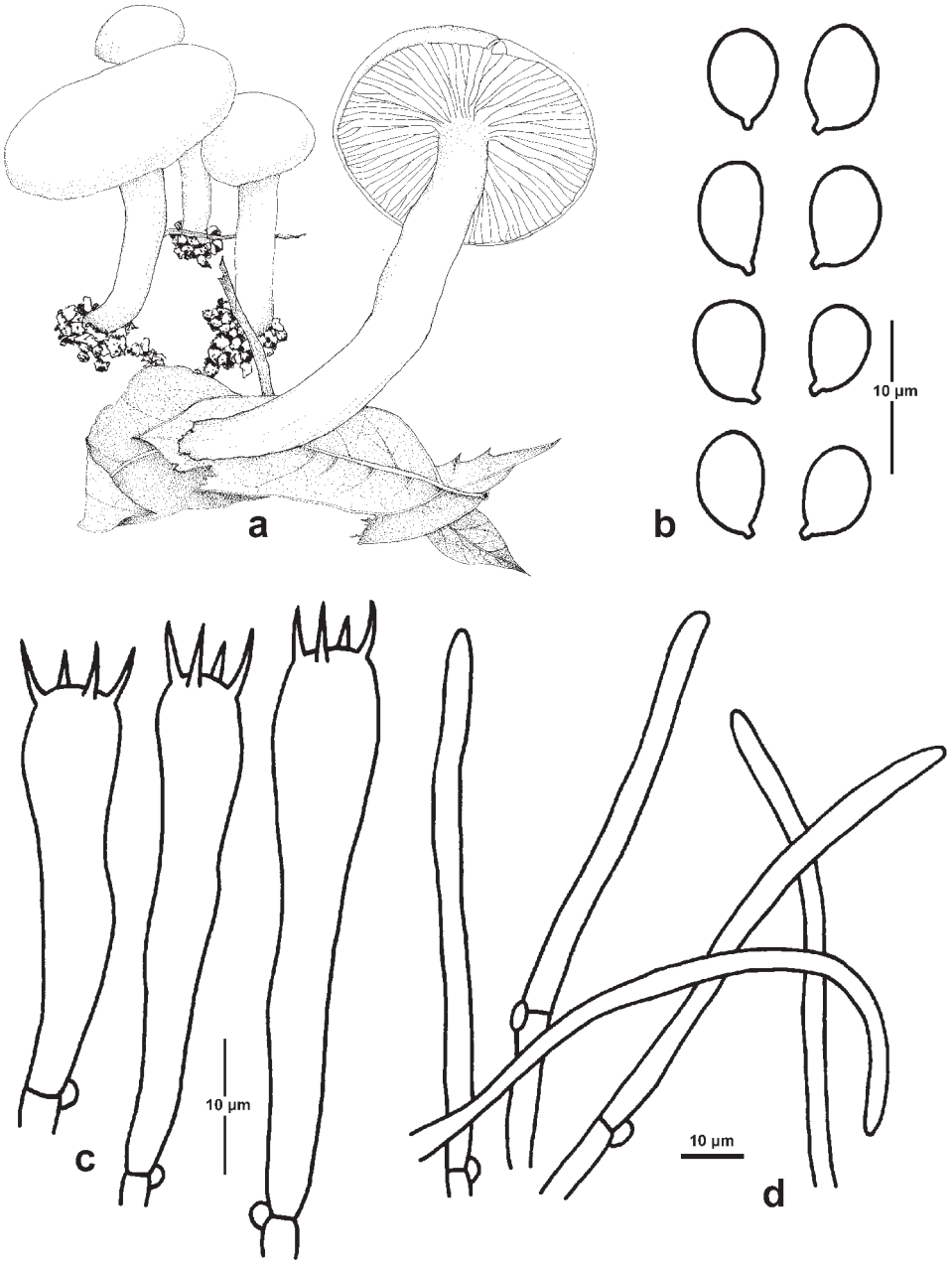

Figure 6. Macro- and microscopic features of *Hygrophorus glutiniceps*. **a** Basidiomata (GDGM42217) **b** Basidiospores (GDGM42188) **c** Basidia (GDGM42188) **d** Terminal cells of pileipellis (GDGM42188).

(5C5) to brown (6E8) when exsiccated. *Lamellae* broadly adnate or with decurrent tooth when young, short to moderately decurrent when mature, white when young, then changing to ochraceous or even brown (6E8), waxy when wet, with 25–30 com-

plete lamellae reaching to stipe and 1–3 lamellulae between two entire lamellae. *Stipe* 25–60 × 3–6 mm, equal but often thinner at the base, cylindrical but usually curved, white, occasionally with yellowish tint (2A2), covered with transparent glutinous materials when wet. *Context* thin, white when young, changing to brown when old.

Basidiospores (5)6–8.5(10) × (3.5)4–5.5(6) μm [mean length = 7.1 μm, mean width = 4.7 μm], Q = (1.2)1.3–1.77(2), Q_m = 1.52, ellipsoid to oblong, smooth, hyaline. *Basidia* 35–47 × 5–8.5 μm, Q values usually more than 5, clavate, thin-walled, 4-spored, with sterigmata up to 7.5 μm long, hyaline. *Pileipellis* an ixotrichoderm, composed of septate hyphae, usually covered with a gelatinous layer; hyphae thin-walled, 3–5 μm wide, with yellowish gluten in KOH. *Stipitipellis* an ixotrichoderm, hyphae 3–5 μm wide, similar to those of pileipellis. *Hymenophoral trama* divergent, composed of septate, thin-walled and cylindrical hyaline in 4–17 μm diam. *Clamp connections* present.

Habit, habitat and distribution. Gregarious to scattered, on the ground of subtropical broad-leaf forest dominated by *Castanopsis*, currently only known from subtropical to tropical areas of China.

Additional specimens examined. China, Guangdong Province, Guangzhou City, Tianluhu Forest Park, 6 September 2012, M. Zhang (GDGM42217); ibidem, 6 September 2012, J. Xu (GDGM42140). Hainan Province, Changjiang County, 3 July 2013, M. Zhang (GDGM45220); Baisha County, Yinggeling National Nature Reserve, elev. ca. 600 m, 1 August 2015, N.K. Zeng 2452 (FHMU1578); Ledong County, Yinggeling National Nature Reserve, elev. ca. 650 m, 4 June 2017, N.K. Zeng 3052 (FHMU2013).

Remarks. *Hygrophorus glutiniceps* is macro-morphologically characterised by its subtropical-tropical distribution, white and sticky pileus and stipe, darkening lamellae when mature or wounded. The size of basidiospores [(5)6–8.5(10) × (3.5)4–5.5(6) μm] and basidia [35–47 × 5–8.5 μm] can be used to confirm the recognition. The association with *Castanopsis fissa* is also helpful for its identification.

Hygrophorus glutiniceps can be morphologically distinguished from closely-related species by the following differences. *Hygrophorus cossus* looks different from *H. glutiniceps* in the different ectomycorrhizal connection (with *Quercus*), the temperate distribution, the longer basidiospores [(7–9.5 μm long in Candusso (1997), 7–9 μm long in Larsson and Jacobsson (2004)] and the higher ratio of length to width [Qm = 1.7–1.75 in Candusso (1997)]. *Hygrophorus eburneus* differs in the different host-connection (with *Fagus*), thicker stipe (7–10 mm in width) and larger basidiospores (8–10 × 4.5–5.5 μm) with larger Qm (1.78–1.82); *H. discoxanthus* differs in the different host-connection (with *Fagus*), the more rusty brown tint on pileus and lamellae and the thicker stipe (5–12 mm in width); *H. hedrychii* differs in the different host-connection (with *Betula*) and larger pileus (30–60 mm broad); *H. laurae* Morgan has a much larger basidioma (with pileus 20–40 mm broad) and a wash of red or brown on the disc; and *H. laurae* var. *decipiens* Peck, described from New York, USA, differs in the absence of the pileus discolouration when dry and the nearly unchangeable lamellae (Morgan 1883, Peck 1905, Candusso 1997, Larsson and Jacobsson 2004).

Hygrophorus griseodiscus **C.Q. Wang & T.H. Li, sp. nov.**
Fungal Names: FN 570000
Figure 7

Typification. China, Sichuan Province, Jiuzhaigou, elev. ca. 3100 m, 11 September 2012, X.L. He (SAAS462, Holotype!), ITS MN378338.

Etymology. "*griseo-*": grey, "*-discus*": pileus. The species epithet "*griseodiscus*" (Lat.) refers to the grey disc of the pileus.

Diagnosis. *Hygrophorus griseodiscus* is distinguished from *H. brunneodiscus* by the greyish pileus with a darker grey pileus disc and larger basidiospores measuring (7)8–10(10.5) × (4)4.5–6(6.5) μm.

Description. *Pileus* 20–45 mm broad, convex, obtusely umbonate at disc, grey to light grey (1C1, 1D1), medium to dark grey or olive grey (1E1, 1F1–4) at disc, white to pale grey (1B1) at margin, glutinous when wet; margin even, slightly involuted to extended. *Lamellae* emarginate with decurrent tooth or subdecurrent, white, thick, subcrowded, unequal, with 1–3 lamellulae between two entire lamellae. *Stipe* 40–70 × 4–6 mm, cylindrical, white to pale grey (1B1), covered with transparent glutinous materials when wet. *Context* slightly thick, white.

Basidiospores (7)8–10(10.5) × (4)4.5–6(6.5) μm [mean length = 9 μm, mean width = 5.2 μm], Q = 1.4–2.1, Qm = 1.74, ellipsoid, oblong to subcylindrical, smooth, hyaline. *Basidia* 29–56.5 × 7–11 μm, Q = 3.05–6(6.9), Qm = 4.39, clavate to cylindrical, thin-walled, 4-spored, with sterigmata up to 6 μm long. *Pileipellis* an ixotrichoderm, covered with a gelatinous layer; hyphae thin-walled, 2.5–6 μm wide. *Hymenophoral trama* divergent, composed of septate, thin-walled and cylindrical hyphae; hyphal cells 5.5–20 μm in width, hyaline. *Clamp connections* present.

Habit, habitat and distribution. Scattered, on the ground of subalpine coniferous forest dominated by *Abies* and *Picea*, often surrounded by mosses, so far only known from Sichuan Province in Southwest China.

Remarks. *Hygrophorus griseodiscus* is characterised by its convex and grey pileus with a dark grey to olive grey disc, emarginate to subdecurrent lamellae. The Asian subalpine coniferous habitat may be a helpful character for its identification.

Morphologically, *H. brunneodiscus* is distinguished from *H.griseodiscus* by the brownish pileus disc and smaller basidiospores (6.5–9.5 × 4–5 μm). *Hygrophorus cossus* differs in the greyish-white lamellae with a cream yellow tint and a thicker stipe (6–20 mm wide) (Candusso 1997, Campo 2015). *Hygrophorus discoxanthus* can be separated by the pure white pileus when young and rusty brown lamellae when mature (Candusso 1997, Campo 2015). *Hygrophorus eburneus* is different by the white pileus and the wider basidiospores (8–10 × 4.5–5.5, Qm = 1.78–1.82) (Candusso 1997). *Hygrophorus glutiniceps* is separated by the white pileus with cream or light yellow to orange tint at the disc, shorter basidiospores [(5)6–8.5(10) × (3.5)4–6 μm] and subtropical to tropical distribution. *Hygrophorus hedrychii* is distinguished by the presence of a pale orange tint on the pileus disc and an orange-pink tint on the lamellae (Larsson

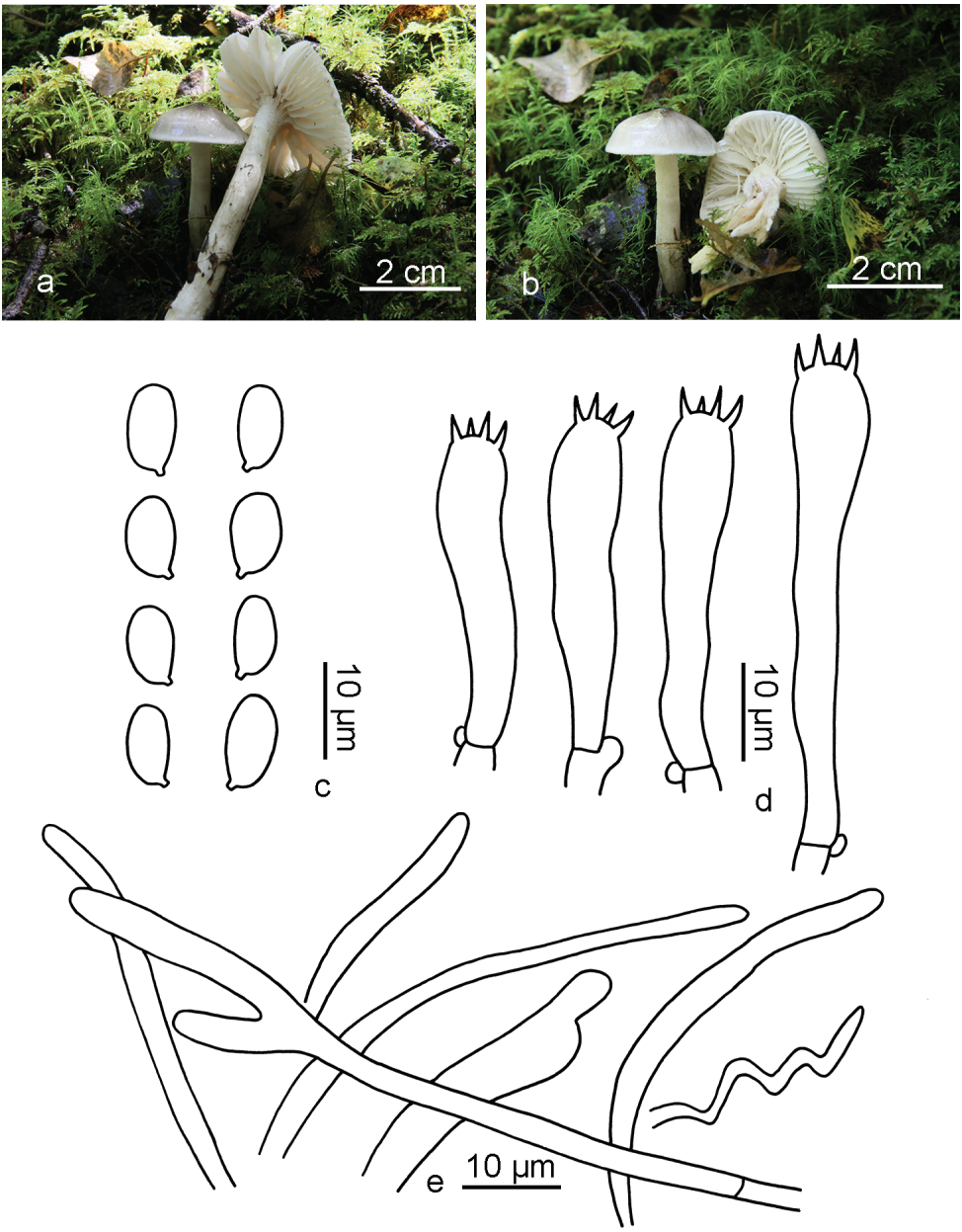

Figure 7. *Hygrophorus griseodiscus* (SAAS462, Holotype). **a, b** Basidiomata **c** Basidiospores **d** Basidia **e** Elements of pileipellis.

and Jacobsson 2004). *Hygrophorus scabrellus* is readily distinguished from *H. brunneodiscus* by its smaller basidiomata (pileus 2.4–2.8 cm broad), dark green tint on pileus and much smaller basidiospores (6.5 × 3.84 µm) (Naseer et al. 2019).

***Hygrophorus hedrychii* (Helen.) K. Kult, Česká Mykol. 10(4): 232 (1956)**
Figure 8

Description. *Pileus* 10–50 mm broad when dried, subglobose when young, becoming hemispherical, convex to nearly plane when mature; margin incurved when young, even, expanded to sometimes slightly upturned when mature; surface covered with a thick layer of transparent and sticky materials, white, with pinkish (7A2) to yellowish (4A2) tones or cream colour (1A2) on the disc. *Lamellae* adnate to short decurrent, white at first, changing to pinkish-white (7A2) or pale yellow (4A3) or cream colour (1A2), waxy, with 1–3 lamellulae between two entire lamellae. *Stipe* 20–85 × 3–10 mm when dried, cylindrical or nearly so, often thinner at apex, usually slightly enlarged at base, uneven, with white short fibrils at apex, sometimes longitudinally lacerated when mature, covered with a layer of transparent sticky materials, white, changing to orange white (5A2, 6A2) where touched. *Context* thick, white when young, pale to pinkish-yellow when mature, with *Cossus* smell.

Basidiospores (6)7–8(9) × (3.5)4–4.5(5) μm, Q = 1.5–2(2.3), Qm = 1.8, ellipsoid to subcylindrical, colourless, thin-walled, smooth. *Basidia* 30–40 × 6–9 μm, Q = 4.1–5.7, clavate, 4-spored; sterigmata 4–5 μm long; basal clamp connections common. *Pileipellis* an ixotrichoderm, composed of septate hyphae, covered with a gelatinous layer; hyphae thin-walled, 4–5 μm wide. *Stipitipellis* a trichoderm; hyphae 7–10 μm wide, light yellowish-brown intracellular pigment presented in a few hyphae when immersed in 5% KOH solution. *Hymenophoral trama* composed of septate, thin-walled and cylindrical hyaline hyphae, size 58–105 × 3–23 μm. *Clamp connections* present.

Habit, habitat and distribution. Scattered to gregarious in the north temperate forests dominated by *Betula*, known from north-eastern China (this study), as well as from Europe where the species was firstly discovered.

Specimens examined. China, Inner Mongolia Autonomous Region, Chifeng City, Harqin Banner, Wangyedian village, 30 August 2007, T.Z. Liu (CFSZ2851); ibidem, 8 August 2017, T.Z. Liu, Y.Q. Guang & N. Liu (CFSZ18159); Hexigten Banner, Jingpeng Town, 15 August 2017, T.Z. Liu & G.L. Yu (CFSZ18269).

Remarks. Macroscopically, *Hygrophorus hedrychii* is a distinctive waxycap, which is relatively easily recognised in the field by its white pileus disc and lamellae changing to pale ochraceous pink when mature and the host association with birch. Microscopically, the Chinese specimens agree with the descriptions by Larsson and Jacobsson (2004) for the Swedish samples and Campo (2015) for the French collections. Molecular phylogenetically, they are also identical to the European species. The Chinese samples from Inner Mongolia are traded as edible fungi at some local markets. The European *H. hedrychii* was not, however, treated as an edible mushroom (Larsson, personal communication). This difference may indicate different dietary habits in different areas.

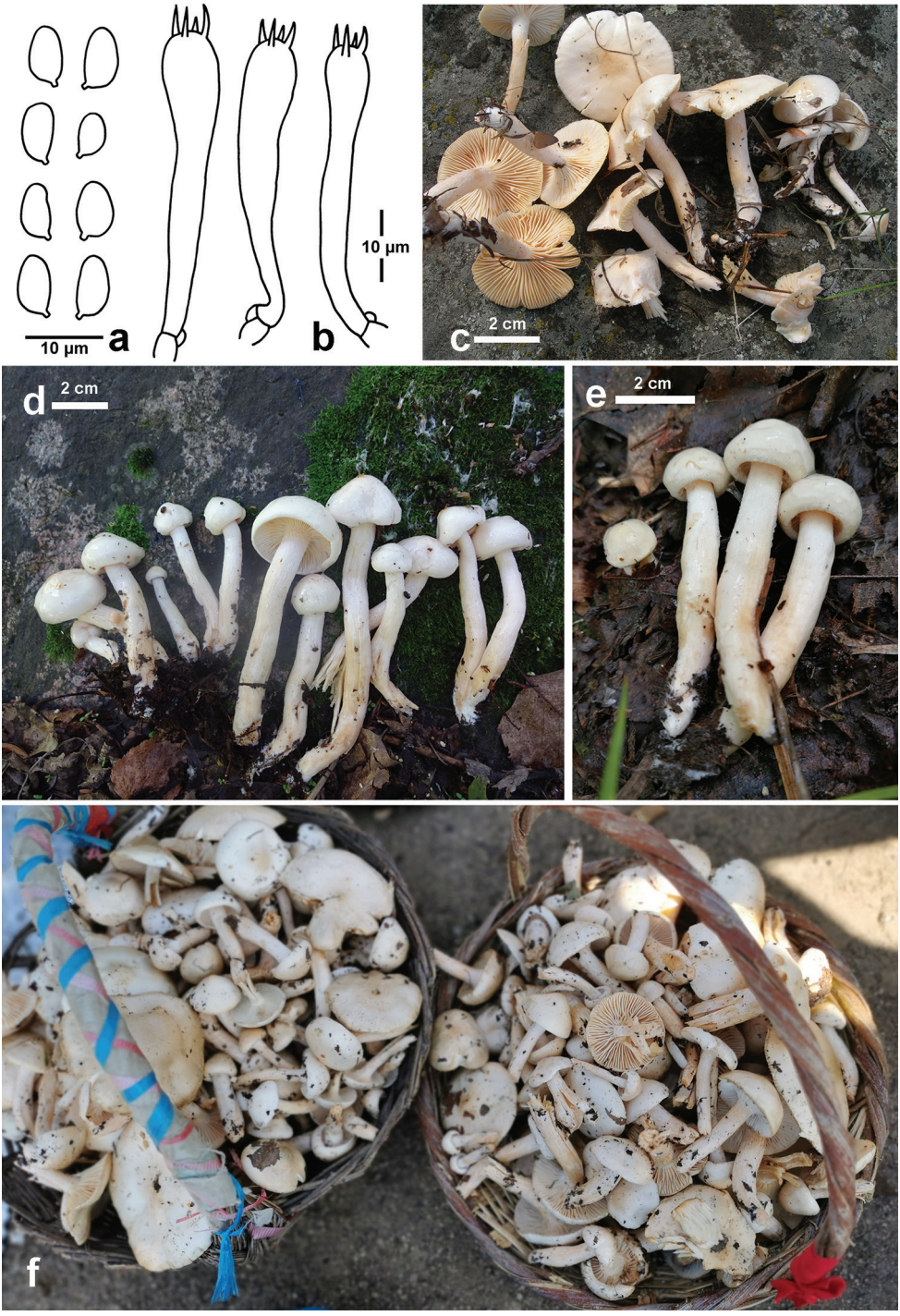

Figure 8. *Hygrophorus hedrychii*. **a** Basidiospores **b** Basidia **c** Basidiomata (CFSZ2851) **d** Basidiomata (CFSZ18159) **e** Basidiomata (CFSZ18269) **f** Sold at a local market, named as "baizhenmo".

Discussion

Phylogeny and circumscription of subsect. *Hygrophorus*

In recent years, the phylogenetic framework of *Hygrophorus* has been reconstructed by Lodge et al. (2014), based on morphological characteristics and 1–4 gene regions, based phylogenetic analyses, thus, the subsect. *Hygrophorus* has been inclusively redefined. In order to assess the monophyly of subsect. *Hygrophorus*, a LSU-based phylogeny overview of the genus *Hygrophorus* and an ITS-based phylogeny overview of subsect. *Hygrophorus* are made in this study. According to the LSU tree, most species' sequences of subsect. *Hygrophorus* are well-grouped in a clade, but three sequences with species names outside of subsect. *Hygrophorus* (MK278183 named as "*H.* cf. *arbustivus*", MK278193 named as "*H. lindtneri*" and MK278194 named as "*H. marzuolus*") are inserted in the clade of subsect. *Hygrophorus.* It is well-known that *H. arbustivus* and *H. lindtneri* are members of subgen. *Hygrophorus*/sect. *Hygrophorus*/subsect. *Fulventes* and *H. marzuolus* is a member of subgen. *Camarophylli*/sect. *Camarophylli*, according to Lodge et al. (2014). If the sequences were well-identified, it is necessary to reassess their taxonomic positions or reconsider the phylogeny framework of subsect. *Hygrophorus*. However, through careful checking, it was found that all three sequences were submitted by Varga et al. (2019), which mainly focused on the phylogeny reconstruction of various higher agaric taxa in a much larger scale, the species identification of the sequences not being the focus of that paper. Therefore, the correctness of the sequences' identification is still questionable.

According to the ITS phylogenetic tree in this study, subsect. *Hygrophorus* is monophyletic. Thus, the concept of subsect. *Hygrophorus* proposed by Lodge et al. (2014) is acceptable at present, since both LSU and ITS analyses are not strongly in conflict with the circumscription. In the future, analyses, based on more samples and additional genes, are still needed.

The species diversity of subsect. *Hygrophorus*

Previously, five species were confirmed as members of subsect. *Hygrophorus*, including *H. cossus*, *H. discoxanthus*, *H. eburneus*, *H. hedrychii* and *H. scabrellus* (Larsson and Jacobsson 2004, Lodge et al. 2014, Naseer et al. 2019). In this study, at least 13 phylogenetic species-level clades are presented as members of subsect. *Hygrophorus*, according to ITS-based analysis (Fig. 2), although some species are still to be verified or to be formally named.

Apart from the four new species from China, proposed in this study (*H. brunneodiscus*, *H. fuscopapillatus*, *H. glutiniceps* and *H. griseodiscus*), two species with American sequence samples ("*H. chrysaspis* Métrod" and *H. occidentalis* A.H. Sm. & Hesler) and two undescribed species, *H.* sp1 from Europe and *H.* sp2 from North America, are present as phylogenetic species under subsect. *Hygrophorus*. Four sequences labelled as "*H. chrysaspis*" from USA are grouped together. Al-

Table 2. Morphological characteristics of known species of subsect. *Hygrophorus*.

Species	Pileus size (cm)	Colour of mature pileus	Colour of lamellae	Stipe width (cm)	Spore size (μm)	Host-connection	Reference
H. brunneodiscus	2–5	White with brownish-orange to light brown at the disc	White	0.4–0.7	6.5–9.5 × 4–5	*Quercus*	This study
H. cossus	3–9	Pale ochraceous grey at the centre of the pileus	Greyish-white with a cream yellow tint	0.6–2.0	7–9 × 4–5	*Quercus*	Larsson and Jacobsson 2004
H. discoxanthus	3–7	White with rusty-brown margin upon drying	White as young, then rusty brown	0.5–1.2	6.5–9 × 3.5–5.5	*Fagus*	Larsson and Jacobsson 2004
H. eburneus	2–7	White	Cream-white as young then cream-yellow	0.4–1.0	7.5–10 × 4–5.5	*Fagus*	Larsson and Jacobsson 2004
H. fuscopapillatus	2–3	White to pale grey at margin, pale grey to olive brown at papilla	White	0.4–0.5	(6)7–9.5(10) × (4)4.5–5.5(6)	Fagaceae	This study
H. glutiniceps	0.8–4	White with cream or light yellow to orange tint at disc	White when young, then changing to ochraceous or even brown	0.3–0.6	(5)6–8.5(10) × (3.5)4–6	*Castanopsis*	This study
H. griseodiscus	2–4.5	Grey to light grey with dark grey at disc	White	0.4–0.6	(7)8–10(10.5) × (4)4.5–6(6.5)	*Abies* or *Picea*	This study
H. hedrychii	3–8	White with orange-pinkish tint at centre	White with orange-pinkish tint	0.5–1.0	6.5–9 × 3.5–5	*Betula*	Larsson and Jacobsson 2004
H. occidentalis	2–8(10)	"hair brown" to "fuscous", at times yellowish or smoky at disc	White then tinged cream	0.3–1(1.5)	6–8 ×3.5–5	unclear	Hesler and Smith 1963
H. scabrellus	2.4–2.8	Off-white with dark green	Off-white to beige	2.1–2.4	6.5 × 3.84	*Quercus*	Naseer et al. 2019

though the North American samples have not been proved to be conspecific with the European *H. chrysaspis* (originally described from France) with molecular evidence due to the absence of the French sequence, the USA samples can still present a member of subsect. *Hygrophorus*; in addition, Hesler and Smith (1963) has also mentioned that the USA *H. chrysaspis* resembled *H. eburneus* (the type species of subsect. *Hygrophorus*). The American species *H. occidentalis*, originally described from Michigan (USA), is further confirmed as a member of subsect. *Hygrophorus* in this study (Table 2), since the isotype's sequence (MH656479) is included; it had been regarded as a grey to fuscous member of *H. eburneus* complex, based on morphological evidence (Hesler and Smith 1963). Thus, *H. occidentalis* should be included in subsect. *Hygrophours* (Table 2).

It is worth mentioning that the species diversity within subsect. *Hygrophorus* may be underestimated for these two main reasons: 1) some species from the well-studied countries may have been left out. For example, *H. occidentalis* had been listed in the North American monograph (Hesler and Smith 1963), but it was not included in Lodge et al. (2014) since the absence of sequences at that time. 2) Many areas

have been less investigated or not at all. Taking the ITS gene sequences as an example (Fig. 2), the majority sequences come from European and USA samples and very few sequences come from Africa, Oceania or South America, where there might be many taxa, different from those of Europe and North America.

Morphology and sequence misidentification in subsect. *Hygrophorus*

Some *Hygrophorus* taxa are difficult to be distinguished with the naked eye by the specific differences of macro-morphological characteristics and it will be harder when considering the infraspecific variations; the microscopic features for distinguishing *Hygrophorus* species are also limited, since they usually lack cystidia and have slight interspecific differences in the size and shape of basidiospores and basidia.

Due to the morphological similarity, misidentifications are common in subsect. *Hygrophorus.* For example, 15 samples with the same name as "*H. eburneus*" are included in the analysis (Fig. 2), but they are nested in different positions in the phylogram, which indicates that at least some of them are misidentified. The sequences of AY242855, AY463484, AY463485 and UDB000555 from Sweden (where the species was originally described) are identified in Larsson and Jacobsson (2004) and they should be the true *H. eburneus*. Some other European sequences, i.e. MK028422 from Switzerland, MK088116 from Hungry, MK627047 from Austria and UDB000021 labelled as "*H. discoxanthus*" from Denmark, are clustered with those real *H. eburneus* sequences from Sweden with strong support (94% BS); they should also be conspecific and treated as *H. eburneus*. These European sequences form a clade of "*H. eburneus* (Europe)". On the other hand, there are eight sequences from USA which are gathered together in the phylogram with 95% BS, forming a sister clade to the European *H. eburneus.* Due to the close molecular similarity and the lack of adequate morphological comparison and other information, they are still treated as *H. eburneus* here as a clade of "*H. eburneus* (North America)". However, the sequence MK737049, labelled as "*H.* cf. *eburneus*" from USA, is isolated from the true *H. eburneus*; thus, it should represent an unidentified species. In addition, the two other sequences, MK575431 from USA and DQ367904 from Canada, labelled as "*H. eburneus*" and "*H. eburneus* var. *eburneus*" respectively, are grouped as a sister clade of the Europe-Asia *H. hedrychii* clade with 100% BS. Obviously, MK575431 and DQ367904 are not the true "*H. eburneus*", though it is not clear whether they are *H. hedrychii* or not since the species boundaries of *H. hedrychii* are not clear enough. The sequence MK564560 from USA, labelled as "*H. eburneus*", should also be misidentified since it is clustered with the sequences (MK575247 and MF686502) of "*H. chrysaspis*".

It is worthy to mention that, although some samples might have been misidentified, their molecular sequences can still provide some useful information for analysing the relationships amongst the samples or even potentially representing some undescribed taxa and reflecting richer species diversity.

The distribution of Chinese species of subsect. *Hygrophorus*

Ecologically, according to the authors' investigation since 2010, *Hygrophorus* species are relatively rare in the subtropical to tropical areas of Guangdong and Hainan Provinces in South China. The reports of the Chinese *Hygrophorus* are mainly concentrated in the temperate regions and in the high-elevation areas of subtropical zone (Zeng and Yang 1991, Yuan and Sun 2007, Chen and Li 2013). With the description of *H. glutiniceps*, it is scientifically confirmed from the genetic level that the distribution of *Hygrophorus* species can extend to the southernmost province of China (tropical Hainan Province).

With the application of integrative taxonomy, considering the morphology characteristics, molecular data, the symbiotic association of plants etc., it is now easier to distinguish species within subsect. *Hygrophorus.* Even the study of genus *Hygrophorus* has entered an era in which a mass of new species have been discovered (Jacobsson and Larsson 2007; Yu et al. 2007; Larsson et al. 2014, 2018; Endo et al. 2018; Moreau et al. 2018; Huang et al. 2018; Naseer et al. 2019). Due to the support of the Chinese government, many mushroom investigations are being carried out. It is foreseeable that, in the next few years, a large number of new species will be reported from China and the distribution of species under subsect. *Hygrophorus* will be expanded.

Acknowledgements

The authors sincerely thank the editors and reviewers for their valuable comments and suggestions. Thanks are given to Dr David Hibbett for giving specimens to the first author. Thanks are given to Dr Yi-Jian Yao and Ms Liu Yang for their help in loaning specimens. Thanks are given to Mr Jun-Yan Xu for identifying plant species. This study is supported by the National Natural Science Foundation of China (Nos. 31800013, 31760004), the GDAS' Project of Science and Technology Development (No. 2020GDASYL-20200104013), the Biodiversity Survey and Assessment Project of the Ministry of Ecology and Environment, China (No. 2019HJ2096001006), the Science and Technology Planning Project of Guangdong Province, China (Nos. 2018B030324001, 2018B020205001) and the Science and Technology Planning Project of Guizhou Province, China (No. Qian Ke He Fu Qi [2019] 4007).

References

Benson DA, Cavanaugh M, Clark K, Karsch-Mizrachi I, Ostell J, Pruitt KD, Sayers EW (2017) GenBank. Nucleic Acids Research 46(D1): D41–D47. https://doi.org/10.1093/nar/gkx1094

Candusso M (1997) *Hygrophorus* s.l., Fungi Europaei 6. Alassio, 1–748.

Campo E (2015) *Hygrophorus*, *Hygrocybe* e *Cuphophyllus* del Friuli Venezia Giulia. Gruppo Mycologico Sacilese, 1–181.

Chen JL, Li Y (2013) The checklist of species in Hygrophoraceae from China and their distribution. Journal of Fungal Research 11: 3–13, 37. [in Chinese]

Endo N, Tokoo R, Fukuda M, Yamada A (2018) *Hygrophorus yukishiro* sp. nov., a new vernal edible mushroom from Nagano Prefecture, Japan. Mycoscience 59: 449–454. https://doi.org/10.1016/j.myc.2018.03.002

Gardes M, Bruns TD (1993) ITS primers with enhanced specificity for basidiomycetes-application to the identification of mycorrhizae and rusts. Molecular Ecology 2: 113–118. https://doi.org/10.1111/j.1365-294X.1993.tb00005.x

Huang HY, Yang SD, Zeng NK, Zhang GL, Hu Y, Tang LP (2018) *Hygrophorus parvirussula* sp. nov., a new edible mushroom from southwestern China. Phytotaxa 373: 139–146. https://doi.org/10.11646/phytotaxa.373.2.4

Jacobsson S, Larsson E (2007) *Hygrophorus penarioides*, a new species identified using morphology and its sequence data. Mycotaxon 99: 337–343.

Katoh K, Rozewicki J, Yamada KD (2017) MAFFT online service: multiple sequence alignment, interactive sequence choice and visualization. Briefings in Bioinformatics, 1–7. https://doi.org/10.1093/bib/bbx108

Kornerup A, Wanscher JH (1978) Methuen Handbook of Colour. Eyre Methuen, London, 1–252.

Larsson E, Jacobsson S (2004) Controversy over *Hygrophorus cossus* settled using ITS sequence data from 200 year-old type material. Mycological Research 108: 781–786. https://doi.org/10.1017/S0953756204000310

Larsson E, Campo E, Carbone M (2014) *Hygrophorus exiguus*, a new species in subgenus *Colorati* section *Olivaceoumbrini*, subsection *Tephroleuci*. Karstenia 54: 41–48. https://doi.org/10.29203/ka.2014.462

Larsson E, Kleine J, Jacobsson S, Krikorev M (2018) Diversity within the *Hygrophorus agathosmus* group (Basidiomycota, Agaricales) in Northern Europe. Mycological Progress 17(2): 1293–1304. https://doi.org/10.1007/s11557-018-1445-y

Letunic I, Bork P (2016) Interactive tree of life (iTOL) v3: an online tool for the display and annotation of phylogenetic and other trees. Nucleic Acids Research 44(W1): W242–W245. https://doi.org/10.1093/nar/gkw290

Liu Y, Tang H, Li XW, Chen ZH, Lei ZY, Xiang L (2016) Identification of medicinal and edible fungi (Agaricales) through internal transcribed spacer barcode. World Chinese Medicine 11: 791–795. [in Chinese]

Lodge DJ, Padamsee M, Matheny PB, Aime MC, Cantrell SA, Boertmann D, Kovalenko A, Vizzini A, Dentinger BTM, Kirk PM, Ainsworth AM, Moncalvo JM, Vilgalys R, Larsson E, Lücking R, Griffith GW, Smith ME, Norvell LL, Desjardin DE, Redhead SA, Ovrebo CL, Lickey EB, Ercole E, Hughes KW, Courtecuisse R, Young A, Binder M, Minnis AM, Lindner DL, Ortiz-Santana B, Haight J, Læssøe T, Baroni TJ, Geml J, Hattori T (2014) Molecular phylogeny, morphology, pigment chemistry and ecology in Hygrophoraceae (Agaricales). Fungal Diversity 64: 1–99. https://doi.org/10.1007/s13225-013-0259-0

Moreau PA, Bellanger JM, Lebeuf R, Athanassiou Z, Athanasiades A, Lambert H, Schwarz C, Larsson E, Loizides M (2018) Hidden diversity uncovered in *Hygrophorus*, sect. *Aurei*, (Hygrophoraceae), including the Mediterranean *H. meridionalis* and the North American *H. boyeri*, spp. nov. Fungal Biology 122: 817–836. https://doi.org/10.1016/j.funbio.2018.04.009

Morgan AP (1883) The mycologic flora of the Miami valley, Ohio. Journal of the Cincinnati Society of Natural History 6: 173–199. https://doi.org/10.5962/bhl.title.4044

Naseer A, Khalid AN, Healy R, Smith ME (2019) Two new species of *Hygrophorus* from temperate Himalayan Oak forests of Pakistan. MycoKeys 56: 33–47. https://doi.org/10.3897/mycokeys.56.30280

Nilsson RH, Larsson KH, Taylor AFS, Bengtsson-Palme J, Jeppesen TS, Schigel D, Kennedy P, Picard K, Glöckner FO, Tedersoo L, Saar I, Kõljalg U, Abarenkov K (2019) The UNITE database for molecular identification of fungi: handling dark taxa and parallel taxonomic classifications. Nucleic Acids Research 47: D259–264. https://doi.org/10.1093/nar/gky1022

Peck CH (1905) Report of the state botanist 1904. Bulletin of the New York State Museum 94: 5–58.

Razaq A, Ilyas S, Khalid AN (2014) Taxonomic and phylogenetic affinities of *Hygrophorus chrysodon* from western Himalayan forests. Austrian Journal of Mycology 23: 21–29.

Singer R (1986) The Agaricales in modern taxonomy, 4th edn. Koeltz Scientific Books, Koenigstein, 981 pp.

Trifinopoulos J, Nguyen LT, von Haeseler A, Minh BQ (2016) W-IQ-TREE: a fast online phylogenetic tool for maximum likelihood analysis. Nucleic Acids Research 44(W1): W232–W235. https://doi.org/10.1093/nar/gkw256

Varga T, Krizsán K, Földi C, Dima B, Sánchez-García M, Sánchez-Ramírez S, Szöllősi GJ, Szarkándi JG, Papp V, Albert L, Andreopoulos W, Angelini C, Antonín V, Barry KW, Bougher NL, Buchanan P, Buyck B, Bense V, Catcheside P, Chovatia M, Cooper J, Dämon W, Desjardin D, Finy P, Geml J, Haridas S, Hughes K, Justo A, Karasiński D, Kautmanova I, Kiss B, Kocsubé S, Kotiranta H, LaButti KM, Lechner BE, Liimatainen K, Lipzen A, Lukács Z, Mihaltcheva S, Morgado LN, Niskanen T, Noordeloos ME, Ohm RA, Ortiz-Santana B, Ovrebo C, Rácz N, Riley R, Savchenko A, Shiryaev A, Soop K, Spirin V, Szebenyi C, Tomšovský M, Tulloss RE, Uehling J, Grigoriev IV, Vágvölgyi C, Papp T, Martin FM, Miettinen O, Hibbett DS, Nagy LG. (2019) Megaphylogeny resolves global patterns of mushroom evolution. Nature Ecology & Evolution 3(4): 668–678. https://doi.org/10.1038/s41559-019-0834-1

Vellinga EC (1988) Glossary. In: Bas C, Kuyper ThW, Noordeloos ME, Vellinga EC (Eds) Flora Agaricina Neerlandica, vol. 1. A.A. Balkema, Rotterdam, 54–64.

White TJ, Bruns T, Lee SS, Taylor J (1990) Amplification and direct sequencing of fungal ribosomal RNA genes for phylogenetics. In: Innis MA, Gelfand DH, Sninsky JJ, White TJ (Eds) PCR protocols: a guide to methods and applications. Academic Press, San Diego, 315–322. https://doi.org/10.1016/B978-0-12-372180-8.50042-1

Yu FQ, Xu GB, Liu PG (2007) A new and noteworthy species of *Hygrophorus* from Yunnan, China. Mycotaxon 100: 169–175.

Young AM (2005) Fungi of Australia: Hygrophoraceae. ABRS, Canberra; CSIRO Publishing, Melbourne.

Yuan MS, Sun PQ (2007) Pictorial Book of Mushrooms of China. Sichuan Science and Technology Press, Chengdu, 1–552. [in Chinese]

Zeng XL, Yang WS (1991) Hygrophoraceae of Jilin province. Journal of Northeast Normal University 2: 71–78. [in Chinese]

MycoKeys 68: 75–113 (2020)
doi: 10.3897/mycokeys.68.52092
http://mycokeys.pensoft.net

RESEARCH ARTICLE

A peer-reviewed open-access journal
MycoKeys
Launched to accelerate biodiversity research

New section and species in *Talaromyces*

Bing-Da Sun[1,2*], Amanda J. Chen[3*], Jos Houbraken[4], Jens C. Frisvad[5], Wen-Ping Wu[6], Hai-Lei Wei[7], Yu-Guang Zhou[1], Xian-Zhi Jiang[3], Robert A. Samson[4]

1 *China General Microbiological Culture Collection Center, Institute of Microbiology, Chinese Academy of Sciences, Beijing 100101, China* **2** *State Key Laboratory of Bioactive Substance and Function of Natural Medicines, Institute of Materia Medica, Chinese Academy of Medical Sciences and Peking Union Medical College, Beijing 100050, China* **3** *Microbiome Research Center, Moon (Guangzhou) Biotech Ltd., Guangzhou 510535, China* **4** *Westerdijk Fungal Biodiversity Institute, Uppsalalaan 8, 3584 CT Utrecht, The Netherlands* **5** *Department of Biotechnology and Biomedicine, Technical University of Denmark, Kongens Lyngby, Denmark* **6** *Novozymes China, No. 14, Xinxi Rd, Shangdi, Beijing, China* **7** *Key Laboratory of Microbial Resources Collection and Preservation, Ministry of Agriculture, Institute of Agricultural Resources and Regional Planning, Chinese Academy of Agricultural Sciences, Beijing 100081, China*

Corresponding author: Xian-Zhi Jiang (jxz@moonbio.com); Robert A. Samson (r.samson@wi.knaw.nl)

Academic editor: Pedro Crous | Received 15 March 2020 | Accepted 29 May 2020 | Published 7 July 2020

Citation: Sun B-D, Chen AJ, Houbraken J, Frisvad JC, Wu W-P, Wei H-L, Zhou Y-G, Jiang X-Z, Samson RA (2020) New section and species in *Talaromyces*. MycoKeys 68: 75–113. https://doi.org/10.3897/mycokeys.68.52092

Abstract

Talaromyces is a monophyletic genus containing seven sections. The number of species in *Talaromyces* grows rapidly due to reliable and complete sequence data contributed from all over the world. In this study agricultural soil samples from Fujiang, Guangdong, Jiangxi, Shandong, Tibet and Zhejiang provinces of China were collected and analyzed for fungal diversity. Based on a polyphasic approach including phylogenetic analysis of partial ITS, *BenA*, *CaM* and *RPB2* gene sequences, macro- and micro-morphological analyses, six of them could not be assigned to any described species, and one cannot be assigned to any known sections. Morphological characters as well as their phylogenetic relationship with other *Talaromyces* species are presented for these putative new species. *Penicillium resedanum* is combined in *Talaromyces* section *Subinflati* as *T. resedanus*.

Keywords

Eurotiales, Penicillium resedanum, polyphasic taxonomy, section Tenues, soil

* Contributed equally as the first authors.

Introduction

The genus *Talaromyces* used to accommodate sexual *Penicillium* species (Benjamin 1955). The generic concept has changed in the last decade due to changes in nomenclatural rules and results of phylogenetic studies. Before 2011, various studies showed that asexual reproducing *Penicillium* species classified in subgenus *Biverticillium* and the sexual *Talaromyces* species form a monophyletic clade distinct from *Penicillium sensu stricto* (LoBuglio et al. 1993; Berbee et al. 1995; Ogawa et al. 1997; Ogawa and Sugiyama 2000; Wang and Zhuang 2007; Houbraken and Samson 2011). In 2011, following the concepts of nomenclatural priority and single name nomenclature, Samson et al. (2011) transferred the majority of accepted *Penicillium* subgenus *Biverticillium* species to *Talaromyces*. A monograph of *Talaromyces* was provided based on a polyphasic species concept with seven sections *Bacillispori*, *Helici*, *Islandici*, *Purpurei*, *Subinflati*, *Talaromyces* and *Trachyspermi* (Yilmaz et al. 2014). This sectional classification was further supported by a four gene phylogeny (Chen et al. 2016). The number of species in *Talaromyces* grows rapidly due to reliable and complete sequence data contributed from all over the world (Visagie et al. 2015; Crous et al. 2016, 2017, 2018; Yilmaz et al. 2016a, b; Guevara-Suarez et al. 2017; Peterson and Jurjević 2017; Barbosa et al. 2018; Varriale et al. 2018; Rodríguez-Andrade et al. 2019; Rajeshkumar et al. 2019; Guevara-Suarez et al. 2020). It is noteworthy that in China many new species were discovered with another 19 new species reported (Chen et al. 2016; Wang QM et al. 2016; Wang XC et al. 2016, 2017; Jiang et al. 2018; Su and Niu 2018).

Talaromyces species are commonly distributed in a wide range of substrates, mostly in soil. Their main interest to food mycologists lies in their production of heat resistant ascospores and association with spoilage of pasteurized fruit juices and fruit-based products; the most commonly isolated heat resistant species include *T. bacilisporus*, *T. helicus*, *T. macrosporus*, *T. stipitatus* and *T. trachyspermus* (Dijksterhuis 2007; Pitt and Hocking 2009; Yilmaz et al. 2014). In addition, *T. flavus*, *T. funiculosus*, *T. pinophilus*, *T. purpurogenus*, *T. rugulosus* and *T. wortmannii* have been found quite frequently in food, including fruit, nuts and cereals (Pitt and Hocking 2009). *Talaromyces islandicus* can cause the yellowing of stored rice and has been reported from e.g. flour, peanuts, pecans, soybeans and maize (Saito et al. 1971; Sakai et al. 2005; Oh et al. 2008; Pitt and Hocking 2009).This species produces unique mycotoxins such as cyclochlorotine, islanditoxin, erythroskyrine and luteoskyrin, which are carcinogenic liver and kidney toxins (Uraguchi et al. 1961, 1972; Uraguchi 1962; Ueno and Ishikawa 1969; Bouhet et al. 1976; Stark et al. 1978). Other mycotoxins produced by *Talaromyces* members include rugulosin and skyrin (by members of section *Islandici*), botryodiploidin (*T. coalescens* and *T. stipitatus*), rubratoxin (*T. purpurogenus*), rugulovasine (*T. purpurogenus* and *T. wortmannii*) and secalonic acid D & F (*T. dendriticus*, *T. flavovirens*, *T. funiculosus*, *T. minioluteus*, *T. pseodostromaticus*, *T. siamensis* and *T. stipitatus*) (Yilmaz et al. 2014).

Talaromyces contains several species that are reported to cause infections in humans. *Talaromyces marneffei* has been exclusively associated with acquired immunodeficiency syndrome (AIDS) caused by human immunodeficiency virus (HIV) infections

(Supparatpinyo et al. 1994; Limper et al. 2017). Other species like *T. indigoticus*, *T. helicus*, *T. piceus*, *T. purpurogenus*, *T. radicus*, *T. rugulosus* and *T. verruculosus* have been reported in superficial or disseminated, fatal infections (Horré et al. 2001; Santos et al. 2006; de Vos et al. 2009; Weisenborn et al. 2010; Tomlinson et al. 2011; de Hoog et al. 2014). Recently, four new members of *Talaromyces* were reported from clinical sources, and more studies are needed to complete the distribution and the relevance of these new fungi in human and animal disease (Guevara-Suarez et al. 2017).

On the other hand, species in *Talaromyces* are good producers of anticancer, antibacterial and antifungal compounds (Bladt et al. 2013; Zhai et al. 2016; Nicoletti et al. 2018), antiproliferative and antioxidative compounds (Kumari et al. 2018), enzymes (Isbelia et al. 1999; Narikawa et al. 2000; Pol et al. 2012; Maeda et al. 2013; Antonopoulou et al. 2018; Lian et al. 2018; Xu et al. 2018) and natural colourants (Frisvad et al. 2013; Zaccarim et al. 2018). Several species also proved to be effective biocontrol agents against soil-borne pathogens. *Talaromyces flavus* suppresses Verticillium wilt of tomato, eggplant and potato (Dutta et al. 1981; Marois et al. 1984; Fahima and Henis 1995), parasitizes *Sclerotinia sclerotiorum*, *Rhizoctonia solani* and *Sclerotium rolfsii* (Boosalis 1956; McLaren et al. 1986), degrades cell walls of *Pythium ultimum* and *Fusarium equisetii* (Inglis and Kawchuk 2002), shows antagonistic activities against *Cylindrocarpon destructans*, *Fusarium oxysporum*, *Rhizoctonia solani*, *Sclerotinia nivalis*, *Botrytis cinerea*, *Phytophthora capsici* and increases the dehiscence ratios of ginseng seed (Kim et al. 2017). *Talaromyces pinophilus* shows antagonistic activity and mycoparasitic behavior on *Rhizoctonia solani* and *Botrytis cinerea* (Alagesaboopathi 1994; Abdel-Rahim and Abo-Elyousr 2018) and shows plant growth-promoting effects on Waito-C rice (Khalmuratova et al. 2015).

In this study, we collected agricultural soil samples from Fujiang, Guangdong, Jiangxi, Shandong, Tibet and Zhejiang provinces in China. After isolation and identification, six *Talaromyces* species could not be assigned to any known species. A polyphasic approach including phylogenetic analysis of partial ITS, β-tubulin (*BenA*), calmodulin (*CaM*) and RNA polymerase II second largest subunit (*RPB2*) gene sequences and macro- and micro-morphological data were used to delimitate the new species and section in this genus.

Materials and methods

Isolates

Soil samples were collected from six provinces from China as mentioned above. A general dilution-plate method was used to isolate fungi, bacteria and actinomycetes. As for fungi, Potato Dextrose Agar (PDA, Guangdong huankai microbiological technology co., LTD) and Rose Bengal Medium (RBM, Beijing luqiao technology co., Ltd) with antibiotics (tetracycline hydrochloride and chloramphenicol with the final concentration of 100 mg/ml) were used. Obtained strains were purified and sub-cultured on

malt extract agar (MEA, Guangdong huankai microbiological technology co., Ltd). Reference strains used in this study were obtained from the China General Microbiological Culture Collection Center (CGMCC), Beijing, China, the CBS culture collection and the working collection of the Applied and Industrial Mycology department (DTO), both housed at the Westerdijk Fungal Biodiversity Institute (Utrecht, the Netherlands). An overview of strains is listed in Table 1. For other strains used in the phylogenetic analyses, readers are referred to Chen et al. 2016; Crous et al. 2016, 2017, 2018; Wang QM et al. 2016; Wang XC et al. 2016, 2017; Yilmaz et al. 2016a, b; Guevara-Suarez et al. 2017; Peterson and Jurjević 2017; Barbosa et al. 2018; Jiang et al. 2018; Su and Niu 2018; Varriale et al. 2018; Rajeshkumar et al. 2019; Rodríguez-Andrade et al. 2019; Guevara-Suarez et al. 2020.

DNA extraction, PCR amplification and sequencing

Strains were grown for 1 wk on MEA prior to DNA extraction. DNA was extracted using the Ultraclean TM Microbial DNA isolation Kit (MoBio, Solana Beach, U.S.A.) and stored at -20 °C. The ITS, *BenA*, *CaM*, and *RPB2* genes were amplified and sequenced using methods and primers previously described (Houbraken and Samson 2011; Yilmaz et al. 2014).

Table 1. *Talaromyces* strains used in this study.

Section	Species name	Strain no.	Substrate and origin	GenBank accession nr.			
				ITS	BenA	CaM	RPB2
Talaromyces	*Talaromyces brevis*	CBS 141833T= DTO 349-E7	Soil, Beijing, China	MN864269	MN863338	MN863315	MN863328
		DTO 307-C1	Soil, Zonguldak, Turkey	MN864270	MN863339	MN863316	MN863329
		CBS 118436 = DTO 004-D8	Soil, Maroc	MN864271	MN863340	MN863317	MN863330
	Talaromyces rufus	CBS 141834 T= DTO 349-D7 = CGMCC 3.13203	Soil, Yunnan, China	MN864272	MN863341	MN863318	MN863331
		DTO 274-C5	Soil, Korea	MN864273	MN863342	MN863319	n.a.
	Talaromyces aspriconidius	CBS 141835 T= DTO 340-F8	Soil, Yunnan, China	MN864274	MN863343	MN863320	MN863332
Tenues	*Talaromyces tenuis*	CBS 141840 T = DTO 340-G9	Soil, Guizhou, China	MN864275	MN863344	MN863321	MN863333
Trachyspermi	*Talaromyces albisclerotius*	CBS 141839 T = DTO 340-G5	Soil, Guizhou, China	MN864276	MN863345	MN863322	MN863334
Subinflati	*Talaromyces guizhouensis*	CBS 141837 T = DTO 340-G8	Soil, Guizhou, China	MN864277	MN863346	MN863323	MN863335
		DTO 054-C8	Soil from rainforest, Langkawi, Malaysia	MN864278	MN863347	MN863324	MN863336
		DTO 054-A7	Soil from rainforest, Langkawi, Malaysia	MN864279	MN863348	MN863325	MN863337
	Talaromyces resedanus	CBS 181.71T = DTO 376-A7 = ATCC 22356 = FRR 578 = IMI 062877 = NRRL 578	Soil, A1 horizon of Podzol, Victoria, Seychelles	MN864280	MN863349	MN863326	n.a.
		CBS 184.90 = DTO 376-A8 = UPSC 2879	Soil in greenhouse, Sweden	MN864281	MN863350	MN863327	n.a.

Phylogenetic analysis

For sectional classification in *Talaromyces*, a four-gene phylogeny combining ITS, *BenA*, *CaM* and *RPB2* sequences was used. Prior to combining the datasets, single gene alignments were generated using MAFFT v. 7 (Katoh et al. 2019), and then trimmed at both ends. Aligned datasets were subsequently concatenated using Mesquite v 3.6 (Maddison and Maddison 2018). For each section, single gene phylogenies were generated to determine the phylogenetic relationship among species. The most suitable substitution model was determined using FindModel (Posada and Crandall 1998). Bayesian analyses were performed with MrBayes v. 3.2 (Ronquist et al. 2012). The sample frequency was set to 100 and the first 25% of trees were removed as burn-in. Maximum likelihood analyses including 1000 bootstrap replicates were run using RAxML (Kozlov et al. 2019). *Trichocoma paradoxa* (CBS 788.83^{T}) was used as an outgroup in the *Talaromyces* phylogeny. Sequences of *T. trachyspermus* (CBS 373.48^{T}), *T. dendriticus* (CBS 660.80^{T}) and *T. purpurogenus* (CBS 286.36^{T}) were used as outgroups in *Talaromyces* sections *Subinflati*, *Talaromyces* and *Trachyspermi*, respectively. The resulting trees were visualized with FigTree v1.4.2 and edited in Adobe Illustrator CS5. Bayesian inference (BI) posterior probabilities (pp) values and bootstrap (bs) values are labelled on nodes. Values less than 0.95 pp and 75% bs are not shown. Branches with posterior probability values of 1 and bootstrap values higher than 95% are thickened. Newly obtained sequences were deposited in GenBank.

Morphological analysis

Macroscopic characters were studied on Czapek yeast autolysate agar (CYA), CYA supplemented with 5% NaCl (CYAS), yeast extract sucrose agar (YES), creatine sucrose agar (CREA), dichloran 18% glycerol agar (DG18), oatmeal agar (OA) and malt extract agar (MEA; Oxoid malt) (Samson et al. 2010). Isolates were inoculated at three points on 90 mm Petri dishes and incubated for 7 d at 25 °C in darkness. Additional CYA plates were incubated at 30 and 37 °C, and an additional MEA plate was incubated at 30 °C. After 7 d of incubation, colony diameters were recorded. The colony texture, degree of sporulation, obverse and reverse colony colors, the production of soluble pigments and exudates were noted. Acid production on CREA is indicated by a change in the pH sensitive bromocresol purple dye, from a purple to yellow color in media surrounding colonies. For ascoma production, OA, MEA and CYA plates were incubated for up to four wks. Color codes used in description refer to Rayner (1970).

Microscope preparations were made from 1 wk-old colonies grown on MEA. Production of ascomata, asci and ascospores was determined on 2–3 wk-old colonies on OA. Size of ascospores and conidia were measured without ornamentation. Lactic acid (60%) was used as mounting fluid and 96% ethanol was applied to remove the excess of conidia. A Zeiss Stereo Discovery V20 dissecting microscope and Zeiss AX10 Imager A2 light microscope equipped with Nikon DS-Ri2 cameras and software NIS-Elements D v4.50 were used to capture digital images.

Results

Phylogeny

The individual ITS, *BenA*, *CaM* and *RPB2* datasets consist of 653, 591, 782 and 802 characters, respectively, and were combined to study the relationship within *Talaromyces*. The most optimal model for each dataset is listed in Table 2. Eight well-supported lineages are present in the multigene phylogenic analysis (Fig. 1). Seven lineages agree with sectional classification by Yilmaz et al. 2014 and one lineage, represented by a new species described here (*Talaromyces tenuis*), could not be assigned to any known section. This lineage is sister to sections *Talaromyces* and *Helici* but cannot be assigned into any of them. Based on its phylogenetic and morphological peculiarity (see description below), the lineage is described as a new section named *Tenues*. Furthermore, five new species are distributed over three sections, *T. brevis*, *T. rufus* and *T. aspriconidius* in section *Talaromyces*; *T. albisclerotius* in section *Trachyspermi* and *T. guizhouensis* in section *Subinflati*.

In section *Talaromyces*, *T. rufus* and *T. aspriconidius* can be separated via each single gene phylogram. *Talaromyces rufus* is close to *T. macrosporus* based on *BenA*, *CaM* and *RPB2* phylograms and forms a separate lineage in ITS phylogram. *Talaromyces aspriconidius* is close to *T. primulinus* based on *RPB2* phylogram, but clusters with *T. flavus* based on *BenA* phylogram, and forms a separate lineage in *CaM* and ITS phylograms. *Talaromyces brevis* is closely related to *T. liani*, it can be differentiated via *BenA*, *CaM* and *RPB2* phylograms, but not via ITS phylogram (Fig. 2; Suppl. materials: 1–3).

In section *Trachyspermi*, *T. albisclerotius* can be well-separated in four single phylograms; this species clusters with *T. diversus* in *BenA*, *CaM* and *RPB2* phylograms, and forms a separate lineage in ITS phylogram (Fig. 3; Suppl. materials: 4–6).

Talaromyces guizhouensis is assigned in section *Subinflati* and *P. resedanum* also belongs to this section according to our multigene analysis. With the newly described *T. tzapotlensis* and *T. omanensis* the total number of taxa belonging to section *Subinflati* increased from two to five since it was established in 2014. *Talaromyces omanensis* shares same ITS, *BenA* and *CaM* sequences with *T. resedanus* CBS 184.90. *Talaromyces guizhouensis* is close to *T. tzapotlensis* and *T. subinflatus* in each single gene phylogram (Fig. 4, Suppl. materials: 7–9).

Identification

The five new species *T. albisclerotius*, *T. aspriconidius*, *T. guizhouensis*, *T. rufus*, *T. tenuis* can be identified by ITS, *BenA*, *CaM* and *RPB2* sequences. *Talaromyces brevis* cannot be separated from *T. liani* (strains CBS 225.66^{T}, CBS 118885, CBS 118434 and DTO 058-F2) by its ITS sequence, but it can be differentiated from *T. liani* by *BenA* (97.3% similarity, 366/376 bp), *CaM* (99.5% similarity, 463/465 bp) and *RPB2* (99% similarity, 838/846 bp).

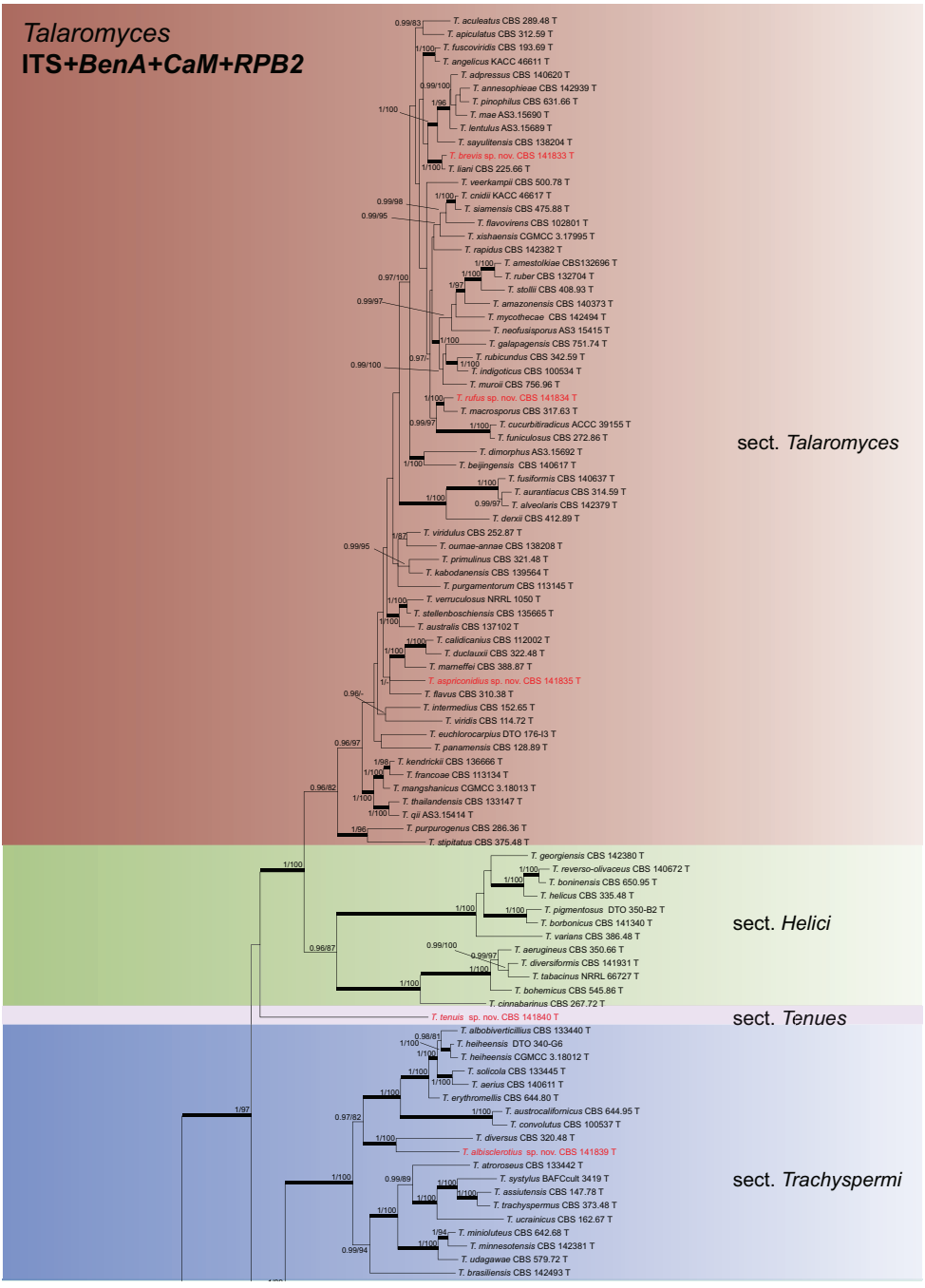

Figure 1. Concatenated phylogeny of the ITS, *BenA*, *CaM* and *RPB2* gene regions of species from *Talaromyces*. Branches with values more than 1 pp and 95% bs are thickened, supports lower than those values are indicated with a dash (-). *Trichocoma paradoxa* (CBS 788.83^{T}) was chosen as outgroup. T: ex-type.

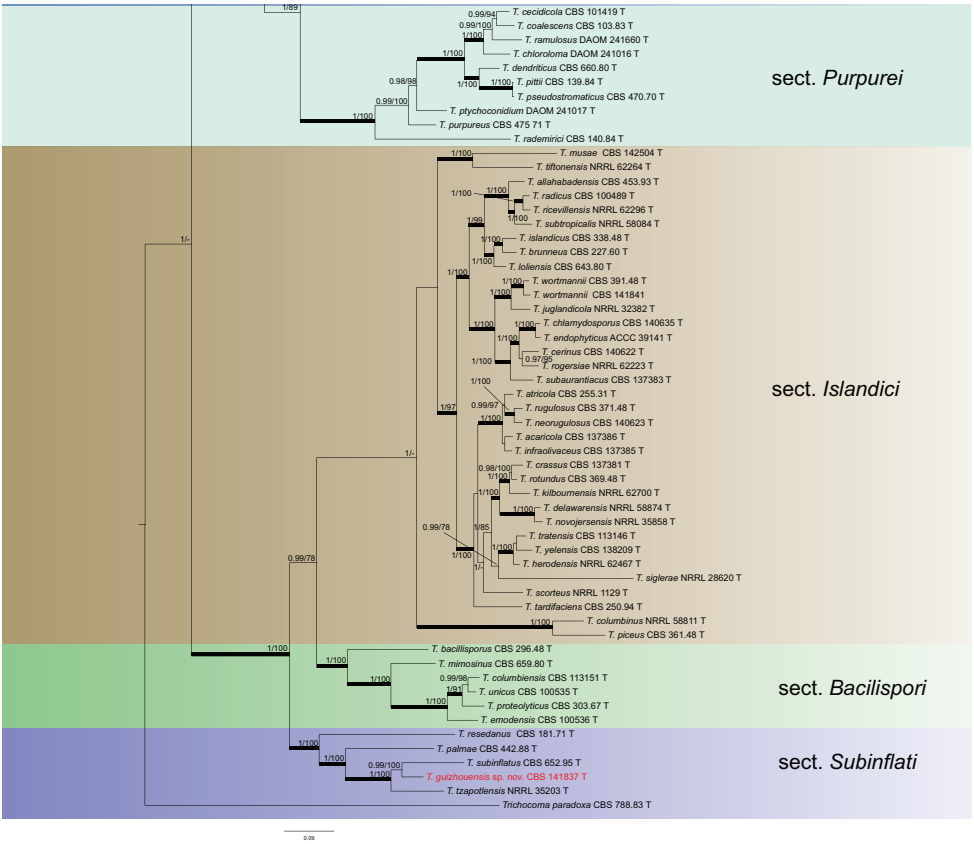

Figure 1. Continued.

Table 2. Sequence data sets and models used in phylogeny.

Section	Sequence data sets							
	ITS (bp)	Substitution model	*BenA*(bp)	Substitution model	*CaM*(bp)	Substitution model	*RPB2*(bp)	Substitution model
Overview *Talaromyces*	653	GTR+G	591	K2P+G	782	GTR+G	802	GTR+G
Section *Subinflati*	751	GTR+G	458	K2P+G	520	GTR+G	893	K2P+G
Section *Talaromyces*	539	GTR+G	398	HKY+G	528	GTR+G	838	GTR+G
Section *Trachyspermi*	505	GTR+G	422	GTR+G	556	GTR+G	852	GTR+G

Taxonomy

***Talaromyces* section *Tenues* B.D. Sun, A.J. Chen, Houbraken & Samson, sect. nov.**
MycoBank No: 833138

Typus. *Talaromyces tenuis* B.D. Sun, A.J. Chen, Houbraken & Samson

Description. Conidiophores monoverticillate or biverticillate, with hyaline, thin stipes, colonies grow restrictedly on CYA, YES, DG18, slightly faster on MEA and OA, no growth on CYAS and CREA at 25 °C and CYA incubated at 37 °C.

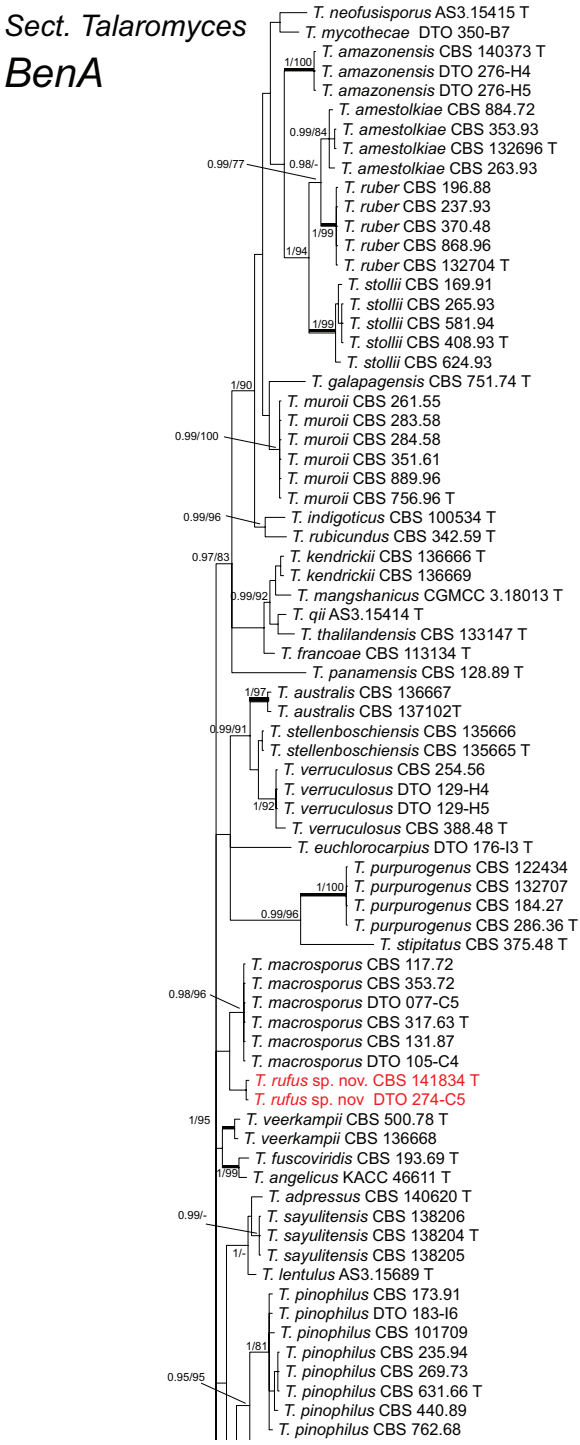

Figure 2. Phylogeny of *BenA* for species classified in *Talaromyces* section *Talaromyces*. Branches with values more than 1 pp and 95% bs are thickened, supports lower than those values are indicated with a dash (-). *Talaromyces dendriticus* (CBS 633.80^{T}) was chosen as outgroup. T: ex-type.

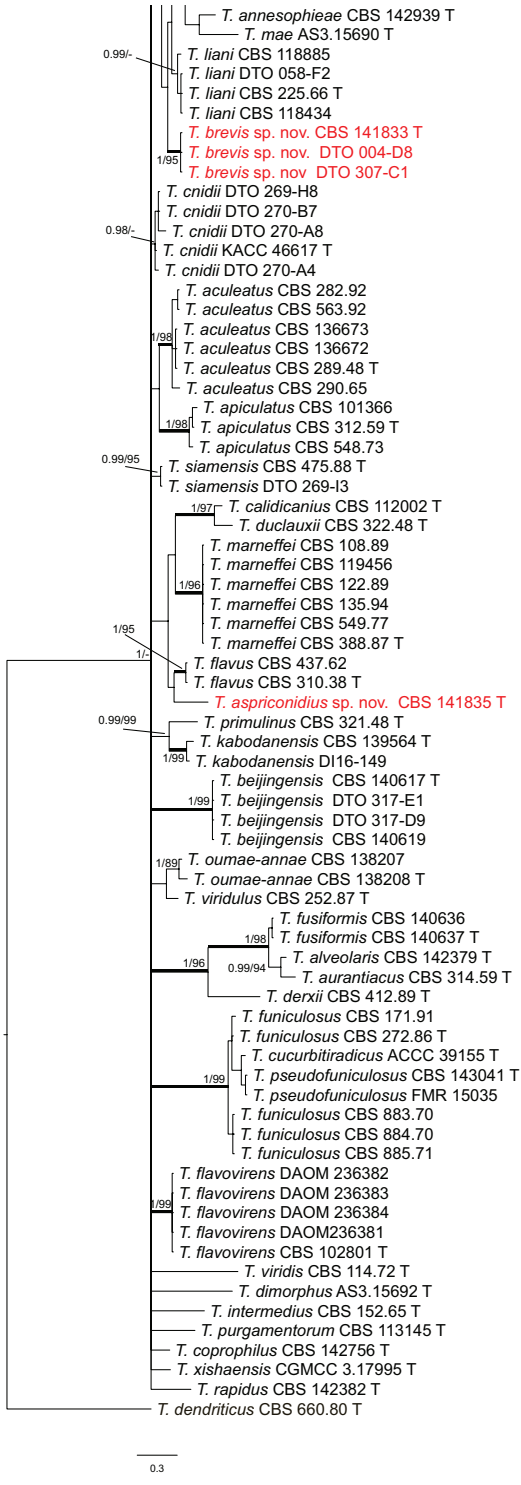

Figure 2. Continued.

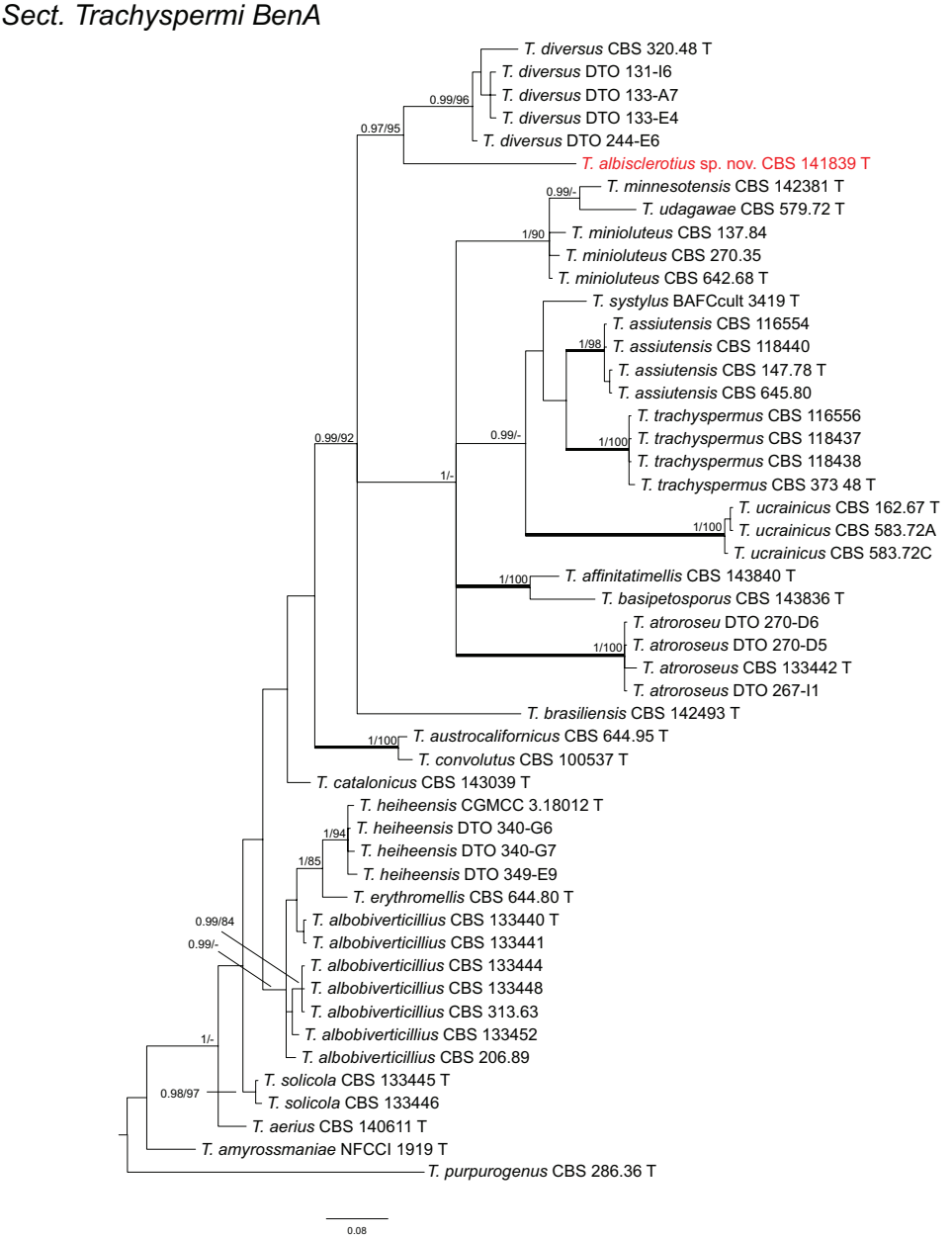

Figure 3. Phylogeny of *BenA* for species classified in *Talaromyces* section *Trachyspermi*. Branches with values more than 1 pp and 95% bs are thickened, supports lower than those values are indicated with a dash (-). *Talaromyces purpurogenus* (CBS 286.36[T]) was chosen as outgroup. T: ex-type.

Phylogenetic analysis places *Talaromyces* section *Tenues* sister to sections *Talaromyces* and *Helici* (Fig. 1); however, statistical support for this relationship is lacking. Using a nine-gene sequence data set, Houbraken et al. (2020) confidently shows that

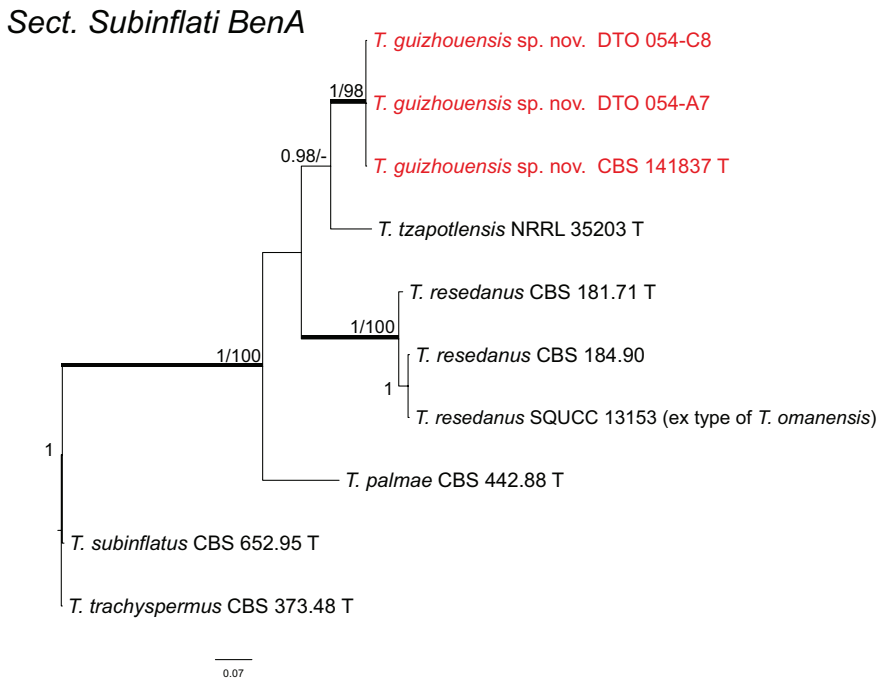

Figure 4. Phylogeny of *BenA* for species classified in *Talaromyces* section *Subinflati*. Branches with values more than 1 pp and 95% bs are thickened, supports lower than those values are indicated with a dash (-). *Talaromyces trachyspermus* (CBS 373.48^{T}) was chosen as outgroup. T: ex-type.

Talaromyces sp. CBS 141840 (= *T. tenuis*, the sole representative of the section) is sister to sect. *Purpurei* and *Trachyspermi*. Section *Trachyspermi* species produce abundant red pigments (Yilmaz et al. 2014), while *Talaromyces tenuis* does not. Section *Purpurei* species generally grow rapidly on CYA and MEA, and usually produce synnemata after two to three weeks of incubation (Yilmaz et al. 2014).

Etymology. Named after the type species of the section, *Talaromyces tenuis*.

Talaromyces tenuis **B.D. Sun, A.J. Chen, Houbraken & Samson, sp. nov.**
MycoBank No: 833136
Fig. 5

Typus. China, Guizhou, soil, 2014, isolated by X.Z. Jiang, Holotype CBS H-22838, culture ex-holotype CBS 141840 = DTO 340-G9.

ITS barcode. MN864275. Alternative identification markers: *BenA* = MN863344, *CaM* = MN863321, *RPB2* = MN863333.

Diagnosis. *Talaromyces tenuis* produces hyaline, thin conidiophores, yellow mycelium on MEA and OA, and grows very restrictedly on CYA, YES and DG18.

In. *Talaromyces* section *Tenues*

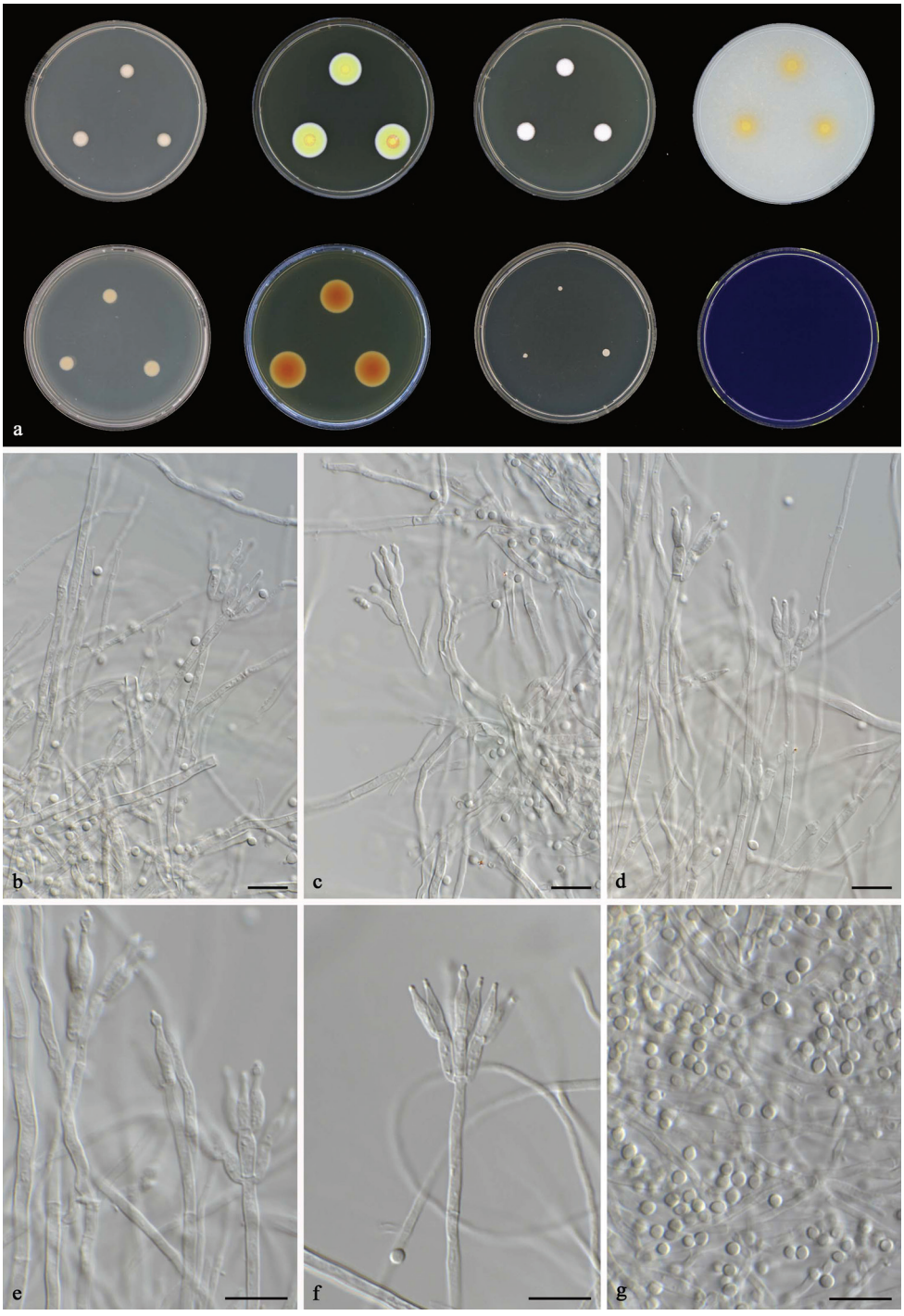

Figure 5. *Talaromyces tenuis* CBS 141840^{T} **a** colonies from left to right (top row) CYA, MEA, YES and OA; (bottom row) CYA reverse, MEA reverse, DG 18 and CREA **b–g** conidiophores and conidia. Scale bars: 10 µm (**b–g**).

Colony diam, 7 d (mm). CYA 7–8; CYA 30 °C 5–8; CYA 37 °C No growth; MEA 18–20; MEA 30 °C 10–11; OA 12–14; YES 9–10; CREA No growth; CYAS No growth; DG18 2–3.

Colony characters. CYA 25 °C, 7 d: Colonies moderately deep, plane; margins entire; mycelium white; texture floccose; sporulation absent; soluble pigments absent; exudates absent; reverse white. MEA 25 °C, 7 d: Colonies moderately deep, plane; margins entire; mycelium sulphur yellow (15) or ochreous (44); texture floccose; sporulation sparse; conidia *en masse* white or greyish yellow-green (68); soluble pigments absent; exudates absent; reverse ochreous (44) to umber (9). YES 25 °C, 7 d: Colonies moderately deep, plane; margins entire; mycelium white; texture floccose; sporulation absent; soluble pigments absent; exudates absent; reverse buff (45). DG18 25 °C, 7 d: Colonies moderately deep, plane; margins entire; mycelium white; texture floccose; sporulation absent; soluble pigments absent; exudates absent; reverse white. OA 25 °C, 7 d: Colonies moderately deep, plane; margins entire; mycelium pale luteous (11); texture floccose; sporulation absent; soluble pigments absent; exudates absent; reverse buff (45).

Micromorphology. Conidiophores monoverticillate or biverticillate, stipes smooth, 80–150 × 2–3 µm; metulae 2–3, divergent, 8–9 × 2–2.5 µm; phialides 2–3, acerose, 8–9.5 × 2–2.5 µm; conidia smooth, globose to subglobose, 2–3 × 2–2.5 µm. Ascomata not observed.

Note. *Talaromyces tenuis* is phylogenetically distinct and is basal to species belonging to sections *Talaromyces* and *Helici* (Fig. 1). In a nine-gene phylogeny, it is sister to sections *Purpurei* and *Trachyspermi* (Houbraken et al. 2020). This species is characterized by hyaline, thin conidiophores, and grows very restrictedly on CYA, YES and DG18; colonies on MEA and OA have prominent yellow mycelia.

Etymology. Latin, *tenuis*, refers to its thin conidiophores.

***Talaromyces albisclerotius* B.D. Sun, A.J. Chen, Houbraken & Samson, sp. nov.**
MycoBank No: 833135
Fig. 6

Typus. China, Xinjiang, soil, 2002, isolated by L. Cai, Holotype CBS H-22837, culture ex-holotype CBS 141839 = DTO 340-G5.

ITS barcode. MN864276. Alternative identification markers: *BenA* = MN863345, *CaM* = MN863322, *RPB2* = MN863334.

Diagnosis. *Talaromyces albisclerotius* produces white sclerotia on OA, grows restrictedly on CYA, YES, DG18 and OA and does not grow on CYAS.

In. *Talaromyces* section *Trachyspermi*

Colony diam, 7 d (mm). CYA 5–8; CYA 30 °C 3–4; CYA 37 °C No growth; MEA 19–20; MEA 30 °C 8–9; OA 13–14; YES 6–7; CREA No growth; CYAS No growth; DG18 5–6.

Colony characters. CYA 25 °C, 7 d: Colonies moderately deep, slight sulcate; margins entire; mycelium white; texture floccose; sporulation dense; conidia *en masse*

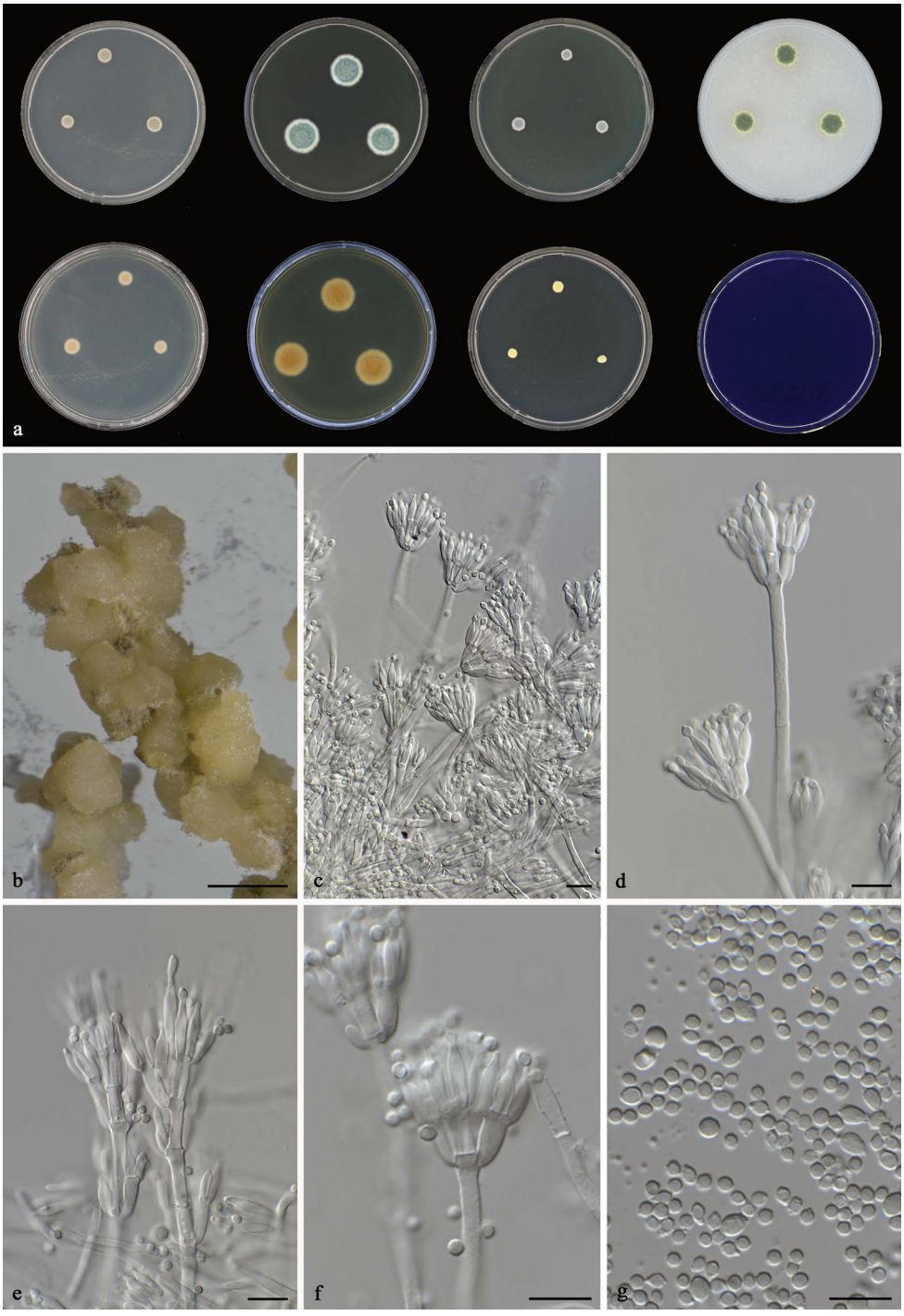

Figure 6. *Talaromyces albisclerotius* CBS 141839^{T} **a** colonies from left to right (top row) CYA, MEA, YES and OA; (bottom row) CYA reverse, MEA reverse, DG 18 and CREA **b** sclerotia on OA after two weeks **c–g** conidiophores and conidia. Scale bars: 1000 µm (**b**), 10 µm (**c–g**).

greyish yellow-green (68); soluble pigments absent; exudates absent; reverse buff (45). MEA 25 °C, 7 d: Colonies moderately deep, sulcate; margins entire; mycelium white and primrose (66); texture floccose; sporulation dense; conidia *en masse* pistachio green (92); soluble pigments absent; exudates absent; reverse ochreous (44). YES 25 °C, 7 d: Colonies moderately deep, plane; margins entire; mycelium white; texture floccose; sporulation moderately dense; conidia *en masse* pistachio green (92); soluble pigments absent; exudates absent; reverse buff (45). DG18 25 °C, 7 d: Colonies moderately deep, plane; margins entire; mycelium sulphur yellow (15); texture floccose; sporulation sparse; conidia *en masse* greyish yellow-green (68); soluble pigments absent; exudates absent; reverse sulphur yellow (15). OA 25 °C, 7 d: Colonies moderately deep, plane; margins entire; mycelium white and primrose (66); texture velvety; sporulation dense; conidia *en masse* yellow green (71); soluble pigments absent; exudates clear droplets; reverse greyish yellow-green (68). CREA 25 °C, 7 d: No growth.

Micromorphology. Conidiophores biverticillate, with a minor proportion having subterminal branches; stipes smooth, 70–130 × 3–4 µm, extra branches 10–20 µm; metulae 3–5, divergent, 8.5–11 × 4–4.5 µm; phialides 4–6, acerose, 9–11 × 3–5 µm; conidia smooth, subglobose to fusiform, 2–4.5× 3–4 µm. Ascomata not observed, white sclerotia present on OA after 1 wk.

Notes. *Talaromyces albisclerotius* is characterized by the production of white sclerotia on OA after 1 wk incubation; these sclerotia remain sterile and no ascospores are observed after prolonged incubation up to eight wk. *Talaromyces assiutensis* and *T. trachyspermus* could produce white ascomata, but their ascomata mature after weeks and release ascospores (Yilmaz et al. 2014). Phylogenetically, *T. albisclerotius* clusters with *T. diversus* and *T. brasiliensis*, but *T. diversus* grows faster on MEA, and *T. brasiliensis* produces rough conidia (Yilmaz et al. 2014; Barbosa et al. 2018).

Etymology. Latin, *albisclerotius*, refers to its white sclerotia produced on OA.

***Talaromyces aspriconidius* B.D. Sun, A.J. Chen, Houbraken & Samson, sp. nov**
MycoBank No: 833134
Fig. 7

Typus. China, Yunnan, soil, 2008, isolated by L. Cai, Holotype CBS H-22833, culture ex-holotype CBS 141835 = DTO 340-F8.

ITS barcode. MN864274. Alternative identification markers: *BenA* = MN863343, *CaM* = MN863320, *RPB2* = MN863332.

Diagnosis. *Talaromyces aspriconidius* produces strikingly roughened, globose conidia, grows moderately on CYA and CYA at 30 °C, reaches 22–23 mm and 25–26 mm after 7 d.

In. *Talaromyces* section *Talaromyces*

Colony diam, 7 d (mm). CYA 22–23; CYA 30 °C 25–26; CYA 37 °C 22–23; MEA 36–37; MEA 30 °C 44–45; OA 38–42; YES 28–29; CREA 7–8; CYAS No growth; DG18 10–11.

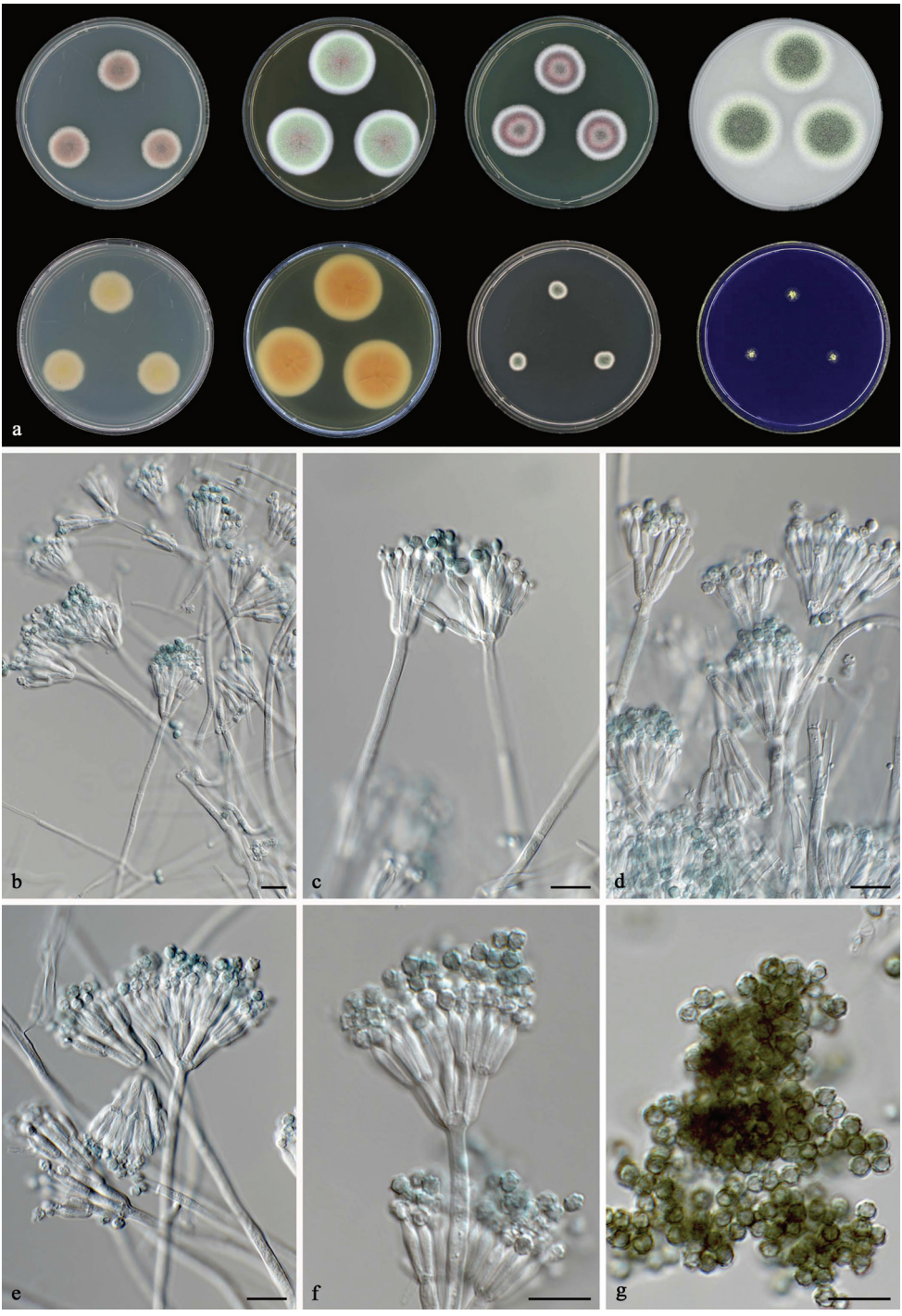

Figure 7. *Talaromyces aspriconidius* CBS 141835^{T} **a** colonies from left to right (top row) CYA, MEA, YES and OA; (bottom row) CYA reverse, MEA reverse, DG 18 and CREA **b–g** conidiophores and conidia. Scale bars: 10 µm (**b–g**).

Colony characters. CYA 25 °C, 7 d: Colonies moderately deep, plane; margins entire; mycelium white and peach (4); texture floccose; sporulation moderately dense; conidia *en masse* greyish yellow-green (68); soluble pigments absent; exudates absent; reverse buff (45). MEA 25 °C, 7 d: Colonies moderately deep, plane; margins entire; mycelium white; texture floccose; sporulation moderately dense; conidia *en masse* leek green (49) and greyish yellow-green (68); soluble pigments absent; exudates brown droplets; reverse saffron (10). YES 25 °C, 7 d: Colonies moderately deep, plane; margins entire; mycelium white and peach (4); texture floccose; sporulation moderately dense; conidia *en masse* greyish yellow-green (68); soluble pigments absent; exudates absent; reverse saffron (10). DG18 25 °C, 7 d: Colonies moderately deep, plane; margins entire; mycelium white and primrose (66); texture floccose; sporulation dense; conidia *en masse* honey (64); soluble pigments absent; exudates absent; reverse greyish yellow-green (68). OA 25 °C, 7 d: Colonies moderately deep, plane; margins entire; mycelium white and primrose (66); texture floccose; sporulation dense; conidia *en masse* yellow-green (71); soluble pigments absent; exudates clear droplets; reverse greyish yellow-green (68). CREA 25 °C, 7 d: Moderate growth, acid production absent.

Micromorphology. Conidiophores biverticillate, stipes smooth, 150–250 × 3–4 µm, metulae 4–5, divergent, 10–12 × 3–3.5 µm; phialides 4–6, acerose to flask shaped, 8–10.5 × 3–3.5 µm; conidia strikingly roughened, globose, 3–4 µm. Ascomata not observed.

Notes. *Talaromyces aspriconidius* is characterized by its strikingly roughened, globose conidia. *Talaromyces aculeatus*, *T. apiculatus*, *T. diversus*, *T. solicola* and *T. verruculosus* also produce this kind of conidia. However, *T. aspriconidius* grows slower than *T. aculeatus*, *T. apiculatus* and *T. verruculosus*, and faster than *T. diversus* and *T. solicola* on CYA and CYA at 30 °C (Yilmaz et al. 2014).

Etymology. Latin, *aspriconidius*, refers to its strikingly roughened conidia.

***Talaromyces brevis* B.D. Sun, A.J. Chen, Houbraken & Samson, sp. nov.**
MycoBank No: 833132
Fig. 8

Typus. China, Beijing, soil, 2010, isolated by B.D. Sun, Holotype CBS H-22831, culture ex-holotype CBS 141833= DTO 349-E7.

Additional material examined. Turkey, Zonguldak, soil, 2014, isolated by Rasime Demirel, culture DTO 307-C1. Maroc, soil, 2005, isolated by J. Dijksterhuis, culture CBS 118436 = DTO 004-D8.

ITS barcode. MN864269. Alternative identification markers: *BenA* = MN863338, *CaM* = MN863315, *RPB2* = MN863328.

Diagnosis. *Talaromyces brevis* produces short conidiophores measuring 15–50 × 3–4 µm, yellow to orange ascomata on OA and spiny ascospores measuring 3.5–4.5 × 3–4 µm.

In. *Talaromyces* section *Talaromyces*

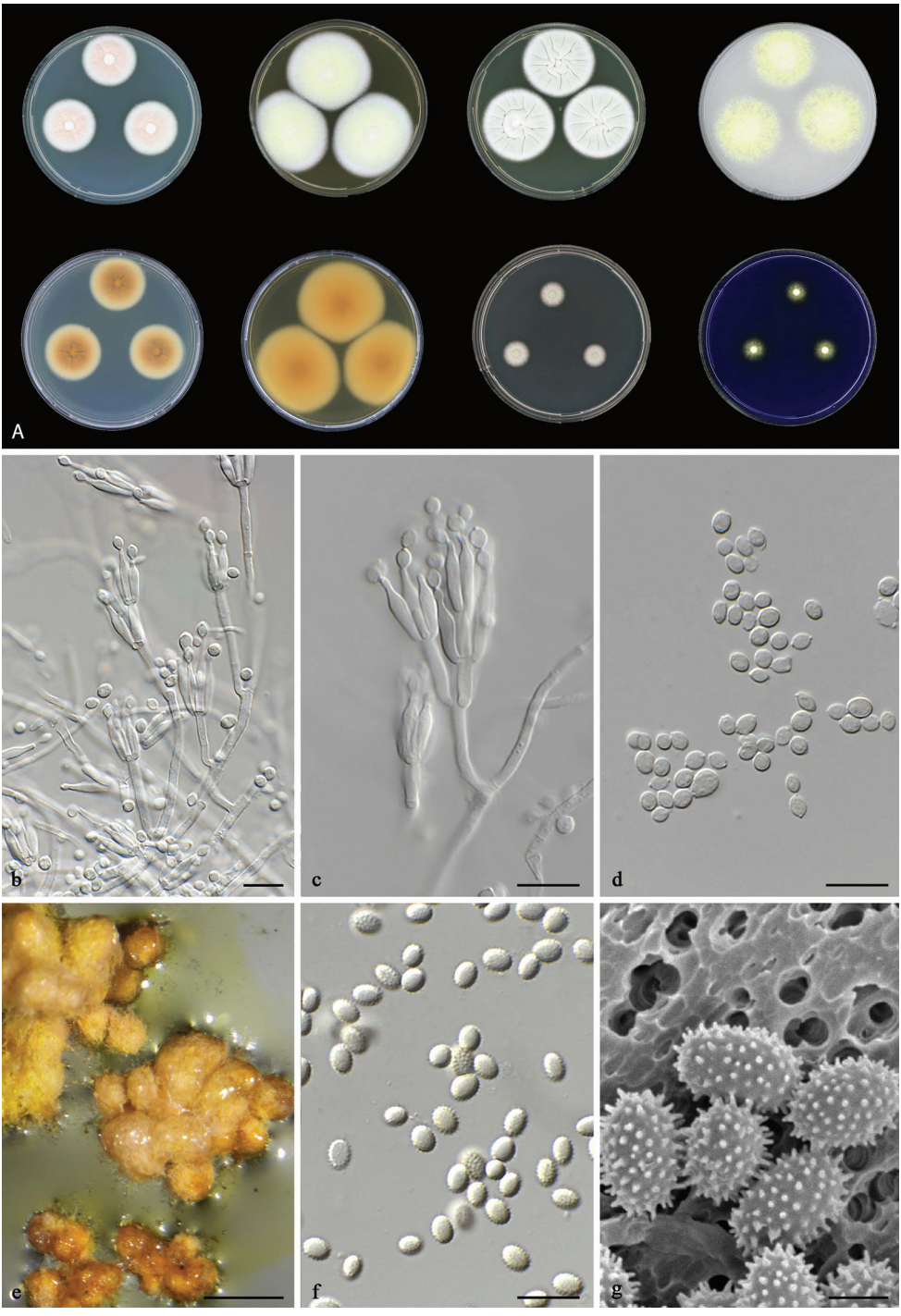

Figure 8. *Talaromyces brevis* CBS 141833^{T} **a** colonies from left to right (top row) CYA, MEA, YES and OA; (bottom row) CYA reverse, MEA reverse, DG 18 and CREA **b–d** conidiophores and conidia **e** ascomata on OA after two weeks **f–g** ascospores. Scale bars: 10 µm (**b–d, f**), 1000 µm (**e**), 2 µm (**g**).

Colony diam, 7 d (mm). CYA 30–31; CYA 30 °C 28–30; CYA 37 °C 25–26; MEA 50–51; MEA 30 °C 57–60; OA 39–43; YES 42–43; CREA 13–14; CYAS No growth; DG18 13–15.

Colony characters. CYA 25 °C, 7 d: Colonies moderately deep, sulcate; margins entire; mycelium white and flesh (37); texture floccose; sporulation sparse; conidia *en masse* white; soluble pigments absent; exudates absent; reverse ochreous (44). MEA 25 °C, 7 d: Colonies moderately deep, plane; margins entire; mycelium white and primrose (66); texture floccose; sporulation sparse; conidia *en masse* white to greyish yellow-green (68); soluble pigments absent; exudates absent; reverse ochreous (44). YES 25 °C, 7 d: Colonies moderately deep, sulcate; margins entire; mycelium white; texture floccose; sporulation absent; soluble pigments absent; exudates absent; reverse ochreous (44). DG18 25 °C, 7 d: Colonies moderately deep, slightly raised at center, plane; margins entire; mycelium white; texture floccose; sporulation moderately dense; conidia *en masse* yellow-green (71); soluble pigments absent; exudates absent; reverse greyish yellow-green (68). OA 25 °C, 7 d: Colonies moderately deep, plane; margins entire; mycelium primrose (66); texture floccose; sporulation absent; soluble pigments absent; exudates absent; reverse primrose (66). Ascomata present. CREA 25 °C, 7 d: Moderate growth, acid production present.

Micromorphology. Conidiophores monoverticillate and biverticillate; stipes smooth, 15–50 × 3–4 µm; metulae 3–5, divergent, 10–15 × 2.5–3 µm; phialides 4–6, flask-shaped, 9–13 × 2–4 µm; conidia smooth, subglobose to fusiform, 3–4(–5) × 2.5–3.5(–4.5) µm. Ascomata maturing after 2–3 wk of incubation on OA, yellow to orange, globose to subglobose, 400–550 µm; ascospores ellipsoidal, spiny, 3.5–4.5 × 3–4 µm.

Notes. *Talaromyces brevis* is morphologically and phylogenetically close to *T. liani*, but the latter produces larger ascospores measuring 4–6 × 2.5–4 µm and does not produce acid on CREA (except *T. liani* CBS 118885 produces very weak acid) (Yilmaz et al. 2014).

Etymology. Latin, *brevis*, refers to its short conidiophores.

***Talaromyces guizhouensis* B.D. Sun, A.J. Chen, Houbraken & Samson, sp. nov.**
MycoBank No: 833131
Fig. 9

Typus. China, Guizhou, soil, 2014, isolated by X.Z. Jiang, Holotype CBS H-22835, culture ex-holotype CBS 141837= DTO 340-G8.

Additional material examined. Malaysia, Langkawi, soil from rainforest, 2007, isolated by J. Houbraken, culture DTO 054-C8. Malaysia, Langkawi, soil from rainforest, 2007, isolated by J. Houbraken, culture DTO 054-A7.

ITS barcode. MN864277. Alternative identification markers: *BenA* = MN863346, *CaM* = MN863323, *RPB2* = MN863335.

Diagnosis. *Talaromyces guizhouensis* grows poorly on CREA and DG18, does not produce synnemata as well as ascospores.

In. *Talaromyces* section *Subinflati*

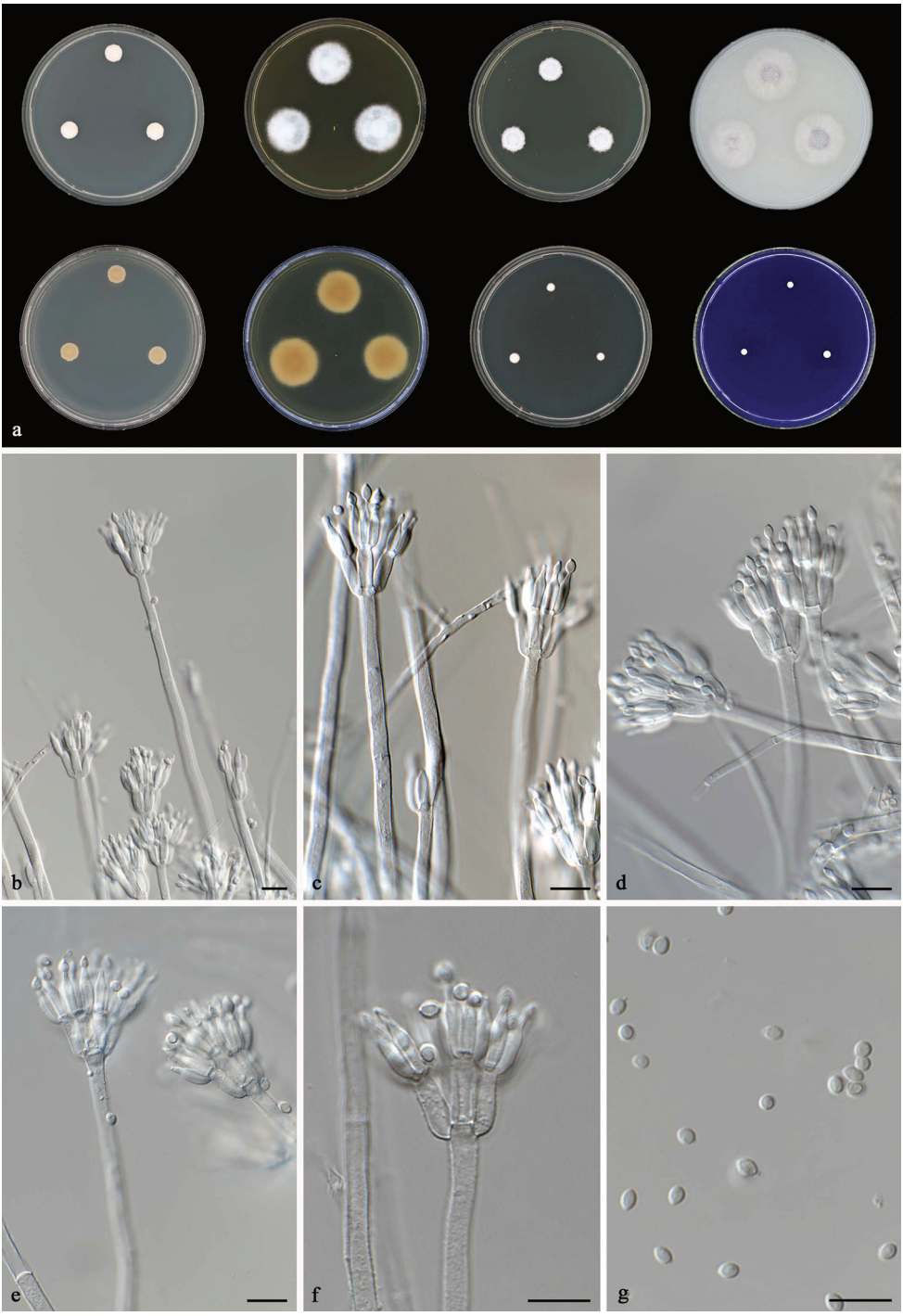

Figure 9. *Talaromyces guizhouensis* CBS 141837^{T} **a** colonies from left to right (top row) CYA, MEA, YES and OA; (bottom row) CYA reverse, MEA reverse, DG 18 and CREA **b–g** conidiophores and conidia. Scale bars: 10 μm (**b–g**).

Colony diam, 7 d (mm). CYA 8–9; CYA 30 °C 10; CYA 37 °C No growth; MEA 24–27; MEA 30 °C 18–19; OA 27–29; YES 12–13; CREA 2–3; CYAS No growth; DG18 4–5.

Colony characters. CYA 25 °C, 7 d: Colonies moderately deep, plane; margins entire; mycelium white; texture floccose; sporulation absent; soluble pigments absent; exudates clear droplets; reverse saffron (10). MEA 25 °C, 7 d: Colonies moderately deep, raised at center, plane; margins entire; mycelium white; texture floccose; sporulation moderately dense; conidia *en masse* pistachio green (92); soluble pigments absent; exudates absent; reverse saffron (10). YES 25 °C, 7 d: Colonies moderately deep, raised at center, plane; margins entire; mycelium white; texture floccose; sporulation absent; soluble pigments absent; exudates clear droplets; reverse cream white. DG18 25 °C, 7 d: Colonies moderately deep, plane; margins entire; mycelium white; texture floccose; sporulation absent; soluble pigments absent; exudates absent; reverse cream white. OA 25 °C, 7 d: Colonies moderately deep, raised at center, plane; margins entire; mycelium white; texture floccose; sporulation moderately dense; conidia *en masse* pistachio green (92); soluble pigments absent; exudates clear droplets; reverse greyish lavender (98) at center, fading into saffron (10). CREA 25 °C, 7 d: Poor growth, acid production absent.

Micromorphology. Conidiophores biverticillate, stipes smooth to finely rough, 150–300 × 3–4.5 µm, metulae 3–5, divergent, 11–13 × 3–5 µm; phialides 3–5, acerose to flask shaped, 9–10 × 3–3.5 µm; conidia finely rough, subglobose to fusiform, 2.5–4.5 × 2.5–3 µm. Ascomata not observed.

Notes. Section *Subinflati* previously contained two species namely *T. subinflatus* and *T. palmae*. These species do not resemble each other, although both grow poorly on CREA and DG18 (Yilmaz et al. 2014). *Talaromyces tzapotlensis* was included more recently (Peterson and Jurjević 2017) and we here expand this section with *T. guizhouensis* and *T. resedanus*. Like the other species in this section, *T. guizhouensis* also grows poorly on CREA and DG18. This species is phylogenetically related to *T. subinflatus*, but the latter grows very restrictedly on common media except MEA (Yilmaz et al. 2014). *Talaromyces palmae* produces indeterminate synnemata and short stipes (up to 85 µm) (Yilmaz et al. 2014) and these are not observed in *T. guizhouensis*. Furthermore, *T. tzapotlensis* grows faster on most media (e.g., 29–30 *vs* 8–9 mm on CYA; 10–11 *vs* 4–5 mm on DG18; 20–22 *vs* 2–3 mm on CREA, all diam. after 7 days (Peterson and Jurjević 2017) and *T. resedanus* does not grow on CREA and produces smaller conidia measuring 2–3 × 1.5–2 µm.

Etymology. Latin, *guizhouensis*, refers to its origin, isolated from Guizhou, China.

***Talaromyces resedanus* (McLennan and Ducker) A.J. Chen, Houbraken & Samson comb. nov.**

MycoBank No: 302422

Fig. 10

Penicillium resedanum McLennan and Ducker, Aust. J. Bot. 2: 360. 1954. Basionym.

= *Talaromyces omanensis* Halo, Maharachch., Al-Yahyai and Al-Sadi, Phytotaxa 404: 192. 2019.

Typus. Australia, Frankston in solo arenoso acido, Holotype IMI 062877, culture ex-holotype CBS 181.71 = DTO 376-A7 = ATCC 22356 = FRR 578 = IMI 062877 = NRRL 578.

Additional material examined. Sweden, soil in greenhouse, 1989, isolated by O. Constantinescu, culture CBS 184.90 = DTO 376-A8 = UPSC 2879.

ITS barcode. MN864280. Alternative identification markers: *BenA* = MN863349, *CaM* = MN863326, *RPB2* = MN969214.

In. *Talaromyces* section *Subinflati*

Colony diam, 7 d (mm). CYA 19–21; CYA 30 °C 18–20; CYA 37 °C 8–11; MEA 23–25; MEA 30 °C 15–21; OA 26–28; YES 17–19; CREA No growth; CYAS 5–7; DG18 8–9.

Colony characters. CYA 25 °C, 7 d: Colonies moderately deep, plane; margins entire; mycelium sulphur yellow (15) at center, white at edge; texture floccose; sporulation absent; soluble pigments absent; exudates clear droplets; reverse saffron (10). MEA 25 °C, 7 d: Colonies moderately deep, plane; margins entire; mycelium white and sulphur yellow (15); texture floccose; sporulation sparse; conidia *en masse* white to greyish yellow-green (68); soluble pigments absent; exudates clear droplets; reverse saffron (10). YES 25 °C, 7 d: Colonies moderately deep, plane; margins entire; mycelium white and buff (45); texture floccose; sporulation sparse; conidia *en masse* white to greyish yellow-green (68); soluble pigments absent; exudates clear droplets; reverse saffron (10). DG18 25 °C, 7 d: Colonies moderately deep, plane; margins entire; mycelium white; texture floccose; sporulation absent; soluble pigments absent; exudates absent; reverse cream white. OA 25 °C, 7 d: Colonies moderately deep, plane; margins entire; mycelium white and sulphur yellow (15); texture floccose; sporulation absent; soluble pigments absent; exudates clear droplets; reverse white. CREA 25 °C, 7 d: No growth.

Micromorphology. Conidiophores monoverticillate, stipes smooth, 50–150 × 3–4.5 µm, phialides 3–9, flask shaped, 9–12 × 3–3.5 µm; conidia finely rough, ellipsoidal, 2–3 × 1.5–2 µm. Ascomata not observed.

Notes. *Talaromyces resedanus* grows restrictedly on DG18 and does not grow on CREA, two features shared with other taxa in section *Subinflati*. The monoverticillate conidiophores can differentiate *T. resedanus* from all reported section *Subinflati* species. *Talaromyces aerugineus*, *T. flavus*, *T. intermedius*, *T. rotundus*, *T. tardifaciens* also produce monoverticillate conidiophores, all of them except *T. aerugineus* can produce ascospores. *Talaromyces aerugineus* differs from *T. resedanus* by its shorter conidiophores (10–20 × 2.5–5 µm) and large, globose to ellipsoidal conidia (3–8.5 × 2.5–5 µm).

This species was introduced as *Penicillium resedanum* (McLennan et al., 1954). Yilmaz et al. (2014) listed it as doubtful species because the ex-type culture CBS 181.71 was not viable at that time. We requested the lyophilized culture of CBS 181.71 and CBS 184.90 deposited in nitrogen, and successfully resurrected them. The concatenated alignment and the single gene phylogenies proved its assignment in section *Subinflati*. *Talaromyces omanensis* described by Halo et al. (2019) shares ITS, *BenA* and *CaM* (all 100% similarity) sequences with *T. resedanus* CBS 184.90, have 99.7% (576/578), 98.3% (357/363), 98.8% (487/493) similarity with *T. resedanus* CBS 181.71^{T}. Its type culture SQUCC 13153 showed good sporulation on CYA and MEA

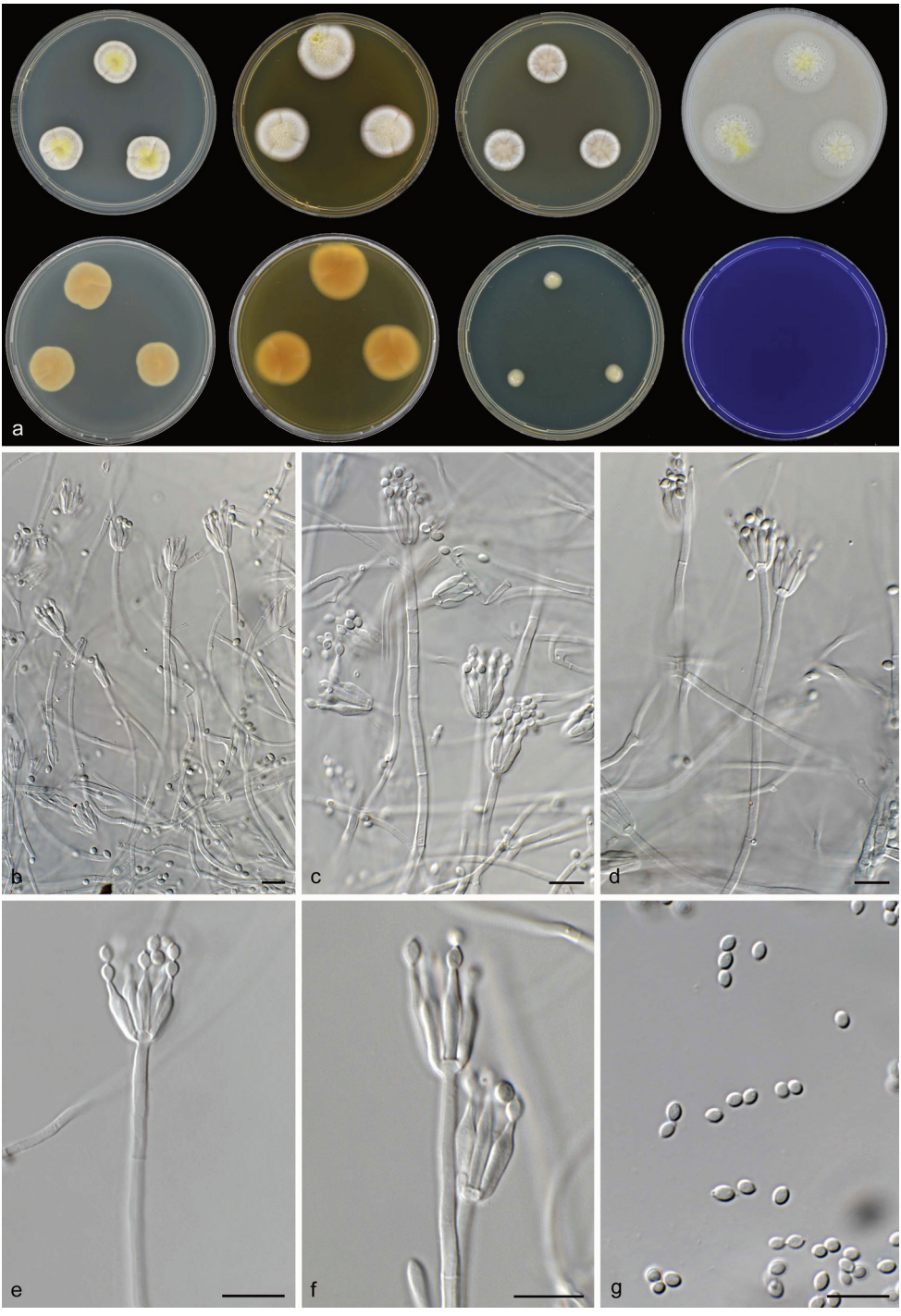

Figure 10. *Talaromyces resedanus* CBS 181.71^{T} **a** colonies from left to right (top row) CYA, MEA, YES and OA; (bottom row) CYA reverse, MEA reverse, DG 18 and CREA **b–g** conidiophores and conidia. Scale bars: 10 μm (**b–g**).

and thus displayed green colony. The monoverticillate conidiophores, size and shape of stipes, phialides and conidia of *T. omanensis* resemble those of *T. resedanus*, except that conidiophores of *T. omanensis* are rough under scanning electron microscope (SEM) (Halo et al. 2019). The photo plate of *T. omanensis* showed smooth conidiophores under microscope. Based on the molecular and morphological similarity, we considered *T. omanensis* a synonym of *T. resedanus*.

***Talaromyces rufus* B.D. Sun, A.J. Chen, Houbraken & Samson, sp. nov.**
MycoBank No: 833133
Fig. 11

Typus. China, Yunnan, soil, 2009, isolated by T.S. Zhou, Holotype CBS H-22832, culture ex-holotype CBS 141834 = DTO 349-D7 = CGMCC 3.13203.

Additional material examined. Korea, soil, 2013, isolated by J. Houbraken, culture DTO 274-C5.

ITS barcode. MN864272. Alternative identification markers: *BenA* = MN863341, *CaM* = MN863318, *RPB2* = MN863331.

Diagnosis. This species produces red, determinate synnemata and ellipsoidal, spiny ascospores measuring 5–6 × 4–5 µm.

In. *Talaromyces* section *Talaromyces*

Colony diam, 7 d (mm). CYA 12–16; CYA 30 °C 18–20; CYA 37 °C 15–16; MEA 37–38; MEA 30 °C 50–51; OA 38–40; YES 26–27; CREA Weak growth; CYAS No growth; DG18 9–13.

Colony characters. CYA 25 °C, 7 d: Colonies deep, plane; margins entire; mycelium white and scarlet (5); texture floccose; sporulation sparse; conidia *en masse* greyish yellow-green (68); soluble pigments scarlet (5); exudates absent; reverse scarlet (5). MEA 25 °C, 7 d: Colonies moderately deep, plane; margins entire; mycelium white and scarlet (5); texture floccose; sporulation sparse; conidia *en masse* greyish yellow-green (68); soluble pigments scarlet (5); exudates absent; reverse scarlet (5). YES 25 °C, 7 d: Colonies moderately deep, raised at center, plane; margins entire; mycelium white and scarlet (5); texture floccose; sporulation absent; soluble pigments absent; exudates scarlet (5) droplets; reverse scarlet (5) at center, fading into peach (4). DG18 25 °C, 7 d: Colonies moderately deep, plane; margins entire; mycelium white; texture smooth and sticky; sporulation absent; soluble pigments absent; exudates absent; reverse cream white. OA 25 °C, 7 d: Colonies low, plane; margins entire; mycelium white and scarlet (5); texture floccose; sporulation absent; soluble pigments scarlet (5); exudates absent; reverse scarlet (5). Ascomata present. CREA 25 °C, 7 d: Acid production absent.

Micromorphology. Conidiophores solitary and monoverticillate; stipes smooth, 5–30 × 2.5–3 µm; phialides1–4, acerose, 10–12 × 3–4 µm; conidia smooth, ellipsoidal to fusiform, 2.5–4.5 × 2–3 µm. Ascomata maturing within 2–3 wk on OA, subglobose to ellipsoildal, 350–600 × 200–350 µm, yellow, ascospores ellipsoidal, spiny, 5–6 × 4–5 µm.

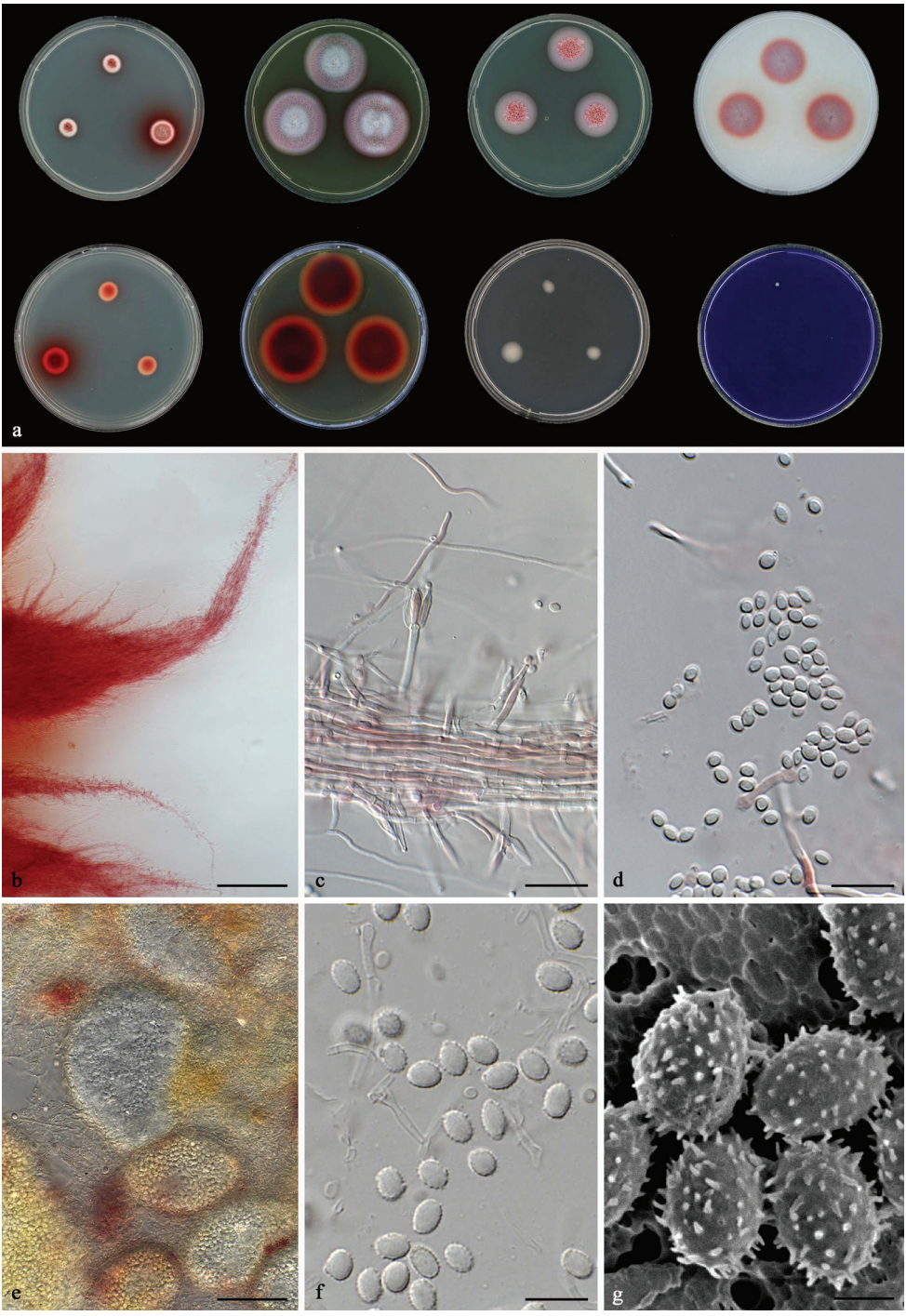

Figure 11. *Talaromyces rufus* CBS 141834^{T} **a** colonies from left to right (top row) CYA, MEA, YES and OA; (bottom row) CYA reverse, MEA reverse, DG 18 and CREA **b** synnemata on MEA after 1 wk incubation **c, d** conidiophores and conidia **e** ascomata **f, g** ascospores. Scale bars: 200 µm (**b**), 10 µm (**c, d, f**), 50 µm (**e**), 2 µm (**g**).

Notes. *Talaromyces rufus* is characterized by its red determinate synnemata on all tested media except DG18, CYAS and CREA. According to Yilmaz et al. (2014), twelve *Talaromyces* species produce determinate or indeterminate synnemata, but *T. rufus* can be easily distinguished from them by its red synnemata. Phylogenetically, *T. rufus* is related to *T. macrosporus*; however, *T. macrosporus* produces broadly ellipsoidal ascospores and does not produce synnemata.

Etymology. Latin, *rufus*, refers to its red synnemata.

Discussion

Previous studies showed that the genus *Talaromyces* comprises seven sections (Yilmaz et al. 2014). In this study, a comprehensive isolation of soil samples was carried out in China; one new section and six new species were described using a polyphasic approach. *Talaromyces* section *Tenues* is newly introduced and contains one species. In our phylogenetic analysis, this section is sister to sections *Talaromyces* and *Helici*, though statistical support is lacking. Houbraken et al. (2020) studied the relationships within the *Eurotiales* and confidently showed that the section is sister to *Purpurei* and *Trachyspermi*. Section *Tenues* is morphologically characterized by restricted growth on CYA, YES and DG18, slightly faster growth on MEA and OA and no growth on CREA. Based on these phenotypic characteristics, section *Tenues* species resemble section *Trachyspermi* species, but the species in section *Trachyspermi* are likely to produce abundant red pigments (Yilmaz et al. 2014), while *Talaromyces tenuis* doesn't. *Talaromyces tenuis* also produces thinner conidiophores, and it is interesting to find out whether this character is shared by other species that will be described in this section in the future.

Three of our new species fall into section *Talaromyces*. This section was first introduced for species that produce yellow ascomata, which can occasionally be white, creamish, pinkish or reddish, and have yellow ascospores (Stolk and Samson 1972). Nowadays, this section is not limited to sexual species, but it still contains the largest number and highest ratio of sexual reproducing species in this genus. Among three new species, *T. brevis* and *T. rufus* produce yellow, spiny ascospores, the ascospores of *T. brevis* are smaller compared to its close relatives *T. liani*, and *T. rufus* can be easily distinguished by its red synnemata. *Talaromyces aspriconidius* is characterized by its strikingly roughened, globose conidia, but ascospores were not observed after long incubation.

Talaromyces albisclerotius is classified in section *Trachyspermi*. Species in section *Trachyspermi* show restricted growth on CYA, YES and DG18, grow slightly faster on MEA, and do not, or poorly grow, on CREA. Conidiophores are generally biverticillate and some species produce creamish white or yellow ascomata (Yilmaz et al. 2014). The morphology of *T. albisclerotius* matches these characters well; however, *T. albisclerotius* produces white sclerotia and does not produce ascomata and ascospores. Yilmaz et al. (2016c) speculated that *Talaromyces* species with no known sexual stage may actually be heterothallic. They successfully induced the sexual reproductive structures in *T. amestolkiae*, which was formerly described as an asexual taxon with black sclerotia. Further study is needed on *T. albisclerotius* to complete this hypothesis.

Talaromyces guizhouensis and *T. resedanus* belong to section *Subinflati*. This section previously contained two morphologically distinct species *T. palmae* and *T. subinflatus*. *Talaromyces palmae* produces short, biverticillate conidiophores and indeterminate synnemata, and *T. subinflatus* produces longer conidiophores, and grows more restrictedly on all tested media (Yilmaz et al. 2014). *Talaromyces tzapotlensis* was described by Peterson and Jurjević (2017), it grows well on CREA and DG18. *Talaromyces omanensis* was considered as a synonym of *T. resedanus* based on molecular and morphological similarity. The growth rate of *T. guizhouensis* falls somewhere in between; it is phylogenetically close to *T. subinflatus* and *T. tzapotlensis*. *Talaromyces resedanus* is the only monoverticillate species in this section.

Talaromyces species have a worldwide distribution and are isolated from a wide range of substrates. Soil is their main habitat, but new species were also isolated from indoor air, dust, clinical samples, plants, seed, leaf litter, honey, pollen and stingless bee nests (Sang et al. 2013; Visagie et al. 2014; Chen et al. 2016; Wang QM et al. 2016; Yilmaz et al. 2016a; Guevara-Suarez et al. 2017; Peterson and Jurjević 2017; Barbosa et al. 2018; Crous et al. 2018; Su and Niu 2018; Rodríguez-Andrade et al. 2019). These studies expanded our knowledge on the substrates where *Talaromyces* species can occur, but on the other hand demonstrated the complicated ecological function of this genus. In this study, one new section and six new species were identified from soil in China. Further research will focus on the *Talaromyces* diversity from a wide range of substrates.

Acknowledgements

This project was supported by the Open Funding Project of the State Key Laboratory of Bioactive Substance and Function of Natural Medicines No. GTZK201903 and Beijing science and technology plan No. Z191100004019025. We acknowledge professor Lei Cai for providing the type culture of *Talaromyces aspriconidius* and *T. albisclerotius*.

References

Abdel-Rahim IR, Abo-Elyousr KAM (2018) *Talaromyces pinophilus* strain AUN-1 as a novel mycoparasite of *Botrytis cinerea*, the pathogen of onion scape and umbel blights. Microbiological Research 212–213: 1–9. https://doi.org/10.1016/j.micres.2018.04.004

Alagesaboopathi C (1994) Biological control of damping-off disease of cotton seedling. Current Science 66: 865–868.

Antonopoulou I, Iancu L, Jütten P, Piechot A, Rova U, Christakopoulos P (2018) Screening of novel feruloyl esterases from *Talaromyces wortmannii* for the development of efficient and sustainable syntheses of feruloyl derivatives. Enzyme and Microbial Technology 120: 124–135. https://doi.org/10.1016/j.enzmictec.2018.08.007

Barbosa RN, Bezerra JDP, Souza-Motta CM, Frisvad JC, Samson RA, Oliveira NT, Houbraken J (2018) New *Penicillium* and *Talaromyces* species from honey, pollen and nests of stingless bees. Antonie van Leeuwenhoek 111: 1–30. https://doi.org/10.1007/s10482-018-1081-1

Benjamin CR (1955) Ascocarps of *Aspergillus* and *Penicillium*. Mycologia 47: 669–687. https://doi.org/10.1080/00275514.1955.12024485

Berbee ML, Yoshimura A, Sugiyama J, Taylor JW (1995) Is *Penicillium* monophyletic? An evaluation of phylogeny in the family Trichocomaceae from 18S, 5.8S and ITS ribosomal DNA sequence data. Mycologia 87: 210–222. https://doi.org/10.1080/00275514.1995.12026523

Bladt TT, Frisvad JC, Knudsen PB, Larsen TO (2013) Anticancer and antifungal compounds from *Aspergillus*, *Penicillium* and other filamentous fungi. Molecules 18: 11338–11376. https://doi.org/10.3390/molecules180911338

Boosalis MG (1956) Effect of soil temperature and green-manure amendment of unsterilized soil on parasitism of *Rhizoctonia solani* by *Penicillium vermiculatum* and *Trichoderma* sp. Phytopathology 46: 473–478.

Bouhet JC, Van Chuong PP, Toma F, Kirszenbaum M, Fromageot P (1976) Isolation and characterization of luteoskyrin and rugulosin, two hepatotoxic anthraquinonoids from *Penicillium islandicum* Sopp and *Penicillium rugulosum* Thom. Journal of Agricultural and Food Chemistry 24: 964–972. https://doi.org/10.1021/jf60207a028

Chen AJ, Sun BD, Houbraken J, Frisvad JC, Yilmaz N, Zhou YG, Samson RA (2016) New *Talaromyces* species from indoor environments in china. Studies in Mycology 84: 119–144. https://doi.org/10.1016/j.simyco.2016.11.003

Crous PW, Wingfield MJ, Burgess TI, Hardy GEStJ, Crane C, Barrett S, Cano-Lira JF, Le Roux JJ, Thangavel R, Guarro J, Stchigel AM, Martín MP, Alfredo DS, Barber PA, Barreto RW, Baseia IG, Cano-Canals J, Cheewangkoon R, Ferreira RJ, Gené J, Lechat C, Moreno G, Roets F, Shivas RG, Sousa JO, Tan YP, Wiederhold NP, Abell SE, Accioly T, Albizu JL, Alves JL, Antoniolli ZI, Aplin N, Araújo J, Arzanlou M, Bezerra JDP, Bouchara JP, Carlavilla JR, Castillo A, Castroagudín VL, Ceresini PC, Claridge GF, Coelho G, Coimbra VRM, Costa LA, da Cunha KC, da Silva SS, Daniel R, de Beer ZW, Dueñas M, Edwards J, Enwistle P, Fiuza PO, Fournier J, García D, Gibertoni TB, Giraud S, Guevara-Suarez M, Gusmão LFP, Haituk S, Heykoop M, Hirooka Y, Hofmann TA, Houbraken J, Hughes DP, Kautmanová I, Koppel O, Koukol O, Larsson E, Latha KPD, Lee DH, Lisboa DO, Lisboa WS, López-Villalba Á, Maciel JLN, Manimohan P, Manjón JL, Marincowitz S, Marney TS, Meijer M, Miller AN, Olariaga I, Paiva LM, Piepenbring M, Poveda-Molero JC, Raj KNA, Raja HA, Rougeron A, Salcedo I, Samadi R, Santos TAB, Scarlett K, Seifert KA, Shuttleworth LA, Silva GA, Silva M, Siqueira JPZ, Souza-Motta CM, Stephenson SL, Sutton DA, Tamakeaw N, Telleria MT, Valenzuela-Lopez N, Viljoen A, Visagie CM, Vizzini A, Wartchow F, Wingfield BD, Yurchenko E, Zamora JC, Groenewald JZ (2016) Fungal Planet description sheets: 469–557. Persoonia 37: 218–403. https://doi.org/10.3767/003158516X694499

Crous PW, Wingfield MJ, Burgess TI, Carnegie AJ, Hardy GEStJ, Smith D, Summerell BA, Cano-Lira JF, Guarro J, Houbraken J, Lombard L, Martín MP, Sandoval-Denis M, Alexandrova AV, Barnes CW, Baseia IG, Bezerra JDP, Guarnaccia V, May TW, Hernández-Restrepo M, Stchigel AM, Miller AN, Ordoñez ME, Abreu VP, Accioly T, Agnello C, Agustin CA, Albuquerque CC, Alfredo DS, Alvarado P, Araújo-Magalhães GR, Arauzo S, Atkinson T, Barili A, Barreto RW, Bezerra JL, Cabral TS, Camello RF, Cruz RHSF, Daniëls PP, da Silva BDB, de Almeida DAC, de Carvalho Júnior AA, Decock CA, Delgat L, Denman S, Dimitrov RA, Edwards J, Fedosova AG, Ferreira RJ, Firmino AL, Flores JA, García D,

Gené J, Góis JS, Gomes AAM, Gonçalves CM, Gouliamova DE, Groenewald M, Guéorguiev BV, Guevara-Suarez M, Gusmão LFP, Hosaka K, Hubka V, Huhndorf SM, Jadan M, Jurjević Ž, Kraak B, Kučera V, Kumar TKA, Kušan I, Lacerda SR, Lamlertthon S, Lisboa WS, Loizides M, Luangsa-ard JJ, Lysková P, Mac Cormack WP, Macedo DM, Machado AR, Malysheva EF, Marinho P, Matočec N, Meijer M, Mešić A, Mongkolsamrit S, Moreira KA, Morozova OV, Nair KU, Nakamura N, Noisripoom W, Olariaga I, Oliveira RJV, Paiva LM, Pawar P, Pereira OL, Peterson SW, Prieto M, Rodríguez-Andrade E, Rojo De Blas C, Roy M, Santos ES, Sharma R, Silva GA, Souza-Motta CM, Takeuchi-Kaneko Y, Tanaka C, Thakur A, Smith MTh, Tkalčec Z, Valenzuela-Lopez N, Van der Kleij P, Verbeken A, Viana MG, Wang XW, Groenewald JZ (2017) Fungal Planet description sheets: 625–715. Persoonia 39: 270–467. https://doi.org/10.3767/persoonia.2017.39.11

Crous PW, Wingfield MJ, Burgess TI, Hardy GEStJ, Gené J, Guarro J, Baseia IG, García D, Gusmão LFP, Souza-Motta CM, Thangavel R, Adamčík S, Barili A, Barnes CW, Bezerra JDP, Bordallo JJ, Cano-Lira JF, de Oliveira RJV, Ercole E, Hubka V, Iturrieta-González I, Kubátová A, Martín MP, Moreau PA, Morte A, Ordoñez ME, Rodríguez A, Stchigel AM, Vizzini A, Abdollahzadeh J, Abreu VP, Adamčíková K, Albuquerque GMR, Alexandrova AV, Álvarez DE, Armstrong-Cho C, Banniza S, Barbosa RN, Bellanger JM, Bezerra JL, Cabral TS, Caboň M, Caicedo E, Cantillo T, Carnegie AJ, Carmo LT, Castañeda-Ruiz RF, Clement CR, Čmoková A, Conceição LB, Cruz RHSF, Damm U, da Silva BDB, da Silva GA, da Silva RMF, de A. Santiago ALCM, de Oliveira LF, de Souza CAF, Déniel F, Dima B, Dong G, Edwards J, Félix CR, Fournier J, Gibertoni TB, Hosaka K, Iturriaga T, Jadan M, Jany JL, Jurjević Ž, Kolařík M, Kušan I, Landell MF, Leite CTR, Lima DX, Loizides M, Luo S, Machado AR, Madrid H, Magalhães OMC, Marinho P, Matočec N, Mešić A, Miller AN, Morozova OV, Neves RP, Nonaka K, Nováková A, Oberlies NH, Oliveira-Filho JRC, Oliveira TGL, Papp V, Pereira OL, Perrone G, Peterson SW, Pham THG, Raja HA, Raudabaugh DB, Řehulka J, Rodríguez-Andrade E, Saba M, Schauflerová A, Shivas RG, Simonini G, Siqueira JPZ, Sousa JO, Stajsic V, Svetasheva T, Tan YP, Tkalčec Z, Ullah S, Valente P, Valenzuela-Lopez N, Abrinbana M, Viana MDA, Wong PTW, Xavier de Lima V, Groenewald JZ (2018) Fungal Planet description sheets: 716–784. Persoonia 40: 240–393. https://doi.org/10.3767/persoonia.2018.40.10

de Hoog GS, Guarro J, Gene J, Figueras MJ (2014) Atlas of Clinical Fungi. CBS-KNAW Fungal Biodiversity Center, Utrecht, 1126 pp.

de Vos JP, van Garderen E, Hensen H, Tange I, Curfs-Breuker I, Vandevelde B, Meis JF (2009) Disseminated *Penicillium radicum* infection in a dog, clinically resembling multicentric malignant lymphoma. Vlaams Diergeneeskundig Tijdschrift 78: 183–188.

Dijksterhuis J (2007) Heat resistant ascospores. In: Dijksterhuis J, Samson RA (Eds) Food Mycology. A Multifaceted Approach to Fungi and Food. CRC Press, Boca Raton, 101–117. https://doi.org/10.1201/9781420020984.ch6

Dutta BK (1981) Studies on some fungi isolated from the rhizosphere of tomato plants and the consequent prospect for control of Verticillium wilt. Plant Soil 63: 209–216. https://doi.org/10.1007/BF02374599

Fahima T, Henis Y (1995) Quantitative assessment of the interaction between the antagonistic fungus *Talaromyces flavus* and the wilt pathogen *Verticillium dahliae* on eggplant roots. Plant Soil 176: 129–137. https://doi.org/10.1007/BF00017683

Frisvad JC, Yilmaz N, Thrane U, Rasmussen KB, Houbraken J, Samson RA (2013) *Talaromyces atroroseus*, a new species efficiently producing industrially relevant red pigments. PLoS ONE 8: e84102. https://doi.org/10.1371/journal.pone.0084102

Guevara-Suarez M, García D, Cano-Lira JF, Guarro J, Gené J (2020) Species diversity in *Penicillium* and *Talaromyces* from herbivore dung, and the proposal of two new genera of penicillium-like fungi in Aspergillaceae. Fungal Systematics and Evolution 5: 39–75. https://doi.org/10.3114/fuse.2020.05.03

Guevara-Suarez M, Sutton DA, Gené J, García D, Wiederhold N, Guarro J, Cano-Lira JF (2017) Four new species of *Talaromyces* from clinical sources. Mycoses 60: 651–662. https://doi.org/10.1111/myc.12640

Halo B, Maharachchikumbura SSN, Al-yahyai RA, Al-nabhani AA, Al-sadi AM (2019) *Talaromyces omanensis* sp. nov.: phenotypic and molecular characterization of a novel species isolated from Rhazya stricta in Oman. Phytotaxa 404: 190–202. https://doi.org/10.11646/phytotaxa.404.5.2

Horré R, Gilges S, Breig P, Kupfer B, de-Hoog GS, Hoekstra E, Poonwan N, Schaal KP (2001) Case report. Fungaemia due to *Penicillium piceum*, a member of the *Penicillium marneffei* complex. Mycoses 44: 502–504. https://doi.org/10.1046/j.1439-0507.2001.00710.x

Houbraken J, Samson RA (2011) Phylogeny of *Penicillium* and the segregation of Trichocomaceae into three families. Studies in Mycology 70: 1–51. https://doi.org/10.3114/sim.2011.70.01

Houbraken J, Kocsubé S, Visagie CM, Yilmaz N, Wang XC, Meijer M, Kraak B, Hubka V, Samson RA, Frisvad JC (2020) Classification of *Aspergillus*, *Penicillium*, *Talaromyces* and related genera (Eurotiales): an overview of families, genera, subgenera, sections, series and species. Studies in Mycology (accepted).

Inglis GD, Kawchuk LM (2002) Comparative degradation of oomycete, ascomycete, and basidiomycete cell walls by mycoparasitic and biocontrol fungi. Canadian Journal of Microbiology 48: 60–70. https://doi.org/10.1139/w01-130

Isbelia R, Louis B, Simard RR, Phillipe T, Hani A (1999) Characteristics of phosphate solubilization by an isolate of a tropical *Penicillium rugulosum* and two UV induced mutants. FEMS Microbiology Ecology 28: 291–295. https://doi.org/10.1016/S0168-6496(98)00118-4

Jiang XZ, Yu ZD, Ruan YM, Wang L (2018) Three new species of *Talaromyces* sect. *Talaromyces* discovered from soil in China. Scientific Reports 8: 1–4932. https://doi.org/10.1038/s41598-018-23370-x

Katoh K, Rozewicki J, Yamada KD (2019) MAFFT online service: multiple sequence alignment, interactive sequence choice and visualization. Briefings in Bioinformatics 20: 1160–1166. https://doi.org/10.1093/bib/bbx108

Khalmuratova I, Kim H, Nam YJ, Oh Y, Jeong MJ, Choi HR, You YH, Choo YS, Lee IJ, Shin JH, Yoon H, Kim JG (2015) Diversity and plant growth promoting capacity of endophytic fungi associated with halophytic plants from the west coast of Korea. Mycobiology 43: 373–383. https://doi.org/10.5941/MYCO.2015.43.4.373

Kim MJ, Shim CK, Kim YK, Hong SJ, Park JH, Han EJ, Kim SC (2017) Enhancement of seed dehiscence by seed treatment with *Talaromyces flavus* GG01 and GG04 in Ginseng (Panax ginseng). The Plant Pathology Journal 33: 1–8. https://doi.org/10.5423/PPJ.OA.06.2016.0146

Kozlov AM, Darriba D, Flouri T, Morel B, Stamatakis A (2019) RA×ML-NG: A fast, scalable, and user-friendly tool for maximum likelihood phylogenetic inference. Bioinformatics 35: 1–3. https://doi.org/10.1093/bioinformatics/btz305

Kumari M, Taritla S, Sharma A, Jayabaskaran C (2018) Antiproliferative and antioxidative bioactive compounds in extracts of marine-derived endophytic fungus *Talaromyces purpureogenus*. Frontiers in Microbiol 9: e1777. https://doi.org/10.3389/fmicb.2018.01777

Lian W, Wang W, Tan CP, Wang J, Wang Y (2018) Immobilized *Talaromyces thermophilus* lipase as an efficient catalyst for the production of LML-type structured lipids. Bioprocess and Biosystems Engineering 42: 321–329. https://doi.org/10.1007/s00449-018-2036-7

Limper AH, Adenis A, Le T, Harrison TS (2017) Fungal infections in HIV/AIDS. Lancet Infectious Diseases 17: e334–e343. https://doi.org/10.1016/S1473-3099(17)30303-1

LoBuglio KF, Pitt JI, Taylor JW (1993) Phylogenetic analysis of two ribosomal DNA regions indicates multiple independent losses of a sexual *Talaromyces* state among asexual *Penicillium* species in subgenus *Biverticillium*. Mycologia 85: 592–604. https://doi.org/10.2307/3760506

Maddison WP, Maddison DR (2018) Mesquite: a modular system for evolutionary analysis. Version 3.6 http://www.mesquiteproject.org

Maeda RN, Barcelos CA, Anna LMMS, Pereira N (2013) Cellulase production by *Penicillium funiculosum* and its application in the hydrolysis of sugar cane bagasse for second generation ethanol production by fed batch operation. Journal of Biotechnology 163: 38–44. https://doi.org/10.1016/j.jbiotec.2012.10.014

Marois JJ, Fravel DR, Papavizas GC (1984) Ability of *Talaromyces flavus* to occupy the rhizosphere. Soil Biology and Biochemistry 16: 387–390. https://doi.org/10.1016/0038-0717(84)90038-5

McLaren DL, Huang HC, Rimmer SR (1986) Hyperparasitism of *Sclerotinia sclerotiorum* by *Talaromyces flavus*. Canadian Journal of Plant Pathology 8: 43–48. https://doi.org/10.1139/b89-279

Mclennan EI, Tucker SC, Thrower LB (1954) New soil fungi from Australian heathland: *Aspergillus*, *Penicillium*, *Spegazzinia*. Australian Journal of Botany 2: 355–364. https://doi.org/10.1071/BT9540355

Narikawa T, Shinoyama H, Fujii T (2000) A β-rutinosidase from *Penicillum rugulosum* IFO 7242 that is a peculiar flavonoid glycosidase. Bioscience, Biotechnology and Biochemistry 64: 1317–1319. https://doi.org/10.1271/bbb.64.1317

Nicoletti R, Salvatore MM, Andolfi A (2018) Secondary metabolites of mangrove-associated strains of *Talaromyces*. Marine Drugs 16: 1–12. https://doi.org/10.3390/md16010012

Ogawa H, Sugiyama J (2000) Evolutionary relationships of the cleistothecial genera with *Penicillium*, *Geosmithia*, *Merimbla* and *Sarophorum* anamorphs as inferred from 18S rDNA sequence divergence. In: Samson RA, Pitt JI (Eds) Integration of Modern Taxonomic Methods for *Penicillium* and *Aspergillus* Classification. Plenum Press, New York, 149–161.

Ogawa H, Yoshimura A, Sugiyama J (1997) Polyphyletic origins of species of the anamorphic genus *Geosmithia* and the relationships of the cleistothecial genera: Evidence from 18S, 5S and 28S rDNA sequence analyses. Mycologia 89: 756–771. https://doi.org/10.1080/00275514.1997.12026842

Oh JY, Kim EN, Ryoo MI, Kim KD (2008) Morphological and molecular identification of *Penicillium islandicum* isolate KU101 from stored rice. Plant Pathology Journal 24: 469–473. https://doi.org/10.5423/PPJ.2008.24.4.469

Peterson SW, Jurjević Ž (2017) New species of *Talaromyces* isolated from maize, indoor air, and other substrates. Mycologia 109: 537–556. https://doi.org/10.1080/00275514.2017.1369339

Pitt JI, Hocking AD (2009) Fungi and Food Spoilage. Springer, New York, 519 pp. https://doi.org/10.1007/978-0-387-92207-2

Pol D, Laxman RS, Rao M (2012) Purification and biochemical characterization of endoglucanase from *Penicillium pinophilum* MS 20. Indian Journal of Biochemistry and Biophysics 49: 189–194.

Posada D, Crandall KA (1998) MODELTEST: testing the model of DNA substitution. Bioinformatics 14: 817–818. https://doi.org/10.1093/bioinformatics/14.9.817

Rajeshkumar KC, Yilmaz N, Marathe SD, Seifert KA (2019) Morphology and multigene phylogeny of *Talaromyces amyrossmaniae*, a new synnematous species belonging to the section *Trachyspermi* from India. MycoKeys 45: 41–56. https://doi.org/10.3897/mycokeys.45.32549

Rayner RW (1970) A Mycological Colour Chart. Commonwealth Mycological Institute, Kew, 34 pp.

Rodríguez-Andrade E, Stchigel AM, Terrab A, Guarro J, Cano-Lira JF (2019) Diversity of xerotolerant and xerophilic fungi in honey. IMA Fungus 10: 1–20. https://doi.org/10.1186/s43008-019-0021-7

Ronquist F, Teslenko M, van der Mark P, Ayres DL, Darling A, Höhna S, Larget B, Liu L, Suchard MA, Huelsenbeck JP (2012) MrBayes 3.2: Efficient Bayesian phylogenetic inference and model choice across a large model space. Systematic Biology 61: 539–542. https://doi.org/10.1093/sysbio/sys029

Saito M, Enomoto M, Tatsuno T (1971) Yellowed rice toxins. Luteoskyrin and related compounds, chlorine-containing compounds, and citrinin. In: Ciegler A, Kadis S, Ajl SJ (Eds) Microbial Toxins. Academic Press Inc., New York, 299–308.

Sakai A, Tanaka H, Konishi Y, Hanazawa R, Ota T, Nakahara Y, Sekiguchi S, Oshida E, Takino M, Ichinoe M, Yoshikawa K, Yoshizawa T, Takatori K (2005) Mycological examination of domestic unpolished rice and mycotoxin production by isolated *Penicillium islandicum*. Journal of the Food Hygienic Society of Japan 46: 205–212. https://doi.org/10.3358/shokueishi.46.205

Samson RA, Houbraken J, Thrane U, Frisvad JC, Andersen B (2010) Food and Indoor Fungi. CBS Laboratory manual. CBS-KNAW Fungal Biodiversity Center, Utrecht, 390 pp.

Samson RA, Yilmaz N, Houbraken J, Spierenburg H, Seifert SW, Peterson SW, Varga J, Frisvad JC (2011) Phylogeny and nomenclature of the genus *Talaromyces* and taxa accommodated in *Penicillium* subgenus *Biverticillium*. Studies in Mycology 70: 159–183. https://doi.org/10.3114/sim.2011.70.04

Sang H, An TJ, Kim CS, Shin GS, Sung GH, Yu SH (2013) Two novel *Talaromyces* species isolated from medicinal crops in Korea. The Journal of Microbiology 51: 704–708. https://doi.org/10.1007/s12275-013-3361-9

Santos PE, Piontelli E, Shea YR, Galluzzo ML, Holland SM, Zelazko ME, Rosenzweig SD (2006) *Penicillium piceum* infection: diagnosis and successful treatment in chronic granulomatous disease. Medical Mycology 44: 749–753. https://doi.org/10.1080/13693780600967089

Stark AA, Townsend JM, Wogan GN, Demain AL, Manmade A, Ghosh AC (1978) Mutagenicity and antibacterial activity of mycotoxins produced by *Penicillium islandicum* Sopp and *Penicillium rugulosum*. Journal of Environmental Pathology and Toxicology 2: 313–324.

Stolk AC, Samson RA (1972) The genus *Talaromyces* – studies on *Talaromyces* and related genera II. Studies in Mycology 2: 1–65. https://doi.org/10.2307/3758303

Su L, Niu YC (2018) Multilocus phylogenetic analysis of *Talaromyces* species isolated from cucurbit plants in China and description of two new species, *T. cucurbitiradicus* and *T. endophyticus*. Mycologia 110: 375–386. https://doi.org/10.1080/00275514.2018.1432221

Supparatpinyo K, Khamwan C, Baosoung V, Nelson KE, Sirisanthana T (1994) Disseminated *Penicillium marneffei* infection in southeast Asia. Lancet 344: 110–113. https://doi.org/10.1016/S0140-6736(94)91287-4

Tomlinson JK, Cooley AJ, Zhang S, Johnson ME (2011) Granulomatous lymphadenitis caused by *Talaromyces helicus* in a labrador retriever. Veterinary Clinical Pathology 40: 553–557. https://doi.org/10.1111/j.1939-165X.2011.00377.x

Ueno Y, Ishikawa I (1969) Production of luteoskyrin, a hepatotoxic pigment, by *Penicillium islandicum* Sopp. Applied Microbiology 18: 406–409. https://doi.org/10.1128/AEM.18.3.406-409.1969

Uraguchi K (1962) Malignant hepatoma and so-called carcinogens, with special reference to the toxicity of luteoskyrin in a small dose. Folia Pharmacologica Japonica 58: 1–19.

Uraguchi K, Uraguchi K, Tatsuno T, Sakaki F, Tsukioka M, Ito H (1961) Isolation of two toxic agents, luteoskyrin and chlorione-containing peptide, from metabolites of *Penicillium islandicum* Sopp, with properties thereof. Journal of Experimental Medicine 31: 193–207.

Uraguchi K, Saito M, Noguchi Y, Takahashi K, Enomoto M, Tatsuno T (1972) Chronic toxicity and carcinogenicity in mice of the purified mycotoxins, luteoskyrin and cyclochlorotine. Food and Cosmetics Toxicology 10: 193–207. https://doi.org/10.1016/S0015-6264(72)80197-4

Varriale S, Houbraken J, Granchi Z, Pepe O, Cerullo G, Ventorino V, Chin-A-Woeng T, Meijer M, Riley R, Grigoriev IV, Henrissat B, de Vries RP, Faraco V (2018) *Talaromyces borbonicus*, sp. nov., a novel fungus from biodegraded Arundo donax with potential abilities in lignocellulose conversion. Mycologia 110: 316–324. https://doi.org/10.1080/00275514.2018.1456835

Visagie CM, Yilmaz N, Frisvad JC, Houbraken J, Seifert KA, Samson RA, Jacobs K (2015) Five new *Talaromyces* species with ampulliform-like phialides and globose rough walled conidia resembling *T. verruculosus*. Mycoscience 56: 486–502. https://doi.org/10.1016/j.myc.2015.02.005

Wang L, Zhuang WY (2007) Phylogenetic analyses of penicillia based on partial calmodulin gene sequences. BioSystems 88: 113–112. https://doi.org/10.1016/j.biosystems.2006.04.008

Wang QM, Zhang YH, Wang B, Wang L (2016) *Talaromyces neofusisporus* and *T. qii*, two new species of section *Talaromyces* isolated from plant leaves in Tibet, China. Scientific Reports 6: 1–18622. https://doi.org/10.1038/srep18622

Wang XC, Chen K, Qin WT, Zhuang WY (2017) *Talaromyces heiheensis* and *T. mangshanicus*, two new species from China. Mycological Progress 16: 73–81. https://doi.org/10.1007/s11557-016-1251-3

Wang XC, Chen K, Xia YW, Wang L, Li TH, Zhuang WY (2016) A new species of *Talaromyces* (Trichocomaceae) from the Xisha Islands, Hainan, China. Phytotaxa 267: 187–200. https://doi.org/10.11646/phytotaxa.267.3.2

Weisenborn JLF, Kirschner R, Cáceres O, Piepenbring M (2010) *Talaromyces indigoticus* Takada & Udagawa, the first record from Panama and the American continent. Mycopathologia 170: 203–208. https://doi.org/10.1007/s11046-010-9305-6

Xu Y, Feng X, Jia J, Chen X, Jiang T, Rasool A, Lv B, Qu L, Li C (2018) A novel β-glucuronidase from *Talaromyces pinophilus* Li-93 precisely hydrolyzes glycyrrhizin into glycyrrhetinic acid 3-O-mono-β-d-glucuronide. Applied and Environmental Microbiology 84: e00755–18. https://doi.org/10.1128/AEM.00755-18

Yilmaz N, Visagie CM, Houbraken J, Frisvad JC, Samson RA (2014) Polyphasic taxonomy of the genus *Talaromyces*. Studies in Mycology 78: 175–341. https://doi.org/10.1016/j.simyco.2014.08.001

Yilmaz N, López-Quintero CA, Vasco-Palacios AM, Frisvad JC, Theelen B, Boekhout T, Samson RA, Houbraken J (2016a) Four novel *Talaromyces* species isolated from leaf litter from Colombian Amazon rain forests. Mycological Progress 15: 1041–1056. https://doi.org/10.1007/s11557-016-1227-3

Yilmaz N, Visagie CM, Frisvad JC, Houbraken J, Jacobs K, Samson RA (2016b) Taxonomic re-evaluation of species in *Talaromyces* section *Islandici*, using a polyphasic approach. Persoonia 36: 37–56. https://doi.org/10.3767/003158516X688270

Yilmaz N, Hagen F, Meis JF, Houbraken J, Samson RA (2016c) Discovery of a sexual cycle in *Talaromyces amestolkiae*. Mycologia 108: 70–79. https://doi.org/10.3852/15-014

Zhai MM, Li J, Jiang CX, Shi XP, Di DL, Crews P, Wu QX (2016) The bioactive secondary metabolites from *Talaromyces* species. Natural Products and Bioprospecting. 6: 1–24. https://doi.org/10.1007/s13659-015-0081-3

Supplementary material 1

Phylogeny of ITS for species classified in *Talaromyces* section *Talaromyces*

Authors: Bing-Da Sun, Amanda J. Chen, Jos Houbraken, Jens C. Frisvad, Wen-Ping Wu, Hai-Lei Wei, Yu-Guang Zhou, Xian-Zhi Jiang, Robert A. Samson

Data type: phylogenetic

Explanation note: Branches with values more than 1 pp and 95% bs are thickened. *Talaromyces dendriticus* was chosen as outgroup.

Link: https://doi.org/10.3897/mycokeys.68.52092.suppl1

Supplementary material 2

Phylogeny of *CaM* for species classified in *Talaromyces* section *Talaromyces*

Authors: Bing-Da Sun, Amanda J. Chen, Jos Houbraken, Jens C. Frisvad, Wen-Ping Wu, Hai-Lei Wei, Yu-Guang Zhou, Xian-Zhi Jiang, Robert A. Samson

Data type: phylogenetic

Explanation note: Branches with values more than 1 pp and 95% bs are thickened. *Talaromyces dendriticus* was chosen as outgroup.

Link: https://doi.org/10.3897/mycokeys.68.52092.suppl2

Supplementary material 3

Phylogeny of *RPB2* for species classified in *Talaromyces* section *Talaromyces*

Authors: Bing-Da Sun, Amanda J. Chen, Jos Houbraken, Jens C. Frisvad, Wen-Ping Wu, Hai-Lei Wei, Yu-Guang Zhou, Xian-Zhi Jiang, Robert A. Samson

Data type: phylogenetic

Explanation note: Branches with values more than 1 pp and 95% bs are thickened. *Talaromyces dendriticus* was chosen as outgroup.

Link: https://doi.org/10.3897/mycokeys.68.52092.suppl3

Supplementary material 4

Phylogeny of ITS for species classified in *Talaromyces* section *Trachyspermi*

Authors: Bing-Da Sun, Amanda J. Chen, Jos Houbraken, Jens C. Frisvad, Wen-Ping Wu, Hai-Lei Wei, Yu-Guang Zhou, Xian-Zhi Jiang, Robert A. Samson

Data type: phylogenetic

Explanation note: Branches with values more than 1 pp and 95% bs are thickened. *Talaromyces purpurogenus* was chosen as outgroup.

Link: https://doi.org/10.3897/mycokeys.68.52092.suppl4

Supplementary material 5

Phylogeny of *CaM* for species classified in *Talaromyces* section *Trachyspermi*

Authors: Bing-Da Sun, Amanda J. Chen, Jos Houbraken, Jens C. Frisvad, Wen-Ping Wu, Hai-Lei Wei, Yu-Guang Zhou, Xian-Zhi Jiang, Robert A. Samson

Data type: phylogenetic

Explanation note: Branches with values more than 1 pp and 95% bs are thickened. *Talaromyces dendriticus* was chosen as outgroup.

Link: https://doi.org/10.3897/mycokeys.68.52092.suppl5

Supplementary material 6

Phylogeny of *RPB2* for species classified in *Talaromyces* section *Trachyspermi*

Authors: Bing-Da Sun, Amanda J. Chen, Jos Houbraken, Jens C. Frisvad, Wen-Ping Wu, Hai-Lei Wei, Yu-Guang Zhou, Xian-Zhi Jiang, Robert A. Samson

Data type: phylogenetic

Explanation note: Branches with values more than 1 pp and 95% bs are thickened. *Talaromyces dendriticus* was chosen as outgroup.

Link: https://doi.org/10.3897/mycokeys.68.52092.suppl6

Supplementary material 7

Phylogeny of ITS for species classified in *Talaromyces* section *Subinflati*

Authors: Bing-Da Sun, Amanda J. Chen, Jos Houbraken, Jens C. Frisvad, Wen-Ping Wu, Hai-Lei Wei, Yu-Guang Zhou, Xian-Zhi Jiang, Robert A. Samson

Data type: phylogenetic

Explanation note: Branches with values more than 1 pp and 95% bs are thickened. *Talaromyces dendriticus* was chosen as outgroup.

Link: https://doi.org/10.3897/mycokeys.68.52092.suppl7

Supplementary material 8

Phylogeny of *CaM* for species classified in *Talaromyces* section *Subinflati*

Authors: Bing-Da Sun, Amanda J. Chen, Jos Houbraken, Jens C. Frisvad, Wen-Ping Wu, Hai-Lei Wei, Yu-Guang Zhou, Xian-Zhi Jiang, Robert A. Samson

Data type: phylogenetic

Explanation note: Branches with values more than 1 pp and 95% bs are thickened. *Talaromyces dendriticus* was chosen as outgroup.

Link: https://doi.org/10.3897/mycokeys.68.52092.suppl8

Supplementary material 9

Phylogeny of *RPB2* for species classified in *Talaromyces* section *Subinflati*

Authors: Bing-Da Sun, Amanda J. Chen, Jos Houbraken, Jens C. Frisvad, Wen-Ping Wu, Hai-Lei Wei, Yu-Guang Zhou, Xian-Zhi Jiang, Robert A. Samson

Data type: phylogenetic

Explanation note: Branches with values more than 1 pp and 95% bs are thickened. *Talaromyces dendriticus* was chosen as outgroup.

Link: https://doi.org/10.3897/mycokeys.68.52092.suppl9

MycoKeys 68: 115–135 (2020)
doi: 10.3897/mycokeys.68.53561
http://mycokeys.pensoft.net

RESEARCH ARTICLE

A peer-reviewed open-access journal
MycoKeys
Launched to accelerate biodiversity research

Taxonomy and phylogeny of *Sidera* (Hymenochaetales, Basidiomycota): four new species and keys to species of the genus

Rui Du[1*], Fang Wu[1*], Genevieve M. Gate[2], Yu-Cheng Dai[1], Xue-Mei Tian[3]

1 *School of Ecology and Nature Conservation, PO Box 61, Beijing Forestry University, Beijing 100083, China* **2** *Tasmanian Institute of Agriculture, Private Bag 98, Hobart, Tasmania 7001, Australia* **3** *Shandong Provincial Key Laboratory of Applied Mycology, Qingdao Agricultural University, Qingdao 266109, China*

Corresponding author: Yu-Cheng Dai (yuchengd@yahoo.com); Xue-Mei Tian (txm@qau.edu.cn)

Academic editor: K. Hosaka | Received 23 April 2020 | Accepted 10 June 2020 | Published 7 July 2020

Citation: Du R, Wu F, Gate GM, Dai Y-C, Tian X-M (2020) Taxonomy and phylogeny of *Sidera* (Hymenochaetales, Basidiomycota): four new species and keys to species of the genus. MycoKeys 68: 115–135. https://doi.org/10.3897/mycokeys.68.53561

Abstract

Sidera is a polypore genus with white to cream or buff basidiomata, whose species in Hymenochaetales are poorly known. We study the phylogeny and diversity of *Sidera* based on our recent collections from tropic and subtropic Asian-Pacific regions. Phylogenetic analyses based on the internal transcribed spacer (ITS) and nuclear large subunit (nLSU) ribosomal RNA gene regions indicate that ten terminal lineages are well supported within *Sidera*. Based on morphological examination and phylogeny, four new species, viz. *Sidera minutissima*, *S. parallela*, *S. srilankensis* and *S. tenuis* are described, and a new combination, *Sidera minutipora*, is proposed. All these species are illustrated. *Sidera minutissima* is characterized by tiny basidiomata with bluish pores when fresh, generative hyphae dominating at the dissepiment edges, the presence of cystidioles, and allantoid basidiospores measuring 3.8–4.4 × 0.9–1.3 µm. *Sidera parallela* differs from other poroid species in the genus by having parallel tramal hyphae in combination with lunate basidiospores measuring 2.8–3.3 × 0.9–1.2 µm. *Sidera srilankensis* have generative and skeletal hyphae co-dominating at the dissepiment edges, and lunate basidiospores measuring 3.5–4 × 1–1.3 µm. *Sidera tenuis* is distinguished by small pores (8–10 per mm) and relatively long allantoid basidiospores measuring 4.2–5 × 0.8–1 µm. *Sidera minutipora* is characterized by buff to olivaceous buff basidiomata when dry, 5–7 pores per mm, rosette-like crystals rare, and allantoid basidiospores measuring 3.7–4.3 × 1–1.3 µm. An identification key to all accepted species is provided.

Keywords

Phylogeny, Rickenellaceae, taxonomy, wood-rotting fungi

* Contributed equally as the first authors.

Introduction

Sidera Miettinen & K.H. Larss. was established by Miettinen and Larsson (2011) based on molecular and morphological analyses, with *S. lenis* (P. Karst.) Miettinen as the type species. Five species are currently accepted in the genus: *S. lenis* (= *Physisporus lenis* P. Karst., Rabenhorst 1886), *S. vulgaris* (Fr.) Miettinen (= *Polyporus vulgaris* Fr., Fries 1821), *S. lowei* (Rajchenb.) Miettinen (= *Ceriporiopsis lowei* Rajchenb., Rajchenberg 1987), *S. lunata* (Romell ex Bourdot & Galzin) K.H. Larss. (= *Grandinia lunata* Romell ex Bourdot & Galzin, Bourdot and Galzin 1928), and *S. vesiculosa* Rui Du & M. Zhou (Du et al. 2019). The genus is characterized by resupinate, white to cream or buff, mostly waxy basidiomata when fresh, poroid or hydnoid hymenophore, a monomitic or dimitic hyphal system with generative hyphae bearing clamp connections, the presence of rosette-like crystals, and allantoid to lunate basidiospores (Miettinen and Larsson 2011; Du et al. 2019). Species grow on decaying wood and cause a white-rot (Dai et al. 2007; Yuan and Dai 2008; Miettinen and Larsson 2011; Du et al. 2019).

In the phylogeny, current five *Sidera* species distributed in Europe, Asia, Pacific Ocean and South America were defined based on ITS and nLSU sequences. *Sidera vesiculosa*, *S. lowei*, *S. vulgaris* have distributions in Asian-Pacific regions. However, samples named as *Sidera vulgaris* from New Zealand and Australia were separated into two lineages (Miettinen and Larsson 2011; Du et al. 2019).

New specimens collected from the tropic and subtropic Asian-Pacific regions have been studied by morphological and DNA methods. As a result, four unknown *Sidera* species are found. Another species, originally described as *Poria minutipora* Rodway & Cleland from Australia, is proposed for transfer to *Sidera*, and the sample from Australia named as *S. vulgaris* by Miettinen and Larsson (2011) is also identified as the species. In addition, specimens or literatures and sequences of all ten accepted *Sidera* species are studied. Furthermore, an identification key to accepted species is provided.

Materials and methods

Morphological studies

The studied specimens are deposited at the herbarium of the Institute of Microbiology, Beijing Forestry University (**BJFC**). Macro-morphological descriptions are based on field notes and dry herbarium specimens. Microscopic measurements and drawings were made from slide preparations of dried specimens stained with Cotton Blue and Melzer's reagent following Dai (2010). In presenting spore size variation, 5% of measurements were excluded from each end of the range and this value is given in parentheses. The following abbreviations were used: KOH = 2% potassium hydroxide, CB = Cotton Blue, CB– = acyanophilous, IKI = Melzer's reagent, IKI– = neither amyloid nor dextrinoid, L = mean spore length (arithmetic average of all spores), W = mean spore width (arithmetic average of all spores), Q = variation in the L/W ratios between specimens studied, n (a/b) = number of spores (a) measured from given number of

specimens (b). Special color terms follow Anonymous (1969) and Petersen (1996). Herbarium abbreviations follow Thiers (2018).

Molecular studies

A CTAB rapid plant genome extraction kit (Aidlab Biotechnologies Co., Ltd., Beijing, China) was used to extract total genomic DNA from dried specimens following the manufacturer's instructions with some modifications (Cui et al. 2019; Shen et al. 2019). ITS regions were amplified with primers ITS4 and ITS5 (White et al. 1990), and the nLSU with primers LR0R and LR7. The PCR procedure for ITS was as follows: initial denaturation at 95 °C for 3 min, followed by 35 cycles at 94 °C for 40 sec, 54 °C for 45 sec and 72 °C for 1 min, and a final extension of 72 °C for 10 min. The PCR procedure for nLSU was as follows: initial denaturation at 94 °C for 1 min, followed by 35 cycles at 94 °C for 1min, 50 °C for 1 min and 72 °C for 1.5 min, and a final extension of 72 °C for 10 min. The PCR products were purified and sequenced in the Beijing Genomics Institute, China, with the same primers used in the PCR reactions.

Phylogenetic analyses

Phylogenetic analyses were applied to ITS+nLSU sequences. Sequences generated in this study were aligned with additional sequences downloaded from GenBank (Table 1) using Clustal X (Thompson et al. 1997) and manually adjusted in BioEdit (Hall 1999). Prior to phylogenetic analysis, ambiguous sequences at the start and the end were deleted and gaps were manually adjusted to optimize the alignment. Sequence alignment was deposited at TreeBase (submission ID 26119). Phylogenetic analysis was done as in Li et al. (2014) and Zhu et al. (2019). Sequences of *Exidia candia* Lloyd and *Exidiopsis calcea* (Pers.) K. Wells outside Hymenochaetales were used as outgroup referred to Miettinen and Larsson (2011) and Yuan et al. (2016), because some species related to *Sidera* in Polyporales, like *Skeletocutis* species, were added in phylogenetic analysis.

Maximum parsimony analysis (MP) was performed in PAUP* version 4.0b10 (Swofford 2002). All characters were equally weighted and gaps were treated as missing data. Trees were inferred using the heuristic search option with TBR branch swapping and 1000 random sequence additions. Max-trees were set to 1000, branches of zero length were collapsed and all parsimonious trees were saved. Clade robustness (BP) was assessed using a bootstrap analysis with 1000 replicates (Felsenstein 1985).

The optimal substitution models for the combined dataset were determined using the Akaike Information Criterion (AIC) implemented in MrModeltest 2.2 (Nylander 2004) after scoring 24 models of evolution by PAUP* version 4.0 beta 10 (Swofford 2002). The selected model applied in the Bayesian phylogenetic inference (BI) analyses and Maximum likelihood (ML) analyses was the model GTR+I+G.

The BI analysis was performed with MrBayes 3.2.5 (Ronquist et al. 2012). Four Markov chains were run for 5 million generations and trees were sampled every 1000

Table 1. Information for the sequences used in this study.

Species	Specimen no.	Locality	GenBank accession no.	
			ITS	nLSU
Ceriporiopsis aneirina	MUAF 888	Czech Republic	EU340895	EU340895
Contumyces rosella	Redhead 7501	–	U66452	U66452
Exidia candida	Spirin 8588	USA	KY801870	KY801895
Exidiopsis calcea	MW 331	Canada	AF291280	AF291326
Gloeoporus dichrous	KHL 11173	Norway	EU118627	EU118627
Gloeoporus hainanensis	Dai 15253	China	KU360402	KU360408
Globulicium hiemale	Hjm 19007	Sweden	DQ873595	DQ873595
Hyphodermella poroides	Dai 12045	China	KX008367	KX011852
Odonticium romellii	Murdoch 38	Finland	MF319073	MF318929
Oxyporus corticola	KHL 13217	Estonia	DQ873641	DQ873641
Phlebia georgica	KHL 12019	Norway	DQ873645	DQ873645
Repetobasidium conicum	KHL 12338	USA	DQ873647	DQ873647
Resinicium furfuraceum	KHL 11738	Finland	DQ873648	DQ873648
Rickenella mellea	Lamoure 74	–	U66438	U66438
Skvortzovia pinicola	KHL 12224	USA	DQ873637	DQ873637
Sidera lenis	Miettinen 11036	Finland	FN907914	FN907914
Sidera lowei	Miettinen X419	Venezuela	FN907917	FN907917
Sidera lunata	JS 15063	Norway	DQ873593	DQ873593
Sidera minutipora	Gates FF257	Australia	FN907922	FN907922
Sidera minutipora	**Cui 16720**	**Australia**	**MN621349**	**MN621348**
Sidera minutissima	**Dai 19529**	**Sri Lanka**	**MN621352**	**MN621350**
Sidera minutissima	**Dai 19587**	**Sri Lanka**	**–**	**MN621351**
Sidera parallela	**Cui 10346**	**China**	**MK346145**	**–**
Sidera parallela	**Cui 10361**	**China**	**MK346144**	**–**
Sidera srilankensis	**Dai 19581**	**Sri Lanka**	**MN621345**	**MN621347**
Sidera srilankensis	**Dai 19654**	**Sri Lanka**	**MN621344**	**MN621346**
Sidera tenuis	**Dai 18697**	**Australia**	**MK331865**	**MK331867**
Sidera tenuis	**Dai 18698**	**Australia**	**MK331866**	**MK331868**
Sidera vesiculosa	BJFC025367	Singapore	NH636565	NH636567
Sidera vesiculosa	BJFC025377	Singapore	NH636564	NH636566
Sidera vulgaris	Ryvarden 37198	New Zealand	FN907918	FN907918
Skeletocutis amorpha	Miettinen 11038	Finland	FN907913	FN907913
Skeletocutis chrysella	Miettinen 9472	Finland	FN907916	FN907916
Skeletocutis lilacina	HHB 10522sp	USA	KY948834	KY948894
Skeletocutis yuchengii	FBCC 1132	China	KY953045	KY953045
Skeletocutis yunnanensis	Dai 15709	China	KU950434	KU950436
Skeletocutis odora	L 13763sp	Canada	KY948830	KY948893
Skeletocutis vulgaris	CBS 465.50	France	MH856711	–

New sequences are shown in bold.

generations. The first 25% of the sampled trees were discarded as burn-in, and the remaining ones were used to reconstruct a majority rule consensus tree and calculate Bayesian posterior probabilities (BPP) of the clades. The ML analysis was conducted on RAxmlGUI 1.31 (Michalak 2012), and all parameters used default settings. Statistical support values (BS) were obtained using non- parametric bootstrapping with 1000 replicates. The best fit maximum likelihood tree from all searches was kept. Branches that received bootstrap support values for MP and ML greater than or equal to 70% and BPP greater than or equal to 0.95 were considered as significantly supported.

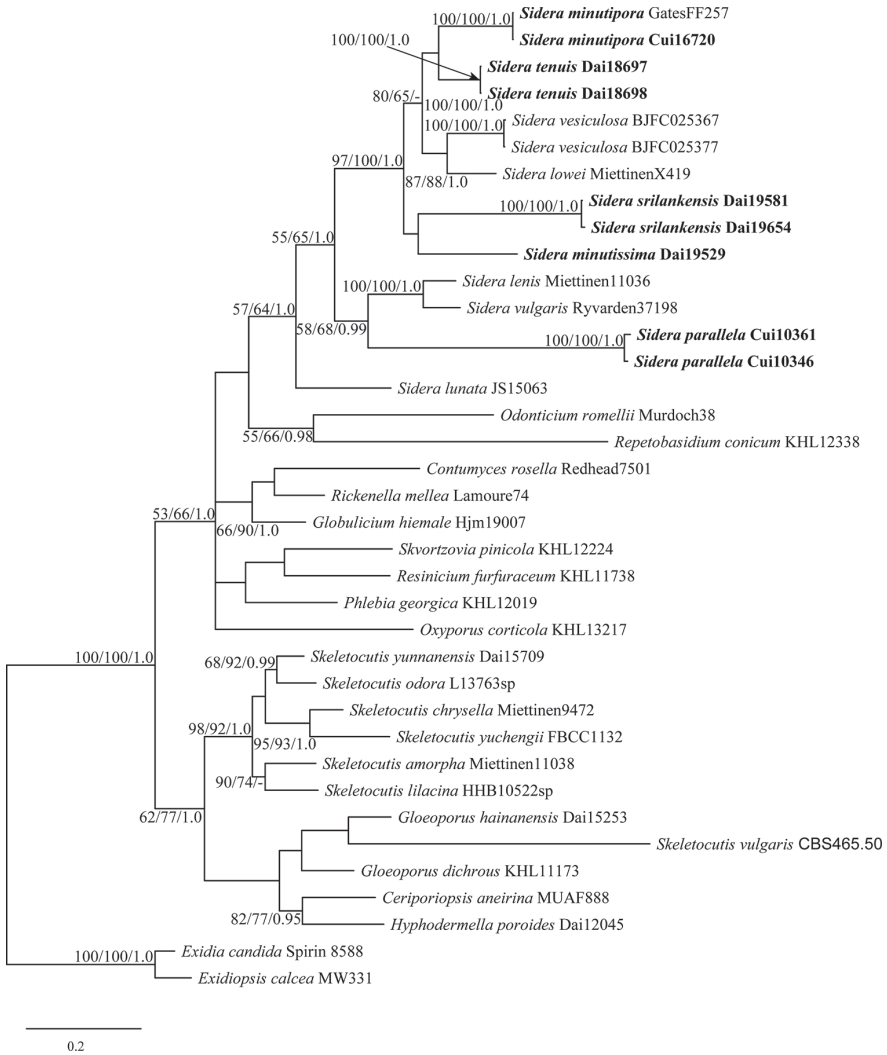

Figure 1. Phylogeny of *Sidera* and related species generated by BI analysis based on combined ITS and nLSU sequences. Branches are labeled with MP and ML bootstrap values higher than 50%, and BI probabilities more than 0.95. New species and a new combination name are indicated in bold.

Results

Phylogenetic analyses

The combined ITS+nLSU dataset included sequences from 37 specimens representing 32 species (Table 1). The specimen Dai 19587 was not included because of its lack of ITS sequence, but it has an nLSU sequence with 100% identity to Dai 19529. The dataset had an aligned length of 1718 characters, of which 909 are constant, 148 are variable but parsimony-uninformative, and 661 are parsimony-informative. BI analyses resulted in a best tree (Figure 1), where the ESSs of all parameters were superior to

1000 and the PSRFs were close to 1.0. MP and ML analyses produced consensus trees similar to BI analysis, and only the BI tree is presented along with support values from MP and ML analyses. Our newly generated sequences formed five robustly supported lineages within the *Sidera* clade, which we interpret as four new species and support for one new combination.

Taxonomy

Sidera minutipora **(Rodway & Cleland) Y.C. Dai, F. Wu, G.M. Gates & Rui Du, comb. nov.**
MycoBank No: 835373
Figures 2, 3

Poria minutipora Rodway & Cleland, Pap. & Proc. Roy. Soc. Tasmania 1929: 17 (1930). Basionym.

Type. Australia. New South Wales, Malanganee, 25 miles west of Casino, August 1917, MBT 35118.

Description. ***Basidiomata*****:** Annual, resupinate, soft when fresh, soft corky to fragile when dry, up to 6.5 cm long, 3 cm wide, and approximately 1 mm thick at

Figure 2. A basidioma of *Sidera minutipora* (Cui 16720). Scale bar: 1 cm. Photo by Bao-Kai Cui.

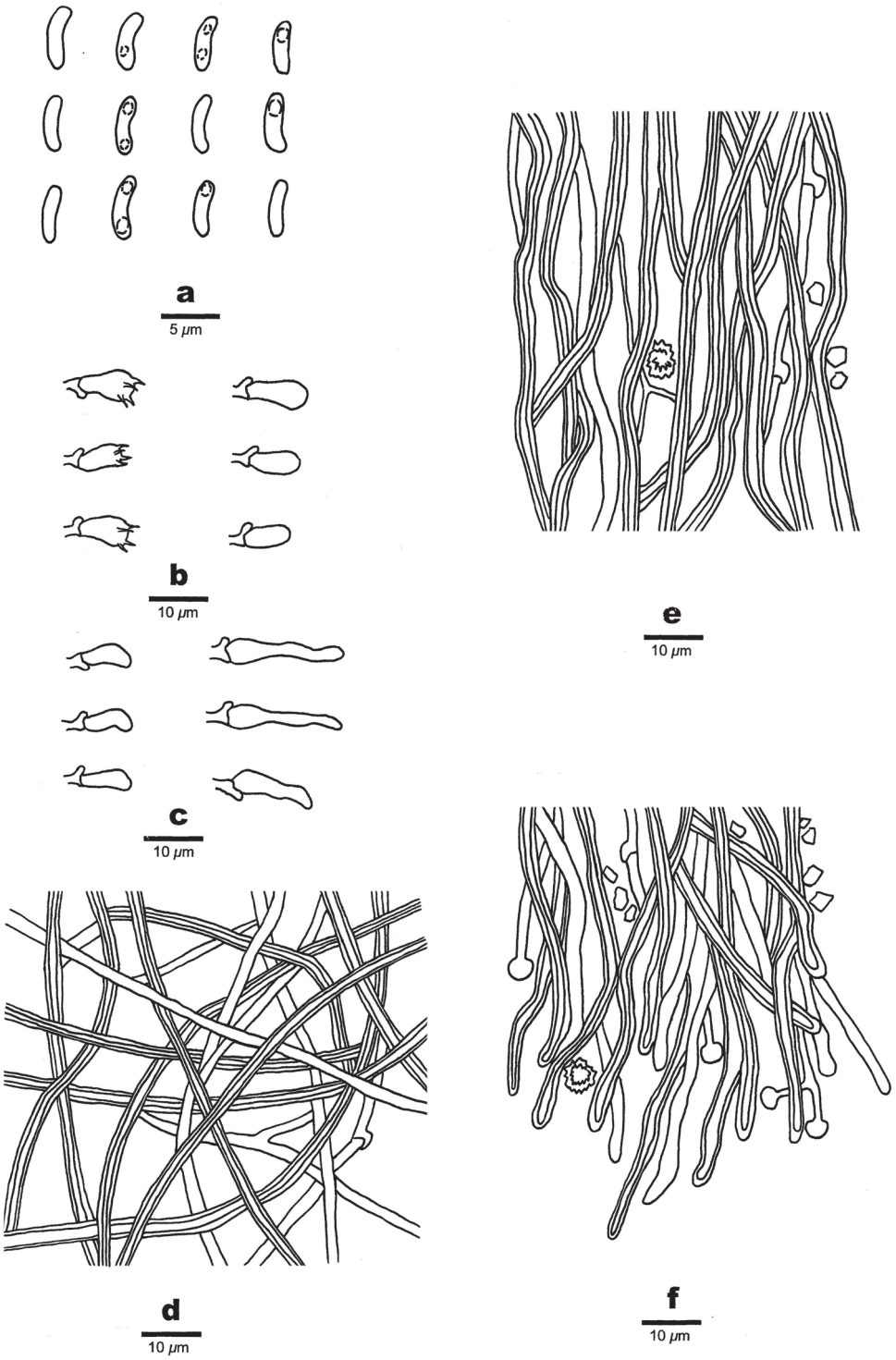

Figure 3. Microscopic structures of *Sidera minutipora* (Cui 16720) **a** basidiospores **b** basidia, basidioles **c** cystidioles **d** hyphae from subiculum **e** hyphae from trama **f** hyphae at dissepiment edge. Drawings by Rui Du.

center; pore surface cream to buff when fresh, become buff to olivaceous buff when dry; sterile margin distinct, fimbriate, thinning out; pores round, 5–7 per mm; dissepiments thin, lacerate; subiculum very thin to almost absent; tubes darker than the poroid surface, up to 1 mm long.

***Hyphal structure*:** Hyphal system dimitic, generative hyphae bearing clamp connections; all hyphae IKI–, CB–, skeletal hyphae swolling in KOH.

***Subiculum*:** Generative hyphae hyaline, thin-walled, occasionally branched, 1–2 μm in diam; skeletal hyphae dominant, unbranched, interwoven, 1.5–2.5 μm diam; rosette-like crystals occasionally present, 1.5–7.0 μm in diam, irregular crystals frequently present.

***Tubes*:** Generative hyphae hyaline, thin-walled, occasionally branched, 1–2 μm in diam, some with swollen tips; skeletal hyphae with a narrow lumen to subsolid, unbranched, interwoven, 1.8–3.0 μm diam; skeletal hyphae and generative hyphae co-dominating at dissepiment edges; rosette-like and irregular rhomboidal crystals occasionally present; cystidioles present, fusoid, hyaline, thin-walled, basally swollen, with a long or hyphoid neck, 7–19 × 2.4–4 μm; basidia barrel-shaped, hyaline, bearing four sterigmata and a basal clamp connection, 6.7–9 × 3.5–4.5 μm; basidioles in shape similar to basidia, but slightly shorter.

***Basidiospores*:** Allantoid, hyaline, thin-walled, smooth, occasionally with one or two guttules, IKI–, CB–, 3.7–4.3(–4.5) × 1–1.3 μm, L = 4.01 μm, W = 1.08 μm, Q = 3.71 (n = 30/1).

Specimen examined. Australia. Tasmania, Arve River Streamside Reserve, on rotten stump of *Eucalyptus*, 15 May 2018, B.K. Cui 16720 (BJFC 030019, Duplication in MEL); Warra LTER, 43°05'4"S, 146°38'5"E, 16.Jan 2007 Gates FF257 (MEL).

***Sidera minutissima* Y.C. Dai, F. Wu, G.M. Gates & Rui Du, sp. nov.**
MycoBank No: 833182
Figures 4, 5

Type material. *Holotype*: Sri Lanka. Wadduwa, South Bolgoda Lake, on rotten angiosperm branch, 28 Feb 2019, Y.C. Dai 19529 (BJFC, isotype in University of Ruhuha).

Etymology. *Minutissima* (Lat.), refers to the species having small basidiomata.

Description. *Basidiomata*: Annual, resupinate, soft when fresh, soft corky to fragile when dry, up to 5 cm long, 3 cm wide, and approximately 1 mm thick at center; pore surface bluish to more or less turquoise when fresh, becoming cream to buff yellow when dry; sterile margin distinct, fimbriate, thinning out; pores round, 7–9 per mm; dissepiments thin, entire; subiculum very thin to almost absent; tubes concolorous with pore surface, up to 1 mm long.

***Hyphal structure*:** Hyphal system dimitic, generative hyphae bearing clamp connections; skeletal hyphae unbranched, interwoven, 2–3 μm diam; all hyphae IKI–, CB–,unchanged in KOH.

***Subiculum*:** Generative hyphae hyaline, thin-walled, frequently branched, 1–2 μm in diam; skeletal hyphae dominant, more or less straight, unbranched, interwoven,

Figure 4. A basidioma of *Sidera minutissima* (paratype, Dai 19587). Scale bar: 1 cm. Photo by Yu-Cheng Dai.

2–3 µm diam; rosette-like crystals frequently present, 2–8.5 µm in diam, some irregular rhomboidal crystals present.

***Tubes*:** Generative hyphae hyaline, thin-walled, frequently branched, 1–2 µm in diam, some with swollen tips, dominating at dissepiment edges; skeletal hyphae with a narrow lumen to subsolid, unbranched, interwoven, 2–3 µm diam; rosette-like and irregular rhomboidal crystals abundant; cystidioles present, fusoid, hyaline, thin-walled, basally swollen, some with a long or hyphoid neck, 8–18 × 2–5 µm; basidia barrel-shaped, hyaline, bearing four sterigmata and a basal clamp connection, 7.1–12 × 3.5–4.8 µm; basidioles in shape similar to basidia, but slightly shorter.

***Basidiospores*:** Allantoid, hyaline, thin-walled, smooth, occasionally with one or two guttules, IKI–, CB–, (3.7–)3.8–4.4(–4.5) × (0.8–)0.9–1.3 µm, L = 4.02 µm, W = 1.07 µm, Q = 3.67–3.85 (n = 60/2).

Additional specimen examined (paratype). Sri Lanka. Kandy, Udawatta kele, Royal Forest Park. on rotten angiosperm wood, 2 Mar 2019, Y.C. Dai 19587 (BJFC).

***Sidera parallela* Y.C. Dai, F. Wu, G.M. Gates & Rui Du, sp. nov.**
MycoBank No: 829166
Figures 6, 7

Type material. *Holotype*: China. Yunnan Province, Lanping County, Luogujing Scenic Spot, on rotten angiosperm trunk, 19 Sep 2011, B.K. Cui 10346 (BJFC 011241).

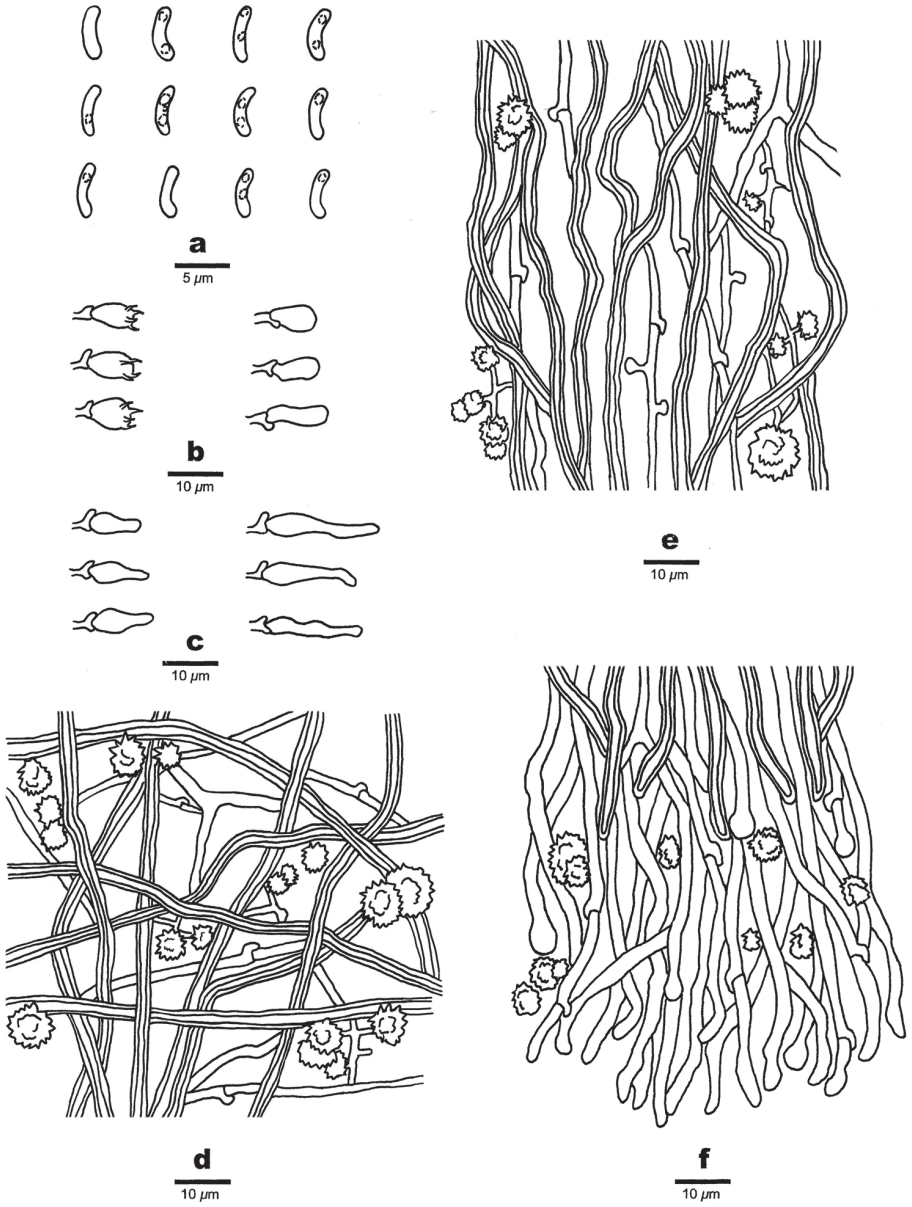

Figure 5. Microscopic structures of *Sidera minutissima* (holotype, Dai 19529) **a** basidiospores **b** basidia, basidioles **c** cystidioles **d** hyphae from subiculum **e** hyphae from trama **f** hyphae at dissepiment edge. Drawings by Rui Du.

Etymology. *Parallela* (Lat.), refers to the species having tubes with parallel tramal hyphae.

Description. ***Basidiomata*:** Annual, resupinate, soft corky when fresh, soft corky when dry, up to 11 cm long, 4 cm wide, and approximately 1.5 mm thick at center;

Figure 6. A basidioma of *Sidera parallela* (holotype, Cui 10346). Scale bar: 1 cm. Photo by Bao-Kai Cui.

pore surface white when fresh, becoming cream to buff yellow upon drying; sterile margin distinct, fimbriate, thinning out; pores round, 6–8 per mm; dissepiments thick, entire; subiculum very thin to almost absent; tubes concolorous with pore surface, up to 1.5 mm long.

***Hyphal structure*:** Hyphal system dimitic, generative hyphae bearing clamp connections; skeletal hyphae dominant, unbranched, interwoven or parallel, 2–3 μm diam; all hyphae IKI–, CB–, unchanged in KOH.

***Subiculum*:** Generative hyphae hyaline, thin-walled, rarely branched, 1–2 μm in diam; skeletal hyphae dominating, more or less straight, unbranched, interwoven, 2–3 μm diam; rosette-like crystals frequently present, 2–8.5 μm in diam, some irregular rhomboidal crystals present.

***Tubes*:** Generative hyphae hyaline, thin-walled, rarely branched, 1–2 μm in diam, dominating at dissepiment edges; skeletal hyphae with a narrow lumen to subsolid, unbranched, parallel along the tubes, 2–3 μm diam; rosette-like and irregular rhomboidal crystals abundant; cystidia absent; cystidioles present, fusoid, hyaline, thin-walled, basally swollen, with a sharp or often hyphoid neck, 8.0–17 × 2.3–4 μm; basidia barrel-shaped, hyaline, bearing four sterigmata and a basal clamp connection, 7–9 × 4–5 μm; basidioles in shape similar to basidia, but slightly shorter.

***Basidiospores*:** Lunate, hyaline, thin-walled, smooth, occasionally with one or two guttules, IKI–, CB–, (2.7–)2.8–3.3 × (0.8–)0.9–1.2 μm, L = 3 μm, W = 1.07 μm, Q = 2.72–2.87 (n = 60/2).

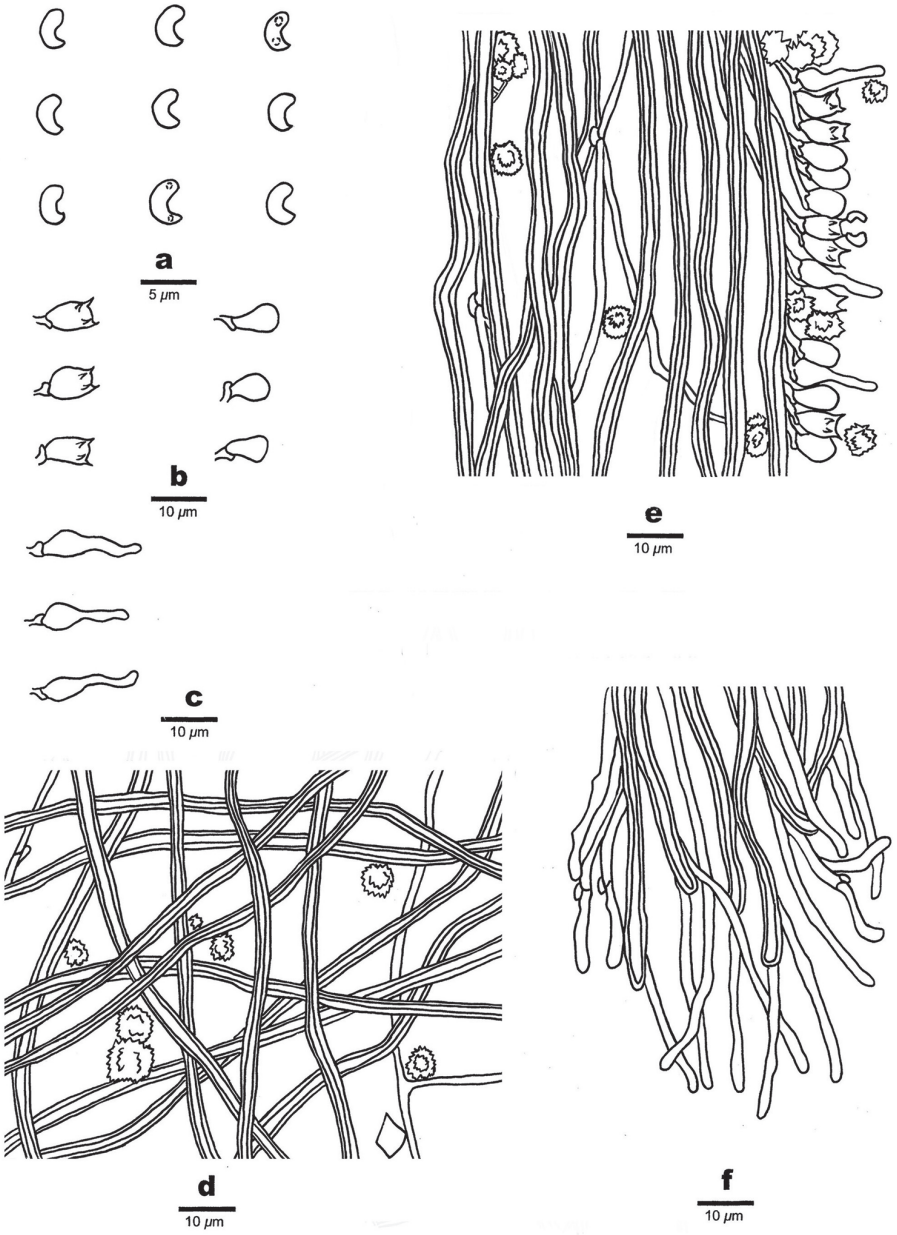

Figure 7. Microscopic structures of *Sidera parallela* (holotype, Cui 10346) **a** basidiospores **b** basidia, basidioles **c** cystidioles **d** hyphae from subiculum **e** hyphae from trama **f** hyphae at dissepiment edge. Drawings by Rui Du.

Additional specimen examined (paratype). China. Yunnan Province, Lanping County, Luogujing Scenic Spot, on fallen angiosperm trunk, 19 Sep 2011, B.K. Cui 10361 (BJFC 011256).

Sidera srilankensis **Y.C. Dai, F. Wu, G.M. Gates & Rui Du, sp. nov.**
MycoBank No: 833183
Figures 8, 9

Type material. ***Holotype*****:** Sri Lanka. Western Province, Mitirigala Nissarana, Vanaya Forest, on rotten angiosperm wood, 4 Mar 2019, Y.C. Dai 19654 (BJFC, isotype in University of Ruhuha).

Etymology. *Srilankensis* (Lat.), refers to the species being found in Sri Lanka.

Description. ***Basidiomata*****:** Annual, resupinate, soft when fresh, soft corky to fragile when dry, up to 16.5 cm long, 3 cm wide, and approximately 1 mm thick at center; pore surface cream when fresh, becoming buff yellow upon drying; sterile margin distinct, fimbriate, thinning out; pores round, 6–8 per mm; dissepiments thin, lacerate; subiculum very thin to almost absent; tubes concolorous with poroid surface, up to 1 mm long.

Hyphal structure**:** Hyphal system dimitic, generative hyphae bearing clamp connections; skeletal hyphae dominant, unbranched, interwoven, 1.5–3 µm diam; all hyphae IKI–, CB–, unchanged in KOH.

Subiculum**:** Generative hyphae hyaline, thin-walled, frequently branched, 1–2 µm in diam; skeletal hyphae dominant, more or less straight, unbranched, interwoven, 1.5–3 µm diam; rosette-like crystals frequently present, 3.5–12 µm in diam, some irregular rhomboidal crystals present.

Figure 8. A basidioma of *Sidera srilankensis* (holotype, Dai 19654). Scale bar: 1 cm. Photo by Yu-Cheng Dai.

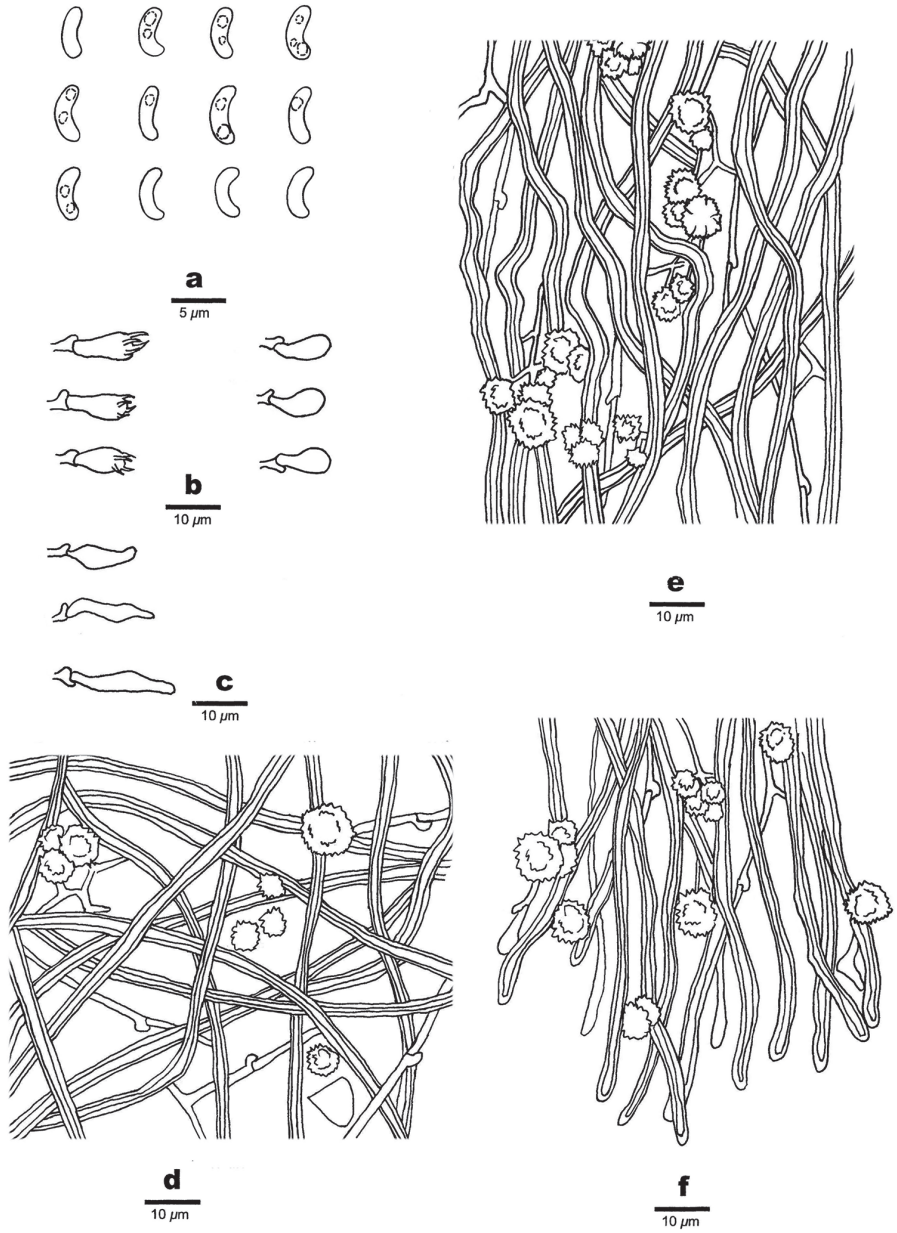

Figure 9. Microscopic structures of *Sidera srilankensis* (holotype, Dai 19654) **a** basidiospores **b** basidia, basidioles **c** cystidioles **d** hyphae from subiculum **e** hyphae from trama **f** hyphae at dissepiment edge. Drawings by Rui Du.

***Tubes*:** Generative hyphae hyaline, thin-walled, frequently branched, 1–2 μm in diam; skeletal hyphae with a narrow lumen to subsolid, unbranched, interwoven, 1.5–3 μm diam; skeletal hyphae and generative hyphae co-dominating at dissepiment edges; rosette-like and irregular rhomboidal crystals abundant; cystidia absent; cystidioles

present, fusoid, hyaline, thin-walled, basally swollen, with a sharp or often hyphoid neck, 8.1–14 × 3–4.1 µm; basidia barrel-shaped, hyaline, bearing four sterigmata and a basal clamp connection, 7.8–13.2 × 3.6–4.5 µm; basidioles in shape similar to basidia, but slightly shorter.

***Basidiospores*:** Lunate, hyaline, thin-walled, smooth, occasionally with one or two guttules, IKI–, CB–, (3.4–)3.5–4(–4.1) × 1–1.3(–1.4) µm, L = 3.83 µm, W = 1.16 µm, Q = 3.28–2.34 (n = 60/2).

Additional specimen examined (paratype). Sri Lanka. Kandy, Udawatta Kele, Royal Forest Park, on rotten angiosperm wood, 2 Mar 2019, Y.C. Dai 19581 (BJFC).

***Sidera tenuis* Y.C. Dai, F. Wu, G.M. Gates & Rui Du, sp. nov.**
MycoBank No: 829165
Figures 10, 11

Type material. *Holotype*: Australia. Tasmania, Hobart, Mt Wellington, on rotten wood of *Eucalyptus*, 13 May 2018, Y.C. Dai 18697 (BJFC 027166, isotype in MEL).

Etymology. *Tenuis* (Lat.), refers to the species having narrow basidiospores.

Description. *Basidiomata*: Annual, resupinate, soft and waxy when fresh, soft corky when dry, up to 10 cm long, 3 cm wide, and approximately 1 mm thick at cent-

Figure 10. A basidioma of *Sidera tenuis* (holotype, Dai 18697). Scale bar: 1 cm. Photo by Yu-Cheng Dai.

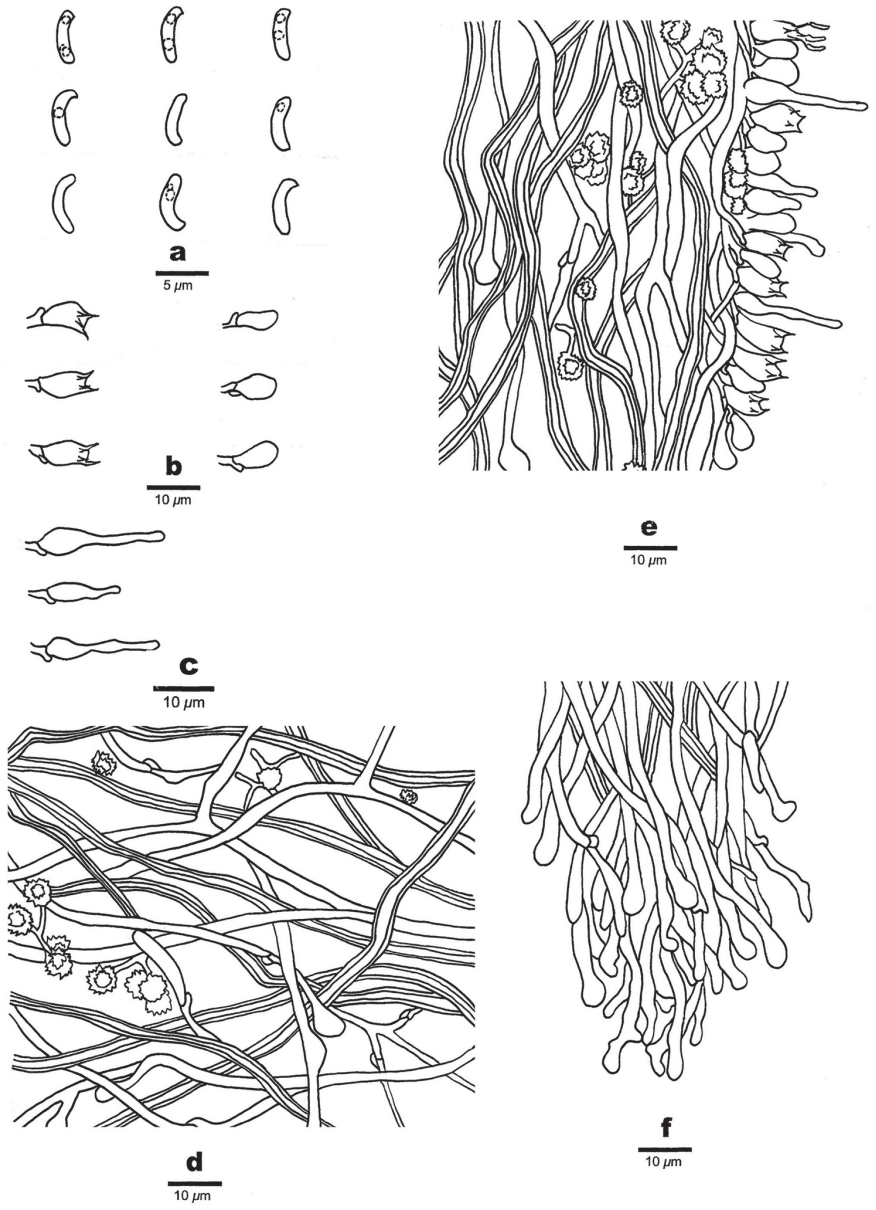

Figure 11. Microscopic structures of *Sidera tenuis* (holotype, Dai 18697) **a** basidiospores **b** basidia, basidioles **c** cystidioles **d** hyphae from subiculum **e** hyphae from trama **f** hyphae at dissepiment edge. Drawings by Rui Du.

er; pore surface white when fresh, becoming cream when dry; sterile margin indistinct; pores round, 8–10 per mm; dissepiments thin, entire; subiculum very thin to almost absent; tubes concolorous with poroid surface, up to 1 mm long.

***Hyphal structure*:** Hyphal system dimitic, generative hyphae bearing clamp connections; skeletal hyphae dominant, unbranched, interwoven, 2–3 μm in diam; all hyphae IKI–, CB–, and unchanged in KOH.

***Subiculum*:** Generative hyphae hyaline, thin-walled, frequently branched, 1–2.5 μm in diam, some with distinctly swollen tips which in shape are globose, bottle-shaped or irregularly elongated; skeletal hyphae dominant, unbranched, interwoven, 2–3 μm in diam; rosette-like crystals frequently present, 2.5–10 μm in diam, some irregular rhomboidal crystals present.

***Tubes*:** Generative hyphae hyaline, thin-walled, frequently branched, 1–2.5 μm in diam, some with swollen tips, dominant at dissepiment edges; skeletal hyphae with a narrow lumen to subsolid, unbranched, interwoven, 2–3 μm diam; rosette-like and irregular rhomboidal crystals abundant; cystidia absent; cystidioles present, fusoid, hyaline, thin-walled, swollen at base, with a sharp or often hyphoid neck, 6–25 × 2.5–4.5 μm; basidia barrel-shaped, hyaline, bearing four sterigmata and a basal clamp connection, 7.3–11 × 3.5–5 μdm; basidioles in shape similar to basidia, but slightly shorter.

***Basidiospores*:** Allantoid, thin-walled, smooth, usually with one or two small guttules, IKI–, CB–, (4.1–)4.2–5(–5.4) × (0.7–)0.8–1(–1.2) μm, L = 4.62 μm, W = 0.95 μm, Q = 4.73–4.95 (n = 60/2).

Additional specimen examined (paratype). Australia. Hobart, Mt Wellington, on rotten wood of *Eucalyptus*, 13 May 2018, Y.C. Dai 18698 (BJFC 027167).

Key to species accepted in *Sidera*

1	Hymenium grandinioid to odontioid	***S. lunata***
–	Hymenium poroid	**2**
2	Hyphal system monomitic	**3**
–	Hyphal system dimitic	**4**
3	Basidiospores 2.9–3.7 × 0.6–1 μm	***S. vesiculosa***
–	Basidiospores 3.5–5 × 1–1.2 μm	***S. lowei***
4	Basidiomata perennial; basidiospores > 1.5 μm in wildth	***S. lenis***
–	Basidiomata annual; basidiospores < 1.5 μm in wildth	**5**
5	Pore surface bluish when fresh	***S. minutissima***
–	Pore surface white to cream or buff when fresh	**6**
6	Pores 8–10 per mm	***S. tenuis***
–	Pores 5–8 per mm	7
7	Tramal hyphae parallel along tubes	***S. parallela***
–	Tramal hyphae interwoven in the tubes	**8**
8	Basidiospores 2.9–3.6 μm long	***S. vulgaris***
–	Basidiospores mostly 3.5–4.3 μm long	**9**
9	Basidiospores lunate, skeletal hyphae unchanged in KOH	***S. srilankensis***
–	Basidiospores allantoid, skeletal hyphae swollen in KOH	***S. minutipora***

Discussion

Previously five species of *Sidera*, viz. *S. lenis*, *S. lowei*, *S. lunata*, *S. vesiculosa* and *S. vulgaris*, were described or transferred to the genus. In this paper, *Sidera minutissima*, *S. parallela*, *S. srilankensis* and *S. tenuis* are described as new to science. In addition, *Sidera minutipora* is proposed as a new combination based on *Poria minutipora*. All these species with resupinate, white to cream or buff, bluish to more or less turquoise basidiomata when fresh, a dimitic hyphal system with generative hyphae bearing clamp connections, the presence of rosette-like crystals and allantoid to lunate basidiospores fit well in *Sidera*. Besides, they formed distinct lineages within the *Sidera* clade inferred from ITS and nLSU datasets (Figure 1).

Eight names were listed as synonyms of *S. lenis* (Index Fungorum and Mycobank): *Poria lunulispora* Pilát (type from Siberia), *P. chakasskensis* Pilát (type from Siberia), *P. earlei* Murrill (type from Jamaica), *P. tenuipora* Murrill (type from Jamaica), *P. montana* Murrill (type from Jamaica), *P. consimilis* Rick (type from Brazil), *P. subvulgaris* Rick (type from Brazil) and *P. minutipora* (type from Tasmania). Buchanan and Ryvarden (1993) indicated that the holotype of *P. minutipora* was not found, but an isotype PDD 7115 labelled part of type collection was studied. This comprised fragments of two species, *Diplomitoporus lenis* (P. Karst.) Gilb. & Ryvarden (=*Sidera lenis*) and *Schizopora flavipora* (Berk. & M.A. Curtis ex Cooke) Ryvarden [=*Xylodon flaviporus* (Berk. & M.A. Curtis ex Cooke) Riebesehl & Langer], and the portion of the isotype conforming to *D. lenis* was selected as lectotype for *P. minutipora*.

Three taxa were treated as synonyms of *Sidera vulgaris* (Index Fungorum and Mycobank): *Boletus papyraceus* Schrank, *B. proteus* Bolton and *B. cellulosus* O.F. Müll, and all of them were originally described from Europe, and they most probably represent a single species of *S. vulgaris* which was originally described from Sweden (Niemelä and Dai 1997).

In our phylogeny Gates FF257 clustered with Cui 16720 with high support within the *Sidera* clade (Figure 1), and both samples were collected from Tasmania, Australia. The sample Gates FF257 was named as *S. vulgaris* by Miettinen and Larsson (2011), but *S. vulgaris* was originally described from Europe and is different from the Australian specimens by having shorter basidiospores (2.9–3.6 × 0.9–1.4 μm according to Niemelä and Dai 1997, vs. 3.7–4.3 × 1–1.3 μm in Cui 16720). According to the protologue of *Poria minutipora* pores are 7 per mm and the only microscopic characteristic mentioned is that hyphae are 2–3 μm wide (Rodway and Cleland 1929). We did not study the type but our specimen Cui 16720 fits well with the description. Cunningham (1965) treated *P. minutipora* as a synonym of *P. lenis* (P. Karst.) Sacc. (=*Sidera lenis*), and indicated that spores were 2.5–4 × 1–1.5 μm. *Sidera tenuis* is also described from Tasmania in the present paper, but differs from *S. minutipora* by smaller pores (8–10 per mm) and longer basidiospores (4.2–5 × 0.8–1 μm). A European ITS sequence of *Skeletocutis vulgaris* (Fr.) Niemelä & Y.C. Dai (ex. CBS 465.50 GenBank: MH856711.1) is close to *Skeletocutis* species and far from *Sidera* species in the phylogeny. Ryvarden 37198 from New Zealand also named as *Sidera vulgaris* by Miettinen and Larsson (2011) clustered with *Sidera lenis* from Finland with high support, but we didn't examine their morphology, thus we keep their name.

Poria chakasskensis and *P. lunulispora* were described from Siberia (Pilát 1933, 1935) and both types were studied by Kotlaba and Pouzar (1989, 1991). The type of *P. chakasskensis* has basidiospores measuring 5.5–8.5 × 2–2.4 μm and represents *Ceriporia purpurea* (Fr.) Donk (Kotlaba and Pouzar 1991). *Poria lunulispora* was collected on wood of *Pinus*, and is true *S. lenis* (Kotlaba and Pouzar 1989, as *Diplomitoporus lenis*). *Poria consimilis* and *P. subvulgaris* were described from Brazil (Rick 1937). Rajchenberg (1987) studied the types and considered them as synonyms of *S. lenis*. *Sidera lenis* is a perennial species, and its basidiospores are more than 1.5 μm wide. Our newly described species have annual basidiomata and basidiospores are less than 1.5 μm wide. *Poria earlei*, *P. montana* and *P. tenuipora* were described from Jamaica (Murrill 1920a, b). Types of these species were studied by Niemelä and Dai (1997). They found that all types are sterile, but also that *P. earlei* and *P. montana* are conspecific and have perennial basidiomata, and that *P. tenuipora* has skeletal hyphae that are 3–4 μm in diam. Our new species are all annual and skeletal hyphae are 2–3 μm in diam.

Phylogenetically, *Sidera minutissima* is closely related to *S. vesiculosa*, *S. lowei*, *S. minutipora*, *S. tenuis* and *S. srilankensis* (Fig. 1). However, *S. vesiculosa* and *S. lowei* are readily distinguished from *S. minutissima* by have a monomitic hyphal structure. *S. minutipora*, *S. tenuis* and *S. srilankensis* differ from *S. minutissima* by having white or cream pores when fresh. *Sidera parallela* is genetically close to *S. lenis* and *S. vulgaris* (Fig. 1), but *S. lenis* has perennial basidiomata and its basidiospores are more than 1.5 μm wide, and *S. vulgaris* has interwoven tramal hyphae.

Morphologically *Sidera minutipora* resembles *S. srilankensis* by sharing similar size of pores and basidiospores. However, the former species has allantoid basidiospores, and its skeletal hyphae become swollen in KOH while basidiospores are lunate and skeletal hyphae are unchanged in KOH in *S. srilankensis*.

Sidera minutissima is similar to *S. tenuis* but differs by the bluish color of fresh basidiomata (white in *S. tenuis*) and by wider basidiospores (0.9–1.3 μm vs 0.8–1.0 μm).

Sidera parallela can be distinguished from other species by its parallel tramal hyphae. *Sidera srilankensis* resembles *S. parallela* by sharing pore size and lunate basidiospores, but in addition to the parallel tramal hyphae *S. parallela* also has smaller basidiospores measuring 2.8–3.3 × 0.9–1.2 μm.

Sidera tenuis has the smallest pores of all species in the genus (8–10 per mm) and also the narrowest basidiospores (0.8–1 μm).

In this paper four new species and a new combination of *Sidera* are described from tropic and subtropic Asian-Pacific regions. Although the type species, *Sidera lenis*, has a distribution in boreal forests, the majority of species are so far found in tropical and subtropical regions.

Acknowledgments

The research is supported by the National Natural Science Foundation of China (Project Nos. U1802231, 31900019).

References

Anonymous (1969) Flora of British Fungi. Colour Identification Chart. Her Majesty´s Stationery Office, London.

Bourdot H, Galzin A (1928) Hyménomycètes de France. France, 764 pp.

Buchanan PK, Ryvarden L (1993) Type studies in the Polyporaceae 24. Species described by Cleland, Rodway and Cheel. Australian Systematic Botany 6: 215–235. https://doi.org/10.1071/SB9930215

Cunningham GH (1965) Polyporaceae of New Zealand. Bulletin of the New Zealand Department Scientific and Industrial Research 64: 1–304.

Cui BK, Li HJ, Ji X, Zhou JL, Song J, Si J, Yang ZL, Dai YC (2019) Species diversity, taxonomy and phylogeny of Polyporaceae (Basidiomycota) in China. Fungal Diversity 97: 137–392. https://doi.org/10.1007/s13225-019-00427-4

Dai YC (2010) Hymenochaetaceae (Basidiomycota) in China. Fungal Diversity 45: 131–343. https://doi.org/10.1007/s13225-010-0066-9

Dai YC, Yu CJ, Wang HC (2007) Polypores from eastern Xizang (Tibet), western China. Annales Botanicci Fennici 44: 135–145.

Du R, Wang L, Zhou M, Chen JJ (2019) A new species of *Sidera* (Hymenochaetales, Basidiomycota) from tropical Asia. Phytotaxa 387: 165–171. https://doi.org/10.11646/phytotaxa.387.2.9

Felsenstein J (1985) Confidence intervals on phylogenetics: an approach using bootstrap. Evolution 39: 783–791. https://doi.org/10.1111/j.1558-5646.1985.tb00420.x

Fries EM (1821) Systema Mycologicum. Berlingius lindae 1: 1–520.

Hall TA (1999) Bioedit: a user-friendly biological sequence alignment editor and analysis program for Windows 95/98/NT. Nucleic Acids Symposium Series 41: 95–98.

Li HJ, Cui BK, Dai YC (2014) Taxonomy and multi-gene phylogeny of Datronia (Polyporales, Basidiomycota). Persoonia 32: 170–182. https://doi.org/10.3767/003158514X681828

Kotlaba F, Pouzar Z (1989) Type studies of polypores described by A. Pilát 2. Ceská Mycology 43: 36–44.

Kotlaba F, Pouzar Z (1991) Type studies of polypores described by A. Pilát 4. Ceská Mycology 45: 91–97.

Michalak S (2012) RaxmlGUI: a graphical front-end for RAxML. Organisms Diversity & Evolution 12: 335–337. https://doi.org/10.1007/s13127-011-0056-0

Miettinen O, Larsson KH (2011) *Sidera*, a new genus in Hymenochaetales with poroid and hydnoid species. Mycological Progress 10: 131–141. https://doi.org/10.1007/s11557-010-0682-5

Murrill WA (1920a) Light-colored resupinate polypores 1. Mycologia 12: 77–92. https://doi.org/10.1080/00275514.1920.12016821

Murrill WA (1920b) Light-colored resupinate polypores 2. Mycologia 12: 299–308. https://doi.org/10.1080/00275514.1920.12016844

Niemelä T, Dai YC (1997) Polypore *Skeletocutis lenis* and its sib *S. vulgaris*. Annales Botanici Fennici 34: 133–140.

Nylander JAA (2004) MrModeltest v2. Program distributed by the author. Evolutionary Biology Centre, Uppsala University, Uppsala.

Petersen JH (1996) The Danish Mycological Society's colour-chart. Foreningen til Svampekundskabens Fremme, Greve.

Pilát A (1933) Additamenta ad floram Sibiriae Asiaeque orientalis mycologicam. Bulletin de la Société Mycologique de France 49: 256–339.

Pilát A (1935) Additamenta ad floram Sibiriae Asiaeque orientalis mycologicam. Pars tertia. Bulletin de la Société Mycologique de France. 51: 351–426.

Rajchenberg M (1987) Type studies of Polyporaceae (Aphyllophorales) described by J. Rick. Nordic Journal of Botany 7: 553–568. https://doi.org/10.1111/j.1756-1051.1987.tb02023.x

Rick J (1937) Poriae Riograndenses. Brotéria Série Trimestral: Ciências Naturais 6: 128–152.

Rodway L, Cleland JB (1929) Notes on the genus *Poria* 3. Papers and Proceedings of the Royal Society of Tasmania 1929: 7–24.

Ronquist F, Teslenko M, van der Mark P, Avres DL, Darling A, Höhna S, Larget B, Liu L, Suchard MA, Huelsenbeck JP (2012) MrBayes3.2: efficient Bayesian phylogenetic inference and model choice, across a large model space. Systematic Biology 61: 539–542. https://doi.org/10.1093/sysbio/sys029

Shen LL, Wang M, Zhou JL, Xing JH, Cui BK, Dai YC (2019) Taxonomy and phylogeny of *Postia*. Multi-gene phylogeny and taxonomy of the brown-rot fungi: *Postia* and its related genera. Persoonia 42: 101–126. https://doi.org/10.3767/persoonia.2019.42.05

Swofford DL (2002) PAUP*: Phylogenetic analysis using parsimony (*and other methods). Version 4.0b10. Sinauer Associates, Sunderland. https://doi.org/10.1002/0471650129.dob0522

Thiers B (2018) Index Herbariorum: A global directory of public herbaria and associated staff. New York Botanical Garden's Virtual Herbarium, New York. http://sweetgum.nybg.org/science/ih/

Thompson JD, Gibson TJ, Plewniak F, Jeanmougin F, Higgins DG (1997) The CLUSTAL X windows interface: flexible strategies for multiple sequence alignment aided by quality analysis tools. Nucleic Acids Research 25: 4876–4882. https://doi.org/10.1093/nar/25.24.4876

White TJ, Bruns T, Lee S, Taylor J (1990) Amplification and direct sequencing of fungal ribosomal RNA genes for phylogenetics. In: Innis MA, Gefand DH, Sninsky JJ, White JT (Eds) PCR Protocols: A Guide to Methods and Applications. Academic Press, San Diego, 315–322. https://doi.org/10.1016/B978-0-12-372180-8.50042-1

Yuan HS, Dai YC (2008) Polypores from northern and central Yunnan Province, Southwestern China. Sydowia 60: 147–159.

Yuan Y, Ji XH, Wu F, He SH, Chen JJ (2016) Two new *Gloeoporus* (Polyporales, Basidiomycota) from tropical China. Nova Hedwigia 103: 169–183. https://doi.org/10.1127/nova_hedwigia/2016/0344

Zhu L, Song J, Zhou JL, Si J, Cui BK (2019) Species diversity, phylogeny, divergence time and biogeography of the genus *Sanghuangporus* (Basidiomycota). Frontiers in Microbiology 10: 1–812. https://doi.org/10.3389/fmicb.2019.00812